

Recent advances in oxidation chemistry

Guest editor: Dan Yang

Department of Chemistry, The University of Hong Kong, Pokfulam Road, Hong Kong, PR China

Contents

Announcement: Tetrahedron Symposia-in-Print
Preface

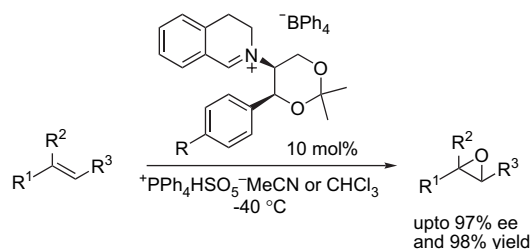
pp 6601–6603
p 6605

ARTICLES

Non-aqueous iminium salt mediated catalytic asymmetric epoxidation

pp 6607–6613

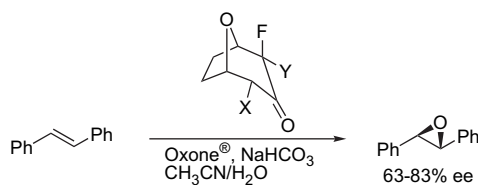
Philip C. Bulman Page,* Benjamin R. Buckley, David Barros, A. John Blacker, Harry Heaney and Brian A. Marples



Bicyclo[3.2.1]octanone catalysts for asymmetric alkene epoxidation: the effect of disubstitution

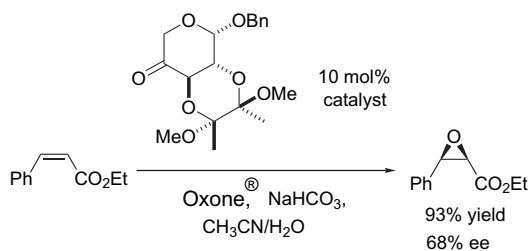
pp 6614–6620

Alan Armstrong,* Belen Dominguez-Fernandez and Tomoki Tsuchiya

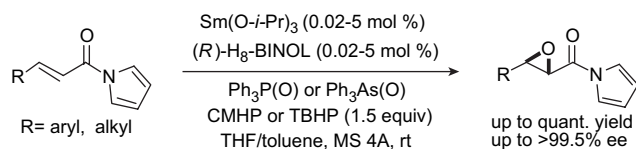


Asymmetric epoxidation of *cis*-alkenes with arabinose-derived ketones: enantioselective synthesis of the side chain of Taxol[®] pp 6621–6629

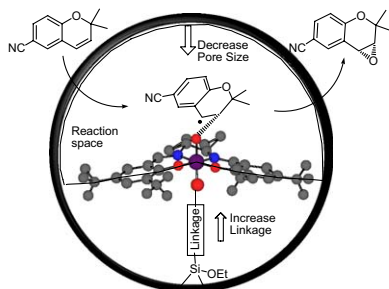
Tony K. M. Shing,* To Luk and Chi M. Lee


Catalytic asymmetric epoxidation of α,β -unsaturated *N*-acylpyrroles as monodentate and activated ester equivalent acceptors pp 6630–6639

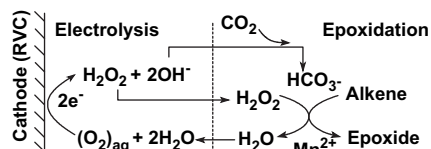
Shigeki Matsunaga,* Hongbo Qin, Mari Sugita, Shigemitsu Okada, Tomofumi Kinoshita, Noriyuki Yamagiwa and Masakatsu Shibasaki*


Asymmetric epoxidation of 6-cyano-2,2-dimethylchromene on Mn(salen) catalyst immobilized in mesoporous materials pp 6640–6649

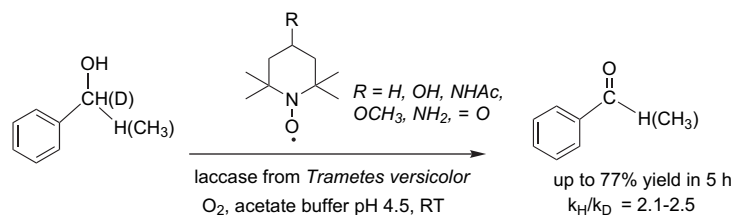
Huidong Zhang and Can Li*


Indirect catalytic epoxidation with hydrogen peroxide electrogenerated in ionic liquids pp 6650–6658

Kam-Piu Ho, Kwok-Yin Wong* and Tak Hang Chan*

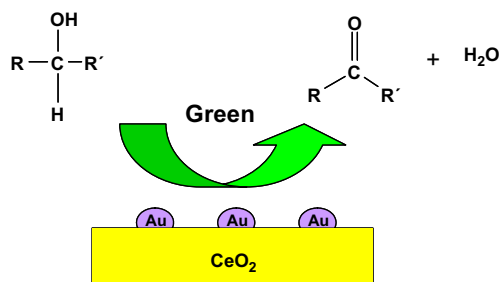


Comparison of TEMPO and its derivatives as mediators in laccase catalysed oxidation of alcohols pp 6659–6665
 Isabel W. C. E. Arends, Yu-Xin Li, Rina Ausan and Roger A. Sheldon*



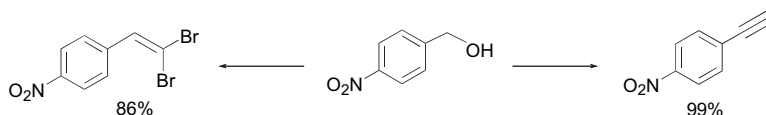
Efficient chemoselective alcohol oxidation using oxygen as oxidant. Superior performance of gold over palladium catalysts pp 6666–6672
 Alberto Abad, Carles Almela, Avelino Corma* and Hermenegildo García*

Alberto Abad, Carles Almela, Avelino Corma* and Hermenegildo García*



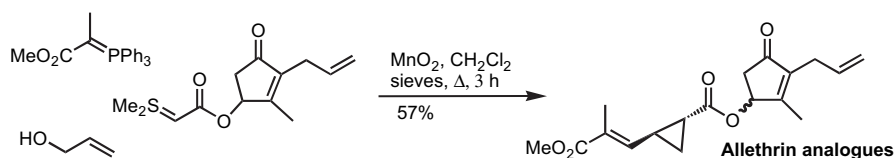
One-pot conversion of activated alcohols into 1,1-dibromoalkenes and terminal alkynes using tandem oxidation processes with manganese dioxide pp 6673–6680
 Ernesto Quesada, Steven A. Raw, Mark Reid, Estelle Roman and Richard J. K. Taylor*

Ernesto Quesada, Steven A. Raw, Mark Reid, Estelle Roman and Richard J. K. Taylor*



The direct preparation of functionalised cyclopropanes from allylic alcohols or α -hydroxyketones using tandem oxidation processes pp 6681–6694
 Graeme D. McAllister, Magalie F. Oswald, Richard J. Paxton, Steven A. Raw and Richard J. K. Taylor*

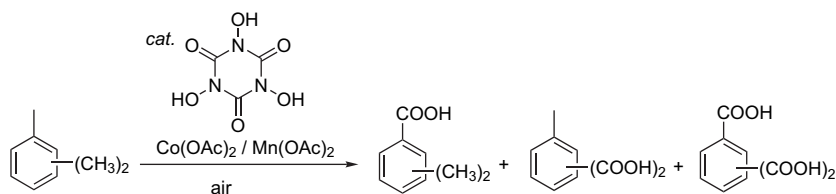
Graeme D. McAllister, Magalie F. Oswald, Richard J. Paxton, Steven A. Raw and Richard J. K. Taylor*



Aerobic oxidation of trimethylbenzenes catalyzed by N,N',N'' -trihydroxyisocyanuric acid (THICA) as a key catalyst

pp 6695–6699

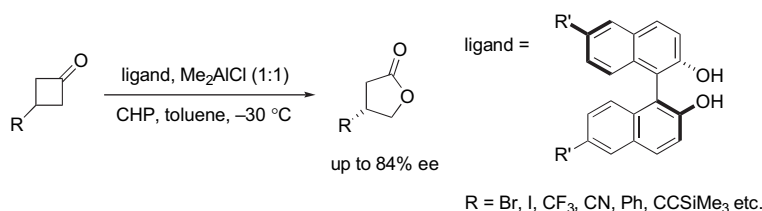
Naruhisa Hirai, Yoshinobu Tatsukawa, Michiko Kameda, Satoshi Sakaguchi and Yasutaka Ishii*



Ligand effects in aluminium-catalyzed asymmetric Baeyer–Villiger reactions

pp 6700–6706

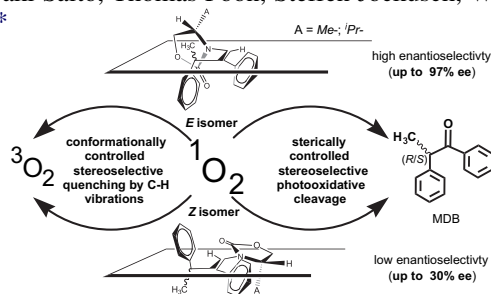
Jean-Cédric Frison, Chiara Palazzi and Carsten Bolm*



Conformationally controlled (entropy effects), stereoselective vibrational quenching of singlet oxygen in the oxidative cleavage of oxazolidinone-functionalized encarbamates through solvent and temperature variations

pp 6707–6717

J. Sivaguru, Marissa R. Solomon, Hideaki Saito, Thomas Poon, Steffen Jockusch, Waldemar Adam, Yoshihisa Inoue and Nicholas J. Turro*



*Corresponding author

COVER

The cover graphic exemplifies several classes of important oxidation reactions that have been covered in this Symposium-in-Print issue. The two words at the bottom of the graphic are the Chinese characters for oxidation.

© 2006 D. Yang. Published by Elsevier Ltd.



Full text of this journal is available, on-line from **ScienceDirect**. Visit www.sciencedirect.com for more information.

Indexed/Abstracted in: AGRICOLA, Beilstein, BIOSIS Previews, CAB Abstracts, Chemical Abstracts. Current Contents: Life Sciences, Current Contents: Physical, Chemical and Earth Sciences, Current Contents Search, Derwent Drug File, Ei compendex, EMBASE/Excerpta Medica, Medline, PASCAL, Research Alert, Science Citation Index, SciSearch



ELSEVIER

ISSN 0040-4020

Tetrahedron Symposia-in-Print

Series Editor

Professor H. H. Wasserman, Department of Chemistry, Yale University, P.O. Box 208107, New Haven, CT 06520-8107, U.S.A.

Tetrahedron Symposia-in-Print comprise collections of original research papers covering timely areas of organic chemistry.

Each symposium is organized by a Symposium Editor who will invite authors, active in the selected field, to submit original articles covering current research, complete with experimental sections. These papers will be rapidly reviewed and processed for publication by the Symposium Editor under the usual refereeing system.

Authors who have not already been invited, and who may have obtained recent significant results in the area of the announced symposium, may also submit contributions for Editorial consideration and possible inclusion. Before submitting such papers authors should send an abstract to the Symposium Editor for preliminary evaluation. Firm deadlines for receipt of papers will allow sufficient time for completion and presentation of ongoing work without loss of the freshness and timeliness of the research results.

Symposia-in-Print—already published

1. Recent trends in organic photochemistry, Albert Padwa, Ed. *Tetrahedron* **1981**, *37*, 3227–3420.
2. New general synthetic methods, E. J. Corey, Ed. *Tetrahedron* **1981**, *37*, 3871–4119.
3. Recent developments in polycyclopentanoid chemistry, Leo A. Paquette, Ed. *Tetrahedron* **1981**, *37*, 4357–4559.
4. Biradicals, Josef Michl, Ed. *Tetrahedron* **1982**, *38*, 733–867.
5. Electron-transfer initiated reactions, Gary B. Schuster, Ed. *Tetrahedron* **1982**, *38*, 1025–1122.
6. The organic chemistry of animal defense mechanisms, Jerrold Meinwald, Ed. *Tetrahedron* **1982**, *38*, 1853–1970.
7. Recent developments in the use of silicon in organic synthesis, Hans Reich, Ed. *Tetrahedron* **1983**, *39*, 839–1009.
8. Linear tetrapyrroles, Ray Bonnett, Ed. *Tetrahedron* **1983**, *39*, 1837–1954.
9. Heteroatom-directed metallations in heterocyclic synthesis, George R. Newkome, Ed. *Tetrahedron* **1983**, *39*, 1955–2091.
10. Recent aspects of the chemistry of β -lactams, J. E. Baldwin, Ed. *Tetrahedron* **1983**, *39*, 2445–2608.
11. New spectroscopic techniques for studying metabolic processes, A. I. Scott, Ed. *Tetrahedron* **1983**, *39*, 3441–3626.
12. New developments in indole alkaloids, Martin E. Kuehne, Ed. *Tetrahedron* **1983**, *39*, 3627–3780.
13. Recent aspects of the chemistry of nucleosides, nucleotides and nucleic acids, Colin B. Reese, Ed. *Tetrahedron* **1984**, *40*, 1–164.
14. Bioorganic studies on receptor sites, Koji Nakanishi, Ed. *Tetrahedron* **1984**, *40*, 455–592.
15. Synthesis of chiral non-racemic compounds, A. I. Meyers, Ed. *Tetrahedron* **1984**, *40*, 1213–1418.
16. Control of acyclic stereochemistry, Teruaki Mukaiyama, Ed. *Tetrahedron* **1984**, *40*, 2197–2344.
17. Recent aspects of anthracycline chemistry, T. Ross Kelly, Ed. *Tetrahedron* **1984**, *40*, 4537–4794.
18. The organic chemistry of marine products, Paul J. Scheuer, Ed. *Tetrahedron* **1985**, *41*, 979–1108.
19. Recent aspects of carbene chemistry, Matthew Platz, Ed. *Tetrahedron* **1985**, *41*, 1423–1612.
20. Recent aspects of singlet oxygen chemistry of photooxidation, Isao Saito and Teruo Matsuura, Eds. *Tetrahedron* **1985**, *41*, 2037–2236.
21. Synthetic applications of dipolar cycloaddition reactions, Wolfgang Oppolzer, Ed. *Tetrahedron* **1985**, *41*, 3447–3568.
22. Selectivity and synthetic applications of radical reactions, Bernd Giese, Ed. *Tetrahedron* **1985**, *41*, 3887–4302.
23. Recent aspects of organoselenium chemistry, Dennis Liotta, Ed. *Tetrahedron* **1985**, *41*, 4727–4890.
24. Application of newer organometallic reagents to the total synthesis of natural products, Martin Semmelhack, Ed. *Tetrahedron* **1985**, *41*, 5741–5900.
25. Formal transfers of hydride from carbon–hydrogen bonds, James D. Wuest, Ed. *Tetrahedron* **1986**, *42*, 941–1208.
26. Synthesis of non-natural products: challenge and reward, Philip E. Eaton, Ed. *Tetrahedron* **1986**, *42*, 1549–1916.
27. New synthetic methods—II, F. E. Ziegler, Ed. *Tetrahedron* **1986**, *42*, 2777–3028.
28. Structure and reactivity of organic radical ions, Heinz D. Roth, Ed. *Tetrahedron* **1986**, *42*, 6097–6350.
29. Organic chemistry in anisotropic media, V. Ramamurthy, J. R. Scheffer and N. J. Turro, Eds. *Tetrahedron* **1987**, *43*, 1197–1746.
30. Current topics in sesquiterpene synthesis, John W. Huffman, Ed. *Tetrahedron* **1987**, *43*, 5467–5722.
31. Peptide chemistry: design and synthesis of peptides, conformational analysis and biological functions, Victor J. Hruby and Robert Schwyzer, Eds. *Tetrahedron* **1988**, *44*, 661–1006.
32. Organosilicon chemistry in organic synthesis, Ian Fleming, Ed. *Tetrahedron* **1988**, *44*, 3761–4292.
33. α -Amino acid synthesis, Martin J. O'Donnell, Ed. *Tetrahedron* **1988**, *44*, 5253–5614.
34. Physical-organic/theoretical chemistry: the Dewar interface, Nathan L. Bauld, Ed. *Tetrahedron* **1988**, *44*, 7335–7626.
35. Recent developments in organocopper chemistry, Bruce H. Lipshutz, Ed. *Tetrahedron* **1989**, *45*, 349–578.
36. Organotin compounds in organic synthesis, Yoshinori Yamamoto, Ed. *Tetrahedron* **1989**, *45*, 909–1230.

37. Mycotoxins, Pieter S. Steyn, Ed. *Tetrahedron* **1989**, *45*, 2237–2464.
38. Strain-assisted syntheses, Léon Ghosez, Ed. *Tetrahedron* **1989**, *45*, 2875–3232.
39. Covalently linked donor-acceptor species for mimicry of photosynthetic electron and energy transfer, Devens Gust and Thomas A. Moore, Eds. *Tetrahedron* **1989**, *45*, 4669–4912.
40. Aspects of modern carbohydrate chemistry, S. Hanessian, Ed. *Tetrahedron* **1990**, *46*, 1–290.
41. Nitroalkanes and nitroalkenes in synthesis, Anthony G. M. Barrett, Ed. *Tetrahedron* **1990**, *46*, 7313–7598.
42. Synthetic applications of anodic oxidations, John S. Swenton and Gary W. Morrow, Eds. *Tetrahedron* **1991**, *47*, 531–906.
43. Recent advances in bioorganic chemistry, Dale L. Boger, Ed. *Tetrahedron* **1991**, *47*, 2351–2682.
44. Natural product structure determination, R. B. Bates, Ed. *Tetrahedron* **1991**, *47*, 3511–3664.
45. Frontiers in natural products biosynthesis. Enzymological and molecular genetic advances, D. E. Cane, Ed. *Tetrahedron* **1991**, *47*, 5919–6078.
46. New synthetic methods—III, S. E. Denmark, Ed. *Tetrahedron* **1992**, *48*, 1959–2222.
47. Organotitanium reagents in organic chemistry, M. T. Reetz, Ed. *Tetrahedron* **1992**, *48*, 5557–5754.
48. Total and semi-synthetic approaches to taxol, J. D. Winkler, Ed. *Tetrahedron* **1992**, *48*, 6953–7056.
49. Synthesis of optically active compounds—prospects for the 21st century, Kenji Koga and Takayuki Shioiri, Eds. *Tetrahedron* **1993**, *49*, 1711–1924.
50. Peptide secondary structure mimetics, Michael Kahn, Ed. *Tetrahedron* **1993**, *49*, 3433–3689.
51. Transition metal organometallics in organic synthesis, Anthony J. Pearson, Ed. *Tetrahedron* **1993**, *49*, 5415–5682.
52. Palladium in organic synthesis, Jan-E. Bäckvall, Ed. *Tetrahedron* **1994**, *50*, 285–572.
53. Recent progress in the chemistry of enediyne antibiotics, Terrence W. Doyle and John F. Kadow, Eds. *Tetrahedron* **1994**, *50*, 1311–1538.
54. Catalytic asymmetric addition reactions, Stephen F. Martin, Ed. *Tetrahedron* **1994**, *50*, 4235–4574.
55. Mechanistic aspects of polar organometallic chemistry, Manfred Schlosser, Ed. *Tetrahedron* **1994**, *50*, 5845–6128.
56. Molecular recognition, Andrew D. Hamilton, Ed. *Tetrahedron* **1995**, *51*, 343–648.
57. Recent advances in the chemistry of zirconocene and related compounds, Ei-ichi Negishi, Ed. *Tetrahedron* **1995**, *51*, 4255–4570.
58. Fluoroorganic chemistry: synthetic challenges and biomedical rewards, Giuseppe Resnati and Vadim A. Soloshonok, Eds. *Tetrahedron* **1996**, *52*, 1–330.
59. Novel applications of heterocycles in synthesis, A. R. Katritzky, Ed. *Tetrahedron* **1996**, *52*, 3057–3374.
60. Fullerene chemistry, Amos B. Smith III, Ed. *Tetrahedron* **1996**, *52*, 4925–5262.
61. New synthetic methods—IV. Organometallics in organic chemistry, István E. Markó, Ed. *Tetrahedron* **1996**, *52*, 7201–7598.
62. Cascade reactions, Ron Grigg, Ed. *Tetrahedron* **1996**, *52*, 11385–11664.
63. Applications of solid-supported organic synthesis in combinatorial chemistry, James A. Bristol, Ed. *Tetrahedron* **1997**, *53*, 6573–6706.
64. Recent applications of synthetic organic chemistry, Stephen F. Martin, Ed. *Tetrahedron* **1997**, *53*, 8689–9006.
65. Chemical biology, Gregory L. Verdine and Julian Simon, Eds. *Tetrahedron* **1997**, *53*, 11937–12066.
66. Recent aspects of S, Se, and Te chemistry, Richard S. Glass and Renji Okazaki, Eds. *Tetrahedron* **1997**, *53*, 12067–12318.
67. Modern organic chemistry of polymerization, H. K. Hall Jr., Ed. *Tetrahedron* **1997**, *53*, 15157–15616.
68. New synthetic methods—V, John L. Wood, Ed. *Tetrahedron* **1997**, *53*, 16213–16606.
69. New developments in organonickel chemistry, Bruce H. Lipshutz and Tien-Yau Luh, Eds. *Tetrahedron* **1998**, *54*, 1021–1316.
70. Solution phase combinatorial chemistry, David L. Coffen, Ed. *Tetrahedron* **1998**, *54*, 3955–4150.
71. Heterocycles in asymmetric synthesis, Alexandre Alexakis, Ed. *Tetrahedron* **1998**, *54*, 10239–10554.
72. Recent advances of phase-transfer catalysis, Takayuki Shioiri, Ed. *Tetrahedron* **1999**, *55*, 6261–6402.
73. Olefin metathesis in organic synthesis, Marc L. Snapper and Amir H. Hoveyda, Eds. *Tetrahedron* **1999**, *55*, 8141–8262.
74. Stereoselective carbon–carbon bond forming reactions, Harry H. Wasserman, Stephen F. Martin and Yoshinori Yamamoto, Eds. *Tetrahedron* **1999**, *55*, 8589–9006.
75. Applications of combinatorial chemistry, Miles G. Siegel and Stephen W. Kaldor, Eds. *Tetrahedron* **1999**, *55*, 11609–11710.
76. Advances in carbon–phosphorus heterocyclic chemistry, François Mathey, Ed. *Tetrahedron* **2000**, *56*, 1–164.
77. Transition metal organometallics in organic synthesis, Kenneth M. Nicholas, Ed. *Tetrahedron* **2000**, *56*, 2103–2338.
78. Organocopper chemistry II, Norbert Krause, Ed. *Tetrahedron* **2000**, *56*, 2727–2904.
79. Carbene complexes in organic chemistry, James W. Herndon, Ed. *Tetrahedron* **2000**, *56*, 4847–5044.
80. Recent aspects of the chemistry of β -lactams—II, Marvin J. Miller, Ed. *Tetrahedron* **2000**, *56*, 5553–5742.
81. Molecular assembly and reactivity of organic crystals and related structures, Miguel A. Garcia-Garibay, Vaidhyanathan Ramamurthy and John R. Scheffer, Eds. *Tetrahedron* **2000**, *56*, 6595–7050.
82. Protein engineering, Richard Chamberlin, Ed. *Tetrahedron* **2000**, *56*, 9401–9526.
83. Recent advances in peptidomimetics, Jeffrey Aubé, Ed. *Tetrahedron* **2000**, *56*, 9725–9842.
84. New synthetic methods—VI, George A. Kraus, Ed. *Tetrahedron* **2000**, *56*, 10101–10282.
85. Oxidative activation of aromatic rings: an efficient strategy for arene functionalization, Stéphane Quideau and Ken S. Feldman, Eds. *Tetrahedron* **2001**, *57*, 265–424.
86. Lewis acid control of asymmetric synthesis, Keiji Maruoka, Ed. *Tetrahedron* **2001**, *57*, 805–914.
87. Novel aromatic compounds, Lawrence T. Scott and Jay S. Siegel, Eds. *Tetrahedron* **2001**, *57*, 3507–3808.
88. Asymmetric synthesis of novel sterically constrained amino acids, Victor J. Hruby and Vadim A. Soloshonok, Eds. *Tetrahedron* **2001**, *57*, 6329–6650.
89. Recognition-mediated self-assembly of organic systems, Vincent M. Rotello, Ed. *Tetrahedron* **2002**, *58*, 621–844.
90. Synthesis of marine natural products containing polycyclic ethers, Masahiro Hirama and Jon D. Rainier, Eds. *Tetrahedron* **2002**, *58*, 1779–2040.

91. Fluorous chemistry, John A. Gladysz and Dennis P. Curran, Eds. *Tetrahedron* **2002**, 58, 3823–4132.
92. Recent developments in chiral lithium amide base chemistry, Peter O'Brien, Ed. *Tetrahedron* **2002**, 58, 4567–4734.
93. Beyond natural product synthesis (Tetrahedron Prize for Creativity in Organic Chemistry 2001 – Yoshito Kishi), Harry H. Wasserman and Stephen F. Martin, Eds. *Tetrahedron* **2002**, 58, 6223–6602.
94. Strained heterocycles as intermediates in organic synthesis, Amy R. Howell, Ed. *Tetrahedron* **2002**, 58, 6979–7194.
95. Molecular design of Lewis and Brønsted acid catalysts—the key to environmentally benign reagents (Tetrahedron Chair 2002), Hisashi Yamamoto, Ed. *Tetrahedron* **2002**, 58, 8153–8364.
96. Recent developments in dendrimer chemistry, David K. Smith, Ed. *Tetrahedron* **2003**, 59, 3787–4024.
97. Art, science and technology in total synthesis (Tetrahedron Prize for Creativity in Organic Chemistry 2002 – K. C. Nicolaou), Stephen F. Martin and Harry H. Wasserman, Eds. *Tetrahedron* **2003**, 59, 6667–7070.
98. New synthetic methods—VII, Brian M. Stoltz, Ed. *Tetrahedron* **2003**, 59, 8843–9030.
99. Oxiranyl and aziridinyl anions as reactive intermediates in synthetic organic chemistry, S. Florio, Ed. *Tetrahedron* **2003**, 59, 9683–9864.
100. Recent advances in rare earth chemistry, Shū Kobayashi, Ed. *Tetrahedron* **2003**, 59, 10339–10598.
101. Biocatalysts in synthetic organic chemistry, S. M. Roberts, Ed. *Tetrahedron* **2004**, 60, 483–806.
102. Recent advances in the chemistry of zirconocenes, Keisuke Suzuki and Peter Wipf, Eds. *Tetrahedron* **2004**, 60, 1257–1424.
103. Atropisomerism, Jonathan Clayden, Ed. *Tetrahedron* **2004**, 60, 4325–4558.
104. Chemistry of biologically and physiologically intriguing phenomena, Daisuke Uemura, Ed. *Tetrahedron* **2004**, 60, 6959–7098.
105. Olefin metathesis: a powerful and versatile instrument for organic synthesis (Tetrahedron prize for creativity in organic chemistry 2003 – R. H. Grubbs), Stephen F. Martin and Harry H. Wasserman, Eds. *Tetrahedron* **2004**, 60, 7099–7438.
106. From synthetic methodology to biomimetic target assembly (Tetrahedron prize for creativity in organic chemistry 2003 – D. Seebach), Léon A. Ghosez, Ed. *Tetrahedron* **2004**, 60, 7439–7794.
107. Solid and solution phase combinatorial chemistry, Rolf Breinbauer and Herbert Waldmann, Eds. *Tetrahedron* **2004**, 60, 8579–8738.
108. Catalytic tools enabling total synthesis (Tetrahedron Chair 2004), Alois Fürstner, Ed. *Tetrahedron* **2004**, 60, 9529–9784.
109. Synthesis and applications of non-racemic cyanohydrins and α -amino nitriles, Michael North, Ed. *Tetrahedron* **2004**, 60, 10371–10568.
110. Synthetic receptors as sensors, Eric V. Anslyn, Ed. *Tetrahedron* **2004**, 60, 11041–11316.
111. Functionalised organolithium compounds, Carmen Nájera and Miguel Yus, Eds. *Tetrahedron* **2005**, 61, 3125–3450.
112. Applications of catalysis in academia and industry, Michael J. Krische, Ed. *Tetrahedron* **2005**, 61, 6155–6472.
113. Development and application of highly active and selective palladium catalysts, Ian J. S. Fairlamb, Ed. *Tetrahedron* **2005**, 61, 9647–9918.
114. Multicomponent reactions, Ilan Marek, Ed. *Tetrahedron* **2005**, 61, 11299–11520.
115. Polymer-supported reagents and catalysts: increasingly important tools for organic synthesis, Patrick Toy and Min Shi, Eds. *Tetrahedron* **2005**, 61, 12013–12192.
116. Organocatalysis in organic synthesis, Pavel Kočovský and Andri V. Malkov, Eds. *Tetrahedron* **2006**, 62, 243–502.
117. Supramolecular chemistry of fullerenes, Nazario Martín and Jean-François Nierengarten, Eds. *Tetrahedron* **2006**, 62, 1905–2132.
118. Chemistry of electron-deficient ynamines and ynamides, Richard P. Hsung, Ed. *Tetrahedron* **2006**, 62, 3771–3938.
119. Microwave assisted organic synthesis, Nicholas E. Leadbeater, Ed. *Tetrahedron* **2006**, 62, 4623–4732.
120. Nature-inspired approaches to chemical synthesis, Erik J. Sorensen and Emmanuel A. Theodorakis, Eds. *Tetrahedron* **2006**, 62, 5159–5354.
121. The chemistry of radical ions, Paul E. Floreancig, Ed. *Tetrahedron* **2006**, 62, 6447–6594.
122. Recent advances in oxidation chemistry, Dan Yang, Ed. *Tetrahedron* **2006**, 62, 6595–6718.



ELSEVIER

Available online at www.sciencedirect.com

SCIENCE @ DIRECT®

Tetrahedron 62 (2006) 6605

Tetrahedron

Preface

Recent advances in oxidation chemistry

Oxidation reactions represent a fundamental class of organic transformations and almost every natural product total synthesis involves an oxidation step. As our living atmosphere contains oxygen, oxidation reactions have been involved in almost every cell. For example, the oxidation of carbon-containing compounds is an important energy source for most living organisms. No doubt, oxidation reactions are essential to organic synthesis as well as life processes, and great progress has been made in the last century on new catalysts, methodologies, and mechanistic studies for oxidation reactions. Nevertheless, the current methods available for oxidation reactions are still far from ideal, in particular, compared to Mother Nature, in terms of regioselectivity, stereoselectivity, mildness of conditions, efficiency, and environmental issues. It is high time for this Symposium-in-Print to focus on the advances in oxidation reactions, and to present the challenges and opportunities for future research in oxidation reactions.

Since it is impossible for this Symposium-in-Print to cover all the significant work done in the area, the following aspects of the recent developments in oxidation reactions have been highlighted instead: enantioselective epoxidation of olefins catalyzed by chiral iminium salts (Page), ketones (Armstrong, Shing), lanthanide/ H_8 -BINOL reagents (Shibasaki),

and chiral Mn(salen) catalysts immobilized on mesoporous materials (Li); epoxidation of olefins using electrochemically generated hydrogen peroxide as the terminal oxidant (Wong and Chan); alcohol oxidation catalyzed by laccases (Sheldon) and gold nanoparticles (Corma and Garcia); manganese dioxide-mediated tandem oxidation processes for alcohols (Taylor); C–H bond oxidation catalyzed by trihydroxycyanuric acid (Ishii); asymmetric Baeyer–Villiger oxidation catalyzed by chiral BINOL/aluminum reagents (Bolm); and photooxidative cleavage of olefins (Turro).

From this selection of 13 contributions, we can see that oxidation chemistry is an active and frontier research field, with great opportunities to explore and significant challenges to meet.

Dan Yang
*Department of Chemistry,
The University of Hong Kong,
Pokfulam Road,
Hong Kong,
PR China*
E-mail address: yangdan@hku.hk

Available online 2 June 2006

Non-aqueous iminium salt mediated catalytic asymmetric epoxidation

Philip C. Bulman Page,^{a,*} Benjamin R. Buckley,^a David Barros,^a A. John Blacker,^b Harry Heaney^a and Brian A. Marples^a

^aDepartment of Chemistry, Loughborough University, Loughborough, Leicestershire LE11 3TU, UK

^bNPIL Pharmaceuticals (UK) Ltd., PO Box 521, Leeds Road, Huddersfield, HD2 1GA, UK

Received 26 August 2005; revised 13 October 2005; accepted 13 October 2005

Available online 5 June 2006

Abstract—A range of substituted dihydroisoquinolinium salts has been tested in the catalytic asymmetric epoxidation of simple alkenes using our newly developed non-aqueous conditions employing tetraphenylphosphonium monoperoxy sulfate (TPPP) as oxidant, giving ees of up to 97%.

© 2006 Elsevier Ltd. All rights reserved.

1. Introduction

In 1976, it was established that oxaziridinium salts are extremely reactive reagents for oxygen transfer to nucleophilic substrates.¹ Since then, there has been significant interest in developing effective iminium salt catalysts for epoxidation of olefins.² The primary oxidant used is oxone and the reactions are usually performed at 0 °C in the presence of a base. In addition to an organic solvent, usually acetonitrile, water is an essential cosolvent, required in order to provide sufficient oxone solubility.

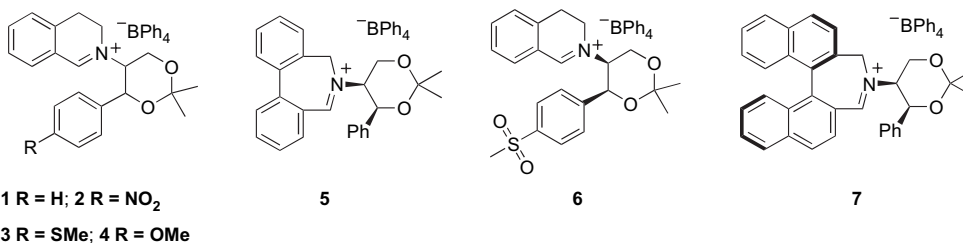
We have previously described our approach to new types of cyclic chiral iminium salts, functionalised with chiral units at the nitrogen atom.³ These enantiomerically pure iminium salts have been successfully employed in the catalytic asymmetric epoxidation of unfunctionalised alkenes, the dioxane-derived catalysts **1–5** giving ees of up to ca. 60%,⁴ catalyst **6** giving ees of up to 97%,⁵ and catalyst **7** ees of up to 95%.⁶

The standard conditions employed by ourselves and others in epoxidation reactions catalysed by iminium salts involve

the use of oxone as stoichiometric oxidant, a base (2 mol equiv of Na₂CO₃ per equiv of oxone) and water/acetonitrile as solvent mixture.

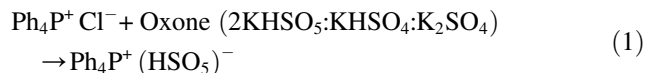
The principal limitation of this system is the restricted range of temperatures at which the epoxidation can be performed (ca. –5 °C to ambient). The upper temperature limit results from the relatively fast decomposition of oxone in basic media at room temperature. The lower limit is determined by the requirement for an aqueous solution (the normal ratio of solvents is (CH₃CN/H₂O; 1:1); aqueous acetonitrile freezes at –8 °C. An additional drawback arising from the dependency on oxone is the large quantity of inorganic salt byproducts produced in the reaction.

We have recently described new reaction conditions for iminium salt-catalysed epoxidation, which eliminate the use of both water and base.⁷ This was achieved through the identification of an effective oxidant, tetraphenylphosphonium monoperoxy sulfate (TPPP), that is soluble in organic solvents. When oxone is treated with tetraphenylphosphonium chloride, TPPP is produced as a colourless solid (Eq. 1).



* Corresponding author. Tel.: +44 1509 222581; fax: +44 1509 223926; e-mail: p.c.b.page@lboro.ac.uk

TPPP has previously been used for the oxidation of manganese(III) porphyrins.⁸



We were pleased to find that the use of TPPP in place of oxone induces efficient epoxidation in organic solvents in the absence of water and furthermore that the presence of base is now not required; indeed, addition of base actually suppresses the epoxidation process. Use of this oxidant also enables greater scope for reaction monitoring and analysis, as water is no longer required. Reactions can be carried out at low temperature, and, when carried out in deuterated solvent, monitored by NMR spectroscopy. We describe herein the catalytic asymmetric epoxidation of several unfunctionalised alkenes using catalysts 2–6 under the new anhydrous conditions, employing (TPPP) as stoichiometric oxidant. The catalysts were first tested in the asymmetric epoxidation of 1-phenylcyclohexene at varying temperatures using TPPP in dichloromethane (Table 1).

As the temperature is reduced there is an increase in enantiomeric excess at the expense of rate of conversion to epoxide. It is interesting that, while catalyst 1 gives the (–)-(1*S*,2*S*) epoxide, when the catalyst contains a strongly electron-withdrawing nitro or sulfone substituent (catalysts 2 and 6),

Table 1. Catalytic asymmetric epoxidation of 1-phenylcyclohexene using TPPP in CH₂Cl₂^a

Entry	Temp (°C)	Catalyst ^b	Conversion (%) ^c	ee (%) ^d	Configuration ^e
1	0	1	100	16	(–)-(1 <i>S</i> ,2 <i>S</i>)
2		2	100	25	(+)-(1 <i>R</i> ,2 <i>R</i>)
3		3	72	16	(+)-(1 <i>R</i> ,2 <i>R</i>)
4		4 ^f	—	—	—
5		6	100	33	(+)-(1 <i>R</i> ,2 <i>R</i>)
6	–30	1	—	—	—
7		2	100	28	(+)-(1 <i>R</i> ,2 <i>R</i>)
8		3	92	33	(+)-(1 <i>R</i> ,2 <i>R</i>)
9		4 ^f	76	25	(+)-(1 <i>R</i> ,2 <i>R</i>)
10		6	100	36	(+)-(1 <i>R</i> ,2 <i>R</i>)
11	–45	1	70	37 ^g	(–)-(1 <i>S</i> ,2 <i>S</i>)
12		2	54	30	(+)-(1 <i>R</i> ,2 <i>R</i>)
13		3	67	33	(+)-(1 <i>R</i> ,2 <i>R</i>)
14		4 ^f	—	—	—
15		6	96	42	(+)-(1 <i>R</i> ,2 <i>R</i>)
16	–78	1	15	23 ^h	(–)-(1 <i>S</i> ,2 <i>S</i>)
17		2	0	—	—
18		3	15	50 ^h	(–)-(1 <i>S</i> ,2 <i>S</i>)
19		4 ^f	13	29 ^h	(+)-(1 <i>R</i> ,2 <i>R</i>)
20		6	—	—	—

^a Epoxidation conditions: iminium salt (10 mol %), TPPP (2 equiv), CH₂Cl₂, 4 h.

^b Catalyst configuration (4*S*,5*S*) unless otherwise stated.

^c Conversions were evaluated from the ¹H NMR spectra by integration of alkene and epoxide signals.

^d Enantiomeric excesses were determined by ¹H NMR spectroscopy in the presence of (+)-Eu(hfc)₃ (0.1 mol equiv).

^e The absolute configurations of the major enantiomers were determined by comparison of optical rotation with literature values.

^f Catalyst configuration (4*R*,5*R*).

^g Reaction carried out at –40 °C.

^h Reaction time 8 h.

a change in the configuration of the enantiomer of epoxide formed preferentially, to the (+)-(1*R*,2*R*) isomer, is observed in every case.

The thiomethyl catalyst 3 also gives the (+)-(1*R*,2*R*) enantiomer of 1-phenylcyclohexene preferentially, but only between temperatures of 0 °C and –50 °C (Table 1, entries 3, 8, 12); at –78 °C the (–)-(1*S*,2*S*) enantiomer is preferentially formed (Table 1, entry 18). We reason that this is due to rapid oxidation of the sulfide to the sulfone at temperatures above –78 °C, generating catalyst 6 in situ. Catalyst 4, which contains an electron-donating methoxy substituent, and has the opposite absolute stereochemistry to catalysts 1, 2, 3 and 6, produces the (+)-(1*R*,2*R*) epoxide enantiomer preferentially, regardless of temperature. Catalyst 4 thus exhibits the same facial selectivity as unsubstituted catalyst 1 (and catalyst 3 at low temperatures).

In the case of catalyst 3, to prove that the active catalyst at temperatures above –78 °C was indeed the corresponding sulfone 6, a standard epoxidation reaction was performed in deuterated dichloromethane solution and the reaction mixture was subjected to ¹H NMR spectroscopic analysis. The chemical shift for the methyl group attached to sulfur had shifted from δ 2.42 to 3.03, confirming that the sulfide had been oxidised to the sulfone, by comparison with authentic catalyst 6. The sulfoxide intermediate was not observed.

In order to determine the effects of solvent on the reaction, several other solvents were screened using our three most enantioselective catalysts 1, 4 and 6 (Table 2). TPPP was found to be insoluble in carbon tetrachloride, ethyl acetate and dimethoxyethane. In dimethylformamide, the TPPP dissolved but no reaction occurred. TPPP is also soluble in dichloroethane, however, and epoxidation reactions of

Table 2. Asymmetric epoxidation of 1-phenylcyclohexene using various solvents^a

Solvent	Catalyst ^b	Time/h	Conversion/% ^c	ee/% ^d	Configuration ^e
CH ₃ CN	1	1.0	42	43 ^f	(–)-(1 <i>S</i> ,2 <i>S</i>)
	4 ^g	0.2	30	44	(+)-(1 <i>R</i> ,2 <i>R</i>)
	6	2.5	89	45	(–)-(1 <i>S</i> ,2 <i>S</i>)
CH ₂ Cl ₂	1	4	70	37 ^f	(–)-(1 <i>S</i> ,2 <i>S</i>)
	4 ^g	4	76	25	(+)-(1 <i>R</i> ,2 <i>R</i>)
	6	4	100	36	(+)-(1 <i>R</i> ,2 <i>R</i>)
C ₂ H ₄ Cl ₂	1	24	29	24	(–)-(1 <i>S</i> ,2 <i>S</i>)
	4 ^g	24	87	17	(+)-(1 <i>R</i> ,2 <i>R</i>)
	6	4	97	32	(+)-(1 <i>R</i> ,2 <i>R</i>)
CHCl ₃	1	24	52	33	(–)-(1 <i>S</i> ,2 <i>S</i>)
	4 ^g	24	73	11	(+)-(1 <i>R</i> ,2 <i>R</i>)
	6	12	100	48	(+)-(1 <i>R</i> ,2 <i>R</i>)

^a Epoxidation conditions: iminium salt (10 mol %), TPPP (2 equiv), solvent, –30 °C.⁹ Catalyst configuration (4*S*,5*S*).

^b Catalyst configuration (4*S*,5*S*) unless otherwise stated.

^c Conversions were evaluated from the ¹H NMR spectra by integration of alkene and epoxide signals.

^d Enantiomeric excesses were determined by ¹H NMR spectroscopy in the presence of (+)-Eu(hfc)₃ (0.1 mol equiv).

^e The absolute configurations of the major enantiomers were determined by comparison of optical rotation with literature values.

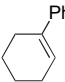
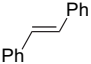
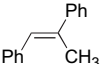
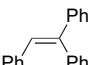
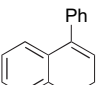
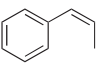
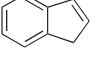
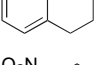
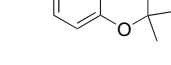
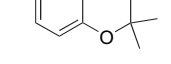
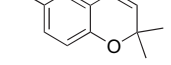
^f Reaction carried out at –40 °C.

^g Catalyst configuration (4*R*,5*R*).

1-phenylcyclohexene performed in this solvent gave almost identical results to those obtained with dichloromethane for catalysts **6** and **4**. Curiously, catalyst **1** was far less reactive in this medium and gave a reduced ee (24% compared to 37%). When the reactions were repeated in chloroform, we observed a dramatic decrease in ee for catalyst **4**, while catalyst **1** gave similar results to those obtained in dichloromethane (33% ee). Catalyst **6** in chloroform, however, gave the best ee for 1-phenylcyclohexene (48% ee) that we have observed with this series of iminium salt catalysts. Interestingly, in acetonitrile at $-30\text{ }^{\circ}\text{C}$ we observed a similar degree of enantioselectivity to that seen in the reaction carried out in chloroform (48% ee, (+)-(1*R*,2*R*) enantiomer), but producing the opposite (–)-(1*S*,2*S*)-enantiomer of phenylcyclohexene oxide in 45% ee. The origins of these solvent effects upon enantioselectivity remain unclear.

Using our most enantioselective catalyst **6**, we next carried out asymmetric epoxidations of several other unfunctionalised alkenes in acetonitrile and in chloroform solution at a standard temperature of $-40\text{ }^{\circ}\text{C}$, using 10 mol % catalyst (Table 3). Remarkably, changing the reaction solvent was found to switch the major enantiomer of epoxide generated from all *trans*- and tri-substituted alkenes tested. Further, *trans*-stilbene, usually a poor substrate with our catalysts (less than 5% ee was observed under our original aqueous conditions using the same catalyst and oxone), afforded the (+)-(*R,R*) enantiomer of *trans*-stilbene oxide in 67% ee when the reaction was carried out in chloroform solution, but the (–)-(*S,S*) isomer, in 30% ee, when performed in acetonitrile. With the exception of α -methylstilbene, it is clear from Table 3 that chloroform is the solvent of choice for catalyst **6** and the enantiomeric excesses are far better

Table 3. Catalytic asymmetric epoxidation of various alkenes using TPPP and catalyst **6**^a

Solvent	Oxone/CH ₃ CN/H ₂ O			CH ₃ CN			CHCl ₃		
	Yield (%) ^b	ee (%) ^c	Configuration ^d	Yield (%) ^b	ee (%) ^c	Configuration ^d	Yield (%) ^b	ee (%) ^c	Configuration ^d
	100 ^e	39	(–)-(1 <i>S</i> ,2 <i>S</i>)	73	45	(–)-(1 <i>S</i> ,2 <i>S</i>)	77	48	(+)-(1 <i>R</i> ,2 <i>R</i>)
	100 ^e	<5	(–)-(<i>S,S</i>)	13 ^e	30	(–)-(<i>S,S</i>)	31	67	(+)-(<i>R,R</i>)
	100 ^e	32	(–)-(1 <i>S</i> ,2 <i>R</i>)	42	48	(–)-(1 <i>S</i> ,2 <i>R</i>)	35	2	(+)-(1 <i>R</i> ,2 <i>S</i>)
	100 ^e	50	(+)-(<i>S</i>)	25	27	(+)-(<i>S</i>)	11 ^e	63	(–)-(<i>R</i>)
	100 ^e	47	(–)-(1 <i>S</i> ,2 <i>R</i>)	56	38	(–)-(1 <i>S</i> ,2 <i>R</i>)	98	59	(+)-(1 <i>R</i> ,2 <i>S</i>)
	—	—	—	71	53	(+)-(1 <i>S</i> ,2 <i>R</i>)	85	70	(+)-(1 <i>S</i> ,2 <i>R</i>)
	—	—	—	—	—	—	83	61	(+)-(1 <i>S</i> ,2 <i>R</i>)
	61	45	(–)-(1 <i>S</i> ,2 <i>R</i>)	80	56	(–)-(1 <i>S</i> ,2 <i>R</i>)	89	82	(–)-(1 <i>S</i> ,2 <i>R</i>)
	—	—	—	—	—	—	52	88	(–)-(1 <i>S</i> ,2 <i>S</i>)
	—	—	—	—	—	—	76	93	(–)-(1 <i>S</i> ,2 <i>S</i>)
	—	—	—	63	80	(–)-(1 <i>S</i> ,2 <i>S</i>)	59	97	(–)-(1 <i>S</i> ,2 <i>S</i>)

^a Epoxidation conditions: iminium salt **6** (10 mol %), TPPP (2 equiv), $-40\text{ }^{\circ}\text{C}$, 24 h.

^b Isolated yields unless otherwise stated.

^c Enantiomeric excesses were determined by ¹H NMR spectroscopy in the presence of (+)-Eu(hfc)₃ (0.1 mol equiv) or by chiral HPLC using a Chiralcel OD column.

^d The absolute configurations of the major enantiomers were determined by comparison of optical rotation with literature values.

^e Conversions, evaluated from the ¹H NMR spectra by integration of alkene and epoxide signals.

than those observed when employing TPPP in acetonitrile as well as in the original aqueous conditions using oxone.

Good enantiomeric excesses were also observed for *cis*- α -methyl styrene (70% ee) and dihydronaphthalene (82% ee). The level of enantioselectivity observed here is remarkable given that the corresponding reaction carried out under our standard aqueous conditions with oxone afforded dihydronaphthalene oxide in only 45% ee. The enantiomeric excess for the epoxidation of indene is somewhat lower (61% ee), but is still much higher than other reported ees for this epoxidation when mediated by oxaziridinium salts.⁴ Epoxidation of the non-aryl *cis*-hept-2-ene produced epoxide with quantitative conversion but with low ee. Electron-deficient alkenes are also poor substrates.

Finally, we turned our attention to the epoxidation of benzopyran substrates. We were delighted to observe excellent enantioselectivities in the epoxidations of 6-nitro-, 6-chloro- and 6-cyano-2,2-dimethylbenzopyrans, with ees up to an unprecedented 97%.⁵ It is interesting to note here that, in these cases, whichever solvent was employed, the same enantiomer of epoxide was observed.

2. Conclusions

A range of iminium salt asymmetric epoxidation catalysts has been tested under non-aqueous conditions at various temperatures in a number of solvents; from these we have identified catalyst **6** as one of the most enantioselective. The reaction solvent has a profound effect on the epoxidation of *trans*- and tri-substituted alkenes and in many cases we are able to produce either enantiomer as the major product by choice of acetonitrile or chloroform as solvent. In terms of enantiomeric excesses, the optimum reaction temperature appears to be $-40\text{ }^{\circ}\text{C}$ and chloroform the solvent of choice. These conditions have provided enantiomeric excesses of up to 97%, in the epoxidation of 6-cyano-2,2-dimethylbenzopyran.

3. Experimental

3.1. General

All infrared spectra were obtained using a Perkin–Elmer Paragon 1000 FTIR spectrophotometer; thin film spectra were acquired using sodium chloride plates. All ^1H and ^{13}C NMR spectra were measured at 250.13 and 62.86 MHz with a Bruker AC 250 MHz spectrometer or at 400.13 and 100.62 MHz with a Bruker DPX 400 MHz spectrometer, in deuteriochloroform solution unless otherwise stated, using TMS (tetramethylsilane) as the internal reference. Mass spectra were recorded using a Jeol-SX102 instrument utilising electron-impact (EI), fast atom bombardment (FAB) and by the EPSRC national mass spectrometry service at the University of Wales, Swansea, utilising electrospray (ES). Analysis by GC–MS utilised a Fisons GC 8000 series (AS 800), using a 15 m \times 0.25 mm DB-5 column and an electron-impact low resolution mass spectrometer. Melting points were recorded using an Electrothermal-IA 9100 melting point instrument and are uncorrected. Optical rotation values were measured with an Optical

Activity-polAAar 2001 instrument, operating at $\lambda=589\text{ nm}$, corresponding to the sodium D line, at the temperatures indicated. Microanalyses were performed on a Perkin–Elmer Elemental Analyser 2400 CHN. All chromatographic manipulations used silica gel as the adsorbent. Reactions were monitored using thin layer chromatography (TLC) on aluminium-backed plates coated with Merck Kieselgel 60 F₂₅₄ silica gel. TLC plates were visualised by UV radiation at a wavelength of 254 nm, or stained by exposure to an ethanolic solution of phosphomolybdic acid (acidified with concentrated sulfuric acid), followed by charring where appropriate. Reactions requiring anhydrous conditions were carried out using glassware dried overnight at $150\text{ }^{\circ}\text{C}$, under a nitrogen atmosphere unless otherwise stated. Reaction solvents were used as obtained commercially unless otherwise stated. Light petroleum (bp $40\text{--}60\text{ }^{\circ}\text{C}$) was distilled from calcium chloride prior to use. Ethyl acetate was distilled over calcium sulfate or chloride. Dichloromethane was distilled over calcium hydride. Tetrahydrofuran was distilled under a nitrogen atmosphere from the sodium/benzophenone ketyl radical or from lithium aluminium hydride. Enantiomeric excesses were determined either by proton nuclear magnetic resonance spectroscopy in the presence of europium (III) tris[3-(hepta-fluoropropyl)-hydroxymethylene-(+)-camphorate] as the chiral shift reagent, or by chiral HPLC using a Chiracel OD column on a TSP Thermo-Separating-Products Spectra Series P200 instrument, with a TSP Spectra Series UV100 ultraviolet absorption detector set at 254 nm and a Chromojet integrator.

3.2. General procedure for the preparation of dihydroisoquinolinium salts from 2-(2-bromoethyl)-benzaldehyde and primary amines

2-(2-Bromoethyl)benzaldehyde (1.60 equiv, 1.10 if freshly distilled) was cooled using an ice bath and a solution of the amine in ethanol (10 ml per g of amine) was added dropwise. After the addition was complete, the ice bath was removed and the reaction mixture was stoppered to retain HBr and stirred overnight. A solution of sodium tetraphenylborate or other anion-exchanging salt (1.10 equiv) in the minimum amount of acetonitrile was added in one portion to the reaction mixture. After stirring for 5 min, the organic solvents were removed under reduced pressure. Ethanol was added to the residue, followed by water. The resulting precipitate was collected by filtration and washed with additional ethanol followed by diethyl ether. If no solid was materialised after the addition of the water, the mixture was allowed to settle and the ethanol/water phase was decanted. The gummy residue was triturated in hot ethanol or methanol, inducing precipitation of the organic salt immediately or upon slow cooling of the hot alcoholic solution. Small quantities of acetonitrile may be added during this process to aid solubility.

3.2.1. (+)-*N*-((4*S*,5*S*)-2,2-Dimethyl-4-phenyl-1,3-dioxan-5-yl)-3,4-dihydroisoquinolinium tetraphenylborate (**1**).⁴

Prepared according to the general procedure from (4*S*,5*S*)-5-amino-2,2-dimethyl-4-phenyl-1,3-dioxane (3.00 g, 14.4 mmol) and purified by recrystallisation from acetone/diethyl ether to give **1** as a yellow solid (6.93 g, 75%), mp $169\text{--}170\text{ }^{\circ}\text{C}$; $[\alpha]_{\text{D}}^{20} +38.6$ (*c* 2.70, CH_3CN); ν_{max} (Nujol)/ cm^{-1} 1637, 1603, 1571, 1480, 1266, 1202, 1166, 1108, 1073; δ_{H}

(250 MHz, CD₃CN), 1.65 (3H, s), 1.94 (3H, s), 2.39–2.48 (1H, m), 2.70–2.82 (1H, m), 3.25–3.40 (1H, m), 3.81–3.97 (1H, m), 4.00–4.10 (1H, m), 4.30 (1H, d, *J* 13.7 Hz), 4.58 (1H, dd, *J* 13.7, 3.1 Hz), 5.70 (1H, d, *J* 2.8 Hz), 6.81 (4H, t, *J* 7.2 Hz), 7.35–7.40 (6H, m), 7.46 (1H, t, *J* 7.3 Hz), 7.65–7.74 (2H, m), 8.92 (1H, s); δ_{C} (62.50 MHz, CD₃CN) 17.9, 24.1, 28.7, 51.6, 61.4, 65.5, 70.7, 104.9, 121.9, 124.3, 125.4, 125.7, 128.1, 128.5, 128.6, 128.0, 134.4, 135.8, 137.0, 137.7, 138.7, 163.5, 167.5; *m/z* 322.1809; C₂₁H₂₄NO₂ (cation) requires 322.1807.

3.2.2. (+)-*N*-((4*S*,5*S*)-2,2-Dimethyl-4-(4-nitrophenyl)-1,3-dioxan-5-yl)-3,4-dihydroisoquinolinium tetraphenylborate (2).⁴ Prepared according to the general procedure from (+)-(4*S*,5*S*)-5-amino-2,2-dimethyl-4-(4-nitrophenyl)-1,3-dioxane (0.19 g, 0.8 mmol) and purified by recrystallisation from CH₂Cl₂/hexane to give **2** as yellow plates (0.36 g, 74%); mp 176–178 °C (dec); [α]_D²⁰ +107.7 (*c* 1.30, acetone). Found C, 77.73; H, 6.23; N, 4.00. C₄₅H₄₃BN₂O₄ · 0.5H₂O requires C, 77.66; H, 6.38; N, 4.03; ν_{max} (film)/cm⁻¹ 1635, 1604, 1571, 1524, 1478, 1384, 1202, 1163, 1107, 1032; δ_{H} (400 MHz, acetone-*d*₆), 1.72 (3H, s, CH₃), 1.76 (3H, s), 2.70–2.80 (1H, m), 2.88–2.96 (1H, m), 3.65–3.74 (1H, m), 4.19–4.23 (1H, m), 4.54 (1H, d, *J* 13.6 Hz), 4.61–4.70 (1H, m), 4.82 (1H, dd, *J* 13.6, 2.8 Hz), 6.11 (1H, d, *J* 2.4 Hz), 6.80 (4H, t, *J* 6.8 Hz), 6.94 (8H, t, *J* 7.2 Hz), 7.36 (8H, m), 7.51 (1H, t, *J* 7.6 Hz), 7.59–7.88 (3H, m), 7.85 (2H, d, *J* 8.4 Hz), 7.95 (2H, d, *J* 8.8 Hz), 9.28 (1H, s); δ_{C} (100 MHz, acetone-*d*₆), 19.2, 25.9, 30.0, 52.8, 63.4, 66.4, 71.9, 102.2, 122.7, 125.3, 125.8, 126.4, 128.3, 129.7, 129.8, 135.9, 137.4, 138.4, 140.1, 145.0, 149.0, 165.0, 169.5; *m/z* 367.1658; C₂₁H₂₃N₂O₄ (cation) requires 367.1658.

3.2.3. (+)-*N*-((4*S*,5*S*)-2,2-Dimethyl-4-(4-(methylthio)phenyl)-1,3-dioxan-5-yl)-3,4-dihydroisoquinolinium tetraphenylborate (3).⁴ Prepared according to the general procedure from (4*S*,5*S*)-5-amino-2,2-dimethyl-4-(4-(methylthio)phenyl)-1,3-dioxane (0.50 g, 2.0 mmol) and purified by recrystallisation from CH₂Cl₂/hexane to give **3** as yellow plates (1.00 g, 73%); mp 146–148 °C (dec); [α]_D²⁰ +115.9 (*c* 1.41, acetone). Found C, 79.05; H, 6.59; N, 1.93. C₄₆H₄₆BNO₂S · 0.5H₂O requires C, 79.27; H, 6.66; N, 2.01; ν_{max} (film)/cm⁻¹ 3053, 2996, 2360, 2341, 1634, 1603, 1571, 1478, 1265, 1201, 1162, 1108, 1075; δ_{H} (250 MHz, acetone-*d*₆) 1.66 (3H, s), 1.72 (3H, s), 2.42 (3H, s), 2.66–2.84 (1H, m), 2.90–3.03 (1H, m), 3.62–3.74 (1H, m), 4.13–4.26 (1H, m), 4.50–4.55 (2H, m), 4.78 (1H, dd, *J* 13.8, 3.1 Hz), 5.91 (1H, d, *J* 2.6 Hz), 6.78 (4H, t, *J* 7.2 Hz), 6.92 (8H, t, *J* 7.40 Hz), 7.34 (8H, m), 7.40–7.56 (6H, m), 7.76–7.87 (2H, m), 9.30 (1H, s); δ_{C} (100 MHz, acetone-*d*₆) 15.4, 18.8, 25.4, 30.0, 52.3, 62.7, 66.5, 71.5, 101.4, 122.3, 125.3, 126.1, 126.9, 127.4, 129.2, 129.3, 133.9, 135.2, 137.0, 137.8, 139.5, 140.5, 165.0, 168.5; *m/z* 368.1682; C₂₂H₂₆NO₂S (cation) requires 368.1684.

3.2.4. (–)-*N*-((4*R*,5*R*)-2,2-Dimethyl-4-(4-methoxyphenyl)-1,3-dioxan-5-yl)-3,4-dihydroisoquinolinium tetraphenylborate (4).⁴ Prepared according to the general procedure from (–)-(4*R*,5*R*)-5-amino-2,2-dimethyl-4-(4-methoxyphenyl)-1,3-dioxane (0.40 g, 1.7 mmol) and purified by recrystallisation from CH₂Cl₂/hexane to give **4** as yellow plates (0.83 g, 74%); mp 171–173 °C (dec); [α]_D²⁰ –108.6 (*c* 1.40, acetone). Found C, 77.70; H, 6.50; N,

1.88. C₄₆H₄₆BNO₃ · 0.5Et₂O requires C, 77.92; H, 6.54; N, 1.98; ν_{max} (film)/cm⁻¹ 1639, 1604, 1573, 1514, 1382, 1254, 1202, 1107, 1031; δ_{H} (400 MHz, CDCl₃) 1.51 (3H, s), 1.52 (3H, s), 2.20–2.25 (1H, m), 2.31–2.35 (1H, m), 2.85–2.90 (1H, m), 3.00–3.10 (1H, m), 2.96–3.07 (1H, m), 3.56 (1H, d, *J* 14.4 Hz), 3.72 (3H, s), 3.90 (1H, dd, *J* 14.0, 2.8 Hz), 5.11 (1H, d, *J* 2.4 Hz), 6.79 (2H, d, *J* 2.0 Hz), 6.87 (4H, t, *J* 7.2 Hz), 7.02 (8H, t, *J* 7.6 Hz), 7.23–7.24 (2H, m) 7.24–7.31 (1H, m), 7.41–7.57 (8H, m), 7.60–7.69 (1H, m), 8.25 (1H, s); δ_{C} (100 MHz, CDCl₃) 18.4, 24.6, 29.4, 50.5, 55.4, 61.9, 64.9, 70.5, 100.4, 114.4, 122.2, 123.7, 125.9, 127.3, 127.9, 128.7, 129.5, 134.0, 134.7, 136.2, 138.8, 159.8, 163.8, 169.5; *m/z* 352.1915; C₂₂H₂₆NO₃ (cation) requires 352.1913.

3.2.5. (+)-*N*-((4*S*,5*S*)-2,2-Dimethyl-4-(4-(methylsulfonyl)phenyl)-1,3-dioxan-5-yl)-3,4-dihydroisoquinolinium tetraphenylborate (6).⁵ Prepared according to the general procedure from (4*S*,5*S*)-5-amino-2,2-dimethyl-4-(4-(methylsulfonyl)phenyl)-1,3-dioxane (0.75 g, 2.96 mmol) and purified by recrystallisation from CH₂Cl₂/hexane to give **6** as yellow plates (1.55 g, 73%); mp 199–201 °C (dec); [α]_D²⁰ +126.7 (*c* 1.20, acetone). Found C, 75.62; H, 6.32; N, 1.84. C₄₆H₄₆BNO₄S · 0.5H₂O requires C, 75.79; H, 6.50; N, 1.92; ν_{max} (film)/cm⁻¹ 1636, 1603, 1572, 1478, 1383, 1314, 1266, 1202, 1150, 1076, 1032, 956; δ_{H} (400 MHz, acetone-*d*₆), 1.69 (3H, s), 1.72 (3H, s), 2.60–2.69 (1H, m), 2.85–2.96 (1H, m), 3.00 (3H, s), 3.65–3.72 (1H, m), 4.12–4.20 (1H, m), 4.49 (1H, d, *J* 13.6 Hz), 4.50–4.64 (1H, m), 4.77 (1H, dd, *J* 13.6, 2.8 Hz), 6.05 (1H, d, *J* 2.8 Hz), 6.80 (4H, t, *J* 7.2 Hz), 6.92 (8H, t, *J* 7.2 Hz), 7.31–7.44 (8H, m), 7.49 (1H, t, *J* 7.6 Hz), 7.73–7.83 (3H, m), 7.82 (2H, d, *J* 8.2 Hz), 7.95 (2, d, *J* 8.2 Hz), 9.28 (1H, s); δ_{C} (100 MHz, acetone-*d*₆), 18.8, 25.4, 29.5, 44.3, 52.3, 62.9, 66.1, 71.5, 101.7, 122.3, 125.3, 126.1, 127.6, 128.8, 129.3, 129.4, 135.4, 137.0, 137.0, 137.9, 142.4, 143.2, 165.0, 168.9; *m/z* 400.1586; C₂₂H₂₆NO₄S (cation) requires 400.1583.

3.2.6. Tetraphenylphosphonium monoperoxysulfate. Oxone™ triple salt (2KHSO₅·KHSO₄·K₂SO₄) (15.0 g, 48.8 mmol with respect to KHSO₅) was dissolved in deionised water (300 ml) and the solution was stirred at 10–15 °C (water bath). A solution of tetraphenylphosphonium chloride (15.0 g, 40.0 mmol) in distilled dichloromethane (300 ml) was added over 5 min and the mixture stirred for an additional 30 min. The organic layer was separated and the solvent was removed under reduced pressure at room temperature. The colourless residue, the crude salt, was transferred to a fritted glass funnel and washed with distilled water (2 × 75 ml). The solid was dissolved in dichloromethane (180 ml) and the solution was dried (MgSO₄). Hexane was added until cloudiness developed and the flask was placed in the freezer (–20 °C) overnight, producing a colourless precipitate of the salt about 85% pure in peroxide (15.4 g, 70%). δ_{H} (250 MHz, CDCl₃) 7.62–7.65 (8H, m), 7.76–7.81 (8H, m), 7.88–7.92 (4H, m), 8.92 (1H, s).

3.3. General procedure for catalytic asymmetric epoxidation of simple alkenes mediated by iminium salts using tetraphenylphosphonium monoperoxysulfate

Tetraphenylphosphonium monoperoxysulfate (2 equiv with respect to the alkene) was dissolved in the desired solvent

(2 ml per 0.1 g oxidant) and the solution cooled to the required temperature. To this was added the iminium salt as a solution in the solvent (0.5 ml per 0.1 g oxidant). This iminium salt solution was cooled to the same temperature as the solution containing the oxidant and added dropwise to it over 15–20 min; the temperature of the reaction vessel was monitored to minimise increase in temperature during the addition. A solution of the alkene in the reaction solvent (0.5 ml per 0.1 g oxidant) was added dropwise. The mixture was stirred at the reaction temperature until the alkene was completely consumed according to TLC. Diethyl ether (pre-cooled to the reaction temperature) (20 ml per 0.1 g oxidant) was added to induce precipitation of the remaining oxidant and the mixture filtered through Celite. The solvents were removed, diethyl ether (40 ml) was added to the residue and the solution was passed through a short pad of silica gel to remove catalyst residues. The solvents were removed to give the epoxide. If the reaction does not reach completion then the epoxide can be separated from the alkene by column chromatography, eluting with ethyl acetate/light petroleum 1:99.

3.4. General procedure for the catalytic asymmetric epoxidation of alkenes mediated by iminium salts using oxone

Oxone (2 equiv with respect to alkene) was added with stirring to an ice-cooled solution of sodium carbonate (4 equiv) in water (12 ml per 1.50 g of sodium carbonate) and the resulting foaming solution was stirred for 5–10 min, until most of the initial effervescence subsided. A solution of the iminium salt (10 mol % with respect to alkene) in acetonitrile (6 ml per 1.50 g of sodium carbonate used) was added, followed by a solution of the alkene in acetonitrile (6 ml per 1.50 g of sodium carbonate used). The suspension was stirred with ice bath cooling until the substrate was completely consumed according to TLC. The reaction mixture was diluted with ice-cooled diethyl ether (20 ml per 100 mg substrate) and the same volume of water was added immediately. The aqueous phase was washed four times with diethyl ether and the combined organic solutions washed with brine and dried (MgSO_4). Filtration and removal of the solvents gave a yellow or light brown residue, which was purified by column chromatography, typically using ethyl acetate/light petroleum (1:99), to provide the pure epoxide.

3.5. General procedure for the formation of racemic epoxides

The alkene was dissolved in CH_2Cl_2 (10 ml/g) and the solution cooled using an ice bath. A solution of *m*-CPBA (2 equiv) in CH_2Cl_2 (10 ml/g, pre-dried over MgSO_4) was added. The reaction was allowed to reach ambient temperature and stirred until complete consumption of the substrate was observed by TLC. Saturated aqueous NaHCO_3 (10 ml/g) was added and the layers were separated. The organic layer was washed with saturated aqueous NaOH (1.0 M, 10 ml/g) and dried (MgSO_4). The solvents were removed under reduced pressure and the residue purified by column chromatography, typically eluting with ethyl acetate/light petroleum (1:99), to give the pure epoxide.

3.5.1. *trans*- α -Methylstilbene oxide.⁹ Colourless oil; $\nu_{\text{max}}(\text{neat})/\text{cm}^{-1}$ 3061, 1602, 1495, 1449, 1381, 1279, 1157,

1118, 1065, 1027, 980; δ_{H} (400 MHz, CDCl_3) 1.46 (3H, s), 3.96 (1H, s), 7.30–7.46 (10H, m); δ_{C} (100 MHz, CDCl_3) 17.1, 63.5, 67.5, 125.6, 126.9, 127.7, 127.9, 128.6, 129.2, 136.4, 142.8.

3.5.2. Triphenylethylene oxide.¹⁰ Colourless oil, which slowly solidified; mp 66–67 °C, (lit. mp 75 °C); $\nu_{\text{max}}(\text{neat})/\text{cm}^{-1}$ 3062, 3030, 2957, 2925, 2856, 1605, 1596, 1499, 1471, 1448, 1262, 1221, 741, 698, 621; δ_{H} (250 MHz, CDCl_3) 4.39–4.41 (1H, m), 7.10–7.47 (15H, m); δ_{C} (62.5 MHz, CDCl_3) 68.0, 68.3, 126.3, 126.8, 127.5, 127.6, 127.7, 127.8, 128.0, 128.2, 128.6, 135.4, 135.9, 141.1.

3.5.3. 1-Phenylcyclohexene oxide.¹¹ Colourless oil; $\nu_{\text{max}}(\text{neat})/\text{cm}^{-1}$ 3084, 1602, 1495, 1446, 1359, 1249, 1173, 1132, 1079, 1030, 993, 974; δ_{H} (250 MHz, CDCl_3) 1.22–1.35 (1H, m), 1.53–1.64 (3H, m), 1.99–2.06 (2H, m), 2.16–2.18 (1H, m), 2.26–2.32 (1H, m), 3.10 (1H, t, *J* 2.0 Hz), 7.28–7.44 (5 H, m); δ_{C} (62.5 MHz, CDCl_3) 19.8, 20.1, 24.7, 28.2, 60.1, 61.8, 125.3, 127.1, 128.2, 142.8.

3.5.4. 1-Phenyl-3,4-dihydronaphthalene oxide.¹¹ Pale yellow solid; mp 104–106 °C, (lit.¹² mp 94–97 °C); $\nu_{\text{max}}(\text{Nujol})/\text{cm}^{-1}$ 1602, 1486, 1307, 1155, 1074, 1042, 953; δ_{H} (250 MHz, CDCl_3) 2.10 (1H, td, *J* 5.8, 13.7 Hz), 2.49–2.60 (1H, m), 2.77 (1H, dd, *J* 5.6, 15.5 Hz), 2.98–3.06 (1H, m), 3.71 (1H, d, *J* 3.1 Hz), 7.11–7.31 (4H, m), 7.45–7.61 (5H, m); δ_{C} (62.5 MHz, CDCl_3) 22.1, 25.4, 60.9, 63.0, 126.0, 127.7, 127.9, 128.1, 128.2, 128.6, 129.8, 135.0, 137.5, 138.8.

3.5.5. *trans*-Stilbene oxide.¹³ Colourless solid; mp 66–67 °C, (lit.¹⁴ mp 61–63 °C); $\nu_{\text{max}}(\text{Nujol})/\text{cm}^{-1}$ 1601, 1492, 1284, 1176, 1157, 1094, 1072, 1025; δ_{H} (400 MHz, CDCl_3) 3.84 (2H, s), 7.28–7.37 (10H, m); δ_{C} (100 MHz, CDCl_3) 63.3, 126.0, 128.6, 129.3, 137.6.

3.5.6. Indene oxide.⁹ Colourless oil; $\nu_{\text{max}}(\text{neat})/\text{cm}^{-1}$ 3027, 2917, 1482, 1464, 1390, 1372, 1232, 1183, 1142, 829, 758, 745, 723; δ_{H} (250 MHz, CDCl_3) 2.97 (1H, dd, *J* 2.7, 18.1 Hz), 3.21 (1H, d, *J* 17.6 Hz), 4.13 (1H, t, *J* 3.0 Hz), 4.26 (1H, dd, *J* 1.1, 2.8 Hz), 7.14–7.29 (3H, m), 7.49 (1H, dd, *J* 1.7, 6.6 Hz); δ_{C} (100 MHz, CDCl_3) 34.6, 57.6, 59.1, 125.2, 126.1, 126.3, 128.6, 141.0, 143.6.

3.5.7. 1,2-Dihydronaphthylene oxide.¹³ Colourless oil; $\nu_{\text{max}}(\text{neat})/\text{cm}^{-1}$ 3059, 3028, 2930, 2850, 1602, 1493, 1316, 1129, 1088, 1030, 964; δ_{H} (400 MHz, CDCl_3) 1.60–1.70 (1H, m), 2.31–2.39 (1H, m), 2.45 (1H, dd, *J* 15.6, 5.6 Hz), 2.65–2.70 (1H, m), 3.65 (1H, t, *J* 4.0 Hz), 3.78 (1H, d, *J* 4.4 Hz), 7.01 (1H, d, *J* 7.2 Hz), 7.14–7.23 (2H, m), 7.33 (1H, d, *J* 7.2 Hz); δ_{C} (100 MHz, CDCl_3) 22.2, 24.8, 55.2, 55.5, 126.5, 128.8, 128.8, 129.9, 132.9, 137.1.

3.5.8. *cis*- β -Methylstyrene oxide.¹³ Colourless oil; $\nu_{\text{max}}(\text{neat})/\text{cm}^{-1}$ 3061, 2994, 1604, 1496, 1450, 1258, 1149, 953, 853, 742, 700, 619; δ_{H} (250 MHz, CDCl_3) 1.12, (3H, d, *J* 5.4 Hz), 3.32–3.40 (1H, m), 4.08 (1H, d, *J* 4.3 Hz), 7.24–7.39 (5H, m); δ_{C} (62.5 MHz, CDCl_3) 12.8, 55.4, 57.8, 126.9, 127.7, 128.3, 135.8.

3.5.9. *cis*-2,3-Epoxyheptene.¹⁵ Colourless oil, 68% yield; $\nu_{\text{max}}(\text{neat})/\text{cm}^{-1}$ 2959, 2930, 2874, 1390, 1259, 1218,

1151, 1114, 1032, 752; δ_{H} (400 MHz, CDCl_3) 0.93 (3H, t, J 8.0 Hz), 1.20 (3H, d, J 4.0 Hz), 1.32–1.50 (6H, m), 2.86–2.91 (1H, m), 2.99–3.06 (1H, m); δ_{C} (100 MHz, CDCl_3) 12.2, 13.0, 21.6, 26.2, 27.6, 51.6, 56.1.

3.5.10. 6-Cyanobenzopyran oxide.¹⁶ Colourless oil, which solidified; ν_{max} (film)/ cm^{-1} 3089, 3038, 2979, 2934, 2226, 1615, 1579, 1490, 1346, 1279, 1157, 1107, 1046, 955; δ_{H} (400 MHz, CDCl_3) 1.22 (3H, s), 1.52 (3H, s), 3.47 (1H, d, J 4.4 Hz), 3.86 (1H, d, J 4.4 Hz), 6.79 (1H, d, J 8.4 Hz), 7.45 (1H, dd, J 2.0, 8.4 Hz), 7.58 (1H, d, J 2.4 Hz); δ_{C} (100 MHz, CDCl_3) 23.4, 25.9, 50.3, 62.7, 75.1, 104.7, 119.0, 119.2, 121.5, 134.2, 134.8, 156.87.

3.5.11. 6-Nitrobenzopyran oxide.¹⁶ Colourless oil, which solidified; ν_{max} (film)/ cm^{-1} 3075, 2926, 2850, 1621, 1590, 1518, 1344, 1281, 1209, 1160, 1088, 955; δ_{H} (400 MHz, CDCl_3) 1.33 (3H, s), 1.63 (3H, s), 3.57 (1H, dd, J 4.4 Hz), 4.00 (1H, d, J 4.4 Hz), 6.89 (1H, d, J 9.0 Hz), 8.15 (1H, dd, J 2.8, 9.0 Hz), 8.30 (1H, d, J 2.8 Hz); δ_{C} (100 MHz, CDCl_3) 23.1, 25.5, 50.0, 62.1, 75.2, 118.5, 120.3, 125.8, 126.3, 141.5, 158.3.

3.5.12. 6-Chlorobenzopyran oxide.¹⁶ Colourless oil: ν_{max} (film)/ cm^{-1} 3080, 2985, 2933, 1611, 1579, 1478, 1366, 1339, 1268, 1237, 1202, 1168, 1103, 1087, 1036, 954; δ_{H} (400 MHz, CDCl_3) 1.17 (3H, s), 1.50 (3H, s), 3.41 (1H, dd, J 4.4 Hz), 3.77 (1H, d, J 4.4 Hz), 6.67 (1H, d, J 8.6 Hz), 7.11 (1H, dd, J 2.6, 8.6 Hz), 7.24 (1H, d, J 2.6 Hz); δ_{C} (100 MHz, CDCl_3) 22.5, 25.6, 50.4, 62.6, 73.4, 119.4, 121.6, 125.7, 129.2, 130.2, 151.2.

Acknowledgements

This investigation has enjoyed the support of the EPSRC and NPIL Pharmaceuticals (UK) Ltd. We are also indebted to the EPSRC Mass Spectrometry Unit, Swansea.

References and notes

- Picot, A.; Millet, P.; Lusinchi, X. *Tetrahedron Lett.* **1976**, *17*, 1573; Hanquet, G.; Lusinchi, X.; Milliet, P. *Tetrahedron Lett.* **1987**, *28*, 6061; Hanquet, G.; Lusinchi, X.; Milliet, P. *Tetrahedron Lett.* **1988**, *29*, 3941.
- Bohé, L.; Hanquet, G.; Lusinchi, M.; Lusinchi, X. *Tetrahedron Lett.* **1993**, *34*, 7271; Bohé, L.; Lusinchi, M.; Lusinchi, X. *Tetrahedron* **1999**, *55*, 141; Bohé, L.; Kammoun, M. *Tetrahedron Lett.* **2002**, *43*, 803; Bohé, L.; Kammoun, M. *Tetrahedron Lett.* **2004**, *45*, 747; Gluszynska, A.; Mackowska, I.; Rozwadowska, M. D.; Sienniak, W. *Tetrahedron: Asymmetry* **2004**, *15*, 2499; Aggarwal, V. K.; Wang, M. F. *J. Chem. Soc., Chem. Commun.* **1996**, 191; Armstrong, A.; Ahmed, G.; Garnett, I.; Gioaccolou, K. *Synlett* **1997**, 1075; Armstrong, A.; Ahmed, G.; Garnett, I.; Gioaccolou, K.; Wailes, J. S. *Tetrahedron* **1999**, *55*, 2341; Minakata, S.; Takemiya, A.; Nakamura, K.; Ryu, I.; Komatsu, M. *Synlett* **2000**, 1810; Wong, M.-K.; Ho, L.-M.; Zheng, Y.-S.; Ho, C.-Y.; Yang, D. *Org. Lett.* **2001**, *16*, 2587; Lacour, J.; Monchaud, D.; Marsol, C. *Tetrahedron Lett.* **2002**, *43*, 8257; Vachon, J.; Pérollier, C.; Monchaud, D.; Marsol, C.; Ditrach, K.; Lacour, J. *J. Org. Chem.* **2005**, *70*, 5903.
- Page, P. C. B.; Rassias, G. A.; Bethell, D.; Schilling, M. B. *J. Chem. Soc., Perkin Trans. 1* **2000**, 3325.
- Page, P. C. B.; Rassias, G. A.; Barros, D.; Ardakani, A.; Buckley, B.; Bethell, D.; Smith, T. A. D.; Slawin, A. M. Z. *J. Org. Chem.* **2001**, *66*, 6926; Page, P. C. B.; Rassias, G. A.; Barros, D.; Ardakani, A.; Bethell, D.; Merrifield, E. *Synlett* **2002**, 580; Page, P. C. B.; Buckley, B. R.; Rassias, G. A.; Blacker, A. J. *Eur. J. Org. Chem.* **2006**, 803.
- Page, P. C. B.; Buckley, B. R.; Heaney, H.; Blacker, A. J. *Org. Lett.* **2005**, *7*, 375.
- Page, P. C. B.; Buckley, B. R.; Blacker, A. J. *Org. Lett.* **2004**, *6*, 1543.
- Page, P. C. B.; Barros, D.; Buckley, B. R.; Ardakani, A.; Marples, B. A. *J. Org. Chem.* **2004**, *69*, 3595.
- Campestrini, S.; Di Furia, G.; Labat, G.; Novello, F. *J. Chem. Soc., Perkin Trans. 1* **1994**, 2175.
- Sasaki, H.; Irie, R.; Hamada, T.; Suzuki, K.; Katsuki, T. *Tetrahedron* **1994**, *50*, 11827; Boyd, D. R.; Sharma, N. D.; Bowers, N. I.; Goodrich, P. A.; Groocok, R. M. *Tetrahedron: Asymmetry* **1996**, *7*, 1559; Sola, L.; Vidal-Ferran, A.; Moyano, A.; Pericas, M. A.; Riera, A. *Tetrahedron: Asymmetry* **1997**, *8*, 1559.
- Fleiser, R.; Galle, D.; Braun, M. *Liebigs Annalen* **1997**, *6*, 1189.
- Tu, Y.; Wang, Z.-X.; Shi, Y. *J. Am. Chem. Soc.* **1996**, *118*, 9806; Brandes, B. D.; Jacobsen, E. N. *J. Org. Chem.* **1994**, *59*, 4378; Belluci, G. *J. Chem. Soc., Perkin Trans. 2* **1973**, 292.
- Padwa, A.; Owens, D. *J. Org. Chem.* **1977**, *42*, 3076.
- Tian, H.; She, X.; Yu, H.; Shu, L.; Shi, Y. *J. Org. Chem.* **2002**, *67*, 2435.
- Solladié-Cavallo, A.; Diep-Vohuule, A.; Sunjic, V.; Vinkovic, V. *Tetrahedron: Asymmetry* **1996**, *7*, 1783; Chang, H.-T.; Sharpless, K. B. *J. Org. Chem.* **1996**, *61*, 6456.
- Kurth, M. J.; Abreo, M. A. *Tetrahedron* **1990**, *46*, 5085; Krief, A.; Heresi, L.; Nagy, J. B.; Derouane, E. G. *Angew. Chem.* **1977**, *89*, 103; Chiappe, C.; Cordoni, A.; Lo Moro, G.; Palese, C. D. *Tetrahedron: Asymmetry* **1998**, *9*, 341.
- Evans, J. M.; Fake, C. S.; Hamilton, T. C.; Poyser, R. H.; Watts, E. A. *J. Med. Chem.* **1983**, *26*, 1582; Bergmann, R.; Eiermann, V.; Gericke, R. *J. Med. Chem.* **1990**, *33*, 2759; Lee, N. H.; Muci, A. R.; Jacobsen, E. N. *Tetrahedron Lett.* **1991**, *32*, 5055.

Bicyclo[3.2.1]octanone catalysts for asymmetric alkene epoxidation: the effect of disubstitution

Alan Armstrong,^{*} Belen Dominguez-Fernandez and Tomoki Tsuchiya

Department of Chemistry, Imperial College London, South Kensington, London SW7 2AZ, UK

Received 5 November 2005; revised 5 December 2005; accepted 7 December 2005

Available online 22 May 2006

Abstract—A series of 2-fluoro-8-oxabicyclo[3.2.1]octan-3-ones are prepared and tested as catalysts for alkene epoxidation with Oxone[®]. These catalysts provide *trans*-stilbene oxide with up to 83% ee, but the highest ee value is obtained with the monofluorinated ketone **2**: both 2,2- and 2,4-disubstituted catalysts afford epoxide of lower ee.

© 2006 Elsevier Ltd. All rights reserved.

1. Introduction

Catalytic asymmetric epoxidation of alkenes is an exceptionally valuable synthetic transformation.¹ The development of efficient methods for asymmetric epoxidation of simple, ‘unfunctionalised’ alkenes is a particular challenge, and some of the most spectacular progress in recent years has come from the use of small organic molecules to promote oxygen transfer by Oxone[®].² While iminium salts are starting to provide promising levels of enantioselectivity,³ chiral dioxiranes derived from chiral ketones have already given excellent results for *trans*- and trisubstituted alkenes.^{4–7} An especially noteworthy feature of these dioxirane systems is that they have allowed greatly improved understanding of the mechanisms of asymmetric induction through synthetic and computational studies.⁸ A further understanding of dioxirane–substrate interactions is especially important for further progress with the challenging terminal alkene class: despite highly encouraging results with styrenes,⁹ these substrates generally still do not reach practical levels of enantioselectivity. In our own contributions to the chiral dioxirane area, we have reported that the bicyclo[3.2.1]octanone system provides a conformationally well-defined framework, which is relatively resistant to Baeyer–Villiger decomposition. The prototype fluoroketone **1** afforded *E*-stilbene oxide with 76% ee at 10 mol % catalyst loading, and, due to its stability, could be recycled.^{10,11} This feature allowed preparation of a silica-supported variant.¹² In exploring the effects of structural modifications, we discovered the more enantioselective oxabicyclic ester **3**.^{13,14} For both catalysts, the major observed enantiomer in the epoxidation of *E*-alkenes fits a spiro-TS (cf. Fig. 1) in which

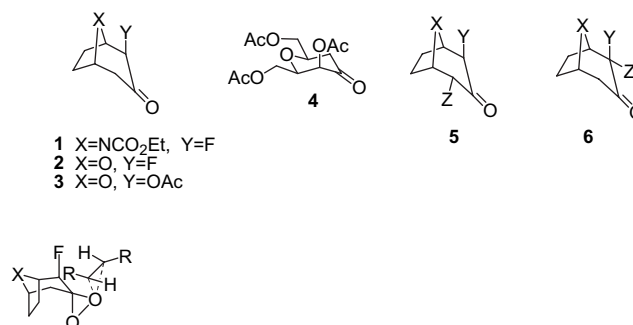


Figure 1.

an olefinic hydrogen substituent sits in the catalyst region occupied by the axial α -substituent. Computational studies¹⁵ on fluorinated cyclohexanone dioxiranes suggest that the axial α heteroatom in catalysts such as **1–3** serve to make the equatorial dioxirane oxygen more reactive than the axial one; in line with this idea, we recently reported¹⁶ that monocyclic ketones **4**, lacking the steric effect of the two-carbon bridge in the bicyclic systems, afford only slightly lowered enantioselectivities.

All of the catalysts we have reported to date have a single substituent α to the ketone carbonyl group. In this paper, we report the first studies of the effect of two electronegative substituents, with the successful synthesis and testing of catalysts of general structure **5** and **6**.¹⁷

2. Results and discussion

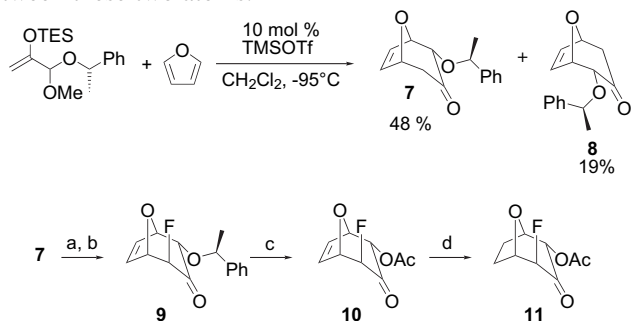
2.1. Ketone synthesis

Our first synthetic targets were ketones of type **5** with an equatorial α' -substituent in addition to the usual axial

Keywords: Epoxidation; Asymmetric; Ketone; Dioxirane.

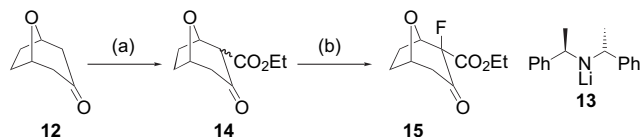
^{*} Corresponding author. Tel.: +44 20 75945876; fax: +44 20 75945804; e-mail: a.armstrong@imperial.ac.uk

α -group. We reasoned that the ‘pseudo- C_2 -symmetry’ of this catalyst class would mean that any approach of the alkene to the *endo*-oxygen of the dioxirane intermediate, would be expected on simple steric expectations to lead to formation of the same product enantiomer as attack on the *exo*-oxygen. Since reaction of enolate derivatives of these bicyclic ketones with electrophiles generally proceeds on the *exo*-face, we introduced the required *endo*-substituent by starting our synthesis with the diastereoselective furan [4+3]-cycloaddition process of Hoffmann,¹⁸ which provides separable diastereomers **7** and **8** (Scheme 1). The major isomer **7** was converted to the corresponding triethylsilyl enol ether, electrophilic fluorination of which with SelectfluorTM (1-chloromethyl-4-fluoro-1,4-diazoniabicyclo[2.2.2]octane bis-(tetrafluoroborate)) provided **9**. Simultaneous removal of the α -methylbenzyl auxiliary and acetylation, followed by hydrogenation of the alkene, afforded the desired α,α' -disubstituted catalyst **11** (Scheme 1). The axial orientation of the fluorine substituent, expected based on the strong precedent for electrophilic attack on the less hindered, *exo*-face of the intermediate silyl enol ether, was confirmed by the analysis of ¹H NMR coupling constants. In particular, the hydrogen α to fluorine displayed a 2.1 Hz coupling to the bridgehead proton. Additionally the proton α to the acetoxy group exhibited a 5.5 Hz coupling to the fluorine, consistent with the expected 1,3-diaxial relationship between these two atoms.



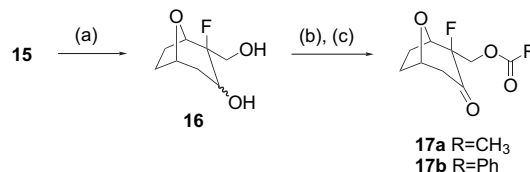
Scheme 1. Reagents and conditions: (a) LDA, Et₃SiCl, THF, –78 °C (96%); (b) 1-chloromethyl-4-fluoro-1,4-diazoniabicyclo[2.2.2]octane bis-(tetrafluoroborate) (SelectfluorTM), CH₃CN, rt (45%); (c) CH₃COCl (3 equiv), FeCl₃ (3 equiv), rt, 15 s (72%); (d) H₂, Pd/C, EtOH (100%).

We next targeted the 2,2-disubstituted catalyst series **6**. Initial attempts to prepare catalysts of this type by further functionalisation of **7** were thwarted by difficulties in effecting enolisation on the side of the ketone bearing the oxygen substituent. We therefore reverted to our earlier strategy in which desymmetrisation of the parent ketone **12** with chiral base **13**¹⁹ was followed by reaction with Mander’s reagent to afford the β -ketoester **14** in 76% yield as a mixture of diastereomers and keto-enol tautomers, which underwent electrophilic fluorination with SelectfluorTM in the absence of added base, leading to **15** (Scheme 2). Chiral GC analysis indicated 98.5% de and 80% ee for **15**.



Scheme 2. Reagents and conditions: (a) **13**, THF, –78 °C, DMPU then NCCO₂Et (76%); (b) 1-chloromethyl-4-fluoro-1,4-diazoniabicyclo[2.2.2]octane bis-(tetrafluoroborate) (SelectfluorTM), CH₃CN, rt (54%).

The synthesis of further interesting 2,2-disubstituted derivatives was planned by conversion of the ester group present in compound **15** to the alcohol oxidation level, which would allow preparation of a wide range of diverse ester derivatives. Thus, a straightforward sequence (Scheme 3) of LiAlH₄ reduction, selective esterification of the primary alcohol and TPAP oxidation²⁰ allowed access to acetate **17a** and benzoate **17b**, the latter being prepared in order to probe for aromatic–aromatic interactions between catalyst and substrate. The ee of these two ketones was determined by chiral GC and was found to be 80%.



Scheme 3. Reagents and conditions: (a) LiAlH₄, THF (70%); (b) Ac₂O, pyridine (51%) or PhCOCl, Et₃N, CH₂Cl₂ (60%); (c) TPAP, NMO, CH₂Cl₂ (87% for **17a**, 100% for **17b**).

2.2. Epoxidation results

The results using ketones **2**, **11**, **15**, **17a** and **17b** as catalysts for alkene epoxidation with Oxone[®] are shown in Table 1. Where the catalysts were not enantiomerically pure, the observed epoxide enantiomeric excess has been converted to ee_{max}, the ee expected assuming a linear relationship

Table 1. Ketone-catalysed Oxone[®] epoxidation of alkenes^a

Entry	Ketone	Alkene	Conversion ^b (%)	ee (%) ^c
1 ^d	2	<i>E</i> -Stilbene	100	83 (<i>R,R</i>)
2 ^c	11	—	100	64 (<i>S,S</i>)
3	15	—	92	77 (<i>R,R</i>)
4	17a	—	84	68 (<i>R,R</i>)
5	17b	—	80	63 (<i>R,R</i>)
6 ^c	11	Styrene	100	2 (<i>S</i>)
7 ^f	15	—	100	14 (<i>R</i>)
8	17a	—	100	29 (<i>R</i>)
9	17b	—	79	25 (<i>R</i>)
10 ^e	11	α -Methylstyrene	100	8 (<i>S</i>)
11 ^f	15	—	100	8 (<i>S</i>)
12	17a	—	61	2 (<i>S</i>)
13	17b	—	100	3 (<i>S</i>)

^a Reaction conditions: alkene (1 equiv), ketone (20 mol %), Oxone[®] (10 equiv of KHSO₅), NaHCO₃ (15.5 equiv), CH₃CN/aq Na₂EDTA (0.4 mmol/dm³ solution) (3:2, 25 mL/mmol), 24 h, rt.

^b Estimated by integration of the ¹H NMR spectrum of the crude reaction mixture.

^c Measured by chiral HPLC or GC (see Section 4). Catalyst **2** was of 76% ee; catalysts **15**, **17a** and **17b** were of 80% ee. For these catalysts, the quoted ee is ee_{max}=100×epoxide ee/ketone ee.

^d Taken from Ref. 13.

^e 10 mol % ketone employed.

^f 100 mol % ketone employed.

between catalyst ee and product ee, which we have shown to be the case for **1** and **3**.^{14,21} Since we have found in the past that performance in the epoxidation of *E*-stilbene is a good general indicator of catalyst selectivity with *trans*-alkenes,¹⁰ we selected this as our test substrate for this olefin class (entries 1–5). All catalysts proved to be reasonably efficient, but the 2,2-disubstituted ketones **17** were less reactive than the other catalysts. In all the cases for *E*-stilbene epoxidation, the major product enantiomer is consistent with predominant reaction via spiro-approach on the *exo*-dioxirane oxygen with the olefinic hydrogen occupying the catalyst quadrant containing the axial fluorine atom (as in Fig. 1). Interestingly, all of the disubstituted catalysts afforded lower epoxide ee than did **2**. Ketone **11** gave the opposite epoxide enantiomer, as expected, but the markedly lower level of selectivity was surprising given the ‘pseudo- C_2 symmetry’ of this system mentioned earlier, and given that in the established spiro-TS-model, only an olefinic hydrogen occupies the quadrant of the catalyst occupied by the acetoxy group. One possible explanation for the low selectivity with **11** comes from our earlier computational studies,¹⁵ which indicated that the TS for epoxidation of ethene with equatorial-fluoro-cyclohexanedioxirane is highly asynchronous, with the developing C–O bond to the end of the olefin closest to the equatorial fluorine being markedly shorter than the other. If this phenomenon was also produced by the equatorial acetoxy group in **11**, it would have the effect of moving the other end of the olefin away from the stereocontrolling axial fluorine substituent, thus lowering epoxidation enantioselectivity. While this explanation is speculative, it is noteworthy that Singleton has recently demonstrated by measuring kinetic isotope effects as well as B3LYP studies that TS-asynchronicity is indeed an important consideration in determining levels of stereocontrol,⁸ suggesting that further mechanistic studies on **11** would be informative. In practical terms, however, the 2,2-disubstituted catalysts **15** and **17** were also less enantioselective than **2**. For the highly challenging terminal alkenes, styrene and α -methylstyrene, again all of the disubstituted catalysts gave disappointing results (entries 6–13). While we did not test catalyst **2** with these substrates, the previously reported results¹⁰ using similar catalyst **1** are 29% ee (*R*) for styrene, and 22% ee (*S*) for α -methylstyrene. Thus for styrene epoxidation, 2,4-disubstitution as in catalyst **11** appears to lower enantioselectivity markedly (entry 6), while the incorporation of the ester unit on the same carbon as the fluorine (catalyst **15**, entry 7) is also deleterious. However, both catalysts **17** appear to give very similar results to the monosubstituted systems (entries 8 and 9). All of the disubstituted catalysts gave very poor results with the challenging 1,1-disubstituted alkene, α -methylstyrene (entries 10–13).

These results suggest that these particular disubstitution motifs are not productive designs for enantioselective ketone catalysts. It is interesting to compare these results, however, with the successful ketone catalysts developed by Shi and co-workers.⁵ Their polysubstituted ketone catalysts generally contain a spirocentre α to the ketone (either as an acetonide or as an oxazolidinone), suggesting that polysubstitution in itself is not disadvantageous and that incorporation of spirocentres adjacent to the ketone in our own catalysts is well worth investigating.

3. Conclusions

In conclusion, we have successfully devised synthetic routes to novel bicyclo[3.2.1]octanones bearing two electron-withdrawing substituents α to the ketone. These are effective catalysts for alkene epoxidation using Oxone[®], but afford lower enantioselectivities than their monosubstituted counterparts. These observations are interesting when compared to the success of polysubstituted ketones containing a spirocentre adjacent to the ketone, developed by Shi and co-workers.⁵ Future studies will therefore examine the effect of incorporation of spirocyclic substitution α to the ketone in our oxabicyclo[3.2.1]octanone framework.

4. Experimental

General experimental details have been described previously.¹⁶

4.1. Ketone synthesis

4.1.1. (1*S*,2*S*,4*S*,5*R*)-2-Fluoro-4-((*S*)-1-phenylethoxy)-8-oxabicyclo[3.2.1]oct-6-en-3-one **9.** To a solution of diisopropylamine (0.36 mL, 2.59 mmol) in THF (4.4 mL) was added 2.5 M ^{*n*}BuLi (1.03 mL, 2.59 mmol) dropwise at –78 °C. After 5 min, the reaction was allowed to warm to room temperature and then cooled to –78 °C. Triethylsilyl chloride (0.50 mL, 2.98 mmol), a solution of oxabicyclic ketone (–)-**7**¹⁸ (0.486 g, 1.99 mmol) in THF and triethylamine (1.25 mL, 8.95 mmol) were then added. After 24 h, the reaction mixture was quenched by the addition of saturated sodium bicarbonate solution (20 mL) at room temperature and the aqueous layer was extracted with diethyl ether (3×100 mL). The combined organic extracts were dried over Na₂SO₄, filtered and concentrated under reduced pressure. The crude product was purified by flash column chromatography (100% petroleum ether) to yield the silyl enol ether (685 mg, 96%) as a colourless oil; [α]_D²⁵ –181.2 (*c* 1.06, CHCl₃); ν_{\max} /cm^{–1} 3026, 2957, 2876, 1637, 1384, 1211, 1093; δ_{H} (250 MHz, CDCl₃) 7.40–7.25 (5H, m, Ph), 6.66 (1H, dd, *J* 6.1, 1.8 Hz, H6), 6.06 (1H, dd, *J* 6.1, 1.8 Hz, H7), 5.31 (1H, d, *J* 4.9 Hz, H4), 4.75 (1H, q, *J* 6.4 Hz, OCHPh), 4.64 (1H, dd, *J* 4.6, 1.8 Hz, H5), 4.58 (1H, dd, *J* 6.1, 1.8 Hz, H1), 3.99 (1H, d, *J* 6.1 Hz, H2), 1.43 (3H, d, *J* 6.4 Hz, CHCH₃), 1.02 (9H, t, *J* 8.0 Hz, CH₂CH₃), 0.74 (6H, q, *J* 8.0 Hz, CH₂CH₃); δ_{C} (62.5 MHz, CDCl₃) 149.5, 144.4, 141.0, 128.5, 127.8, 127.5, 126.5, 108.4, 79.9, 76.5, 73.4, 24.1, 6.7, 5.1. These spectroscopic data agreed with the literature values.¹⁸

To a stirred solution of the silyl enol ether (179 mg, 0.502 mmol) in acetonitrile (5 mL) at room temperature under a nitrogen atmosphere, Selectfluor[™] (178 mg, 0.502 mmol) was added and the mixture stirred for 24 h at room temperature. Tetra-*n*-butylammonium fluoride (0.5 mL, 1 M in THF, 0.50 mmol) was then added to the reaction mixture. After stirring for 0.5 h at room temperature, water (20 mL) and diethyl ether (20 mL) were added to the reaction mixture and the organic layer was separated. The aqueous layer was extracted with diethyl ether (3×25 mL) and the combined organic extracts were dried over Na₂SO₄. After filtration, the filtrate was concentrated under reduced

pressure and purified by flash column chromatography (9:1 petroleum ether/diethyl ether) to afford **9** (59.0 mg, 45%) as a white solid; mp 123–124 °C; $[\alpha]_D^{22}$ –140.0 (*c* 1.10, CHCl₃); *R*_f 0.34 (9:1 petroleum ether/diethyl ether); $\nu_{\max}/\text{cm}^{-1}$ 3057, 2986, 1739, 1603, 1266, 1114; δ_{H} (400 MHz, CDCl₃) 7.40–7.29 (5H, m, Ph), 6.60–6.53 (1H, m, H6), 6.16 (1H, dd, *J* 6.0, 1.5 Hz, H7), 5.01 (1H, d, *J* 9.2 Hz, H1), 4.80 (1H, q, *J* 6.4 Hz, OCHPh), 4.70 (1H, dd, *J* 5.0, 1.6 Hz, H5), 4.40 (1H, dd, *J* 49.1, 1.4 Hz, H2), 4.26 (1H, dd, *J* 5.1, 1.6 Hz, H4), 1.50 (3H, d, *J* 6.4 Hz, CHCH₃); δ_{C} (100 MHz, CDCl₃, DEPT, hmqc) 200.9 (C, ²*J*_{C-F} 18.4 Hz, C₃), 142.8 (C, Ar-C), 137.1 (CH, ⁴*J*_{C-F} 2.8 Hz, C6), 128.7 (CH, Ar-H), 128.7 (CH, C7), 128.1 (CH, Ar-H), 126.4 (CH, Ar-H), 90.5 (CH, ¹*J*_{C-F} 192.2 Hz, C2), 81.6 (CH, C4), 80.9 (CH, ²*J*_{C-F} 20.5 Hz, C1), 80.4 (CH, C5), 79.4 (CH, OCHPh), 24.0 (CH₃, CH₃); MS (CI–NH₃): *m/z* (%) 280 (100, M+NH₄⁺); Found: M+NH₄⁺, 280.1350. C₁₅H₁₉NO₃F requires 280.1349.

4.1.2. (1S,2S,4S,5R)-2-Fluoro-4-acetoxy-8-oxabicyclo[3.2.1]oct-6-en-3-one 10. To a solution of oxabicyclic ketone **9** (59 mg, 0.225 mmol) in dry CH₂Cl₂ (10 mL) at room temperature under a nitrogen atmosphere, anhydrous FeCl₃ (100 mg, 0.617 mmol) and acetyl chloride (48.0 μL, 0.675 mmol) were added and the reaction mixture was stirred for 15 s at room temperature under nitrogen. Water (20 mL) and diethyl ether (20 mL) were added to the reaction mixture and the organic layer was separated. The aqueous layer was extracted with diethyl ether (3×25 mL) and the combined organic extracts were dried over Na₂SO₄. After filtration, the filtrate was concentrated under reduced pressure and purified by flash column chromatography (8:2 petroleum ether/ethyl acetate) to afford **10** (32.6 mg, 72%) as a pale yellow oil; $[\alpha]_D^{22}$ +24.5 (*c* 1.31, CHCl₃); *R*_f 0.20 (8:2 petroleum ether/ethyl acetate); $\nu_{\max}/\text{cm}^{-1}$ 3100, 2977, 2941, 1759, 1745, 1228, 1079; δ_{H} (250 MHz, CDCl₃) 6.55–6.49 (1H, m, H6), 6.25 (1H, dd, *J* 6.1, 1.8 Hz, H7), 5.74 (1H, dd, *J* 5.1, 1.2 Hz, H4), 5.15 (1H, d, *J* 9.1 Hz, H1), 5.02 (1H, dd, *J* 5.1, 1.5 Hz, H5), 4.50 (1H, dd, *J* 48.8, 1.5 Hz, H2), 2.16 (3H, s, CH₃); δ_{C} (100 MHz, CDCl₃, hmqc) 195.0 (²*J*_{C-F} 18.9 Hz, C3), 169.1 (C=OCH₃), 136.0 (C6), 129.7 (C7), 90.1 (¹*J*_{C-F} 193.4 Hz, C2), 81.2 (²*J*_{C-F} 20.5 Hz, C1), 79.0 (C5), 76.4 (C4), 20.4 (C=OCH₃); MS (CI–NH₃): *m/z* (%) 218 (100, M+NH₄⁺); Found: M+H⁺, 201.0564. C₉H₁₀FO₄ requires 201.0563.

4.1.3. (1S,2S,4S,5R)-2-Fluoro-4-acetoxy-8-oxabicyclo[3.2.1]oct-3-one 11. To a stirred solution of oxabicyclic ketone **9** (19.7 mg, 0.0984 mmol) in dry ethanol (4 mL), Pd/C (20 mg, 10% Pd on C) was added. The reaction vessel was then flushed with hydrogen gas and the reaction mixture was stirred for 24 h at room temperature under a positive hydrogen pressure. The reaction mixture was filtered through Celite, with diethyl ether as an eluent, and the filtrate was concentrated under reduced pressure and purified by flash column chromatography (1:9 petroleum ether/ether) to obtain the title compound (20.8 mg, 100%) as a colourless oil; $[\alpha]_D^{22}$ –30.2 (*c* 1.13, CHCl₃); *R*_f 0.83 (diethyl ether); $\nu_{\max}/\text{cm}^{-1}$ 2962, 2929, 2863, 1757, 1743, 1468, 1376, 1230, 1082; δ_{H} (250 MHz, CDCl₃) 5.62 (1H, ddd, *J* 5.5, 3.7, 0.9 Hz, H5), 4.78 (1H, m, H1), 4.69 (1H, apparent t, *J* 5.5 Hz, H4), 4.52 (1H, dd, *J* 49.1, 2.1 Hz, H2), 2.18 (3H, s, CH₃), 2.14 (1H, m, H7), 2.02–1.90 (1H, m, H6), 1.90–1.80 (1H, m, H6), 1.60–1.46 (1H, m, H7); δ_{C} (100 MHz, CDCl₃, DEPT, hmqc) 196.5 (C, ²*J*_{C-F} 20.5 Hz,

C3), 169.0 (C, C=OCH₃), 93.7 (CH, ¹*J*_{C-F} 187.0 Hz, C2), 78.2 (CH, ²*J*_{C-F} 19.0 Hz, C1), 77.5 (CH, C4), 76.1 (CH, C5), 23.8 (CH₂, C6), 23.1 (CH₂, ³*J*_{C-F} 4.6 Hz, C7), 20.5 (CH₃, C=OCH₃); MS (CI–NH₃): *m/z* (%) 220 (100, M+NH₄⁺); Found: M+NH₄⁺, 220.0990. C₉H₁₅NFO₄ requires 220.0985.

4.1.4. (1R,2R,5S)-2-Fluoro-3-oxo-8-oxabicyclo[3.2.1]oct-2-carboxylic acid ethyl ester 15. To a solution of the chiral base **13** (4.44 g, 17.00 mmol) in THF (68 mL) at –78 °C was slowly added 2.70 M ⁿBuLi (12.7 mL, 34.44 mmol). After 15 min, the solution was allowed to warm to –10 °C and then cooled again to –78 °C. The starting ketone **12** (2 g, 15.87 mmol) dissolved in THF (16 mL) was slowly added and the mixture was stirred at this temperature for 30 min followed by slow addition of DMPU (1.9 mL, 15.87 mmol) and ethylcyanoformate (2 mL, 19.04 mmol). Formation of a precipitate was observed before the complete addition of the acylating agent, which dissolves allowing the solution to warm to –45 °C once all the NCCO₂Et has been added. The mixture was further stirred at this temperature for 30 min and then allowed to warm up to 0 °C. After 3 h of reaction, the solution was poured into cold water (100 mL). The expected product was extracted into Et₂O (3×150 mL), and some products were extracted into EtOAc (3×120 mL). The combined organic extracts were dried, filtered and the volatiles evaporated under reduced pressure to give a crude oil. Purification by flash chromatography on silica gel (CH₂Cl₂) afforded the ketoester **14** (2.4 g, 76%) as a colourless oil, as a mixture of diastereomers and tautomers by ¹H NMR analysis; $\nu_{\max}/\text{cm}^{-1}$ 3500, 2978, 1737, 1720, 1657, 1383, 1299, 1200, 1060, 825; *m/z* (CI) MH⁺ 199; Found: MH⁺, 199.0969. C₁₀H₁₅O₄ requires 199.0970.

To a solution of non-racemic **14** (1.50 g, 7.57 mmol) in CH₃CN (90 mL) was added Selectfluor™ (2.67 g, 7.57 mmol). The mixture was stirred for 18 h, concentrated to half volume and the residue partitioned between H₂O and CH₂Cl₂ 1:2 (95 mL). The organic extracts were washed with water (20 mL) and the organic layer was dried (MgSO₄), filtered and the volatiles evaporated under reduced pressure to give a crude product, which was purified by flash chromatography on silica gel (CH₂Cl₂) to give the fluorinated ketone **15** (1.40 g, 54%) as a colourless oil together with unreacted starting material **14** (608 mg, 41%).

Data for 15: $[\alpha]_D^{22}$ –6.5 (*c* 0.15, CH₂Cl₂) at 80% ee; $\nu_{\max}/\text{cm}^{-1}$ 2964, 2929, 1752, 1729, 1470, 1370, 1290, 1260, 1091, 1061, 1030; δ_{H} (300 MHz, CDCl₃) 4.80 (1H, t, *J* 5.5 Hz, H-5), 4.73 (1H, t, *J* 8.3 Hz, H-1), 4.38–4.31 (2H, m, OCH₂CH₃), 3.15 (1H, dt, *J* 15.0, 4.0 Hz, H-4_{ax}), 2.41 (1H, d, *J* 15.0 Hz, H-4_{eq}), 2.20–2.05 (3H, m, 2 H-7&H-6), 1.80–1.72 (1H, m, H-6), 1.35 (3H, t, *J* 7.0 Hz, CH₃); δ_{C} (75.6 MHz, CDCl₃) 197.7 (C=O ketone, d, *J*_{C-F} 22.5 Hz), 165.3 (C=O ester, d, *J*_{C-F} 23.7 Hz), 95.0 (CF, d, *J*_{C-F} 197.5 Hz), 79.1 (CH, d, *J*_{C-F} 19.0 Hz), 75.85 (CH), 62.4 (CH₂), 47.3 (CH₂), 28.2 (CH₂), 24.3 (CH₂), 14.0 (CH₃); *m/z* (GC–MS) (CI); Found: (M+NH₄)⁺, 234.1141. C₁₀H₁₇NO₄F requires 234.1142. λ_{\max} 234.8 nm.

GC conditions: G-TA column (γ-cyclodextrin, trifluoroacetyl), 20 m×0.25 mm; carrier gas: helium; thermalchiral

method: ee 80%, de 98.5%, major diastereoisomer: t_R 15.9 and 16.7, minor diastereoisomer: t_R 16.2 and 16.4.

Diol 16: To a solution of **15** (3.0 g, 13.8 mmol) in THF (130 mL) at 0 °C was slowly added LiAlH₄ (1 g, 26.3 mmol) and the mixture was allowed to warm to room temperature. After 2 h, Na₂SO₄·10H₂O was slowly added at 0 °C and further stirred at room temperature for 1 h. The mixture was filtered over MgSO₄ and further washed with EtOAc (300 mL). Evaporation of the volatiles gave a crude oil, which was purified by flash chromatography on silica gel (Et₂O to EtOAc) to give **16** (1.70 g, 70%) as 1.7:1 mixture of two diastereoisomers, $\nu_{\max}/\text{cm}^{-1}$ 3392, 2957, 1459, 1260, 1075, 1027, 862; m/z (CI); Found: (M+NH₄)⁺, 194.1189. C₈H₁₇NO₃F requires 194.1192. The two isomers could be separated for analytical purposes: less polar isomer, mp 72–73 °C; δ_H (250 MHz, CDCl₃) 4.44 (1H, br t), 4.22 (1H, br t), 4.13–4.04 (1H, m, H-1), 3.91–3.73 (2H, m, H-3,5), 2.37–2.25 (1H, m, H-4), 2.23–2.11 (3H, m, 2OH, H-4), 2.01–1.90 (3H, m, 7, H6), 1.64 (1H, d, J 15.0 Hz, H-6); δ_C (75.5 MHz, CDCl₃) (less polar) 95.4 (C, J_{C-F} 172.6 Hz), 75.9 (CH, J_{C-F} 18.1 Hz), 73.4 (CH), 66.0 (CH, J_{C-F} 35.0 Hz), 63.9 (CH₂, J_{C-F} 21.3 Hz), 35.5 (CH₂), 27.7 (CH₂), 24.9 (CH₂, J_{C-F} 6.0 Hz).

More polar isomer, mp 102–103 °C; δ_H (250 MHz, CDCl₃) 4.54–4.48 (2H, m, CH₂-OH), 4.08 (1H, dd, J 17.0, 12.8 Hz), 3.80–3.65 (2H, m, H-3,5), 2.35–2.29 (2H, br s, 2OH), 2.04–1.96 (2H, m, 2H-4), 1.91–1.66 (4H, m, 2H-6, 2H-7); δ_C (75.6 MHz, CDCl₃) 95.9 (C, J_{C-F} 180.7 Hz), 76.3 (CH, J_{C-F} 18.3 Hz), 73.9 (CH), 64.9 (CH, J_{C-F} 20.5 Hz), 63.9 (CH₂, J_{C-F} 24.4 Hz), 37.9 (CH₂), 27.3 (CH₂), 25.3 (CH₂, J_{C-F} 5.0 Hz).

4.1.5. (1R,2R,5S)-2-Fluoro-2-methyleneacetoxy-8-oxabicyclo[3.2.1]octan-3-one 17a. A mixture of diastereoisomers **16** (885 mg, 5.2 mmol) was dissolved in pyridine (5 mL) and treated with Ac₂O (0.65 mL, 5.7 mmol) at –10 °C. After 2 h, the solution was quenched by the addition of H₂O (11 mL) and extracted into EtOAc (35×3 mL). The combined organic layers were dried, filtered and the volatiles evaporated under reduced pressure to give a crude product, which was purified by flash chromatography (4:1 CH₂Cl₂/Et₂O) to give a mixture of diastereoisomers (565 mg, 51%), $\nu_{\max}/\text{cm}^{-1}$ 3454, 2959, 1746, 1374, 1239, 1065, 1033, 969; m/z (CI); Found: (M+NH₄)⁺, 236.1299. C₁₀H₁₉NO₄F requires 236.1298. The diastereoisomers could be separated for analytical purposes; less polar isomer, white solid, mp 82–83 °C; δ_H (300 MHz, CDCl₃) 4.64–4.46 (3H, m, CHHOAc, H-1,3), 4.23 (1H, dd, J 13.0, 28.8 Hz, CHHOAc), 3.77–3.65 (1H, m, H-5), 2.13 (3H, s, CH₃), 2.07–1.77 (5H, m, OH, 2H-4, 2H-7), 1.71–1.67 (2H, m, 2H-6); δ_C (75.5 MHz, CDCl₃) 170.0 (C=O), 92.8 (C, J_{C-F} 180.0 Hz), 76.1 (CH, J_{C-F} 18.4 Hz), 73.9 (CH, J_{C-F} 12.1 Hz), 65.8 (CH), 63.6 (CH₂, J_{C-F} 24.7 Hz), 38.1 (CH₂), 27.2 (CH₂), 25.2 (CH₂, J 5.4), 20.7 (CH₃).

More polar isomer, colourless oil, δ_H (300 MHz, CDCl₃) 4.56 (1H, dd, J 27.6, 12.6 Hz, CHHOAc), 4.49–4.39 (1H, m, H-1), 4.26–4.14 (2H, m, H-3, CHHOAc), 3.98–3.83 (1H, m, H-5), 2.57 (1H, br s, OH), 2.33–2.18 (1H, m, H-4), 2.16–2.04 (2H, m, H-4, H-7), 2.15 (3H, s, CH₃), 1.98–1.80 (2H, m, H-7, H-6), 1.63 (1H, d, J 14.5 Hz, H-6);

δ_C (75.5 MHz, CDCl₃) 171.6 (C=O), 92.8 (C, J_{C-F} 180.0 Hz), 76.1 (CH, J_{C-F} 17.7 Hz), 73.4 (CH), 66.0 (CH, J_{C-F} 34.5 Hz), 64.5 (CH₂, J_{C-F} 18.9 Hz), 35.5 (CH₂), 27.7 (CH₂), 24.8 (CH₂, J_{C-F} 5.3 Hz), 20.8 (CH₃).

To a solution of the mixture of diastereoisomeric acetates (430 mg, 1.97 mmol) in CH₂Cl₂ (50 mL) was added molecular sieves 4 Å (1.15 g), 4-NMO (406 mg, 3.5 mmol) followed by a catalytic amount of TPAP. The mixture was stirred at room temperature and after 45 min filtered through a silica path and rinsed with EtOAc (75 mL). The volatiles were evaporated under reduced pressure and the crude product was purified by flash chromatography (petroleum ether/Et₂O 3:2) to give **17a** (370 mg, 87%) as a white solid, mp 58–59 °C; $[\alpha]_D^{20}$ +20.6 (*c* 0.34, CH₂Cl₂) at 80% ee; $\nu_{\max}/\text{cm}^{-1}$ 2986, 2969, 1747, 1729, 1233, 1053, 1055; δ_H (250 MHz, CDCl₃) 4.80–4.69 (2H, m, H-1,5), 4.53 (1H, dd, J 15.0, 13.7 Hz, CHHOAc), 4.37 (1H, dd, J 31.8, 13.7 Hz, CHHOAc), 3.15 (1H, dt, J 14.6, 4.3 Hz, H-4_{ax}), 2.33 (1H, d, J 14.6 Hz, H-4_{eq}), 2.13 (3H, s, CH₃), 2.09–2.03 (2H, m, H-6,7), 1.86–1.59 (2H, m, H-6,7); δ_C (75.5 MHz, CDCl₃) 201.1 (C=O, J 24.1 Hz), 170.3 (C=O), 94.4 (C, J 187.4 Hz), 78.0 (CH, J 20.1 Hz), 77.2 (CH), 61.3 (CH₂, J 21.4 Hz), 47.6 (CH₂, J 1.3 Hz), 28.0 (CH₂), 23.7 (CH₂, J 4.0 Hz), 20.7 (CH₃); m/z (CI); Found: (M+NH₄)⁺, 234.1137. C₁₀H₁₇NO₄F requires 234.1142.

GC conditions: G-TA column (γ -cyclodextrin, trifluoroacetyl), 20 m×0.25 mm; carrier gas: helium; Isotherm3 method 130 °C (40 min); ee 80%, de 98.5%, major diastereoisomer: t_R 19.5 and 21.2, minor diastereoisomer: t_R 23.0 and 24.0.

4.1.6. (1R,2R,5S)-2-Fluoro-2-methylenebenzoate-8-oxabicyclo[3.2.1]octan-3-one 17b. To a solution of **16** (major diastereomer) (50 mg, 0.28 mmol) in CH₂Cl₂ (1 mL) was added Et₃N (43 μ L, 0.28 mmol). The mixture was cooled to –40 °C and benzoyl chloride (36 μ L, 0.31 mmol) was added slowly. After 2 h, the mixture was allowed to warm to room temperature and quenched by the addition of a saturated solution of NaHCO₃ (aq) and extracted into Et₂O (5×3 mL). The combined organic extracts were dried (MgSO₄), filtered and the volatiles evaporated to give a crude residue purified by flash chromatography on silica gel (1:1 CH₂Cl₂/Et₂O) to give the benzoate (47 mg, 60%) as a white solid, mp 110–111 °C; $\nu_{\max}/\text{cm}^{-1}$ 3410, 2960, 2928, 1722, 1250, 1050; δ_H (300 MHz, CDCl₃) 8.10–8.07 (2H, m, 2H_{ar}), 7.64–7.57 (1H, m, 1H_{ar}), 7.51–7.44 (2H, m, 2H_{ar}), 4.85–4.75 (1H, m), 4.63–4.57 (1H, m), 4.53–4.49 (2H, m), 3.91–3.69 (1H, m, H-5), 2.11–1.88 (6H, m), 1.84–1.70 (2H, m); δ_C (75.6 MHz, CDCl₃) 166.15 (C=O), 133.5 (CH, J_{C-F} 21.9 Hz), 130.0 (CH, J_{C-F} 31.9 Hz), 129.5 (C), 128.6 (CH, J_{C-F} 4.3 Hz), 93.2 (C, J_{C-F} 181.0 Hz), 76.3 (CH, J_{C-F} 18.7 Hz), 74.0 (CH), 64.5 (CH, J 20.4 Hz), 64.1 (CH₂, J_{C-F} 25.1 Hz), 38.2 (CH₂), 27.2 (CH₂), 25.2 (CH₂, J_{C-F} 5.0 Hz); m/z (CI); Found: (M+NH₄)⁺, 298.1453. C₁₅H₂₁NO₄F requires 298.1455.

To a solution of the benzoate (45 mg, 0.16 mmol) in CH₂Cl₂ (6 mL) was added activated MS 4 Å (120 mg), followed by 4-NMO (41 mg, 0.35 mmol) and tetra-*n*-propylammonium perruthenate (TPAP) (3 mg, 5 mol %). After 1 h, the solution

was filtered through a silica gel path and rinsed with Et₂O (25 mL). The volatiles were evaporated under reduced pressure to give **17b** (44 mg, 100%) as a white solid, mp 84–85 °C; $[\alpha]_D^{24} +12.8$ (*c* 0.39, Et₂O); $\nu_{\max}/\text{cm}^{-1}$ 2985, 1729, 1286, 1074, 1002; δ_{H} (300 MHz, CDCl₃) 8.08 (2H, dd, *J* 8.2, 1.3 Hz, 2H_{ar}), 7.62 (1H, dd, *J* 7.9, 1.1 Hz, 1H_{ar}), 7.47 (2H, dd, *J* 7.7, 0.8 Hz, 2H_{ar}), 4.88–4.81 (2H, m, HHC–CF, H-1), 4.77 (1H, s, H-5), 4.69 (1H, dd, *J* 21.7, 13.7 Hz, HHC–CF), 3.21 (1H, dt, *J* 14.7, 4.4 Hz, H-4_{ax}), 2.38 (1H, d, *J* 14.7 Hz, H-4_{eq}), 2.19–2.04 (2H, m, H-6,7_{endo}), 1.74 (2H, d, *J* 8.5 Hz, H-6,7_{exo}); δ_{C} (75.6 MHz, CDCl₃) 201.1 (C=O, *J*_{C–F} 22 Hz), 165.9 (C=O), 133.4 (CH), 129.8 (CH), 129.4 (C), 128.5 (CH), 94.7 (C, *J*_{C–F} 186.4 Hz), 78.0 (CH, *J*_{C–F} 19.6 Hz), 75.7 (CH), 61.9 (CH₂, *J*_{C–F} 21.6 Hz), 47.6 (CH₂, *J*_{C–F} 2.0 Hz), 28.1 (CH₂), 23.8 (CH₂, *J*_{C–F} 4.0 Hz); *m/z* (CI); Found: (M+NH₄)⁺, 296.1290. C₁₅H₁₉NO₄F requires (M+NH₄)⁺ 296.1298.

GC conditions: G-TA column (γ -cyclodextrin, trifluoroacetyl), 20 m \times 0.25 mm; carrier gas: helium; thermalchiral method: *T*_{init}: 50 °C (3 min), 10 °C/min to *T*_{final}: 180 °C (15 min); 80% ee; *R*_t 25.5 (minor) and 26.7 (major).

4.2. Epoxidation procedure

To a solution of ketone and alkene (0.1 mmol) in acetonitrile (1.5 mL) was added aqueous Na₂EDTA solution (1.0 mL of a 0.4 mM aqueous solution). Oxone[®] (307 mg, 1.0 mmol KHSO₅) and NaHCO₃ (130 mg, 1.55 mmol) were added in portions simultaneously over 60 min. The reaction mixture was stirred vigorously at room temperature until completion (monitored by TLC) and for 24 h, and then diluted with water (10 mL) and the reaction mixture extracted into petrol ether or diethyl ether as appropriate (3 \times 25 mL). The combined organic extracts were dried over Na₂SO₄, filtered and evaporated to dryness under reduced pressure. Flash column chromatography on silica, previously washed with 2% Et₃N in petroleum ether, eluting with appropriate proportion of petroleum ether and diethyl ether afforded the relevant epoxide.

4.3. Determination of epoxide enantiomeric purity in Table 1

E-Stilbene oxide: chiral HPLC on Chiracel OD (Diacel Chemical Industries Ltd., Catalogue Number: 14025), 20% *i*-PrOH/hexane, 1.0 mL/min at 30 °C in oven detecting at 254 nm, as detailed by Shi.²² Absolute configuration determined by comparison to Shi's results.

Styrene oxide: chiral GC on Chiraldex G-TA (Advanced Separation Technologies Ltd., Catalogue Number: 71020), helium head pressure 13 psi at 75 °C in oven, injection temperature 200 °C, detection by FID at 250 °C, as detailed by Shi.²² Absolute configuration was determined by comparison to Shi's results.

α -Methylstyrene oxide: chiral HPLC on Chiracel OD (Diacel Chemical Industries Ltd., Catalogue Number: 14025), 5% *i*-PrOH/hexane, 0.8 mL/min at 30 °C in oven detecting at 254 nm, as detailed by Shi.²² Absolute configuration determined by comparison to Shi's results.

Acknowledgements

We are grateful to the EPSRC (GR/M84534) for support. We also thank Bristol-Myers Squibb, Pfizer and Merck Research Laboratories for unrestricted support of our work.

References and notes

- Xia, Q. H.; Ge, H. Q.; Ye, C. P.; Liu, Z. M.; Su, K. X. *Chem. Rev.* **2005**, *105*, 1603–1662.
- Armstrong, A. *Angew. Chem., Int. Ed.* **2004**, *43*, 1460–1462.
- Page, P. C. B.; Buckley, B. R.; Heaney, H.; Blacker, A. *J. Org. Lett.* **2005**, *7*, 375–377; Page, P. C. B.; Buckley, B. R.; Blacker, A. *J. Org. Lett.* **2004**, *6*, 1543–1546; Page, P. C. B.; Rassias, G. A.; Barros, D.; Bethell, D.; Schilling, M. B. *J. Chem. Soc., Perkin Trans. 1* **2000**, 3325–3334.
- Yang, D. *Acc. Chem. Res.* **2004**, *37*, 497–505.
- Shi, Y. *Acc. Chem. Res.* **2004**, *37*, 488–496.
- Recent examples: Shing, T. K. M.; Leung, G. Y. C.; Yeung, K. W. *Tetrahedron Lett.* **2003**, *44*, 9225–9228; Shing, T. K. M.; Leung, Y. C.; Yeung, K. W. *Tetrahedron* **2003**, *59*, 2159–2168; Crane, Z.; Goeddel, D.; Gan, Y. H.; Shi, Y. *Tetrahedron* **2005**, *61*, 6409–6417.
- For other examples of epoxidation catalysis with fluorocyclohexanones, see: Denmark, S. E.; Matsuhashi, H. *J. Org. Chem.* **2002**, *67*, 3479–3486; Denmark, S. E.; Wu, Z. C. *Synlett* **1999**, 847–859; Denmark, S. E.; Wu, Z. C.; Crudden, C. M.; Matsuhashi, H. *J. Org. Chem.* **1997**, *62*, 8288–8289; Denmark, S. E.; Wu, Z. C. *J. Org. Chem.* **1998**, *63*, 2810–2811; Solladie-Cavallo, A.; Roje, M.; Giraud-Roux, M.; Chen, Y.; Berova, N.; Sunjic, V. *Chirality* **2004**, *16*, 196–203; Solladie-Cavallo, A.; Bouerat, L. *Org. Lett.* **2000**, *2*, 3531–3534; Solladie-Cavallo, A.; Bouerat, L.; Jierry, L. *Eur. J. Org. Chem.* **2001**, 4557–4560; Solladie-Cavallo, A.; Jierry, L.; Bouerat, L.; Taillason, P. *Tetrahedron: Asymmetry* **2001**, *12*, 883–891; Solladie-Cavallo, A.; Jierry, L.; Bouerat, L.; Schmitt, M. *Tetrahedron* **2002**, *58*, 4195–4199; Solladie-Cavallo, A.; Jierry, L.; Klein, A. C. R. *Chim.* **2003**, *6*, 603–606; Solladie-Cavallo, A.; Lupattelli, P.; Jierry, L.; Bovicelli, P.; Angeli, F.; Antonioletti, R.; Klein, A. *Tetrahedron Lett.* **2003**, *44*, 6523–6526; Solladie-Cavallo, A.; Jerry, L.; Klein, A.; Schmitt, M.; Welter, R. *Tetrahedron: Asymmetry* **2004**, *15*, 3891–3898; Solladie-Cavallo, A.; Jierry, L.; Lupattelli, P.; Bovicelli, P.; Antonioletti, R. *Tetrahedron* **2004**, *60*, 11375–11381; Solladie-Cavallo, A.; Jierry, L.; Norouzi-Arasi, H.; Tahmassebi, D. *J. Fluorine Chem.* **2004**, *125*, 1371–1377; Freedman, T. B.; Cao, X.; Nafie, L. A.; Solladie-Cavallo, A.; Jierry, L.; Bouerat, L. *Chirality* **2004**, *16*, 467–474.
- Singleton, D. A.; Wang, Z. H. *J. Am. Chem. Soc.* **2005**, *127*, 6679–6685.
- Shu, L. H.; Wang, P. Z.; Gan, Y. H.; Shi, Y. *Org. Lett.* **2003**, *5*, 293–296; Hickey, M.; Goeddel, D.; Crane, Z.; Shi, Y. *Proc. Natl. Acad. Sci. U.S.A.* **2004**, *101*, 5794–5798; Tian, H. Q.; She, X. G.; Xu, J. X.; Shi, Y. *Org. Lett.* **2001**, *3*, 1929–1931.
- Armstrong, A.; Ahmed, G.; Dominguez-Fernandez, B.; Hayter, B. R.; Wailes, J. S. *J. Org. Chem.* **2002**, *67*, 8610–8617.
- Armstrong, A.; Hayter, B. R. *Chem. Commun.* **1998**, 621–622.
- Sartori, G.; Armstrong, A.; Maggi, R.; Mazzacani, A.; Sartorio, R.; Bigi, F.; Dominguez-Fernandez, B. *J. Org. Chem.* **2003**, *68*, 3232–3237.
- Armstrong, A.; Hayter, B. R.; Moss, W. O.; Reeves, J. R.; Wailes, J. S. *Tetrahedron: Asymmetry* **2000**, *11*, 2057–2061.

14. Armstrong, A.; Moss, W. O.; Reeves, J. R. *Tetrahedron: Asymmetry* **2001**, *12*, 2779–2781.
15. Armstrong, A.; Washington, I.; Houk, K. N. *J. Am. Chem. Soc.* **2000**, *122*, 6297–6298.
16. Armstrong, A.; Tsuchiya, T. *Tetrahedron* **2006**, *62*, 257–263.
17. Subsequent to our first report (Ref. 13) on the use of 8-oxabicyclo[3.2.1]octanones, some related ketone catalysts with additional alkyl substituents were described: Klein, S.; Roberts, S. M. *J. Chem. Soc., Perkin Trans. 1* **2002**, 2686–2691.
18. Stark, C. B. W.; Pierau, S.; Wartchow, R.; Hoffmann, H. M. R. *Chem.—Eur. J.* **2000**, *6*, 684–691; Misske, A. M.; Hoffmann, H. M. R. *Chem.—Eur. J.* **2000**, *6*, 3313–3320.
19. Bunn, B. J.; Cox, P. J.; Simpkins, N. S. *Tetrahedron* **1993**, *49*, 207–218.
20. Ley, S. V.; Norman, J.; Griffith, W. P.; Marsden, S. P. *Synthesis* **1994**, 639–666.
21. Reeves, J. R. PhD thesis, University of London, 2002.
22. Tu, Y.; Wang, Z. X.; Shi, Y. *J. Am. Chem. Soc.* **1996**, *118*, 9806–9807.



Asymmetric epoxidation of *cis*-alkenes with arabinose-derived ketones: enantioselective synthesis of the side chain of Taxol®

Tony K. M. Shing,* To Luk and Chi M. Lee

Department of Chemistry, The Chinese University of Hong Kong, Shatin, Hong Kong, China

Received 18 November 2005; revised 30 December 2005; accepted 25 January 2006

Available online 26 May 2006

Abstract—The ee values of asymmetric epoxidation of *cis*-ethyl cinnamate **15** with arabinose-derived ketones as catalyst and Oxone® as the terminal oxidant were found to increase inversely with the size of the catalyst acetal blocking group. Ketone catalyst **2**, with the least bulky methoxy acetal group, displayed the best enantioselectivity and afforded ethyl (2*R*,3*R*)-3-phenylglycidate **16** in 68% ee. Epoxide **16** was readily converted into a protected side chain of Taxol® in five steps with an overall yield of 89%. The enantioselectivity of the epoxidation of other *cis*-alkenes was moderate to poor.

© 2006 Elsevier Ltd. All rights reserved.

1. Introduction

Catalytic asymmetric epoxidation of alkenes is a versatile synthetic method used to induce chirality into organic molecules and the resultant epoxide moiety can be transformed into a variety of target molecules.¹ Great success has been achieved in the epoxidation of allylic alcohols,² *trans*- and trisubstituted alkenes.^{3–11} For asymmetric epoxidation of unfunctionalized *cis*-alkenes, Mn-salen catalyst is very effective and practical.¹² In recent years, chiral ketones¹³ and iminium salts,¹⁴ also have become promising reagents for asymmetric epoxidation of unfunctionalized *cis*-alkenes.

Our long-term interest in the application of carbohydrates in asymmetric synthesis has employed arabinose-derived alcohols as chiral auxiliaries in asymmetric Diels–Alder¹⁵ and Hosomi–Sakurai reactions.¹⁶ Our efforts towards enantioselective epoxidation of alkenes have furnished chiral ketone catalysts derived from *D*-glucose¹⁷ as well as 2-uloses and 3-uloses derived from *L*-arabinose.¹⁸ We then have concentrated our research on arabinose because it is commercially available in large quantities for both enantiomers. Recently, we reported a series of arabinose-derived 4-uloses,¹⁹ containing a tunable steric blocker, which displayed increasing enantioselectivity with the size of the acetal alkoxy group in catalytic asymmetric epoxidation of *trans*-disubstituted and trisubstituted alkenes. However, most organocatalytic epoxidation of *cis*-alkenes proceeded with moderate enantioselectivity.^{13,14} In this paper, we report our study of the asymmetric epoxidation of *cis*-alkenes with arabinose-derived ketones, using Oxone® as an oxidant

and the conversion of ethyl (2*R*,3*R*)-3-phenylglycidate into a protected side chain of Taxol®.

2. Results and discussion

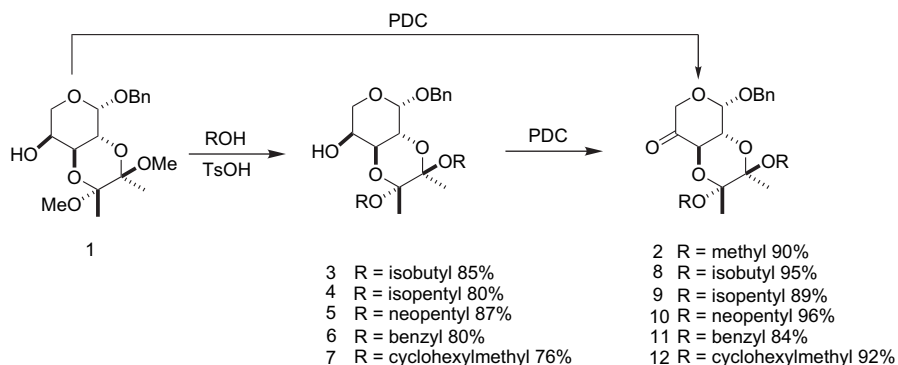
Dimethyl acetal **1**^{19,20} was readily accessible from *L*-arabinose in two steps involving Fischer glycosidation²¹ and *trans*-diol protection²² with 2,2,3,3-tetramethoxybutane in 76% overall yield. Oxidation of the free alcohol in **1** with pyridinium dichromate (PDC) gave ketone **2** in 90% yield. Ketones **8–12** were readily accessible from dimethyl acetal **1** via transacetalization²³ and oxidation in good overall yields (Scheme 1).¹⁹

We also prepared a ketone catalyst **14**, which had a dioxane in place of the diacetal unit. Reduction of acetal **1** using Et₃SiH and BF₃·Et₂O²⁴ in acetonitrile gave 1,4-dioxane **13** in 88% yield. Oxidation of the free alcohol in **13** with PDC afforded ketone **14** in 92% yield (Scheme 2). In the ¹H NMR spectrum, the coupling constant between the two new protons in ketone **14** was 9.0 Hz, which showed that they were diaxially disposed.

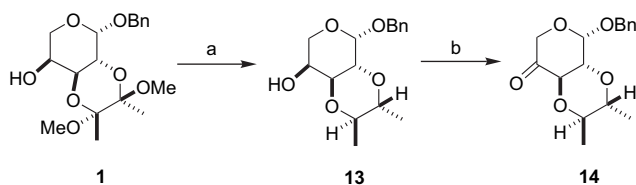
On the basis of our previous studies,^{17–19} the enantioselectivity towards *trans*-disubstituted and trisubstituted alkenes is sensitive to the size of the acetal steric blocker. For example, ketone **10** with a more bulky neopentyl acetal group displayed better chiral induction than ketone **2**, as the ee of epoxidation of *trans*-stilbene was improved from 42% to 83%.^{19a} Encouraged by these results, we went on to investigate the chiral induction capabilities of these ketones in the asymmetric epoxidation of *cis*-ethyl cinnamate, a starting material for the synthesis of Taxol® side chain.²⁵

Keywords: Asymmetric synthesis; Dioxirane; Epoxidation.

* Corresponding author. Tel.: +852 2609 6344; fax: +852 2603 5057; e-mail: tonyshing@cuhk.edu.hk



Scheme 1. Preparation of chiral ketone catalysts.



Scheme 2. Reagents and conditions: (a) $\text{BF}_3 \cdot \text{Et}_2\text{O}$ (3 equiv), Et_3SiH (6 equiv), CH_3CN , $-20^\circ\text{C} \rightarrow 0^\circ\text{C}$, 8 h, 88%; (b) PDC (1.5 equiv), 4 Å MS, CH_2Cl_2 , rt, 12 h, 92%.

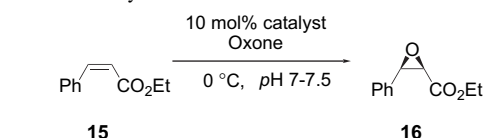
Chemical synthesis of Taxol[®] side chain has drawn much attention during the past decade.^{26–28} Asymmetric epoxidation catalyzed by the readily available and low costing (salen)-Mn(III) complex on *cis*-ethyl cinnamate **15** was reported by Jacobsen.^{12d} Since only *trans*-ethyl cinnamate is commercially available, the desired *cis*-ethyl cinnamate **15** was synthesized (Scheme 3).^{12d} Partial reduction of ethyl phenyl propiolate with Lindlar catalyst under H_2 gave the desired *cis*-ethyl cinnamate **15** in high yield (Scheme 3).²⁹



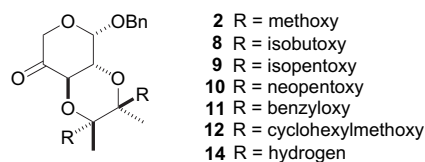
Scheme 3. H_2 , Lindlar catalyst, *n*-hexane, 96%.

The epoxidation reactions were carried out at 0°C with 0.1 mmol of alkene and 10 mol % of catalyst in different solvents at almost neutral conditions (pH 7–7.5). Table 1 shows that acetonitrile (entry 1) was more suitable than *tert*-butanol and 1,4-dioxane as a solvent (entries 2 and 3). In all cases, the epoxides were isolated in high chemical yields (79–95% yield), indicating that all the ketones are efficient catalysts in terms of turnover. Ketones **2** and **14**, with the least bulky blocking groups, displayed the best chiral induction (67–68% ee) (entries 1 and 9). Ketones with bulkier acetal groups did not display better chiral induction with *cis*-alkene **15** as the ee decreased from 68% to 63% in the best case (entries 1 and 7). When the R group changes to the very bulky isopentoxy and neopentoxy groups (entries 5 and 6), the ee drops to 44% and 36%, respectively. It is noteworthy that ketone **10**, with the most bulky neopentoxy group, gave the poorest results (36% ee) whereas this ketone afforded the best enantioselectivities with *trans*-disubstituted and trisubstituted alkenes.^{19a} Anyway, ethyl (2*R*,3*R*)-3-phenylglycidate

Table 1. Asymmetric epoxidation of *cis*-ethyl cinnamate using ketones **2**, **8–12** and **14** as catalysts at 0°C



Catalysts:



Entry ^a	Catalysts	Solvent	Yield (%) ^b	ee (%) ^c	Config. ^d
1	2	CH_3CN	93	68	(+)-(2 <i>R</i> ,3 <i>R</i>) ²⁵
2	2	<i>t</i> BuOH	85	37	(+)-(2 <i>R</i> ,3 <i>R</i>) ²⁵
3	2	1,4-dioxane	95	61	(+)-(2 <i>R</i> ,3 <i>R</i>) ²⁵
4	8	CH_3CN	83	56	(+)-(2 <i>R</i> ,3 <i>R</i>) ²⁵
5	9	CH_3CN	79	44	(+)-(2 <i>R</i> ,3 <i>R</i>) ²⁵
6	10	CH_3CN	84	36	(+)-(2 <i>R</i> ,3 <i>R</i>) ²⁵
7	11	CH_3CN	93	63	(+)-(2 <i>R</i> ,3 <i>R</i>) ²⁵
8	12	CH_3CN	87	49	(+)-(2 <i>R</i> ,3 <i>R</i>) ²⁵
9	14	CH_3CN	93	67	(+)-(2 <i>R</i> ,3 <i>R</i>) ²⁵

^a All epoxidations were carried out with substrate (0.1 mmol), ketone (0.01 mmol), Oxone[®] (1 mmol) and NaHCO_3 (3.1 mmol) in $\text{CH}_3\text{CN}/4 \times 10^{-4}$ M aqueous EDTA (5:1, v/v) for 24 h.

^b Isolated yield.

^c Enantioselectivity was determined by ^1H NMR analysis of the epoxide products directly with shift reagent $\text{Eu}(\text{hfc})_3$.

^d The absolute configuration of the enantiomer in excess was determined by comparing the sign of the optical rotation with the reported one.

16 was obtained in 68% ee using ketone **2** as the catalyst, which is better than existing chiral ketone catalysts (Shi's 44% ee^{13d} and Seki's 26% ee³⁰). The Jacobsen (salen)-Mn(III) catalyst (95–97% ee) is still the best choice for this epoxidation.^{12d}

In our previous studies, we have presented a facile and stereocontrolled synthetic avenue for the construction of the functionalized CD ring of Taxol[®].³¹ With ethyl (2*R*,3*R*)-3-phenylglycidate **16** readily accessible, we now describe a synthesis of a protected form of *N*-benzoyl-(2*R*,3*S*)-phenylisoserine **17** (Fig. 1), Taxol[®] side chain.

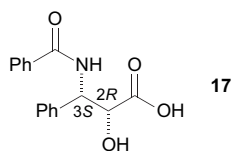


Figure 1. *N*-benzoyl-(2*R*,3*S*)-phenylisoserine.

Asymmetric epoxidation catalyzed by catalyst **2** gave epoxide **16** in 93% yield with 68% ee (Scheme 4). The optical rotation of epoxide **16** was positive in sign, which is in agreement with the literature data of the enantiomerically enriched product.²⁵ Mild acid catalyzed epoxide opening at the benzylic position with NaN_3 and NH_4Cl gave azide **18**, which was then benzoylated under standard conditions to give benzoate **19** in 94% yield. The azide was readily reduced under hydrogenolysis conditions to give an amine. Owing to the stability of an amide being greater than that of an ester, the benzoyl group migrated to the amine group in the presence of *p*-TsOH^{27b} to give benzamide **20** in very good yield. To prevent the epimerization of the hydroxyl group during further manipulation, protection became necessary, which was accomplished by acetalization using 2-methoxypropene in PPTS to give acetal **21** in 98% yield. The ee of **21** was determined to be 68% using ^1H NMR spectral analysis with chiral shift reagent, $\text{Eu}(\text{hfc})_3$. Under basic conditions (LiOH , MeOH , H_2O), the ester **21** was saponified to give acid **22** in 93% yield as a crystalline solid.

At this point, the ee of acid **22** was at best 68%. Huge efforts to increase the ee of **22** were made using recrystallization, the excess amount of the desired (2*R*,3*S*)-enantiomer still remained in the mother liquor. An X-ray crystallographic analysis of a crystal confirmed the structure of acid **22** (Fig. 2).

The specific rotations of the crystals and the concentrated mother liquor were measured. As shown in Scheme 5, the crystals gave almost no specific rotation, which hinted at a racemic mixture. On the other hand, the specific rotation of the mother liquor was +70 and the literature value^{27a} for the enantiomerically enriched acid was +99.1. Enantiomeric excess measurement using chiral shift reagent was performed to determine the relative amount of the enantiomers in the mixture. The results showed that the ee of the mother

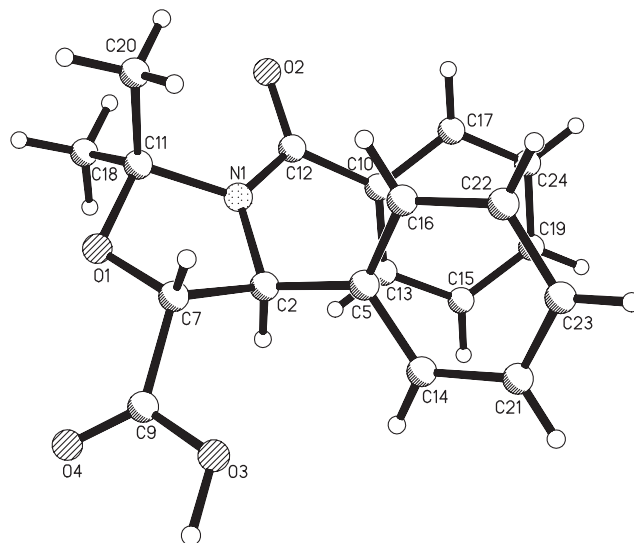
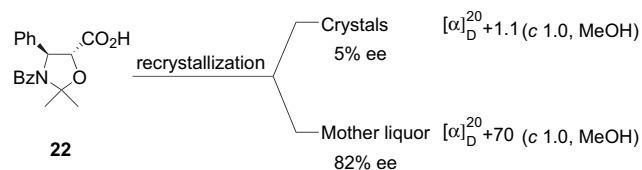


Figure 2. X-ray structure of acid **22** (ORTEP view) (CCDC no. 185892).

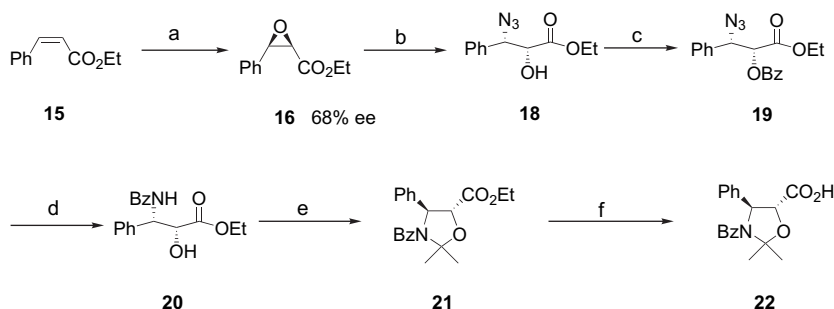
liquor was 82% while that of the crystal counterpart was only 5%.³²



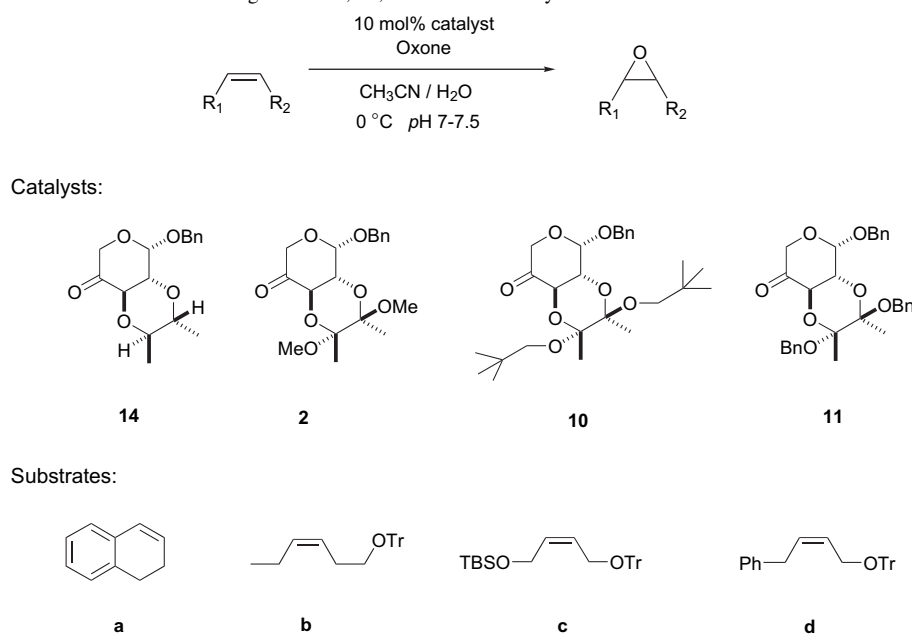
Scheme 5. Specific rotations of solid **22** and liquid **22**.

The asymmetric epoxidation of other *cis*-alkenes was studied using ketones **2**, **10**, **11** and **14** as catalysts and the results are shown in Table 2. In all cases, the epoxides were isolated in high chemical yields (80–96% yield), indicating that all the ketones are conversion-efficient. Ketones **14** and **2**, with the least bulky group, again consistently displayed the best chiral induction (12–33% ee) (entries 1, 2, 5, 6, 9, 10, 13 and 14) among the ketones except for entry 9. Ketones **10** and **11** with the more bulky acetal group consistently displayed poor results.

On the basis of the established spiro transition states^{6i,10h} for chiral dioxirane epoxidation and of our previous studies on *trans*-disubstituted and trisubstituted alkenes,^{18,19} we found



Scheme 4. Reagents and conditions: (a) catalyst **2** (0.1 equiv), Oxone[®] (9 equiv), NaHCO_3 (29 equiv), CH_3CN – EDTA (1:1, v/v), 93%; (b) NaN_3 (2 equiv), NH_4Cl , EtOH , reflux, 92%; (c) Et_3N (4 equiv), DMAP, BzCl (1.5 equiv), 94%; (d) H_2 , 10% Pd/C , *p*-TsOH, 98%; (e) 2-methoxypropene (10 equiv), PPTS, toluene, reflux, 98%; (f) LiOH (2 equiv), MeOH , H_2O , 93%.

Table 2. Asymmetric epoxidation of *cis*-alkenes using ketones **2**, **10**, **11** and **14** as catalysts at 0 °C

Entry ^a	Catalysts	Substrates	Yield (%) ^b	ee (%) ^c	Config. ^d
1	14	a	93	33	(-)-(1 <i>S</i> ,2 <i>R</i>) ³³
2	2	a	93	32	(-)-(1 <i>S</i> ,2 <i>R</i>) ³³
3	10	a	81	11	(-)-(1 <i>S</i> ,2 <i>R</i>) ³³
4	11	a	85	11	(-)-(1 <i>S</i> ,2 <i>R</i>) ³³
5	14	b	84	17	(+) ^e
6	2	b	88	14	(+) ^e
7	10	b	80	9	(+) ^e
8	11	b	86	3	(+) ^e
9	14	c	92	12	(+) ^e
10	2	c	92	21	(+) ^e
11	10	c	83	5	(+) ^e
12	11	c	81	6	(+) ^e
13	14	d	96	24	(+) ^e
14	2	d	93	18	(+) ^e
15	10	d	80	8	(+) ^e
16	11	d	88	8	(+) ^e

^a All epoxidations were carried out with substrate (0.1 mmol), ketone (0.01 mmol), Oxone[®] (1 mmol) and NaHCO₃ (3.1 mmol) in CH₃CN/4 × 10⁻⁴ M aqueous EDTA (5:1, v/v) for 24 h.

^b Isolated yield.

^c Enantioselectivity was determined by ¹H NMR analysis of the epoxide products directly with shift reagent Eu(hfc)₃.

^d The absolute configuration of the enantiomer in excess was determined by comparing the sign of the optical rotation with the reported one.

^e The major absolute configurations were not determined.

that the enantioselectivity was sensitive and increased with the size of the acetal steric blocker.¹⁹ However, in the present case with *cis*-alkenes, the ee increases inversely with the size of the blocking groups. These evidences showed that the transition state for epoxide formation of *cis*-alkenes may be different with that of *trans*-alkenes. In order to rationalize all the possible transition states and the corresponding stereochemistry of the epoxides, more *cis*-alkene substrates need to be investigated. This research is underway.

In conclusion, the ee of the asymmetric epoxidation of *cis*-alkenes decreased with the size of the acetal blocking groups using arabinose-derived ketones. Ketone catalyst **2** with the least bulky acetal group displayed the best enantioselectivity and afforded ethyl (2*R*,3*R*)-3-phenylglycidate **16** in 69% ee. Epoxide **16** was converted into acid **22**, the protected side chain of Taxol[®], in five steps with an overall yield of 89%.

3. Experimental

3.1. General

For general experimental section and procedure for ee determination, see Ref. 15a.

3.1.1. General epoxidation procedure at 0 °C. To a stirred solution of 1,2-dihydronaphthalene (0.1 mmol), ketone (10 mol %) and *n*-Bu₄NHSO₄ (0.5 mg) in CH₃CN (10 mL) was added an aqueous buffer (5 mL, 4 × 10⁻⁴ M aqueous EDTA). The resulting solution was cooled to 0 °C (bath temperature). A solution of Oxone[®] (307 mg, 0.5 mmol) in aqueous EDTA (5 mL, 4 × 10⁻⁴ M) and a solution of NaHCO₃ (252 mg, 3.0 mmol) in H₂O (5 mL) were added dropwise concomitantly via two dropping funnels. The pH of the mixture was maintained at about 7–7.5 over a period of 24 h. The reaction mixture was then poured into water

(10 mL), extracted with Et₂O (3×), dried with anhydrous magnesium sulfate, and filtered. The filtrate was concentrated under reduced pressure to give a residue that was purified by flash column chromatography to give the epoxide.

3.1.2. Alcohol 13. To a solution of dimethyl acetal **1** (160 mg, 0.45 mmol) in dry CH₃CN (8 mL) at –20 °C was added slowly BF₃·Et₂O (0.17 mL, 1.35 mmol). The mixture was stirred for 1 h and Et₃SiH (0.43 mL, 2.71 mmol) was added at –20 °C. The temperature of the resulting mixture was raised to 0 °C and stirred for another 8 h. The cooled reaction mixture was then treated with saturated aqueous NaHCO₃ and extracted with EtOAc (3×20 mL). The combined organic extracts were dried over anhydrous MgSO₄ and filtered. The filtrate was concentrated under reduced pressure. The crude residue was purified by flash column chromatography to give alcohol **13** as a pale yellow syrup (117 mg, 88%): *R*_f 0.30 (hexane–EtOAc, 1:1); [α]_D²⁰ +140.03 (*c* 1.64, CHCl₃); IR (thin film) 3473 (OH) cm⁻¹; ¹H NMR (CDCl₃) δ 7.31–7.17 (5H, m), 4.91 (1H, d, *J*=1.8 Hz), 4.70 (1H, d, *J*=12.6 Hz), 4.56 (1H, d, *J*=12.3 Hz), 3.89 (1H, d, *J*=1.5 Hz), 3.80 (2H, m), 3.75 (1H, d, *J*=1.5 Hz), 3.66 (1H, dd, *J*=12.6, 1.8 Hz), 3.48 (1H, dq, *J*=8.7, 6.2 Hz), 3.32 (1H, dq, *J*=9.0, 6.3 Hz), 2.08 (1H, br s), 1.09 (3H, d, *J*=6.3 Hz), 1.06 (3H, d, *J*=6.0 Hz); ¹³C NMR (acetone) δ 139.5, 129.3, 128.7, 128.5, 98.4, 78.4, 78.3, 74.4, 74.0, 69.9, 68.9, 64.8, 18.0, 17.9; MS (EI) *m/z* (relative intensity) 294 ([M]⁺, 100), 295 (15); HRMS (EI) calcd for C₁₆H₂₂O₅ [M]⁺ 294.1462, found 294.1461; Anal. Calcd for C₁₆H₂₂O₅: C, 65.29; H, 7.53. Found: C, 64.94; H, 7.69.

3.1.3. Ketone 14. To a solution of alcohol **13** (170 mg, 0.57 mmol) in dry CH₂Cl₂ (10 mL) were added slowly PDC (261 mg, 0.69 mmol) and powdered 4 Å molecular sieves (260 mg). The mixture was stirred at room temperature for 12 h. The mixture was suction filtered through a pad of silica gel and the filtrate was concentrated under reduced pressure. The crude residue was purified by flash column chromatography to afford ketone **14** as a colourless syrup (154 mg, 92%): *R*_f 0.22 (hexane–EtOAc, 1:1); [α]_D²⁰ +136.43 (*c* 5.98, CHCl₃); IR (thin film) 1742 (C=O) cm⁻¹; ¹H NMR (CDCl₃) δ 7.37–7.26 (5H, m), 5.08 (1H, d, *J*=3.3 Hz), 4.79 (1H, d, *J*=12.3 Hz), 4.70 (1H, d, *J*=12.3 Hz), 4.59 (1H, d, *J*=10.2 Hz), 4.15 (1H, d, *J*=14.7 Hz), 3.86 (1H, d, *J*=14.7 Hz), 3.74 (1H, dd, *J*=10.4, 3.3 Hz), 3.45 (1H, dq, *J*=9.0, 6.3 Hz), 3.34 (1H, dq, *J*=8.7, 6.3 Hz), 1.17 (3H, d, *J*=6.3 Hz), 1.14 (3H, d, *J*=6.0 Hz); ¹³C NMR (CDCl₃) δ 199.3, 136.5, 128.1, 127.6, 127.3, 96.0, 77.3, 77.2, 76.9, 76.4, 69.7, 66.3, 16.7, 16.4; MS (EI) *m/z* (relative intensity) 292 ([M]⁺, 100), 290 (35); HRMS (EI) calcd for C₁₆H₂₀O₅ [M]⁺ 292.1305, found 292.1303.

3.1.4. Epoxide 16. To a stirred solution of *cis*-ethyl cinnamate (32 mg, 0.18 mmol), ketone **2** (7 mg, 10 mol %) and *n*-Bu₄NHSO₄ (0.5 mg) in CH₃CN (10 mL) was added an aqueous buffer (5 mL, 4×10⁻⁴ M aqueous EDTA). The resulting solution was cooled to 0 °C (bath temperature). A solution of Oxone[®] (550 mg, 0.9 mmol) in aqueous EDTA (5 mL, 4×10⁻⁴ M) and a solution of NaHCO₃ (453 mg, 5.2 mmol) in H₂O (5 mL) were added dropwise concomitantly via two dropping funnels. The pH of the mixture was maintained at about 7–7.5 over a period of 24 h. The

reaction mixture was then poured into water (10 mL), extracted with Et₂O (3×), dried with anhydrous magnesium sulfate and filtered. The filtrate was concentrated under reduced pressure to give a residue that was purified by flash column chromatography to give the epoxide **16** as a colourless syrup (32 mg, 93%): *R*_f 0.40 (hexane–Et₂O, 5:1); The ee of the epoxide was determined to be 68% by ¹H NMR analysis with chiral shift reagent, Eu(hfc)₃. Data for epoxide **16**: [α]_D²⁰ +33.9 (*c* 0.32, CHCl₃); IR (thin film) 1740, 1697, 1649, 1542 cm⁻¹; ¹H NMR (CDCl₃) δ 7.42 (2H, m), 7.33 (3H, m), 4.27 (1H, d, *J*=4.5 Hz), 3.99 (2H, m), 3.82 (1H, d, *J*=4.5 Hz), 1.01 (3H, t, *J*=7.2 Hz); ¹³C NMR (CDCl₃) δ 166.6, 132.8, 128.4, 127.9, 126.6, 61.2, 57.4, 55.7, 13.8; MS (CI) *m/z* (relative intensity) 193 ([M+H]⁺, 100), 165 (20), 119 (40), 91 (42); HRMS (CI) calcd for C₁₁H₁₃O₃ [M+H]⁺ 193.0895, found 193.0861.

3.1.5. Azide 18. Sodium azide (14 mg, 0.208 mmol) and NH₄Cl (2.5 mg, 14 mmol) were added to a stirred solution of epoxide **16** (20 mg, 0.104 mmol) in 80% aqueous EtOH (3 mL) at room temperature. The reaction mixture was refluxed for 24 h and quenched with saturated NaHCO₃. The aqueous phase was extracted with Et₂O (3×) and the combined organic layers were dried over anhydrous MgSO₄ and filtered. The filtrate was concentrated under reduced pressure. The crude residue was purified by flash column chromatography to afford azide **18** as a colourless oil (22 mg, 92%): *R*_f 0.25 (hexane–Et₂O, 2:1); IR (thin film) 3462, 2359, 2107, 1736, 1266, 1112 cm⁻¹; ¹H NMR (CDCl₃) δ 7.42 (5H, m), 4.85 (1H, d, *J*=3.0 Hz), 4.37 (1H, dd, *J*=6.9, 3.0 Hz), 4.29 (2H, q, *J*=7.2 Hz), 3.13 (1H, d, *J*=6.6 Hz), 1.30 (3H, t, *J*=7.2 Hz); ¹³C NMR (CDCl₃) δ 171.9, 128.8, 128.7, 128.6, 127.8, 73.9, 67.1, 62.4, 14.1; MS (CI) *m/z* (relative intensity) 236 ([M+H]⁺, 5), 208 (100), 193 ([M–N₃]⁺, 76); HRMS (CI) calcd for C₁₁H₁₄N₃O₃ [M+H]⁺ 236.1030, found 236.1031.

3.1.6. Benzoate 19. Et₃N (1.7 mL, 11.9 mmol) and benzoyl chloride (0.56 mL, 4.8 mmol) were added to a stirring solution of azide **18** (700 mg, 2.98 mmol) and DMAP (5 mg) in dry CH₂Cl₂ (20 mL) under N₂. The reaction mixture was stirred for 30 min and quenched with saturated NH₄Cl. The mixture was extracted with Et₂O (3×) and the combined organic layers were dried over anhydrous MgSO₄ and filtered. The filtrate was concentrated under reduced pressure. The crude residue was purified by flash column chromatography to give benzoate **19** as a colourless oil (950 mg, 94%): *R*_f 0.58 (hexane–Et₂O, 2:1); IR (thin film) 3328, 2106, 2107, 1729, 1250, 1110, 1020, 707 cm⁻¹; ¹H NMR (CDCl₃) δ 8.13 (2H, m), 7.38 (8H, m), 5.45 (1H, d, *J*=5.1 Hz), 5.15 (1H, d, *J*=5.1 Hz), 4.15 (2H, dq, *J*=7.2, 0.9 Hz), 1.14 (3H, t, *J*=7.2 Hz); ¹³C NMR (CDCl₃) δ 167.2, 165.5, 134.5, 133.6, 130.5, 129.9, 129.0, 128.7, 128.5, 127.8, 127.5, 126.4, 75.5, 65.5, 61.9, 13.8; MS (CI) *m/z* (relative intensity) 340 ([M+H]⁺, 22), 298 ([M–N₃]⁺, 100), 266 (100); HRMS (CI) calcd for C₁₈H₁₈N₃O₄ [M+H]⁺ 340.1292, found 340.1294.

3.1.7. Benzamide 20. A suspension of 10% palladium on charcoal (100 mg, excess) in EtOAc (10 mL) was degassed and refilled with hydrogen gas three times and then stirred for 10 min. A solution of benzoate **19** (960 mg, 2.83 mmol) and *p*-TsOH (10 mg) in EtOAc (10 mL) was added. The

reaction mixture was stirred for 24 h under H₂, quenched with Et₃N, and filtered with filter paper. The solvents of the filtrate were removed under reduced pressure and the residue was purified by flash chromatography to afford benzamide **20** as a white solid (868 mg, 98%); mp 143–144 °C; *R_f* 0.38 (hexane–EtOAc, 2:1); IR (thin film) 3431, 3349, 1718, 1637, 1535, 1095 cm⁻¹; ¹H NMR (CDCl₃) δ 7.76 (2H, d, *J*=6.9 Hz), 7.45 (8H, m), 6.99 (1H, d, *J*=9.0 Hz), 5.76 (1H, dd, *J*=9.3, 2.1 Hz), 4.63 (1H, d, *J*=2.1 Hz), 4.28 (2H, m), 3.31 (1H, br s), 1.31 (3H, t, *J*=7.2 Hz); ¹³C NMR (CDCl₃) δ 172.9, 166.8, 138.7, 134.1, 131.7, 128.6, 128.5, 127.8, 127.6, 127.0, 126.9, 73.3, 62.6, 54.8, 14.1; MS (CI) *m/z* (relative intensity) 314 ([M+H]⁺, 45), 297 ([M–OH]⁺, 17), 208 (84), 193 (100); HRMS (CI) calcd for C₁₈H₂₀NO₄ [M+H]⁺ 314.1387, found 314.1383.

3.1.8. Acetal 21. 2-Methoxypropene (0.31 mL, 3.19 mmol) was added to a stirred solution of benzamide **20** (100 mg, 0.319 mmol) in dry toluene (7 mL) under N₂. Pyridinium *p*-toluenesulfonate (PPTS) (3 mg) was added to the mixture, which was refluxed for 20 h under N₂. The reaction mixture was quenched with aqueous NaHCO₃ and the aqueous phase was extracted with Et₂O (3×). The combined organic layers were dried over anhydrous MgSO₄ and filtered. The filtrate was concentrated under reduced pressure. The crude residue was purified by flash column chromatography to give acetal **21** as a colourless oil (110 mg, 98%); *R_f* 0.38 (hexane–EtOAc, 1:1); IR (thin film) 3368, 1736, 1645, 1528, 1275, 1112, 704 cm⁻¹; ¹H NMR (CDCl₃) δ 7.14 (9H, m), 6.93 (1H, br s), 5.24 (1H, d, *J*=5.7 Hz), 4.55 (1H, d, *J*=6.0 Hz), 4.25 (2H, m), 1.96 (3H, s), 1.87 (3H, s), 1.27 (3H, t, *J*=7.2 Hz); ¹³C NMR (CDCl₃) δ 169.4, 169.1, 138.9, 137.6, 129.3, 128.4, 128.0, 127.7, 126.8, 126.1, 97.8, 81.2, 65.4, 61.9, 26.0, 25.6, 14.1; MS (EI) *m/z* (relative intensity) 353 ([M]⁺, 17), 338 ([M–CH₃]⁺, 99), 295 (100); HRMS (EI) calcd for C₂₁H₂₃NO₄ [M]⁺ 353.1622, found 353.1632. The ee was determined to be 68% by ¹H NMR spectral analysis upon chiral shift reagent addition.

3.1.9. Acid 22. Lithium hydroxide (120 mL, 3.96 mmol) was added to a stirred solution of ester **21** (700 mg, 1.98 mmol) in 70% aqueous MeOH (9 mL) at room temperature. The reaction mixture was stirred for 24 h at room temperature. The solvent was removed in vacuo and H₂O (3 mL) was added to the residue. Saturated NH₄Cl (3 mL) was added to the mixture until the pH reached 4. The aqueous phase was extracted with CH₂Cl₂ (3×). The combined organic layers were dried over anhydrous MgSO₄ and filtered. The filtrate was concentrated under reduced pressure. The crude residue was purified by flash column chromatography to afford acid **22** as a white solid (600 mg, 93%). A single crystal suitable for X-ray crystallographic analysis was obtained in MeOH. The optical rotations of the crystals and the mother liquor obtained from recrystallization were different as indicated below.

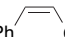
Data for crystals: mp 175–176 °C (lit.^{27a} for enantiomerically enriched acid, mp 213 °C); [α]_D²⁰ +1.1 (*c* 0.7, MeOH); *R_f* 0.32 (CHCl₃–MeOH, 4:1); IR (thin film) 3449, 2933, 1740, 1639, 1390, 1250, 1209 cm⁻¹; ¹H NMR (CD₃OD) δ 7.18 (8H, m), 6.95 (2H, br s), 5.26 (1H, d, *J*=5.7 Hz), 4.57 (1H, d, *J*=5.7 Hz), 1.92 (3H, s), 1.84 (3H, s); ¹³C NMR (CDCl₃) δ 172.8, 169.5, 138.8, 137.2, 129.5,

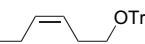
128.5, 128.0, 127.7, 126.8, 126.1, 97.9, 81.1, 65.4, 26.1, 25.4; MS (EI) *m/z* (relative intensity) 325 ([M]⁺, 15), 310 ([M–CH₃]⁺, 87), 105 (100); HRMS (EI) calcd for C₁₉H₁₉NO₄ [M]⁺ 325.1309, found 325.1304.

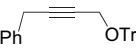
Data for the mother liquor: [α]_D²⁰ +70.3 (*c* 0.6, MeOH) (lit.^{27a} for enantiomerically enriched acid, [α]_D²⁰ +99.1 (*c* 0.36, EtOH)). The acid **22** is not sensitive to chiral shift reagent Eu(hfc)₃ under various solvents and concentrations. To overcome this, the mother liquor from recrystallization was esterified to convert **22** back to ester **21**, which displayed better resolution of the separated signals in the ¹H NMR spectrum upon Eu(hfc)₃ addition. DBU (13 μL, 0.09 mmol) and ethyl bromide (7 μL, 0.09 mmol) were added to a stirred solution of the liquid acid **22** (15 mg, 0.046 mmol) in dry benzene (2 mL). The reaction mixture was stirred at reflux for 1 h and quenched with saturated NH₄Cl. The aqueous phase was extracted with Et₂O (3×). The combined organic layers were dried over anhydrous MgSO₄ and filtered. The filtrate was concentrated under reduced pressure. The crude residue was purified by flash column chromatography to afford ester **21** as a colourless oil (15 mg, 92%). The ee of ester **21** was measured to be 82% by the same method described above.

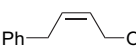
In the same manner, the ee of the ester prepared from crystalline acid **22** was determined to be 5%.


3.2. Preparation of alkene substrates


3.2.1.  **cis-Ethyl cinnamate.**²⁹ To a stirred mixture of ethyl phenyl propiolate (1 g, 5.74 mmol), *n*-hexane (25 mL) and 1-octene (6 mL) was added quinoline (1.03 g, 8 mmol). Palladium on calcium carbonate (Lindlar catalyst 290 mg, 1.7 mmol) was added and the resulting reaction mixture was stirred under H₂ with a hydrogen balloon at room temperature for 20 h. The resulting mixture was filtered through filter paper. The filtrate was concentrated under reduced pressure. The crude residue was purified by flash column chromatography to afford *cis*-ethyl cinnamate as a colourless oil (960 mg, 96%); *R_f* 0.78 (hexane–Et₂O, 5:1); ¹H NMR (CDCl₃) δ 7.58 (2H, m), 7.35 (3H, m), 6.95 (1H, d, *J*=12.6 Hz), 5.95 (1H, d, *J*=12.6 Hz), 4.18 (2H, q, *J*=7.2 Hz), 1.25 (3H, t, *J*=7.2 Hz); ¹³C NMR (CDCl₃) δ 142.9, 129.6, 128.9, 127.9, 119.9, 60.3, 14.1.

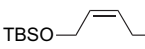
3.2.2.  **cis-1-Trityloxy-3-hexene.** Trityl chloride (2.46 g, 8.86 mmol) and DMAP (7 mg) were added to a stirring mixture of *cis*-3-hexen-1-ol (807 mg, 8.05 mmol) and pyridine (0.98 mL, 12.1 mmol) in dry CH₂Cl₂ (20 mL). The reaction mixture was stirred for 24 h. The reaction was with saturated aqueous NH₄Cl and extracted with Et₂O (3×30 mL). The combined organic extracts were dried over anhydrous MgSO₄ and filtered. The filtrate was concentrated under reduced pressure. The crude residue was purified by flash column chromatography to afford *cis*-1-trityloxy-3-hexene as a colourless oil (2.79 g, 92%); *R_f* 0.33 (hexane–Et₂O, 30:1); ¹H NMR (CDCl₃) δ 7.48–7.23 (15H, m), 5.48 (1H, m), 5.39 (1H, m), 3.11 (2H, t, *J*=6.9 Hz), 2.41 (1H, d, *J*=6.9 Hz), 2.34 (1H, d, *J*=6.9 Hz), 2.12 (1H, dq, *J*=7.5, 7.2 Hz), 0.99 (3H, t, *J*=7.5 Hz); ¹³C NMR (CDCl₃) δ 144.7, 133.8, 129.0, 128.0, 127.2, 125.7, 86.8, 63.9, 28.5, 21.0, 14.7.


3.2.3.  **1-Trityloxy-4-phenyl-2-butyne.** ⁿBuLi (1.6 M, 12.5 mL, 19.0 mmol) was added to a solution of the 1-trityloxy-2-propyne³⁴ (2.97 g, 9.96 mmol) in dry THF at 0 °C. The mixture was stirred at room temperature. After 1 h, BnBr was added to the reaction mixture. BnBr (2.37 mL, 19.0 mmol) was added to the mixture and the resulting solution was stirred for 24 h. The reaction was with saturated aqueous NH₄Cl and extracted with Et₂O (3×30 mL). The combined organic extracts were dried over anhydrous MgSO₄ and filtered. The filtrate was concentrated under reduced pressure. The crude residue was purified by flash column chromatography to afford 1-trityloxy-4-phenyl-2-butyne as a yellow oil (3.21 g, 79%); *R*_f 0.44 (hexane–Et₂O, 10:1); ¹H NMR (CDCl₃) δ 7.59–7.29 (20H, m), 3.91 (2H, t, *J*=2.1 Hz), 3.71 (2H, s); ¹³C NMR (CDCl₃) δ 143.9, 136.9, 128.9, 128.8, 128.2, 128.1, 127.7, 127.4, 126.9, 87.7, 83.7, 79.2, 53.9, 25.6; MS (EI) *m/z* (relative intensity) 388 ([M]⁺, 100), 243 (98), 211 (100); HRMS (EI) calcd for C₂₉H₂₄O₁ [M]⁺ 388.1822, found 388.1816.

3.2.4.  **cis-1-Trityloxy-4-phenyl-2-butene.** To a stirred mixture of 1-trityloxy-4-phenyl-2-butyne (200 mg, 0.49 mmol), *n*-hexane (12 mL) and 1-octene (3 mL) was added quinoline (98 mg, 0.76 mmol). Palladium on calcium carbonate (Lindlar catalyst 30 mg, 0.25 mmol) was added and the resulting reaction mixture was stirred under H₂ with a hydrogen balloon at room temperature for 20 h. The resulting mixture was filtered through filter paper. The filtrate was concentrated under reduced pressure. The crude residue was purified by flash column chromatography to afford *cis*-1-trityloxy-4-phenyl-2-butene as a pale yellow oil (181 mg, 90%); *R*_f 0.50 (hexane–Et₂O, 10:1); ¹H NMR (CDCl₃) δ 7.53–7.26 (20H, m), 5.86 (1H, m), 5.82 (1H, m), 3.80 (2H, d, *J*=6.3 Hz), 3.27 (2H, d, *J*=7.2 Hz); ¹³C NMR (CDCl₃) δ 144.5, 131.1, 129.0, 128.8, 128.7, 128.2, 127.9, 127.7, 127.3, 126.3, 87.2, 60.6, 34.3; MS (ESI) *m/z* (relative intensity) 413 ([M+Na]⁺, 100), 414 (30); HRMS (ESI) calcd for C₂₉H₂₆O₁ [M+Na]⁺ 413.1876, found 413.1882.

3.2.5.  **1-Trityloxy-4-phenyl-2,3-epoxybutane.** Colourless oil: *R*_f 0.25 (hexane–Et₂O, 10:1); ¹H NMR (CDCl₃) δ 7.53–7.26 (20H, m), 3.55 (1H, dd, *J*=10.2, 5.4 Hz), 3.33 (1H, dd, *J*=5.4, 4.2 Hz), 3.24 (2H, m), 2.78 (1H, dd, *J*=15.0, 6.0 Hz), 2.66 (1H, dd, *J*=15.0, 6.3 Hz); ¹³C NMR (CDCl₃) δ 144.1, 137.8, 129.2, 129.0, 128.9, 128.2, 127.5, 126.9, 87.3, 62.4, 57.1, 55.7, 34.6; MS (CI) *m/z* (relative intensity) 389 (100), 390 (30), 407 ([MH]⁺, 10); HRMS (CI) calcd for C₂₉H₂₆O₂ [MH]⁺ 407.2006, found 407.1995.

3.2.6.  **1-Trityloxy-3,4-epoxyhexane.** Colourless oil: *R*_f 0.23 (hexane–Et₂O, 10:1); ¹H NMR (CDCl₃) δ 7.47–7.21 (15H, m), 3.28 (1H, t, *J*=6.3 Hz), 3.15 (1H, q, *J*=5.1 Hz), 2.93 (1H, q, *J*=5.1 Hz), 1.85 (2H, m), 1.54 (2H, dt, *J*=14.1, 6.9 Hz), 1.04 (3H, t, *J*=7.5 Hz); ¹³C NMR (CDCl₃) δ 144.5, 129.0, 128.1, 127.3, 87.0, 61.5, 58.6, 55.4, 29.0, 21.5, 11.0; MS (CI) *m/z* (relative intensity) 358 ([M]⁺, 30), 341 (100); HRMS (CI) calcd for C₂₅H₂₆O₂ [M]⁺ 358.1927, found 358.1918.

3.2.7.  **(Z)-1-Trityloxy-4-tert-butylidimethylsilyloxy-2-butene.** Trityl chloride (3.44 g, 15.7 mmol) and DMAP (8 mg) were added to a stirring mixture of (Z)-1-tert-butylidimethylsilyloxy-2-buten-4-ol³⁵ (2.50 mg, 12.3 mmol) and pyridine (1.0 mL, 15.7 mmol) in dry CH₂Cl₂ (40 mL). The reaction mixture was stirred for 24 h. The reaction was with saturated aqueous NH₄Cl and extracted with Et₂O (3×40 mL). The combined organic extracts were dried over anhydrous MgSO₄ and filtered. The filtrate was concentrated under reduced pressure. The crude residue was purified by flash column chromatography to afford (Z)-1-trityloxy-4-tert-butylidimethylsilyloxy-2-butene as a colourless oil (5.10 g, 93%); *R*_f 0.33 (hexane–Et₂O, 20:1); ¹H NMR (CDCl₃) δ 7.51–7.26 (15H, m), 5.75–5.65 (2H, m), 4.12 (2H, d, *J*=5.7 Hz), 3.71 (2H, d, *J*=5.4 Hz), 0.90 (9H, s), 0.04 (6H, s); ¹³C NMR (CDCl₃) δ 144.4, 132.1, 129.0, 128.2, 127.5, 127.3, 87.2, 60.7, 60.1, 26.3, 18.6, –4.82.

3.2.8.  **1-Trityloxy-4-tert-butylidimethylsilyloxy-2,3-epoxybutane.** Colourless oil: *R*_f 0.34 (hexane–Et₂O, 10:1); ¹H NMR (CDCl₃) δ 7.53–7.26 (15H, m), 3.72 (1H, dd, *J*=12.0, 6.0 Hz), 3.55 (1H, dd, *J*=12.0, 4.2 Hz), 3.37–3.29 (2H, m), 3.21–3.16 (2H, m), 0.91 (9H, s), 0.04 (3H, s), 0.03 (3H, s); ¹³C NMR (CDCl₃) δ 144.1, 128.9, 128.2, 127.4, 87.2, 62.7, 62.1, 56.8, 55.4, 26.2, 18.6, –4.88, –5.05; MS (CI) *m/z* (relative intensity) 461 ([MH]⁺, 10), 444 (45), 443 (100); HRMS (CI) calcd for C₂₉H₃₆O₃Si₁ [MH]⁺ 461.2508, found 461.2503.

Acknowledgements

This research was supported by a CUHK Direct Grant.

References and notes

- Xia, Q. H.; Ge, H. Q.; Ye, C. P.; Liu, Z. M.; Su, K. X. *Chem. Rev.* **2005**, *105*, 1603.
- (a) Katsuki, T.; Martin, V. S. *Org. React.* **1996**, *48*, 1; (b) Johnson, R. A.; Sharpless, K. B. *Catalytic Asymmetric Synthesis*; Ojima, I., Ed.; VCH: New York, NY, 1993, Chapter 4.1; (c) Rossiter, B. E.; Katsuki, T.; Sharpless, K. B. *J. Am. Chem. Soc.* **1981**, *103*, 464; (d) Katsuki, T.; Sharpless, K. B. *J. Am. Chem. Soc.* **1980**, *102*, 5974.
- For reviews, see: (a) Yang, D. *Acc. Chem. Res.* **2004**, *37*, 497; (b) Shi, Y. *Acc. Chem. Res.* **2004**, *37*, 488; (c) Frohn, M.; Shi, Y. *Synthesis* **2000**, *14*, 1979.
- (a) Matsumoto, K.; Tomioka, K. *Tetrahedron Lett.* **2002**, *43*, 631; (b) Klein, S.; Roberts, S. M. *J. Chem. Soc., Perkin Trans. 1* **2002**, 2686; (c) Stearman, C. J.; Behar, V. *Tetrahedron Lett.* **2002**, *43*, 1943; (d) Seki, M.; Furutani, T.; Hatsuda, M.; Imashiro, R. *Tetrahedron Lett.* **2000**, *41*, 2149; (e) Carnell, A. J.; Johnstone, R. A. W.; Parsy, C. C.; Sanderson, W. R. *Tetrahedron Lett.* **1999**, *40*, 8029; (f) Dakin, L. A.; Panek, J. S. *Chemtracts* **1998**, *11*, 531; (g) Bergbreiter, D. E. *Chemtracts* **1997**, *10*, 661; (h) Song, C. E.; Kim, Y. H.; Lee, K. C.; Lee, S. G.; Jin, B. W. *Tetrahedron: Asymmetry* **1997**, *8*, 2921.
- (a) Curci, R.; D'Accolti, L.; Fiorentino, M.; Rosa, A. *Tetrahedron Lett.* **1995**, *36*, 5831; (b) Curci, R.; Fiorentino, M.; Serio, M. R. *J. Chem. Soc., Chem. Commun.* **1984**, 155.

6. (a) Yang, D.; Jiao, G.-S.; Yip, Y.-C.; Lai, T.-H.; Wong, M.-K. *J. Org. Chem.* **2001**, *66*, 4619; (b) Yang, D.; Jiao, G.-S. *Chem.—Eur. J.* **2000**, *6*, 3517; (c) Yang, D.; Jiao, G.-S.; Yip, Y.-C.; Wong, M.-K. *J. Org. Chem.* **1999**, *64*, 1635; (d) Yang, D.; Wong, M.-K.; Yip, Y.-C.; Wang, X.-C.; Tang, M.-W.; Zheng, J.-H.; Cheung, K.-K. *J. Am. Chem. Soc.* **1998**, *120*, 5943; (e) Yang, D.; Yip, Y.-C.; Chen, J.; Cheung, K.-K. *J. Am. Chem. Soc.* **1998**, *120*, 7659; (f) Yang, D.; Yip, Y.-C.; Tang, M.-W.; Wong, M.-K.; Cheung, K.-K. *J. Org. Chem.* **1998**, *63*, 9888; (g) Yang, D.; Yip, Y.-C.; Jiao, G.-S.; Wong, M.-K. *J. Org. Chem.* **1998**, *63*, 8952; (h) Yang, D.; Yip, Y.-C.; Tang, M.-W.; Wong, M.-K.; Zheng, J.-H.; Cheung, K.-K. *J. Am. Chem. Soc.* **1996**, *118*, 491; (i) Yang, D.; Wang, X.-C.; Wong, M.-K.; Yip, Y.-C.; Tang, M.-W. *J. Am. Chem. Soc.* **1996**, *118*, 11311.
7. (a) Adam, W.; Saha-Möller, C. R.; Zhao, C.-G. *Tetrahedron: Asymmetry* **1999**, *10*, 2749; (b) Adam, W.; Zhao, C.-G. *Tetrahedron: Asymmetry* **1997**, *8*, 3995.
8. (a) Armstrong, A.; Ahmed, G.; Dominguez-Fernandez, B.; Hayter, B. R.; Wailes, J. S. *J. Org. Chem.* **2002**, *67*, 8610; (b) Armstrong, A.; Moss, W. O.; Reeves, J. R. *Tetrahedron: Asymmetry* **2001**, *12*, 2779; (c) Armstrong, A.; Hayter, B. R.; Moss, W. O.; Reeves, J. R.; Wailes, J. S. *Tetrahedron: Asymmetry* **2000**, *11*, 2057; (d) Armstrong, A. *Chem. Commun.* **1998**, 621.
9. (a) Denmark, S. E.; Wu, Z.; Crudden, C. M.; Matsushashi, H. *J. Org. Chem.* **1997**, *62*, 8288; (b) Denmark, S. E.; Forbes, D. C.; Hays, D. S.; DePue, J. S.; Wilde, R. G. *J. Org. Chem.* **1995**, *60*, 1391.
10. (a) Lorenz, J. C.; Frohn, M.; Zhou, X. M.; Zhang, J. R.; Tang, Y.; Burke, C.; Shi, Y. *J. Org. Chem.* **2005**, *70*, 2904; (b) Shu, L.; Shen, Y.-M.; Burke, C.; Goeddel, D.; Shi, Y. *J. Org. Chem.* **2003**, *68*, 4963; (c) Wu, X.-Y.; She, X.; Shi, Y. *J. Am. Chem. Soc.* **2002**, *124*, 8792; (d) Tian, H.; She, X.; Xu, J.; Shi, Y. *Org. Lett.* **2001**, *3*, 1929; (e) Tian, H.; She, X.; Shi, Y. *Org. Lett.* **2001**, *3*, 715; (f) Wang, Z.-X.; Miller, S. M.; Anderson, O. P.; Shi, Y. *J. Org. Chem.* **2001**, *66*, 521; (g) Shu, L.; Shi, Y. *Tetrahedron* **2001**, *57*, 5213; (h) Warren, J. D.; Shi, Y. *J. Org. Chem.* **1999**, *64*, 7675; (i) Wang, Z.-X.; Cao, G.-A.; Shi, Y. *J. Org. Chem.* **1999**, *64*, 7646; (j) Wang, Z.-X.; Miller, S. M.; Anderson, O. P.; Shi, Y. *J. Org. Chem.* **1999**, *64*, 6443; (k) Frohn, M.; Dalkiewicz, M.; Tu, Y.; Wang, Z.-X.; Shi, Y. *J. Org. Chem.* **1998**, *63*, 2948; (l) Cao, G.-A.; Wang, Z.-X.; Tu, Y.; Shi, Y. *Tetrahedron Lett.* **1998**, *39*, 4425; (m) Zhu, Y.; Tu, Y.; Yu, H.; Shi, Y. *Tetrahedron Lett.* **1998**, *39*, 7819; (n) Wang, Z.-X.; Shi, Y. *J. Org. Chem.* **1997**, *62*, 8622; (o) Tu, Y.; Wong, Z.-X.; Shi, Y. *J. Am. Chem. Soc.* **1996**, *118*, 9806.
11. (a) Solladié-Cavallo, A.; Jierry, L.; Lupattelli, P.; Bovicelli, P.; Antonioletti, R. *Tetrahedron* **2004**, *60*, 11375; (b) Solladié-Cavallo, A.; Jierry, L.; Klein, A.; Schmitt, M.; Welter, R. *Tetrahedron: Asymmetry* **2004**, *15*, 3891; (c) Solladié-Cavallo, A.; Jierry, L.; Norouzi-Arasi, H.; Tahmassebi, D. *J. Fluorine Chem.* **2004**, *125*, 1371; (d) Solladié-Cavallo, A.; Bouérat, L.; Jierry, L. *Eur. J. Org. Chem.* **2001**, *23*, 4557; (e) Solladié-Cavallo, A.; Jierry, L.; Bouérat, L.; Taillisson, P. *Tetrahedron: Asymmetry* **2001**, *12*, 883; (f) Solladié-Cavallo, A.; Bouérat, L. *Org. Lett.* **2000**, *2*, 3531.
12. (a) Mukaiyama, T. *Aldrichimica Acta* **1996**, *29*, 59; (b) Palucki, M.; McCormick, G. J.; Jacobsen, E. N. *Tetrahedron Lett.* **1995**, *36*, 5457; (c) Katsuki, T. *Coord. Chem. Rev.* **1995**, *140*, 189; (d) Deng, L.; Jacobsen, E. N. *J. Org. Chem.* **1992**, *57*, 4320; (e) Jacobsen, E. N.; Zhang, W.; Muci, A. R.; Ecker, J. R.; Deng, L. *J. Am. Chem. Soc.* **1991**, *113*, 7063; (f) Lee, N. H.; Muci, A. R.; Jacobsen, E. N. *Tetrahedron Lett.* **1991**, *32*, 5055.
13. (a) Shu, L.; Shi, Y. *Tetrahedron Lett.* **2004**, *45*, 8115; (b) Shu, L.; Wang, P.; Gan, Y.; Shi, Y. *Org. Lett.* **2003**, *5*, 293; (c) Tian, H.; She, X.; Yu, H.; Shu, L.; Shi, Y. *J. Org. Chem.* **2002**, *67*, 2435; (d) Tian, H.; She, X.; Shu, L.; Yu, H.; Shi, Y. *J. Am. Chem. Soc.* **2000**, *122*, 11551.
14. (a) Page, P. C. B.; Buckley, B. R.; Heaney, H.; Blacker, A. J. *Org. Lett.* **2005**, *7*, 375; (b) Page, P. C. B.; Buckley, B. R.; Blacker, A. J. *Org. Lett.* **2004**, *6*, 1543.
15. (a) Shing, T. K. M.; Chow, H.-F.; Chung, I. H. F. *Tetrahedron Lett.* **1996**, *37*, 3713; (b) Shing, T. K. M.; Lloyd-Williams, P. *J. Chem. Soc., Chem. Commun.* **1987**, 423.
16. Shing, T. K. M.; Li, L.-H. *J. Org. Chem.* **1997**, *62*, 1230.
17. Shing, T. K. M.; Leung, G. Y. C. *Tetrahedron* **2002**, *58*, 7545.
18. Shing, T. K. M.; Leung, Y. C.; Yeung, K. W. *Tetrahedron* **2003**, *59*, 2159.
19. (a) Shing, T. K. M.; Leung, Y. C.; Luk, T. J. *J. Org. Chem.* **2005**, *70*, 7279; (b) Shing, T. K. M.; Leung, Y. C.; Yeung, K. W. *Tetrahedron Lett.* **2003**, *44*, 9225.
20. For a review on 1,2-diacetals, see: Ley, S. V.; Baeschlin, D. K.; Dixon, D. J.; Foster, A. C.; Ince, S. J.; Priepke, W. M. H.; Reynolds, D. J. *Chem. Rev.* **2001**, *101*, 53.
21. Bennett, M.; Gill, G. B.; Pattenden, G.; Shuker, A. J.; Stapleton, A. *J. Chem. Soc., Perkin Trans. 1* **1991**, 929.
22. Montchamp, J. L.; Tian, F.; Hart, M. E.; Frost, J. W. *J. Org. Chem.* **1996**, *61*, 3897.
23. Isidor, J. L.; Carlson, R. M. *J. Org. Chem.* **1973**, *38*, 554.
24. Lewis, M. D.; Cha, J. K.; Kishi, Y. *J. Am. Chem. Soc.* **1982**, *104*, 9806.
25. Jacobsen, E. N.; Deng, L.; Furukawa, Y.; Martinez, L. E. *Tetrahedron* **1994**, *50*, 4323.
26. (a) Song, C. E.; Oh, C. M.; Roh, E. J.; Lee, S. G.; Choi, J. H. *Tetrahedron: Asymmetry* **1999**, *10*, 671; (b) Kobayashi, S.; Ishitani, H.; Ueno, M. *J. Am. Chem. Soc.* **1998**, *120*, 431; (c) Mukaiyama, T.; Shiina, I.; Uchiro, H.; Kobayashi, S. *Bull. Chem. Soc. Jpn.* **1994**, *67*, 1708; (d) Sharpless, K. B.; Amberg, W.; Bennani, Y. L.; Crispino, G. A.; Hartung, J.; Jeong, K.-S.; Kwong, H.-L.; Morikawa, K.; Wang, Z.-M.; Xu, D.; Zhang, X.-L. *J. Org. Chem.* **1992**, *57*, 2768.
27. (a) Mukaiyama, T.; Shiina, I.; Iwadare, H.; Saitoh, M.; Nishimura, T.; Ohkawa, N.; Sakoh, H.; Nishimura, K.; Tani, Y.; Hasegawa, M.; Yamada, K.; Saitoh, K. *Chem.—Eur. J.* **1999**, *5*, 121; (b) Kang, S. H.; Kim, C. M.; Youn, J.-H. *Tetrahedron Lett.* **1999**, *40*, 3581; (c) Lee, K.-Y.; Kim, Y.-H.; Park, M.-S.; Ham, W.-H. *Tetrahedron Lett.* **1998**, *39*, 8129; (d) Bunnage, M. E.; Davies, S. G.; Goodwin, C. J. *J. Chem. Soc., Perkin Trans. 1* **1994**, 2385; (e) Commercon, A.; Bezard, D.; Bernard, F.; Bourzat, J. D. *Tetrahedron Lett.* **1992**, *33*, 5185.
28. (a) Song, C. E.; Lee, S. W.; Roh, E. J.; Lee, S.-G.; Lee, W.-K. *Tetrahedron: Asymmetry* **1998**, *9*, 983; (b) Farina, V.; Hauck, S. I.; Walker, D. G. *Synlett* **1992**, 761; (c) Ojima, I.; Habus, I.; Zhao, M.; Zucco, M.; Park, Y. H.; Sun, C. M.; Brigaud, T. *Tetrahedron* **1992**, *48*, 4323.
29. Akbulut, N.; Hartsough, D.; Kim, J.-I.; Schuster, G. B. *J. Org. Chem.* **1989**, *54*, 2549.
30. Imashiro, R.; Seki, M. *J. Org. Chem.* **2004**, *69*, 4216.
31. (a) Shing, T. K. M.; Lee, C. M.; Lo, H. Y. *Tetrahedron* **2004**, *60*, 9179; (b) Shing, T. K. M.; Lee, C. M.; Lo, H. Y. *Tetrahedron Lett.* **2001**, *42*, 8361; (c) Shing, T. K. M.; Lo, H. Y.; Mak, T. C. W. *Tetrahedron* **1999**, *55*, 4643.

32. Acid **22** was not sensitive to the chiral shift reagent under various solvents and concentrations. To overcome this problem, acid **22** was esterified by EtBr and DBU back to acetal **21**, which gave better resolution of the separated peaks in the ^1H NMR spectrum upon shift reagent addition.
33. Zhang, W.; Loebach, J. L.; Wilson, S. R.; Jacobsen, E. N. *J. Am. Chem. Soc.* **1990**, *112*, 2801.
34. Yasukouchi, T.; Kanematsu, K. *Tetrahedron Lett.* **1989**, *30*, 6559.
35. Sodeoka, M.; Yamada, H.; Shabasaki, M. *J. Am. Chem. Soc.* **1990**, *112*, 4906.

Catalytic asymmetric epoxidation of α,β -unsaturated *N*-acylpyrroles as monodentate and activated ester equivalent acceptors

Shigeki Matsunaga,* Hongbo Qin, Mari Sugita, Shigemitsu Okada, Tomofumi Kinoshita, Noriyuki Yamagiwa and Masakatsu Shibasaki*

Graduate School of Pharmaceutical Sciences, The University of Tokyo, Hongo 7-3-1, Bunkyo-ku, Tokyo 113-0033, Japan

Received 28 October 2005; revised 5 December 2005; accepted 7 December 2005

Available online 30 May 2006

Abstract—Catalytic asymmetric epoxidation of α,β -unsaturated *N*-acylpyrroles as monodentate and activated ester equivalent acceptors is described. A Sm(*O*-*i*-Pr)₃/(*R*)-H₈-BINOL complex promoted the epoxidation reaction to afford products in high yield (up to quant) and high enantiomeric excess (up to >99.5% ee). Reaction proceeded smoothly using cumene hydroperoxide (CMHP) with low explosive hazard, and completed within 0.2–0.5 h with 5 mol % catalyst. Catalyst loading was successfully reduced to as little as 0.02 mol %. The *N*-acylpyrrole properties as well as efficient synthesis of α,β -unsaturated *N*-acylpyrroles are also described.

© 2006 Elsevier Ltd. All rights reserved.

1. Introduction

Catalytic asymmetric epoxidation of α,β -unsaturated carbonyl compounds is one of the most important transformations in organic synthesis.¹ Although we and others have achieved efficient catalytic asymmetric epoxidation of enones,^{1,2} there are few examples of α,β -unsaturated esters as substrates using a salen/Mn complex³ or chiral ketones⁴ as the catalysts. We also recently reported a yttrium/biphenyldiol catalyst for the epoxidation of α,β -unsaturated esters.^{5,6} Although excellent enantiomeric excess and yield were achieved with various α,β -unsaturated esters (up to 97% yield, up to 99% ee), there are some practical problems: (a) catalyst loading and reaction rate: 2–10 mol % catalyst loading was essential for good conversion; in many cases it was difficult to complete the conversion with less than 1 mol % catalyst; (b) turnover frequency (TOF) of the catalyst was, in most cases, approximately 1–3 h⁻¹; a higher TOF is desirable. (c) Oxidant: *tert*-butyl hydroperoxide (TBHP) with explosive hazard was essential for good reactivity. From a practical viewpoint, it is desirable to use less explosive (less reactive) cumene hydroperoxide (CMHP). In this manuscript, we report the use of α,β -unsaturated *N*-acylpyrrole (Fig. 1, **1**) as a monodentate and activated α,β -unsaturated ester surrogate to overcome the above-mentioned problems. A Sm(*O*-*i*-Pr)₃/(*R*)-H₈-BINOL (Fig. 1)

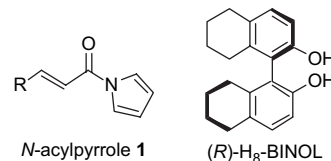


Figure 1. Structures of α,β -unsaturated *N*-acylpyrrole **1** and (*R*)-H₈-BINOL.

complex promoted the epoxidation reaction to afford products in high yield (up to quant) and high enantiomeric excess (up to >99.5% ee). Catalyst loading was also successfully reduced to as little as 0.02 mol % and a high TOF (>3000 h⁻¹) was realized.⁷

2. Design and synthesis of α,β -unsaturated *N*-acylpyrroles

The postulated catalytic cycle of the asymmetric epoxidation reaction is shown in Figure 2. A rare earth metal alkoxide moiety changes to a rare earth metal-peroxide through proton exchange (I). The rare earth metal/BINOL complex also functions as a Lewis acid to activate electron deficient olefins through monodentate coordination (II). Enantioselective 1,4-addition of rare earth metal-peroxide gives intermediate enolate (III), followed by epoxide formation to regenerate the catalyst (IV). In the transition state for the 1,4-addition step, the rare earth metal/BINOL complex,

* Corresponding authors. Tel.: +81 3 5841 4830; fax: +81 3 5684 5206; e-mail addresses: smatsuna@mol.f.u-tokyo.ac.jp; mshibasa@mol.f.u-tokyo.ac.jp

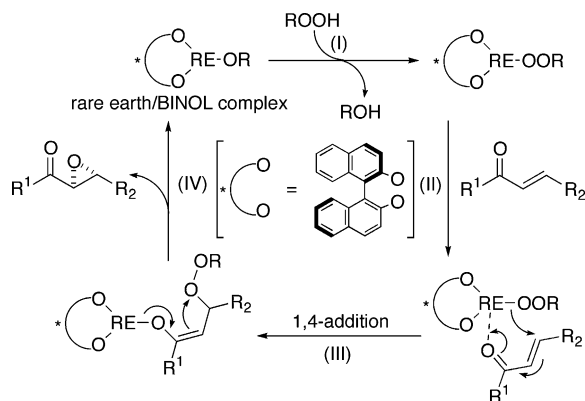
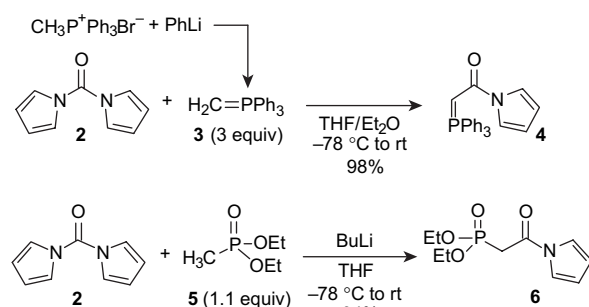


Figure 2. Postulated catalytic cycle of asymmetric epoxidation promoted by rare earth metal alkoxide/BINOL complex.

originally optimized for enones,² is postulated to favor the monodentate coordination mode for high enantioselectivity. When a bidentate α,β -unsaturated oxazolidinone amide is used as an activated carboxylic acid derivative, epoxide is obtained in only 73% yield and 87% ee after 24 h, using as much as 20 mol % catalyst loading, probably due to a coordination mode mismatch.⁶

The ideal substrates for epoxidation with rare earth metal/BINOL complexes should (i) favor a monodentate coordination mode similar to enones, (ii) have the same oxidation state as carboxylic acids, and (iii) be activated as an electrophile. To meet these criteria, an α,β -unsaturated *N*-acylpyrrole **1** (Fig. 1) was selected as a template for investigation of the following reasons. The unique properties and reactivity of *N*-acylpyrroles were reported by Evans and co-workers.⁸ Because the lone electron pair of the nitrogen in the pyrrole ring is delocalized in an aromatic system, the properties of the carbonyl group are similar to those of a phenyl ketone rather than an amide or an ester. The reactivity of α,β -unsaturated *N*-acylpyrrole is thus much higher than that of simple amide and ester. In contrast to the bidentate α,β -unsaturated oxazolidinone amide, *N*-acylpyrrole is supposed to favor monodentate coordination. Furthermore, the *N*-acylpyrrole moiety is relatively stable compared with the *N*-acylimidazole moiety, as predicted from the difference in the p*K*_a values of pyrrole (23.0 in DMSO) and imidazole (18.6 in DMSO). Thus, the *N*-acylpyrrole moiety would be compatible with various catalytic asymmetric reaction conditions. We recently demonstrated the utility of *N*-acylpyrroles as activated monodentate ester equivalents in various other catalytic asymmetric reactions.^{9,10} The *N*-acylpyrrole moiety can be transformed to various functional groups.^{8,9,10}

In the literature, the most efficient synthesis of α,β -unsaturated *N*-acylpyrrole was the condensation of cinnamamide and 2,5-dimethoxytetrahydrofuran in acetic acid or with SOCl₂ at high temperature,^{8a,11} affording **1a** in 60–68% yield. For the synthesis of α,β -unsaturated *N*-acylpyrroles with various functional groups, however, a milder method is necessary. One reason for not using α,β -unsaturated *N*-acylpyrrole widely as an acceptor for 1,4-addition reactions might be the lack of efficient preparation methods under mild conditions. Our synthetic procedure for α,β -unsaturated *N*-acylpyrroles using Wittig reagent **4** and HWE reagent **6** are summarized in Scheme 1, and in Tables 1



Scheme 1. Synthesis of Wittig reagent **4** and HWE reagent **6**.

and **2**. The reaction of carbonyldipyrrole **2**¹² with ylide **3** afforded **4** in 98% yield when 3 equiv of **3** was used (Scheme 1).¹³ The HWE reagent **6** was also synthesized by the reaction of **2** with 1.1 equiv of lithiated **5** in 94% yield. The Wittig reaction to afford α,β -unsaturated *N*-acylpyrroles is summarized in Table 1. With aromatic (entries 1–9) and heteroaromatic (entries 10–12) aldehydes, both the chemical yield and *E/Z* ratio were good using Wittig reagent **4**. Both the electron donating (entries 3 and 4) and withdrawing (entries 5 and 6) substituents at the *para*-position gave products in high yield and *E/Z* ratio (>20/1). With *ortho*-substituents, the *E/Z* ratio decreased to 7/1 (entry 8) and 10/1 (entry 9). For enolizable aliphatic aldehydes, HWE reactions with **6** under Masamune–Roush conditions¹⁴ were appropriate (Table 2), and afforded various β -alkyl substituted

Table 1. Synthesis of α,β -unsaturated *N*-acylpyrrole **1** using Wittig reagent **4**

Entry	Aldehyde R	Product	Temp (°C)	Time (h)	Yield (%)	<i>E/Z</i>
1	Ph-, 7a	1a	100	48	97	>20/1
2	2-naphthyl, 7b	1b	100	48	Quant	>20/1
3	4-Me-C ₆ H ₄ -, 7c	1c	100	48	98	>20/1
4	4-MeO-C ₆ H ₄ -, 7d	1d	110	84	97	>20/1
5	4-Br-C ₆ H ₄ -, 7e	1e	100	36	98	>20/1
6	4-Cl-C ₆ H ₄ -, 7f	1f	100	24	Quant	>20/1
7	3-Cl-C ₆ H ₄ -, 7g	1g	100	24	98	>15/1
8	2-Cl-C ₆ H ₄ -, 7h	1h	100	24	95	7/1
9	1-naphthyl, 7i	1i	100	48	Quant	10/1
10	2-furyl, 7j	1j	100	48	91	>15/1
11	2-thienyl, 7k	1k	100	36	Quant	>20/1
12	4-pyridyl, 7l	1l	100	48	Quant	>20/1
13	PhCH ₂ C(CH ₃) ₂ -, 7m	1m	110	84	63	>20/1
14	BnOCH ₂ C(CH ₃) ₂ -, 7n	1n	110	84	63	>20/1

Table 2. Synthesis of α,β -unsaturated *N*-acylpyrrole **1** using HWE reagent **6**

Entry	Aldehyde R	Product	Time (h)	Yield (%)	<i>E/Z</i>
1	(CH ₃) ₂ CHCH ₂ -, 7o	1o	13	96	>20/1
2	<i>n</i> -Pr, 7p	1p	12	90	>20/1
3	PhCH ₂ CH ₂ -, 7q	1q	22	89	>20/1
4	CH ₂ =CH(CH ₂) ₈ -, 7r	1r	15	94	>20/1
5	<i>i</i> -Pr, 7s	1s	10	90	>20/1
6	<i>cyclo</i> -Hex, 7t	1t	24	98	>20/1

α,β -unsaturated *N*-acylpyrroles in good yield and with high *E*-selectivity.

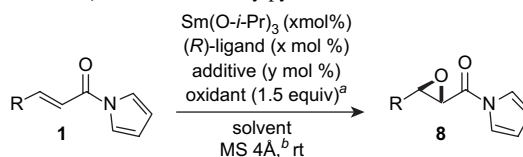
3. Catalytic asymmetric epoxidation of α,β -unsaturated *N*-acylpyrroles

The catalytic asymmetric epoxidation of **1a** proceeded smoothly, as summarized in Table 3. With 10 mol % of the Sm(*O*-*i*-Pr)₃/(*R*)-BINOL complex,¹⁵ 10 mol % of Ph₃As(O), and 1.5 equiv of TBHP, the reaction was completed within 0.5 h and afforded **8a** in 93% yield and 94% ee (entry 1). The reaction rate was much faster than when using other carboxylic acid derivatives^{5,6} and as fast as that using enones.^{1,16} The reaction also proceeded smoothly with 5 mol % catalyst (entry 2: 85% yield, 96% ee). To improve the enantioselectivity, various BINOL derivatives were screened to determine that H₈-BINOL functioned best. The H₈-BINOL complex gave better results than the BINOL complex, probably due to the large bite angle.¹⁷ With a Sm(*O*-*i*-Pr)₃/(*R*)-H₈-BINOL complex, **8a** was obtained in 99% ee (entry 3). Ph₃P(O) was also effective for *N*-acylpyrrole **1a** (entries 4–6). THF/toluene mixed solvent produced better results than THF alone, and **8a** was obtained in 96–99% ee, depending on the amount of Ph₃P(O) (entries 7–9). Both the reaction rate and selectivity were highest with 100 mol % of Ph₃P(O) (entry 9). Under the best conditions (THF/toluene, Ph₃P(O): 100 mol %), less explosive and less reactive CMHP was also applicable and the reaction reached completion within 0.2 h with 5 mol % catalyst (entry 10, 98% yield, >99.5% ee). The result in entry 10 gave additional practical benefits to the present system compared with our previous reports.^{5,6} The substrate scopes for the epoxidation reactions are summarized in entries 10–17.¹⁸ In all the substrates, commercially available CMHP (tech. 80% grade) was used without purification. Various β -aryl substituted α,β -unsaturated *N*-acylpyrroles

had high reactivity regardless of the substituents on the aromatic rings, providing epoxides in 91–98% yield and in 99 to >99.5% ee after 0.2 h (entries 10–14). β -Alkyl substituted α,β -unsaturated *N*-acylpyrroles had slightly lower reactivity. The reaction completed within 0.2–0.5 h, giving epoxides in 90–95% yield and 99–>99.5% ee (entries 15–17). Because the reaction proceeded via 1,4-addition of samarium peroxide, chemoselective epoxidation of electron deficient carbon–carbon double bond was realized with α,β -unsaturated *N*-acylpyrrole **1r**.

We then tried to reduce the catalyst loading. As expected from the high reaction rate with 5 mol % catalyst loading (Table 3), catalyst loading was easily reduced. TBHP was utilized instead of CMHP to reduce the catalyst loading and to achieve a higher reaction rate. As summarized in Table 4, the epoxidation reaction of **1a** completed using as little as 1, 0.5, or 0.2 mol % of Sm(*O*-*i*-Pr)₃/H₈-BINOL complex with 100 mol % of Ph₃P(O), giving product **8a** in high yield (94% quant) and high ee (96–99% ee) after 0.3–1 h (entries 2–4). The reaction proceeded well with as little as 0.1 mol % catalyst loading (substrate/catalyst=1000), affording product in 90.4% yield (turnover number [TON]=904) and 96% ee (entry 5). With the Sm(*O*-*i*-Pr)₃/H₈-BINOL/Ph₃As(O)=1/1/1 complex, catalyst loading was further reduced to 0.1, 0.05, and 0.02 mol % (substrate/catalyst=up to 5000) as summarized in entries 6–8. The high catalyst TON (TON=4710) and high TOF (up to >3000 h⁻¹) in entry 8 was far better compared with previous reports from our group.^{5,6} Because the commercially available TBHP solution in decane (5–6 M) contains up to 4% water, use of the wet TBHP solution in decane was not suitable for reduced catalyst loading (entries 3–8). Thus, TBHP in toluene (ca. 4.5 M) dried with 4 Å MS (water content $\leq 0.4\%$) was alternatively used to avoid decomposition of the Sm(*O*-*i*-Pr)₃/H₈-BINOL catalyst by excess H₂O.

Table 3. Catalytic asymmetric epoxidation reaction of α,β -unsaturated *N*-acylpyrrole

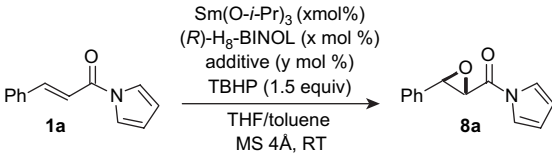


Entry	<i>N</i> -Acylpyrrole R	Sm(<i>O</i> - <i>i</i> -Pr) ₃ (x mol %)	Ligand (x mol %)	Additive (y mol %)	Solvent	Oxidant	Time (h)	Yield (%)	ee (%)
1	Ph, 1a	10	BINOL (10)	Ph ₃ As(O) (10)	THF	TBHP	0.5	93	94
2	Ph, 1a	5	BINOL (5)	Ph ₃ As(O) (5)	THF	TBHP	0.5	85	96
3	Ph, 1a	5	H ₈ -BINOL (5)	Ph ₃ As(O) (5)	THF	TBHP	0.5	94	99
4	Ph, 1a	5	H ₈ -BINOL (5)	Ph ₃ P(O) (15)	THF	TBHP	0.5	84	94
5	Ph, 1a	5	H ₈ -BINOL (5)	Ph ₃ P(O) (50)	THF	TBHP	0.5	88	98
6	Ph, 1a	5	H ₈ -BINOL (5)	Ph ₃ P(O) (100)	THF	TBHP	0.5	85	97
7	Ph, 1a	5	H ₈ -BINOL (5)	Ph ₃ P(O) (15)	THF/toluene	TBHP	0.4	85	96
8	Ph, 1a	5	H ₈ -BINOL (5)	Ph ₃ P(O) (50)	THF/toluene	TBHP	0.5	92	99
9	Ph, 1a	5	H ₈ -BINOL (5)	Ph ₃ P(O) (100)	THF/toluene	TBHP	0.2	97	99
10	Ph, 1a	5	H ₈ -BINOL (5)	Ph ₃ P(O) (100)	THF/toluene	CMHP	0.2	98	>99.5
11	2-naphthyl, 1b	5	H ₈ -BINOL (5)	Ph ₃ P(O) (100)	THF/toluene	CMHP	0.2	93	>99.5
12	4-Me-C ₆ H ₄ -, 1c	5	H ₈ -BINOL (5)	Ph ₃ P(O) (100)	THF/toluene	CMHP	0.2	98	>99.5
13	4-MeO-C ₆ H ₄ -, 1d	5	H ₈ -BINOL (5)	Ph ₃ P(O) (100)	THF/toluene	CMHP	0.2	91	99
14	4-Cl-C ₆ H ₄ -, 1f	5	H ₈ -BINOL (5)	Ph ₃ P(O) (100)	THF/toluene	CMHP	0.2	97	>99.5
15 ^c	PhCH ₂ CH ₂ -, 1q	5	H ₈ -BINOL (5)	Ph ₃ P(O) (100)	THF/toluene	CMHP	0.5	91	99
16	H ₂ C=CH(CH ₂) ₈ -, 1r	5	H ₈ -BINOL (5)	Ph ₃ P(O) (100)	THF/toluene	CMHP	0.3	95	99
17	Cyclohex, 1t	5	H ₈ -BINOL (5)	Ph ₃ P(O) (100)	THF/toluene	CMHP	0.2	90	>99.5

^a TBHP in decane (5–6 M) and CMHP (80% tech. grade) purchased from Aldrich were used as received.

^b 1000 mg of 4 Å MS mmol⁻¹ of compound **1** was used.

^c CMHP (2.5 equiv) was used.

Table 4. Catalytic asymmetric epoxidation reaction of α,β -unsaturated *N*-acylpyrrole with reduced catalyst loading


Entry	Sm(<i>O</i> - <i>i</i> -Pr) ₃ (x mol %)	H ₈ -BINOL (x mol %)	Additive (y mol %)	MS 4 Å (mg mmol ⁻¹ of 1a)	Concd Of [1a] (M)	Time (h)	Yield (%)	ee (%)
1 ^a	5	5	Ph ₃ P(O) (100)	1000	0.1	0.2	97	99
2 ^a	1	1	Ph ₃ P(O) (100)	500	1	0.3	94	99
3 ^b	0.5	0.5	Ph ₃ P(O) (100)	250	1	0.6	Quant	97
4 ^b	0.2	0.2	Ph ₃ P(O) (100)	100	2	1	99	97
5 ^b	0.1	0.1	Ph ₃ P(O) (100)	100	2	2	90	96
6 ^b	0.1	0.1	Ph ₃ As(O) (0.1)	100	3	0.6	Quant	99
7 ^b	0.05	0.05	Ph ₃ As(O) (0.05)	100	3	1	Quant	98
8 ^b	0.02	0.02	Ph ₃ As(O) (0.02)	100	3	1.5	94	99

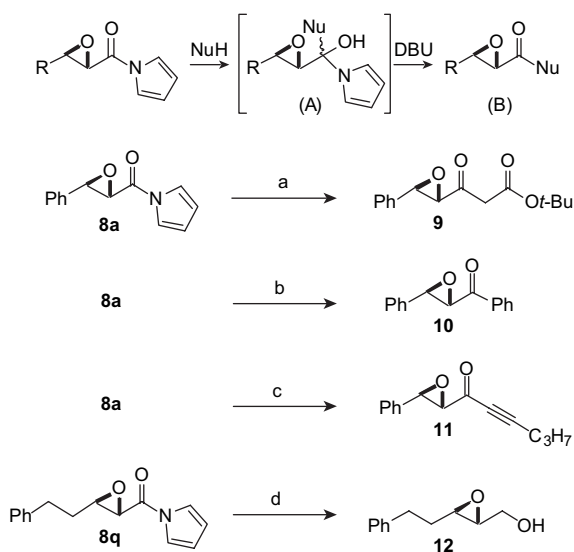
^a Commercially available TBHP solution in decane (5–6 M) was used.

^b Dried TBHP solution in toluene was used.

To reduce the catalyst loading, it was important to keep the concentration of the catalyst within 1–5 mM, which was similar to the best conditions with 5 mol % catalyst loading ([Sm(*O*-*i*-Pr)₃/H₈-BINOL]=5 mM). Thus, the concentration of substrate **1a** increased accordingly when the reaction shown in Table 4 was performed. For example, [**1a**] was 2 M in entry 5 and 3 M in entries 6–8. High volumetric productivity of the present system together with reduced catalyst loading is noteworthy for large scale synthesis. Further experiments to reduce catalyst loading were unsuccessful because it was difficult to maintain the appropriate concentration of Sm catalyst due to solubility problems of product **8a**.

4. Transformation of *N*-acylpyrrole unit

To demonstrate the synthetic utility of the *N*-acylpyrrole unit, several transformations were performed (Scheme 2).¹⁹



Scheme 2. Transformations of *N*-acylpyrrole units: reagents and conditions: (a) *t*-butyl acetate, BuLi, THF, –78 °C, 10 min; then DBU, CH₂Cl₂, 25 °C, 20 min, 74% yield (two steps); (b) PhLi, THF, –78 °C, 10 min; then DBU, CH₂Cl₂, 25 °C, 20 min, 88% yield (two steps); (c) BuLi, 1-pentyne, THF, –78 °C, 10 min; then DBU, CH₂Cl₂, 0 °C, 10 min, 84% yield (two steps); (d) LiBH₄, THF, 0–25 °C, 1 h; then NaBH₄, 25 °C, 4 h, 72% yield (two steps).

Reactions with carbon nucleophiles were examined using the procedure reported by Evans and co-workers.^{8a} The addition of various nucleophiles afforded relatively stable pyrrole carbinol intermediate (A) in Scheme 2. Treatment of the pyrrole carbinol with DBU promoted the elimination of pyrrole to afford the corresponding product (B). Pyrrolyl epoxide **8a** was converted to β -ketoester **9** in 74% yield by the addition of lithium enolate prepared from *t*-butyl acetate, followed by treatment with DBU. α,β -Epoxy ketone **10** was obtained in 88% yield using PhLi and DBU. The addition of lithiated alkyne gave **11** in 84% yield after treatment with DBU. In two steps, **8q** was reduced to epoxyalcohol **12**; successive treatment with LiBH₄ and NaBH₄ gave **12** in 72% yield.

5. Conclusion

In summary, the utility of α,β -unsaturated *N*-acylpyrroles as monodentate and activated ester equivalent acceptors was demonstrated in catalytic asymmetric epoxidation reactions. Various α,β -unsaturated *N*-acylpyrroles were synthesized using either Wittig reagent **4** or HWE reagent **6**. A Sm(*O*-*i*-Pr)₃/(*S*)-H₈-BINOL complex promoted the epoxidation reaction to afford products in high yield (up to quant) and high enantiomeric excess (up to >99.5% ee). The reaction proceeded smoothly using the less explosive CMHP, and completed within 0.2–0.5 h. Catalyst loading was also successfully reduced to as little as 0.02 mol % with TBHP as an oxidant, realizing high TON (up to 4710) and TOF (up to >3000 h⁻¹) of the catalyst.

6. Experimental

6.1. General

Infrared (IR) spectra were recorded on a JASCO FTIR 410 Fourier transform infrared spectrophotometer. NMR spectra were recorded on a JEOL JNM-LA500 spectrometer, operating at 500 MHz for ¹H NMR and 125.65 MHz for ¹³C NMR. Chemical shifts in CDCl₃ were reported downfield from TMS (=0) or in the scale relative to CHCl₃ (7.24 ppm) for ¹H NMR. For ¹³C NMR, chemical shifts were reported in

the scale relative to CHCl_3 (77.0 ppm) as an internal reference. Optical rotations were measured on a JASCO P-1010 polarimeter. ESI mass spectra were measured on Waters-ZQ4000. FAB mass spectra were measured on JMS-MS 700V. Column chromatography was performed with silica gel Merck 60 (230–400 mesh ASTM). The enantiomeric excess (ee) was determined by HPLC analysis. HPLC was performed on JASCO HPLC systems consisting of the following: pump, PU-2080; detector, UV-2075, measured at 254 nm; column, DAICEL CHIRALCEL OJ, CHIRALPAK AD, AS, AD-H; mobile phase, hexane/2-propanol; flow rate, 1.0 mL min^{-1} . Reactions were carried out in dry solvent under argon atmosphere, unless otherwise stated. Tetrahydrofuran (THF) was distilled from sodium benzophenone ketyl. $\text{Sm}(O-i\text{-Pr})_3$ was purchased from Kojundo Chemical Laboratory Co., Ltd (fax: +81 492 84 1351; e-mail: sales@kojundo.co.jp). Cumene hydroperoxide (CMHP: 80% tech. grade) and *tert*-butyl hydroperoxide (TBHP: 5–6 M in decane) were purchased from Aldrich and used as received. Other reagents were purified by the usual methods.

6.2. Synthesis of pyrrolylmethylenetriphenylphosphorane (ylide: 4)

To a suspension of methyltriphenylphosphonium bromide (12.9 g, 36 mmol) in THF (14 mL) at 0 °C was added PhLi (Et_2O solution, 28.1 mL, 36 mmol). The mixture was stirred at 25 °C for 60 min to afford methylenetriphenylphosphorane **3**. Then, the mixture was cooled down to –78 °C, and then the solution of 1,1'-carbonyldipyrrole **2** (1.92 g, 12 mmol) in THF (18 mL) was added. The cooling bath was removed and the reaction mixture was stirred overnight at room temperature. H_2O was added and the mixture was extracted with ethyl acetate/ CH_2Cl_2 =5/1 ($\times 3$). The organic layers were washed with brine and dried over MgSO_4 . After evaporation, the residue was purified by silica gel flash column chromatography to afford ylide **4** (4.33 g, 11.7 mmol, 98% yield); IR (KBr) ν 3434, 3048, 1601, 1438 cm^{-1} ; ^1H NMR (CDCl_3) δ 7.68 (m, 6H), 7.56 (m, 3H), 7.47 (m, 6H), 7.33–7.35 (m, 2H), 6.15–6.18 (m, 2H), 3.71 (d, $J=9.3$ Hz, 1H); ^{13}C NMR (CDCl_3) δ 38.0 (d, $J_{\text{C-P}}=125$ Hz), 109.3, 118.3, 126.4 (d, $J_{\text{C-P}}=91.5$ Hz), 128.8 (d, $J_{\text{C-P}}=12.4$ Hz), 132.1 (d, $J_{\text{C-P}}=2.1$ Hz), 132.9 (d, $J_{\text{C-P}}=10.3$ Hz); ESIMS m/z 370 $[\text{M}+\text{H}]^+$; HRMS (FAB) m/z calcd for $\text{C}_{24}\text{H}_{21}\text{ONP}$ $[\text{M}+\text{H}]^+$: 370.1361; found: 370.1369.

6.3. General procedure of Wittig reaction for the synthesis of α,β -unsaturated *N*-acylpyrroles 1

To the suspension of ylide **4** (240 mg, 0.65 mmol) in toluene (1.25 mL) was added benzaldehyde **7a** (50.8 μL , 0.5 mmol). The suspension was stirred for 48 h at 100 °C, and cooled down to room temperature. The reaction mixture was evaporated under reduced pressure, and the residue was purified by silica gel flash column chromatography (hexane/ethyl acetate=20/1) to give **1a** in 97% yield.

6.4. Preparation of HWE reagent 6

To a stirred solution of diethyl methylphosphonate (**5**, 12.4 mL, 84.9 mmol) in THF (300 mL) at –78 °C was added BuLi (85.2 mmol, 53.9 mL, 1.58 M in hexane) slowly over 30 min. The mixture was stirred at –65 °C for 90 min,

and then carbonyldipyrrole (**2**, 12.5 g, 77.6 mmol) in THF (35 mL) was added slowly over 20 min. The mixture was stirred at the same temperature for 1 h, and then the mixture was gradually warmed to room temperature over 2 h. The reaction mixture was quenched with satd aq NH_4Cl and the mixture was vigorously stirred for 2 h at room temperature. The mixture was extracted with ethyl acetate. The organic layer was washed with brine, and dried over Na_2SO_4 . After removing the solvent, the residue was purified by silica gel flash column chromatography (hexane/ethyl acetate=2/1 to 0/1) to give **6** (18.0 g, 94% yield); IR (neat) ν 587, 746, 922, 973, 1025, 1164, 1255, 1336, 1472, 1713, 2985, 3288 cm^{-1} ; ^1H NMR (CDCl_3) δ 1.26–1.29 (m, 6H), 3.43 (d, $J=22.5$ Hz, 2H), 4.11–4.16 (m, 4H), 6.27–6.28 (m, 2H), 7.30 (br s, 2H); ^{13}C NMR (CDCl_3) δ 162.6, 119.6, 113.5, 62.8, 34.9 (d, $J_{\text{C-P}}=133$ Hz), 16.0; ESIMS m/z 268 $[\text{M}+\text{Na}]^+$; HRMS (FAB) m/z calcd for $\text{C}_{10}\text{H}_{16}\text{O}_4\text{NCsP}$ $[\text{M}+\text{Cs}]^+$: 377.9871; found: 377.9868.

6.5. Representative HWE procedure for the synthesis of α,β -unsaturated *N*-acylpyrrole 1

LiCl (2.54 g, 60 mmol) in a 500 mL flask was flame dried prior to use. Then, CH_3CN (200 mL) was added, and the mixture was cooled at 0 °C. To the mixture were added phosphonate **6** (8.06 g, 33 mmol) and Hünig's base (10.2 mL, 60 mmol). The mixture was stirred at 0 °C for 20 min, and then was added aldehyde **7a** (3.22 mL, 30 mmol). The mixture was stirred at room temperature for 13 h, and H_2O was added. The mixture was extracted with ethyl acetate. The organic layer was washed with brine, and was dried over Na_2SO_4 . After removing the solvent, the residue was purified by silica gel flash column chromatography (hexane/ethyl acetate=30/1) to give **1a** (5.16 g, 96% yield).

6.5.1. (2*E*)-3-Phenyl-1-pyrrol-1-yl-2-propen-1-one (1a).

Colorless solid; IR (KBr) ν 1688, 1624, 1467, 1351 cm^{-1} ; ^1H NMR (CDCl_3) δ 7.98 (d, $J=15.6$ Hz, 1H), 7.61 (dd, $J=3.7, 3.4$ Hz, 2H), 7.40–7.49 (m, 4H), 7.13 (d, $J=15.6$ Hz, 1H); ^{13}C NMR (CDCl_3) δ 162.9, 147.5, 134.2, 130.9, 129.0, 128.4, 119.2, 115.7, 113.3; ESIMS: m/z 220 $[\text{M}+\text{Na}]^+$; HRMS (FAB) m/z calcd for $\text{C}_{13}\text{H}_{12}\text{ON}$ $[\text{M}+\text{H}]^+$: 198.0920; found: 198.0919.

6.5.2. (2*E*)-3-(2-Naphthyl)-1-pyrrol-1-yl-2-propen-1-one (1b).

Colorless solid; IR (KBr) ν 1680, 1617, 1466, 1300 cm^{-1} ; ^1H NMR (CDCl_3) δ 8.15 (d, $J=15.3$ Hz, 1H), 8.03 (s, 1H), 7.84–7.91 (m, 3H), 7.75 (m, 1H), 7.51–7.57 (m, 4H), 7.26 (d, $J=15.3$ Hz, 1H), 6.30–6.35 (m, 2H); ^{13}C NMR (CDCl_3) δ 163.0, 147.6, 134.5, 133.3, 131.7, 130.8, 128.8, 128.7, 127.6, 126.9, 123.4, 119.3, 115.8, 113.3; ESIMS: m/z 270 $[\text{M}+\text{Na}]^+$; HRMS (FAB) m/z calcd for $\text{C}_{17}\text{H}_{14}\text{ON}$ $[\text{M}+\text{H}]^+$: 248.1075; found: 248.1075.

6.5.3. (2*E*)-3-(4-Methylphenyl)-1-pyrrol-1-yl-2-propen-1-one (1c).

Colorless solid; IR (KBr) ν 1686, 1621, 1467, 1352 cm^{-1} ; ^1H NMR (CDCl_3) δ 7.96 (d, $J=15.6$ Hz, 1H), 7.51 (d, $J=8.0$ Hz, 2H), 7.45 (br s, 2H), 7.22 (d, $J=8.0$ Hz, 2H), 7.09 (d, $J=15.6$ Hz, 1H), 2.39 (s, 3H); ^{13}C NMR (CDCl_3) δ 163.1, 147.6, 141.6, 131.5, 129.7, 128.5, 119.2, 114.5, 113.2, 21.5; ESIMS: m/z 234 $[\text{M}+\text{Na}]^+$; HRMS (FAB) m/z calcd for $\text{C}_{14}\text{H}_{14}\text{NO}$ $[\text{M}+\text{H}]^+$: 212.1075; found: 212.1076.

6.5.4. (2E)-3-(4-Methoxyphenyl)-1-pyrrol-1-yl-2-propen-1-one (1d). Colorless solid; IR (KBr) ν 1687, 1625, 1603, 1512, 1466, 1248 cm^{-1} ; ^1H NMR (CDCl_3) δ 7.94 (d, $J=15.3$ Hz, 1H), 7.57 (d, $J=8.5$ Hz, 2H), 7.45 (br s, 2H), 6.99 (d, $J=15.3$ Hz, 1H), 6.93 (d, $J=8.5$ Hz, 2H), 6.33 (br s, 2H), 3.85 (s, 3H); ^{13}C NMR (CDCl_3) δ 163.2, 161.9, 147.3, 130.2, 127.0, 119.2, 114.4, 113.0, 55.4; ESIMS: m/z 250 $[\text{M}+\text{Na}]^+$; HRMS (FAB) m/z calcd for $\text{C}_{14}\text{H}_{14}\text{O}_2\text{N}$ $[\text{M}+\text{H}]^+$: 228.1024; found: 228.1020.

6.5.5. (2E)-3-(4-Bromophenyl)-1-pyrrol-1-yl-2-propen-1-one (1e). Colorless solid; IR (KBr) ν 2922, 1685, 1622, 1471 cm^{-1} ; ^1H NMR (CDCl_3) δ 7.92 (d, $J=15.6$ Hz, 1H), 7.45–7.59 (m, 6H), 7.13 (d, $J=15.6$ Hz, 1H), 6.36–6.38 (m, 2H); ^{13}C NMR (CDCl_3) δ 162.7, 146.1, 133.1, 132.3, 129.8, 125.3, 119.2, 116.3, 113.5; ESIMS: m/z 298, 300 $[\text{M}+\text{Na}]^+$; HRMS (FAB) m/z calcd for $\text{C}_{13}\text{H}_{11}\text{ONBr}$ $[\text{M}+\text{H}]^+$: 276.0014; found: 276.0019.

6.5.6. (2E)-3-(4-Chlorophenyl)-1-pyrrol-1-yl-2-propen-1-one (1f). Colorless solid; IR (KBr) ν 1674, 1620, 1469, 1352, 1255 cm^{-1} ; ^1H NMR (CDCl_3) δ 7.87 (d, $J=15.6$ Hz, 1H), 7.49 (d, $J=8.6$ Hz, 2H), 7.39 (dd, $J=2.5$, 2.2 Hz, 2H), 7.34 (d, $J=8.6$ Hz, 2H), 7.04 (d, $J=15.6$ Hz, 1H), 6.30 (dd, $J=2.5$, 2.2 Hz, 2H); ^{13}C NMR (CDCl_3) δ 162.6, 146.0, 136.9, 132.7, 129.6, 129.3, 119.2, 116.2, 113.5; ESIMS: m/z 254 $[\text{M}+\text{Na}]^+$; HRMS (FAB) m/z calcd for $\text{C}_{13}\text{H}_{11}\text{ONCl}$ $[\text{M}+\text{H}]^+$: 232.0529; found: 232.0529.

6.5.7. (2E)-3-(3-Chlorophenyl)-1-pyrrol-1-yl-2-propen-1-one (1g). Colorless solid; IR (KBr) ν 1685, 1623, 1466 cm^{-1} ; ^1H NMR (CDCl_3) δ 7.90 (d, $J=15.6$ Hz, 1H), 7.60 (s, 1H), 7.35–7.49 (m, 5H), 7.14 (d, $J=15.6$ Hz, 1H), 6.36–6.39 (m, 2H); ^{13}C NMR (CDCl_3) δ 162.5, 145.8, 136.0, 135.0, 130.7, 130.3, 127.9, 126.8, 119.2, 117.1, 113.6; ESIMS: m/z 254, 256 $[\text{M}+\text{Na}]^+$; HRMS (FAB) m/z calcd for $\text{C}_{13}\text{H}_{11}\text{ONCl}$ $[\text{M}+\text{H}]^+$: 232.0529; found: 232.0534.

6.5.8. (2E)-3-(2-Chlorophenyl)-1-pyrrol-1-yl-2-propen-1-one (1h). Colorless solid; IR (KBr) ν 1685, 1621, 1469, 1349, 1285 cm^{-1} ; ^1H NMR (CDCl_3) δ 8.30 (d, $J=15.6$ Hz, 1H), 7.64 (d, $J=5.8$ Hz, 1H), 7.39 (br s, 3H), 7.28 (m, 2H), 7.09 (d, $J=15.6$ Hz, 1H), 6.30 (br s, 2H); ^{13}C NMR (CDCl_3) δ 162.5, 143.3, 135.4, 132.6, 131.5, 130.4, 127.9, 127.1, 119.3, 118.6, 113.5; ESIMS: m/z 254 $[\text{M}+\text{Na}]^+$; HRMS (FAB) m/z calcd for $\text{C}_{13}\text{H}_{11}\text{ONCl}$ $[\text{M}+\text{H}]^+$: 232.0529; found: 232.0526.

6.5.9. (2E)-3-(1-Naphthyl)-1-pyrrol-1-yl-2-propen-1-one (1i). Colorless solid; IR (KBr) ν 1682, 1616, 1471, 1357 cm^{-1} ; ^1H NMR (CDCl_3) δ 8.76 (d, $J=15.0$ Hz, 1H), 8.18 (d, $J=8.3$ Hz, 1H), 7.88 (d, $J=8.3$ Hz, 1H), 7.79 (d, $J=7.0$ Hz, 1H), 7.42–7.57 (m, 5H), 6.31 (br s, 2H); ^{13}C NMR (CDCl_3) δ 162.8, 144.6, 133.7, 131.7, 131.5, 131.2, 128.8, 127.1, 126.4, 125.4, 125.2, 123.3, 119.3, 118.4, 113.4, 113.2; ESIMS: m/z 270 $[\text{M}+\text{Na}]^+$; HRMS (FAB) m/z calcd for $\text{C}_{17}\text{H}_{14}\text{ON}$ $[\text{M}+\text{H}]^+$: 248.1075; found: 248.1077.

6.5.10. (2E)-3-(2-Furyl)-1-pyrrol-1-yl-2-propen-1-one (1j). Colorless solid; IR (KBr) ν 1688, 1618, 1468 cm^{-1} ; ^1H NMR (CDCl_3) δ 7.73 (d, $J=15.3$ Hz, 1H), 7.55 (br s, 1H), 7.45–7.48 (m, 2H), 7.04 (d, $J=15.3$ Hz, 1H), 6.74 (d, $J=3.1$ Hz, 1H), 6.53 (dd, $J=1.9$, 3.1 Hz, 1H), 6.34–6.37

(m, 2H); ^{13}C NMR (CDCl_3) δ 162.8, 150.9, 145.2, 133.1, 119.1, 116.6, 113.2, 113.0, 112.7; ESIMS: m/z 210 $[\text{M}+\text{Na}]^+$; HRMS (FAB) m/z calcd for $\text{C}_{11}\text{H}_{10}\text{O}_2\text{N}$ $[\text{M}+\text{H}]^+$: 188.0711; found: 188.0716.

6.5.11. (2E)-1-Pyrrol-1-yl-3-(2-thienyl)-2-propen-1-one (1k). Colorless solid; IR (KBr) ν 1686, 1609, 1466 cm^{-1} ; ^1H NMR (CDCl_3) δ 8.10 (d, $J=15.0$ Hz, 1H), 7.43–7.47 (m, 3H), 7.37 (d, $J=3.4$ Hz, 1H), 7.10 (dd, $J=3.4$, 4.5 Hz, 1H), 6.92 (d, $J=15.0$ Hz, 1H), 6.34–6.38 (m, 2H); ^{13}C NMR (CDCl_3) δ 162.7, 139.8, 139.5, 132.4, 129.3, 128.4, 119.1, 114.2, 113.3; ESIMS: m/z 226 $[\text{M}+\text{Na}]^+$; HRMS (FAB) m/z calcd for $\text{C}_{11}\text{H}_{10}\text{ONS}$ $[\text{M}+\text{H}]^+$: 204.0483; found: 204.0489.

6.5.12. (2E)-3-(4-Pyridyl)-1-pyrrol-1-yl-2-propen-1-one (1l). Colorless solid; IR (KBr) ν 1687, 1466 cm^{-1} ; ^1H NMR (CDCl_3) δ 8.70 (d, $J=4.9$ Hz, 1H), 7.87 (d, $J=15.5$ Hz, 1H), 7.43–7.46 (m, 4H), 7.29 (d, $J=15.5$ Hz, 1H), 6.36–6.38 (m, 2H); ^{13}C NMR (CDCl_3) δ 162.0, 150.7, 144.4, 141.2, 121.9, 120.3, 119.2, 113.9; ESIMS: m/z 199 $[\text{M}+\text{H}]^+$; HRMS (FAB) m/z calcd for $\text{C}_{12}\text{H}_{11}\text{ON}_2$ $[\text{M}+\text{H}]^+$: 199.0871; found: 199.0871.

6.5.13. (2E)-4,4-Dimethyl-5-phenyl-1-pyrrol-1-yl-2-penten-1-one (1m). IR (KBr) ν 2956, 1682, 1629, 1469, 1349, 1297 cm^{-1} ; ^1H NMR (CDCl_3) δ 7.05–7.38 (m, 8H), 6.25–6.29 (m, 3H), 2.71 (s, 2H), 1.12 (s, 6H); ^{13}C NMR (CDCl_3) δ 163.0, 160.7, 137.4, 130.4, 130.2, 128.1, 127.9, 126.4, 119.2, 116.3, 113.1, 48.5, 38.5, 26.1; ESIMS: m/z 276 $[\text{M}+\text{Na}]^+$; HRMS (FAB) m/z calcd for $\text{C}_{17}\text{H}_{20}\text{ON}$ $[\text{M}+\text{H}]^+$: 254.1545; found: 254.1542.

6.5.14. (2E)-5-Benzyloxy-4,4-dimethyl-1-pyrrol-1-yl-2-penten-1-one (1n). Pale yellow oil; IR (neat) ν 2963, 2868, 1697, 1637, 1467, 1344, 1305, 1267 cm^{-1} ; ^1H NMR (CDCl_3) δ 7.22–7.36 (m, 8H), 6.50 (d, $J=15.6$ Hz, 1H), 6.29 (dd, $J=2.5$, 2.2 Hz, 2H), 4.51 (s, 2H), 3.31 (s, 2H), 1.15 (s, 6H); ^{13}C NMR (CDCl_3) δ 163.1, 158.8, 138.2, 128.3, 127.5, 127.4, 119.2, 117.0, 113.0, 77.9, 73.3, 38.8, 23.9; ESIMS: m/z 306 $[\text{M}+\text{Na}]^+$; HRMS m/z calcd for $\text{C}_{18}\text{H}_{21}\text{O}_2\text{N}$ $[\text{M}+\text{H}]^+$: 284.1650; found: 284.1647.

6.5.15. (2E)-5-Methyl-1-pyrrol-1-yl-2-hexen-1-one (1o). Colorless liquid; IR (neat) 3150, 2958, 1697, 1641, 1468, 1408, 1356, 1281, 1122, 742 cm^{-1} ; ^1H NMR (CDCl_3) δ 7.41 (t, $J=2.1$ Hz, 2H), 7.29 (dt, $J=7.6$, 15.3 Hz, 1H), 6.58 (dd, $J=15.3$ Hz, 1H), 6.35 (t, $J=2.1$ Hz, 2H), 2.29–2.22 (m, 2H), 1.87 (sept, $J=6.7$ Hz, 1H), 1.00 (d, $J=6.7$ Hz, 6H); ^{13}C NMR (CDCl_3) δ 162.7, 151.8, 120.4, 119.2, 113.1, 42.0, 27.9, 22.4; EIMS: m/z 177 $[\text{M}]^+$; HRMS (EI) m/z calcd for $\text{C}_{11}\text{H}_{15}\text{NO}$ $[\text{M}]^+$: 177.1154; found: 177.1163.

6.5.16. (2E)-1-Pyrrol-1-yl-2-hexen-1-one (1p). Light yellow liquid; IR (neat) 3149, 2961, 1698, 1641, 1468, 1355, 1277, 1121, 1072, 940 cm^{-1} ; ^1H NMR (CDCl_3) δ 7.38 (t, $J=2.3$ Hz, 2H), 7.27 (dt, $J=7.2$, 15.2 Hz, 1H), 6.56 (d, $J=15.2$ Hz, 1H), 6.32 (t, $J=2.3$ Hz, 2H), 2.34–2.29 (m, 2H), 1.62–1.51 (m, 2H), 0.98 (t, $J=7.5$ Hz, 3H); ^{13}C NMR (CDCl_3) δ 162.8, 152.7, 119.5, 119.2, 113.1, 34.8, 21.3, 13.7; MS: m/z 163 $[\text{M}]^+$; HRMS (EI) m/z calcd for $\text{C}_{10}\text{H}_{13}\text{NO}$ $[\text{M}]^+$: 163.0997; found: 163.0997.

6.5.17. (2E)-5-Phenyl-1-pyrrol-1-yl-2-penten-1-one (1q). Colorless oil; IR (neat) ν 1694, 1643, 1467, 1363, 1280 cm^{-1} ; ^1H NMR (CDCl_3) δ 7.38–7.16 (m, 8H), 6.53 (d, $J=15.0$ Hz, 1H), 6.31 (dd, $J=2.5, 2.2$ Hz, 2H), 2.85 (t, $J=7.6$ Hz, 2H), 2.71–2.62 (m, 2H); ^{13}C NMR (CDCl_3) δ 162.6, 151.2, 140.4, 128.5, 128.3, 126.2, 120.1, 119.1, 113.1, 34.3, 34.2; ESIMS: m/z 308 $[\text{M}+\text{Na}]^+$; HRMS (FAB) m/z calcd for $\text{C}_{15}\text{H}_{16}\text{ON}$ $[\text{M}+\text{H}]^+$: 226.1232; found: 226.1234.

6.5.18. (2E)-1-Pyrrol-1-yl-tridec-2,12-dien-1-one (1r). Colorless oil; IR (neat) ν 2926, 2854, 1702, 1642, 1467, 1351, 1291 cm^{-1} ; ^1H NMR (CDCl_3) δ 7.38 (t, $J=2.4$ Hz, 2H), 7.27 (m, 1H), 6.55 (d, $J=15.0$ Hz, 1H), 6.32 (dd, $J=2.5, 2.2$ Hz, 2H), 5.81 (m, 1H), 4.99 (d, $J=16.9$ Hz, 1H), 4.93 (d, $J=10.1$ Hz, 1H), 2.33 (m, 2H), 2.03 (m, 2H), 1.25–1.59 (m, 12H); ^{13}C NMR (CDCl_3) δ 167.8, 152.9, 139.1, 119.3, 119.2, 114.1, 113.1, 33.7, 32.8, 29.3, 29.3, 29.1, 29.0, 28.8, 28.0; ESIMS: m/z 282 $[\text{M}+\text{Na}]^+$; HRMS (FAB) m/z calcd for $\text{C}_{17}\text{H}_{26}\text{ON}$ $[\text{M}+\text{H}]^+$: 260.2014; found: 260.2014.

6.5.19. (2E)-3-Cyclohexyl-1-pyrrol-1-yl-2-propen-1-one (1t). Colorless oil; IR (neat) ν 2926, 2852, 1696, 1634, 1468, 1346, 1286 cm^{-1} ; ^1H NMR (CDCl_3) δ 7.38 (dd, $J=2.5, 2.2$ Hz, 2H), 7.22 (dd, $J=15.3, 7.1$ Hz, 1H), 6.50 (dd, $J=15.3, 1.3$ Hz, 1H), 6.32 (dd, $J=2.5, 2.2$ Hz, 2H), 2.26 (m, 1H), 1.65–1.90 (m, 5H), 1.15–1.40 (m, 5H); ^{13}C NMR (CDCl_3) δ 163.1, 157.6, 119.1, 116.9, 113.0, 41.0, 31.6, 25.8, 25.6; ESIMS: m/z 226 $[\text{M}+\text{Na}]^+$; HRMS (FAB) m/z calcd for $\text{C}_{15}\text{H}_{23}\text{O}_4$ $[\text{M}+\text{H}]^+$: 204.1388; found: 204.1382.

6.6. General procedure for catalytic asymmetric epoxidation reaction with 5 mol % catalyst loading

MS (4 Å, 500 mg, powdered) in a flask was dried prior to use at 160 °C under vacuum (0.7 KPa) for 3 h. To a stirred suspension of $\text{Ph}_3\text{P}(\text{O})$ (139 mg, 0.5 mmol), (*R*)- H_8 -BINOL (7.36 mg, 0.025 mmol), and 4 Å MS in THF (1.0 mL) and toluene (1.2 mL) at 25 °C was added $\text{Sm}(\text{O}-i\text{-Pr})_3$ (0.125 mL, 0.025 mmol, 0.2 M in THF). The mixture was stirred for 10 min at 25 °C and cumene hydroperoxide (CMHP) (0.14 mL, 0.75 mmol, 80% tech. grade) was added. After 5 min, the color of the mixture became pale orange, and then **1a** (98.6 mg, 0.5 mmol) was added. The reaction was quenched with 2.5% aq citric acid. The mixture was extracted with ethyl acetate ($\times 3$). Then combined organic layers were washed successively with satd aq NaHCO_3 and brine, and then dried over MgSO_4 . The solvent was evaporated and the resulting crude residue was purified by flash silica gel column chromatography (ethyl acetate/hexane=1/20) to afford **8a** (98% yield, >99.5% ee).

6.7. Procedure for catalytic asymmetric epoxidation reaction with reduced catalyst loading (0.02 mol %)

MS (4 Å, 1000 mg, powdered) in a flask was dried prior to use at 160 °C under vacuum (0.7 KPa) for 3 h. To a stirred suspension of **1a** (1.97 g, 10 mmol), $\text{Ph}_3\text{As}(\text{O})$ (0.644 mg, 0.002 mmol), and (*R*)- H_8 -BINOL (0.589 mg, 0.002 mmol) in THF (2.0 mL) at 25 °C was added $\text{Sm}(\text{O}-i\text{-Pr})_3$ (10 μL , 0.002 mmol, 0.2 M in THF). The mixture was stirred for

15 min at 25 °C and then the mixture was cooled to 0 °C. *tert*-Butyl hydroperoxide (TBHP) (15 mmol, 4.5 M in toluene, dried with 4 Å MS) was added slowly over 60 min (45 min at 0 °C, then 15 min at 25 °C). The stirring was continued for additional 30 min at 25 °C and quenched with 2.5% aq citric acid. The mixture was filtered through Celite and the filtrate was extracted with ethyl acetate. Then combined organic layers were washed successively with satd aq NaHCO_3 and brine, and then dried over MgSO_4 . The solvent was evaporated and the resulting crude residue was purified by flash silica gel column chromatography (ethyl acetate/hexane=1/15) to afford **8a** (2.01 g, 94.2% yield, 99% ee).

6.7.1. (2S,3R)-trans-2,3-Epoxy-3-phenyl-1-pyrrol-1-yl-propan-1-one (8a). IR (KBr) ν 3149, 1714, 1287, 904 cm^{-1} ; ^1H NMR (CDCl_3) δ 7.32–7.42 (m, 7H), 6.33–6.36 (m, 2H), 4.20 (d, $J=1.9$ Hz, 1H), 4.01 (d, $J=1.9$ Hz, 1H); ^{13}C NMR (CDCl_3) δ 57.3, 58.8, 114.1, 119.0, 125.7, 128.8, 129.2, 134.4, 164.3; ESIMS m/z 236 $[\text{M}+\text{Na}]^+$; $[\alpha]_D^{24} +150$ (c 1.07, CHCl_3) (>99.5% ee); HRMS calcd for $\text{C}_{13}\text{H}_{12}\text{NO}_2$ $[\text{M}+\text{H}]^+$: 214.0868; found: 214.0870; HPLC (DAICEL CHIRALPAK AD, 2-propanol/hexane=2/98, flow 1.0 mL min^{-1} , detection at 254 nm) t_R 28.0 min (minor) and 36.0 min (major).

6.7.2. (2S,3R)-trans-2,3-Epoxy-3-(2-naphthyl)-1-pyrrol-1-yl-propan-1-one (8b). IR (KBr) ν 1716, 1288, 910, 818 cm^{-1} ; ^1H NMR (CDCl_3) δ 7.82–7.89 (m, 4H), 7.50–7.53 (m, 2H), 7.41 (br, 1H), 7.37 (dd, $J=8.3, 1.2$ Hz, 1H), 6.33–6.36 (m, 2H), 4.37 (br, 1H), 4.11 (d, $J=1.8$ Hz, 1H); ^{13}C NMR (CDCl_3) δ 57.5, 59.1, 114.2, 119.1, 122.2, 125.9, 126.8, 126.8, 127.9, 127.9, 128.9, 131.8, 133.0, 133.7, 164.3; ESIMS m/z 286 $[\text{M}+\text{Na}]^+$; $[\alpha]_D^{24} +169$ (c 1.01, CHCl_3); HRMS calcd for $\text{C}_{17}\text{H}_{14}\text{NO}_2$ $[\text{M}+\text{H}]^+$: 264.1024; found: 264.1023; HPLC (DAICEL CHIRALPAK AD, 2-propanol/hexane=2/98, flow 1.0 mL min^{-1} , detection at 254 nm) t_R 31.4 min (minor) and 40.0 min (major).

6.7.3. (2S,3R)-trans-2,3-Epoxy-3-(4-methylphenyl)-1-pyrrol-1-yl-propan-1-one (8c). IR (KBr) ν 3152, 1713, 1284, 800 cm^{-1} ; ^1H NMR (CDCl_3) δ 7.20–7.26 (m, 2H), 6.35–6.37 (m, 2H), 4.18 (d, $J=1.7$ Hz, 1H), 4.02 (d, $J=1.7$ Hz, 1H), 2.38 (s, 3H); ^{13}C NMR (CDCl_3) δ 21.2, 57.3, 58.9, 114.1, 119.0, 125.7, 129.5, 131.4, 139.3, 164.5; ESIMS m/z 250 $[\text{M}+\text{Na}]^+$; $[\alpha]_D^{25} +153$ (c 1.22, CHCl_3); HRMS calcd for $\text{C}_{14}\text{H}_{14}\text{NO}_2$ $[\text{M}+\text{H}]^+$: 228.1024; found: 228.1026; HPLC (DAICEL CHIRALCEL OJ, 2-propanol/hexane=2/98, flow 1.0 mL min^{-1} , detection at 254 nm) t_R 33.1 min (major) and 50.2 min (minor).

6.7.4. (2S,3R)-trans-2,3-Epoxy-3-(4-methoxyphenyl)-1-pyrrol-1-yl-propan-1-one (8d). IR (KBr) ν 1715, 1288, 910, 818 cm^{-1} ; ^1H NMR (CDCl_3) δ 7.39 (br, 2H), 7.26 (d, $J=8.7$ Hz, 2H), 6.91 (d, $J=8.7$ Hz, 2H), 6.33–6.35 (m, 2H), 4.14 (d, $J=1.9$ Hz, 1H), 4.00 (d, $J=1.9$ Hz, 1H), 3.81 (s, 3H); ^{13}C NMR (CDCl_3) δ 55.4, 57.3, 58.8, 114.1, 114.3, 119.0, 126.3, 127.2, 160.5, 164.5; ESIMS m/z 266 $[\text{M}+\text{Na}]^+$; $[\alpha]_D^{25} +163$ (c 0.93, CHCl_3); HRMS calcd for $\text{C}_{14}\text{H}_{14}\text{NO}_3$ $[\text{M}+\text{H}]^+$: 244.0973; found: 244.0968; HPLC (DAICEL CHIRALPAK AS-H, 2-propanol/hexane=20/80, flow 1.0 mL min^{-1} , detection at 254 nm) t_R 20.2 min (minor) and 37.1 min (major).

6.7.5. (2*S*,3*R*)-3-(4-Chlorophenyl)-trans-2,3-epoxy-1-pyrrol-1-yl-propan-1-one (8f). IR (KBr) ν 1740, 1288, 798 cm^{-1} ; ^1H NMR (CDCl_3) δ 7.35–7.39 (m, 4H), 7.26–7.28 (m, 2H), 6.34–6.36 (m, 2H), 4.18 (d, $J=1.7$ Hz, 1H), 3.96 (d, $J=1.7$ Hz, 1H); ^{13}C NMR (CDCl_3) δ 56.5, 57.4, 113.5, 118.2, 126.3, 128.3, 132.2, 134.5, 163.2; ESIMS m/z 270 (for ^{35}Cl), 272 (for ^{37}Cl) $[\text{M}+\text{Na}]^+$; $[\alpha]_{\text{D}}^{25} +153$ (c 1.11, CHCl_3); HRMS calcd for $\text{C}_{13}\text{H}_{11}\text{ClNO}_2$ $[\text{M}+\text{H}]^+$: 248.0478; found: 248.0474; HPLC (DAICEL CHIRALPAK AD-H, 2-propanol/hexane=5/95, flow 1.0 mL min^{-1} , detection at 254 nm) t_{R} 15.9 min (major) and 18.3 min (minor).

6.7.6. (2*S*,3*R*)-trans-2,3-Epoxy-5-phenyl-1-pyrrol-1-yl-pentan-1-one (8g). IR (neat) ν 1723, 1288 cm^{-1} ; ^1H NMR (CDCl_3) δ 7.25–7.30 (m, 2H), 7.16–7.23 (m, 5H), 6.28–6.31 (m, 2H), 3.69 (d, $J=1.9$ Hz, 1H), 3.30 (dt, $J=5.8$, 1.9 Hz, 1H), 2.85–2.91 (m, 1H), 2.75–2.82 (m, 1H), 2.00–2.11 (m, 2H); ^{13}C NMR (CDCl_3) δ 31.7, 33.0, 53.7, 58.8, 113.9, 118.9, 126.4, 128.3, 128.7, 140.2, 165.4; ESIMS m/z 264 $[\text{M}+\text{Na}]^+$; $[\alpha]_{\text{D}}^{24} +3.74$ (c 0.98, CHCl_3); HRMS calcd for $\text{C}_{15}\text{H}_{16}\text{NO}_2$ $[\text{M}+\text{H}]^+$: 242.1181; found: 242.1178; HPLC (DAICEL CHIRALPAK AD, 2-propanol/hexane=2/98, flow 1.0 mL min^{-1} , detection at 254 nm) t_{R} 22.3 min (minor) and 29.6 min (major).

6.7.7. (2*S*,3*R*)-trans-2,3-Epoxy-1-pyrrol-1-yl-tridec-12-en-1-one (8r). IR (KBr) ν 2918, 1719, 1296, 922 cm^{-1} ; ^1H NMR (CDCl_3) δ 7.39–7.41 (m, 2H), 6.33–6.35 (m, 2H), 5.74–5.83 (m, 1H), 4.94–5.00 (m, 1H), 4.89–4.93 (m, 1H), 3.75 (d, $J=1.8$ Hz, 1H), 3.25 (ddd, $J=4.9$, 3.1, 1.8 Hz, 1H), 1.99–2.04 (m, 2H), 1.63–1.78 (m, 2H), 1.42–1.53 (m, 2H), 1.22–1.39 (m, 10H); ^{13}C NMR (CDCl_3) δ 25.7, 28.9, 29.0, 29.2, 29.3, 29.3, 31.6, 33.8, 53.8, 59.5, 113.9, 114.2, 119.0, 139.1, 165.7; ESIMS m/z 298 $[\text{M}+\text{Na}]^+$; $[\alpha]_{\text{D}}^{25} +0.87$ (c 1.05, CHCl_3); HRMS calcd for $\text{C}_{17}\text{H}_{26}\text{NO}_2$ $[\text{M}+\text{H}]^+$: 276.1963; found: 276.1960; HPLC (DAICEL CHIRALPAK AD, 2-propanol/hexane=2/98, flow 1.0 mL min^{-1} , detection at 254 nm) t_{R} 15.8 min (minor) and 18.6 min (major).

6.7.8. (2*S*,3*R*)-3-Cyclohexyl-trans-2,3-epoxy-1-pyrrol-1-yl-propan-1-one (8t). IR (KBr) ν 3147, 2926, 1718, 1290, 901 cm^{-1} ; ^1H NMR (CDCl_3) δ 7.38–7.41 (m, 2H), 6.32–6.35 (m, 2H), 3.82 (d, $J=2.2$ Hz, 1H), 3.07 (dd, $J=2.2$, 6.7 Hz, 1H), 1.86–1.91 (m, 1H), 1.73–1.80 (m, 3H), 1.65–1.70 (m, 1H), 1.38–1.47 (m, 1H), 1.11–1.31 (m, 5H); ^{13}C NMR (CDCl_3) δ 25.3, 25.4, 25.9, 28.7, 29.3, 39.6, 52.7, 63.5, 113.8, 118.9, 165.8; ESIMS m/z 242 $[\text{M}+\text{Na}]^+$; $[\alpha]_{\text{D}}^{24} -26.1$ (c 1.02, CHCl_3); HRMS calcd for $\text{C}_{13}\text{H}_{18}\text{NO}_2$ $[\text{M}+\text{H}]^+$: 220.1337; found: 220.1336; HPLC (DAICEL CHIRALPAK AD, 2-propanol/hexane=2/98, flow 1.0 mL min^{-1} , detection at 254 nm) t_{R} 11.9 min (minor) and 15.9 min (major).

6.8. Transformation of *N*-acylpyrrole unit (Scheme 2)

6.8.1. tert-Butyl (4*R*,5*S*)-trans-4,5-epoxy-3-oxo-5-phenyl-pentanoate (9). To a solution of 0.75 M LDA in THF/hexane (1.0 mL, 0.75 mmol) at -78 °C was added *t*-butyl acetate (0.10 mL, 0.742 mmol) slowly over 4 min. The mixture was stirred for 20 min at -78 °C. To this mixture a solution of **8a** (56 mg, 0.262 mmol) in THF (0.8 mL) was added at -78 °C. After stirring for 10 min at -78 °C, satd aq NH_4Cl (1 mL) was added. The mixture was extracted with

ethyl acetate. Organic layer was washed with 1 M HCl, pH 7 phosphate buffer, brine, and then dried over Na_2SO_4 . After evaporation, the residual oil was dissolved in CH_2Cl_2 (5 mL), DBU (90 mg, in 1 mL CH_2Cl_2) was then added and stirred for 20 min at 25 °C. To the reaction mixture was added CHCl_3 , and then 1 M HCl was added. The organic layer was washed with pH 7 phosphate buffer, brine, and then dried over Na_2SO_4 , filtered, and concentrated. After evaporation, the residue was purified by silica gel column chromatography (hexane/diethyl ether=15/1 to 10/1) to give **9** (51.5 mg, 0.196 mmol, 74% yield) as pale yellow oil: IR (neat) 3437, 2979, 2932, 1733, 1713, 1652, 1457, 1369, 1325, 1253, 1154 cm^{-1} ; ^1H NMR (CDCl_3) δ 7.24–7.43 (m, 5H), 4.06 (d, $J=1.7$ Hz, 1H), 3.60 (d, $J=1.7$ Hz, 1H), 3.43 (d, $J=3.1$ Hz, 2H), 1.47 (s, 9H); ^{13}C NMR (CDCl_3) major peaks δ 198.8, 165.6, 134.7, 129.1, 128.7, 128.6, 125.6, 91.7, 82.5, 63.0, 58.0, 45.3, 28.2, 28.1, 27.9; minor peaks δ 172.0, 170.2, 135.7, 81.6, 59.3, 59.1, 31.1; ESIMS m/z 285 $[\text{M}+\text{Na}]^+$; $[\alpha]_{\text{D}}^{24} +40.5$ (c 0.7, CHCl_3); HRMS (FAB) m/z calcd for $\text{C}_{15}\text{H}_{19}\text{O}_4$ $[\text{M}+\text{H}]^+$: 263.1283; found: 263.1283.

6.8.2. (2*S*,3*R*)-trans-2,3-Epoxy-1,3-diphenylpentan-1-one (10). To a solution of bromobenzene (116 mg, 0.738 mmol) in THF (1.2 mL) at -78 °C was added BuLi (1.58 M in hexane, 0.47 mL, 0.695 mmol). The mixture was stirred for 10 min at the same temperature. A solution of **8a** (96 mg, 0.45 mmol) in THF (1.2 mL) was added at -78 °C. After stirring for 10 min at -78 °C, satd aq NH_4Cl (1.5 mL) was added. The mixture was extracted with ethyl acetate. The organic layer was washed with aq NaH_2PO_4 , satd aq NaHCO_3 , brine, and then dried over Na_2SO_4 . After evaporation, the residue was dissolved in CH_2Cl_2 , DBU (50 μL) was then added, and the mixture was stirred for 20 min at 25 °C. The mixture was diluted with CHCl_3 , washed with 1 M HCl, satd aq NaHCO_3 , brine, and then dried over Na_2SO_4 . After evaporation, the residue was purified by silica gel column chromatography (hexane/diethyl ether=10/1) to give **10** (89 mg, 0.3968 mmol, 88% yield) as colorless oil. Analytical data were identical to the reported data.

6.8.3. (1*S*,2*R*)-trans-1,2-Epoxy-3-oxo-1-phenyl-4-octyne (11). To a solution of 1-pentyne (0.167 mL, 1.7 mmol) in THF (1.4 mL) at -78 °C was added BuLi (1.56 M in hexane, 0.96 mL, 1.5 mmol). The mixture was stirred for 30 min at the same temperature. To this mixture a solution of **8a** (105 mg, 0.492 mmol) in THF (1.4 mL) was added at -78 °C. After stirring for 10 min at -78 °C, satd aq NH_4Cl (2 mL) was added. The mixture was extracted with ethyl acetate. The organic layer was washed with 1 M HCl, satd aq NaHCO_3 , brine, and then dried over Na_2SO_4 . After evaporation, the obtained residue was dissolved in CH_2Cl_2 (15 mL), DBU (0.184 M in CH_2Cl_2 , 0.1 mL, 0.0184 mmol) was then added, and stirred for 10 min at 0 °C. The mixture was diluted with CHCl_3 , washed with 1 M HCl, satd aq NaHCO_3 , brine, and then dried over Na_2SO_4 . After evaporation, the residue was purified by silica gel column chromatography (hexane/diethyl ether=15/1 to 10/1) to give **11** (88.7 mg, 0.414 mmol, 84% yield) as yellow oil: IR (neat) 2965, 2935, 2875, 2210, 1667, 1457, 1405, 1257, 1179 cm^{-1} ; ^1H NMR (CDCl_3) δ 7.27–7.50 (m, 5H), 4.17 (d, $J=1.5$ Hz, 1H), 3.61 (d, $J=1.8$ Hz, 1H), 2.41 (t, $J=7.3$ Hz, 2H), 1.65 (dq, $J=7.3$, 7.3 Hz, 2H), 1.04

(t, $J=7.3$ Hz, 3H); ^{13}C NMR (CDCl_3) δ 182.6, 134.8, 129.0, 128.7, 125.7, 98.8, 78.3, 63.6, 58.6, 21.1, 13.4; ESIMS m/z 237 $[\text{M}+\text{Na}]^+$; $[\alpha]_{\text{D}}^{24} +166$ (c 0.95, CHCl_3); HRMS (FAB) m/z calcd for $\text{C}_{14}\text{H}_{15}\text{O}_2$ $[\text{M}+\text{H}]^+$: 215.1072; found: 215.1074.

6.8.4. (2R,3R)-trans-2,3-Epoxy-5-phenyl-1-pentanol (12).

To a suspension of LiBH_4 (15.6 mg, 0.72 mmol) in THF (0.8 mL) at 0°C , was added a solution of **8q** (50.5 mg, 0.209 mmol) in THF (0.8 mL). The mixture was stirred for 20 min at 0°C , and then at 25°C for 40 min. The reaction mixture was poured to ethyl acetate/satd aq NH_4Cl mixture at 0°C . The organic layer was separated, washed with pH 7 phosphate buffer, brine, and then dried over Na_2SO_4 . After evaporation, the residual oil was dissolved in THF (1 mL), and the solution was added to the suspension of NaBH_4 (27 mg, 0.71 mmol) in THF (1.5 mL) at 25°C . After stirring for 4 h, the reaction mixture was poured to ethyl acetate/satd aq NH_4Cl mixture at 0°C . Organic layer was separated, washed with pH 7 phosphate buffer, brine, and then dried over Na_2SO_4 . After evaporation, the residue was purified by silica gel column chromatography (hexane/ethyl acetate=3/1) to give **12** (0.151 mmol, 72% yield) as colorless oil: IR (neat) 3409, 2926, 1603, 1496, 1454, 1231, 1087, 878 cm^{-1} ; ^1H NMR (CDCl_3) δ 7.18–7.32(m, 5H), 3.81–3.88 (m, 1H), 3.54–3.60 (m, 1H), 2.98–3.02 (m, 1H), 2.80–2.88 (m, 2H), 2.70–2.78 (m, 1H), 1.84–1.97 (m, 2H); ^{13}C NMR (CDCl_3) δ 141.0, 128.4, 128.3, 126.0, 61.6, 58.7, 55.3, 33.2, 32.1; ESIMS m/z 201 $[\text{M}+\text{Na}]^+$; $[\alpha]_{\text{D}}^{25} +42.6$ (c 2.41, CHCl_3); HRMS (FAB) m/z calcd for $\text{C}_{11}\text{H}_{15}\text{O}_2$ $[\text{M}+\text{H}]^+$: 179.1072; found: 179.1073.

Acknowledgements

This work was supported by Grant-in-Aid for Specially Promoted Research and Grant-in-Aid for Encouragements for Young Scientists (B) (for SM) from JSPS and MEXT.

References and notes

- For recent reviews see: (a) Porter, M. J.; Skidmore, J. *Chem. Commun.* **2000**, 1215; (b) Nemoto, T.; Ohshima, T.; Shibasaki, M. *J. Synth. Org. Chem. Jpn.* **2002**, *60*, 94; Polyamino acid catalysis: (c) Porter, M. J.; Roberts, S. M.; Skidmore, J. *Bioorg. Med. Chem.* **1999**, *7*, 2145; Chiral ketone as catalyst: (d) Frohn, M.; Shi, Y. *Synthesis* **2000**, 1979; For selected leading references, see also: (e) Enders, D.; Zhu, J.; Raabe, G. *Angew. Chem., Int. Ed.* **1996**, *35*, 1725; (f) Elston, C. L.; Jackson, R. F. W.; MacDonald, S. J. F.; Murray, P. J. *Angew. Chem., Int. Ed.* **1997**, *36*, 410.
- For epoxidation of α,β -unsaturated ketone by rare earth metal/BINOL complexes, see: (a) Bougauchi, M.; Watanabe, T.; Arai, T.; Sasai, H.; Shibasaki, M. *J. Am. Chem. Soc.* **1997**, *119*, 2329; (b) Nemoto, T.; Ohshima, T.; Yamaguchi, K.; Shibasaki, M. *J. Am. Chem. Soc.* **2001**, *123*, 2725; See, also: (c) Daikai, K.; Kamaura, M.; Inanaga, J. *Tetrahedron Lett.* **1998**, *39*, 7321.
- Jacobsen, E. N.; Deng, L.; Furukawa, Y.; Martinez, L. E. *Tetrahedron* **1994**, *50*, 4323.
- (a) Wu, X.-Y.; She, X.; Shi, Y. *J. Am. Chem. Soc.* **2002**, *124*, 8792; (b) Armstrong, A.; Hayter, B. R. *Chem. Commun.* **1998**, 621; (c) Solladié-Cavallo, A.; Bouérat, L. *Org. Lett.* **2000**, *2*, 3531; (d) Seki, M.; Furutani, T.; Imashiro, R.; Kuroda, T.; Yamanaka, T.; Harada, N.; Arakawa, H.; Kusama, M.; Hashiyama, T. *Tetrahedron Lett.* **2001**, *42*, 8201; (e) Shing, T. K. M.; Leung, G. Y. C.; Luk, T. *J. Org. Chem.* **2005**, *70*, 7279; See, also: (f) Yang, D.; Yip, Y.-C.; Tang, M.-W.; Wong, M.-K.; Zheng, J.-H.; Cheung, K.-K. *J. Am. Chem. Soc.* **1996**, *118*, 491.
- Takei, H.; Tuji, R.; Ohshima, T.; Shibasaki, M. *J. Am. Chem. Soc.* **2005**, *127*, 8962.
- For α,β -unsaturated carboxylic acid imidazolide, see: (a) Nemoto, T.; Ohshima, T.; Shibasaki, M. *J. Am. Chem. Soc.* **2001**, *123*, 9474; (b) Ohshima, T.; Nemoto, T.; Tosaki, S.-y.; Takei, H.; Gnanadesikan, V.; Shibasaki, M. *Tetrahedron* **2003**, *59*, 10485. For α,β -unsaturated amide, see: (c) Nemoto, T.; Takei, H.; Gnanadesikan, V.; Tosaki, S.-y.; Ohshima, T.; Shibasaki, M. *J. Am. Chem. Soc.* **2002**, *124*, 14544.
- A part of this article was reported previously. See: (a) Kinoshita, T.; Okada, S.; Park, S.-R.; Matsunaga, S.; Shibasaki, M. *Angew. Chem., Int. Ed.* **2003**, *42*, 4680; (b) Matsunaga, S.; Kinoshita, T.; Okada, S.; Shibasaki, M. *J. Am. Chem. Soc.* **2004**, *126*, 7559.
- (a) Evans, D. A.; Borg, G.; Scheidt, K. A. *Angew. Chem., Int. Ed.* **2002**, *41*, 3188. For application to catalytic asymmetric reactions, see: (b) Evans, D. A.; Johnson, D. S. *Org. Lett.* **1999**, *1*, 595; (c) Evans, D. A.; Scheidt, K. A.; Johnston, J. N.; Willis, M. C. *J. Am. Chem. Soc.* **2001**, *123*, 4480. For application to diastereoselective reactions using chiral auxiliary, see: (d) Arai, Y.; Matsunda, T.; Masaki, Y. *Chem. Lett.* **1997**, 145; (e) Arai, Y.; Ueda, K.; Xie, J.; Masaki, Y. *Chem. Pharm. Bull.* **2001**, *49*, 1609; (f) Arai, Y.; Kasai, M.; Ueda, K.; Masaki, Y. *Synthesis* **2003**, 1511 and references therein. For other application of pyrrole carbinol as useful building blocks, see: (g) Dixon, D. J.; Scott, M. S.; Luckhurst, C. A. *Synlett* **2003**, 2317; (h) Dixon, D. J.; Scott, M. S.; Luckhurst, C. A. *Synlett* **2005**, 2420.
- For the use of α,β -unsaturated *N*-acylpyrroles in other catalytic asymmetric conjugate additions, see: (a) Yamagiwa, N.; Qin, H.; Matsunaga, S.; Shibasaki, M. *J. Am. Chem. Soc.* **2005**, *127*, 13419; (b) Mita, T.; Sasaki, K.; Kanai, M.; Shibasaki, M. *J. Am. Chem. Soc.* **2005**, *127*, 514. See, also: (c) Shintani, R.; Kimura, T.; Hayashi, T. *Chem. Commun.* **2005**, 3213.
- For the use of *N*-acylpyrrole as a donor in direct Mannich-type reaction, see: Harada, S.; Handa, S.; Matsunaga, S.; Shibasaki, M. *Angew. Chem., Int. Ed.* **2005**, *44*, 4365.
- Ekkati, A. R.; Bates, D. K. *Synthesis* **2003**, 1959 and references therein. The scope of the reaction was limited to aromatic amides and cinnamamide.
- For synthesis and application of carbonyldipyrrole **2** reported by Evans co-workers, see Ref. 8a.
- For related procedure for the reaction of *N*-acylimidazole and ylide **3** to afford alkanoylmethylenetriphenylphosphorane, see: Miyano, M.; Stealey, M. A. *J. Org. Chem.* **1975**, *40*, 2840.
- Blanchette, M. A.; Choy, W.; Davis, J. T.; Essefeld, A. P.; Masamune, S.; Roush, W. R.; Sakai, T. *Tetrahedron Lett.* **1984**, *25*, 2183.
- Standard conditions for catalytic asymmetric epoxidation is lanthanide metal alkoxide/BINOL derivative=1/1 with $\text{Ph}_3\text{As}(\text{O})$ or $\text{Ph}_3\text{P}(\text{O})$ as an additive. Among lanthanide metals screened (La, Pr, Nd, Sm, Gd, Er, and Yb), Sm had best reactivity and selectivity. La, Pr, Nd, Gd, and Er complexes also afforded **11a** in $>90\%$ ee and $>80\%$ yield. Yb was not suitable for **1a**. Sm(*O*-*i*-Pr)₃ was purchased from Kojundo Chemical

- Laboratory Co., Ltd (fax: +81 492 84 1351; e-mail: sales@kojundo.co.jp).
16. Reaction rate tendency: chalcone > *N*-acylpyrrole **1a** > benzalacetone. *N*-Acylpyrrole **1a** had slightly lower reactivity than chalcone, and showed slightly higher reactivity than benzalacetone.
 17. For review on H₈-BINOL, see: Terry, T.-L. A.-Y.; Chan, S.-S.; Chan, A. S. C. *Adv. Synth. Catal.* **2003**, 345, 537.
 18. The present catalysis is applicable to various α,β -unsaturated *N*-acylpyrroles shown in Tables 1 and 2 to give epoxides in good yield and ee, except for **1m** and **1n**. Epoxidation of α,β -unsaturated *N*-acylpyrroles **1m** and **1n** did not proceed due to steric hindrance.
 19. *N*-Acylpyrrole unit can also be transformed into ethyl ester in good yield by treatment with either EtSLi in EtOH or NaOEt in EtOH. See, Refs. 7, 9, and 10.



Asymmetric epoxidation of 6-cyano-2,2-dimethylchromene on Mn(salen) catalyst immobilized in mesoporous materials

Huidong Zhang and Can Li*

State Key Laboratory of Catalysis, Dalian Institute of Chemical Physics, Chinese Academy of Sciences, Dalian 116023, China

Received 2 November 2005; revised 6 January 2006; accepted 25 January 2006

Available online 30 May 2006

Abstract—This article reports our recent work on the heterogeneous asymmetric epoxidation catalyzed by chiral Mn(salen) catalyst axially immobilized via phenoxy groups and organic sulfonic groups. The asymmetric epoxidation of 6-cyano-2,2-dimethylchromene was especially presented in detail. The factors that affected the asymmetric induction, such as the nanopores and the external surface, the linkage length, and the modification of nanopores with methyl groups were discussed. It was found that the enantioselectivities increased with decreasing the nanopore sizes or increasing the linkage length in nanopore, and the Mn(salen) catalyst immobilized into nanopores generally gave higher ee values than those on the external surface. The heterogeneous Mn(salen) catalysts with modified nanopores gave a TOF of 14.8 h^{-1} and an ee value of 90.6% for the asymmetric epoxidation of 6-cyano-2,2-dimethylchromene, which were higher than the results (TOF 10.8 h^{-1} , ee 80.1%) obtained for the homogeneous catalyst.

© 2006 Elsevier Ltd. All rights reserved.

1. Introduction

Chiral building blocks are widely used in the synthesis of fine chemicals, pharmaceuticals, vitamins, agrochemicals, flavors, fragrances, and functional materials.¹ How to prepare the chiral compounds via asymmetric catalysis has received great attention. Catalytic enantioselective epoxidation is one of the most important processes for the synthesis of chiral epoxides, which can be further converted into many important chiral building blocks via stereoselective ring-opening or functional group transformations. Chiral Mn(salen) complexes are excellent catalysts for the asymmetric epoxidation of unfunctionalized conjugated *cis*-olefins.² However, the homogeneous asymmetric epoxidation always suffers some difficulties in practical applications, such as the separation of catalysts and purification of products. The heterogeneous Mn(salen) catalysts have received much attention in recent years due to their potential advantages of easy separation, recycling catalysts, purification of products, and better handling properties.³

In the last two decades, many kinds of mesoporous materials with new structures and well-ordered pore arrays have been synthesized, which offer large surface area, uniform pore size distribution, and tunable pore diameters.⁴ Among the mesoporous materials, MCM-41 and SBA-15 are the most promising supports for the immobilization of homogeneous

catalysts for chiral synthesis. First, MCM-41 and SBA-15 have narrow and tunable nanopore size distributions in the range 2–20 nm, which is suitable for the synthesis of fine chemicals and pharmaceuticals. Second, the hydrothermal stability of the materials is good enough for the chiral synthesis under mild reaction conditions. Finally, their nanopores can be chemically modified. Therefore, the nanopores of the mesoporous materials could be employed as ideal nano-reactors for the chiral synthesis.^{3e}

The earlier examples of the heterogeneous chiral Mn(salen) catalysts were the chiral Mn(salen) embedded into mesoporous silicates⁵ or encapsulated within the cages of zeolite Y (a microporous material).⁶ Chiral Mn(salen) catalyst attached with soluble or insoluble polymers for the heterogeneous asymmetric epoxidation was also reported.⁷ In the last several years, various strategies have been reported to immobilize Mn(salen) complexes, including covalent grafting of Mn(salen) on mesoporous materials⁸ or carbon materials,⁹ ion-exchange of Mn(salen) into clay materials¹⁰ or Al-MCM-41,¹¹ encapsulation of Mn(salen) in zeolites,¹² and co-condensation of VO(salen) into periodic mesoporous materials.¹³ It was reported that the Mn(salen)Cl complexes were prone to form the inactive dimers in homogeneous catalytic systems.¹⁴ The immobilization of Mn(salen) catalysts onto the supports could isolate the active sites of Mn(salen), which might greatly reduce the formation of the dimers and increase the catalytic stability.

It is generally believed that tuning the steric and electronic properties of chiral ligands can alter the enantioselectivity for the asymmetric catalysis. Notably, the nanopores of

Keywords: Heterogeneous chiral catalysis; Asymmetric epoxidation; Mn(salen); Confinement effect; Nanopore; Enantioselective.

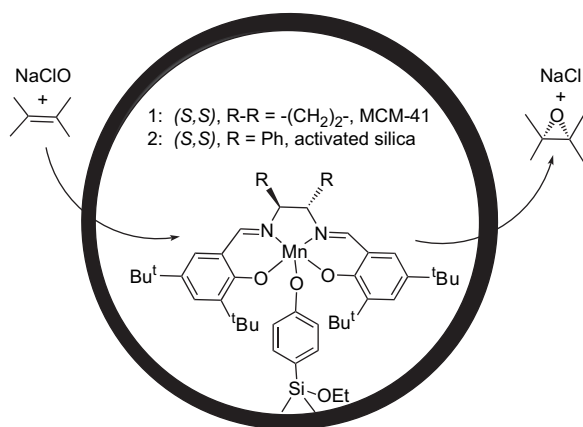
* Corresponding author. Tel.: +86 411 84379070; fax: +86 411 84694447; e-mail: canli@dicp.ac.cn

mesoporous supports might influence the chiral induction for the asymmetric epoxidation when the chiral Mn(salen) catalysts immobilize into the nanopores of mesoporous supports.^{3d,e} A few heterogeneous Mn(salen) catalysts have been reported to give higher ee values than those of the homogeneous ones for the asymmetric epoxidation and this was attributed to the confinement effect of supports.^{8a–d,f–h,10b} It was proposed by Thomas et al. that the confinement effect originating from the nanopores enhances the chiral induction for the heterogeneous asymmetric hydrogenation.¹⁵ Hutchings et al. also proposed that confinement effect of the supports improves the enantioselectivities for the heterogeneous asymmetric aziridination of styrene and hydrogenation of carbonyl- and imino-ene.¹⁶ Herein, the factors that could affect the chiral induction in a confined environment for the asymmetric epoxidation of unfunctionalized olefins were studied to understand the nature of the confinement effect. Accordingly, the effects of the different grafting modes, the linkage length, the types of supports, the nanopores or the external surface of supports, and the modification of the nanopore surface on the heterogeneous asymmetric epoxidation have been systematically investigated.

2. Background of the research

2.1. Immobilization via phenoxy groups

Mn(salen) catalysts were grafted onto mesoporous materials generally via the salen ligands. However, the axial immobilization of Mn(salen) catalysts from Mn atom has seldom been reported.³ Our group has shown the first example of the chiral Mn(salen) complex axially immobilized into the nanopores of MCM-41 via the phenoxy groups.^{8d} The heterogeneous Mn(salen) catalyst (**1**, Scheme 1) showed an ee value of 72% for the asymmetric epoxidation of α -methylstyrene, higher than 56% ee obtained for the homogeneous catalyst. And the immobilized catalysts were quite stable and could be recycled several times with constant ee values for the asymmetric epoxidation.



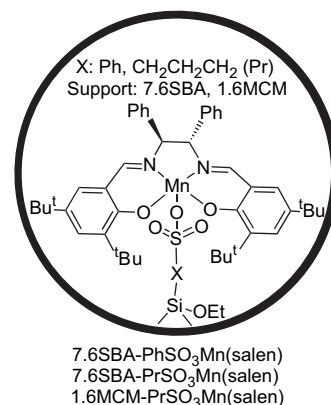
Scheme 1. The chiral Mn(salen) complex immobilized into the nanopores of mesoporous materials via phenoxy groups.^{8d,g}

Then we tried to find out the reasons for the increase in the enantioselectivities for the heterogeneous asymmetric epoxidation in the nanopores. Firstly, the preparation of the heterogeneous Mn(salen) catalyst was improved by the direct

oxidation of the phenyl groups on supports to phenoxy groups.^{8g} And the heterogeneous Mn(salen) catalyst grafted via the phenoxy group (**2**, Scheme 1) gave 79.9% ee for the asymmetric epoxidation of α -methylstyrene, much higher than 26.4% ee for the homogeneous catalyst. The *cis/trans* ratio of epoxides was also increased from 0.46 for homogeneous catalyst to 21 for the catalyst **2** for the asymmetric epoxidation of *cis*- β -methylstyrene. The supports used in this work included MCM-41 (nanopore sizes 1.6 and 2.7 nm), SBA-15 (nanopore sizes 6.2 and 7.6 nm), and activated silica (nanopore size 9.7 nm), which are, respectively, marked as 1.6MCM, 2.7MCM, 6.2SBA, 7.6SBA, and 9.7AS. Supports with different nanopore sizes obviously affected the enantioselectivity for the heterogeneous asymmetric epoxidation. The free Mn(salen)OPh catalyst gave similar reaction results to those of the Mn(salen)Cl catalyst under the same conditions.^{8g} Therefore, the increase in ee values and change in *cis/trans* ratio are mainly attributed to the axial grafting mode and the support effect of the heterogeneous catalysts.

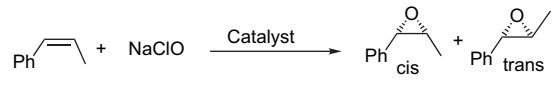
2.2. Immobilization via organic sulfonic groups

We have axially immobilized the chiral Mn(salen) complexes onto inorganic mesoporous materials via phenyl sulfonic groups (Scheme 2, X=Ph).^{8f} The recyclable heterogeneous catalyst 7.6SBA-PhSO₃Mn(salen) offered 92.6% ee (*cis*-epoxide) for the asymmetric epoxidation of *cis*- β -methylstyrene, higher than 25.3% ee obtained for the homogeneous catalyst (entries 1 and 2, Table 1). The ratio of *cis/trans* of epoxides was also increased from 0.46 for the homogeneous Mn(salen)Cl to 7.71 for the heterogeneous Mn(salen) catalyst under the same conditions.

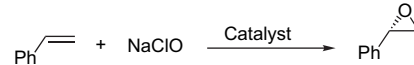


Scheme 2. The chiral Mn(salen) catalyst axially immobilized via organic sulfonic groups.^{8f,17}

In order to study the effect of the grafting modes on the catalytic reaction, the chiral Mn(salen) was immobilized into the nanopores or onto external surface of supports via rigid phenyl sulfonic groups or flexible propyl sulfonic groups (Scheme 2, X=Ph or Pr).¹⁷ Table 1 shows that the Mn(salen) catalyst immobilized via phenyl sulfonic groups gave higher ee value (for *cis*-epoxide) and *cis/trans* ratio than those of the catalyst grafted via propyl sulfonic groups for the asymmetric epoxidation of *cis*- β -methylstyrene (entries 2 and 3). The molecular sizes of Mn(salen) complex was larger than that of the nanopores of 1.6MCM, and the results of N₂ adsorption also proved that the Mn(salen)

Table 1. Asymmetric epoxidation of *cis*- β -methylstyrene^{8f,17,19}


Entry	Catalyst	cis		trans		cis/trans ratio
		Yield (%)	ee (%) ^a	Yield (%)	ee (%) ^b	
1	Mn(salen)Cl	25.3	25.3	55.0	93.3	0.46
2	7.6SBA-PhSO ₃ Mn(salen)	34.7	92.6	4.5	81.4	7.71
3	7.6SBA-PrSO ₃ Mn(salen)	21.0	71.7	24.3	87.0	0.87
4	PS-PhSO ₃ Mn(salen)	43.3	68.8	42.5	89.2	1.02

^a (*S,R*)-Configuration.^b (*S,S*)-Configuration.**Table 2.** Asymmetric epoxidation of styrene¹⁷


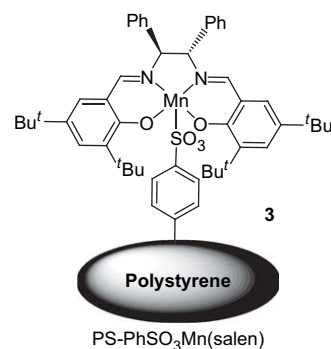
Entry	Catalyst	T (h)	Conv. (%)	Sel. (%) ^a	ee (%) ^b
1	Mn(salen)Cl	6	100	100	58.0
2	7.6SBA-PhSO ₃ Mn(salen)	24	44.5	78.4	50.6
3	7.6SBA-PrSO ₃ Mn(salen)	24	75.5	94.5	60.0
4	1.6MCM-PrSO ₃ Mn(salen)	24	91.5	87.6	52.5

^a Benzaldehyde and acetophenone as by-products.^b (*S*)-Configuration.

complex was anchored on the external surface of 1.6MCM and in the nanopores of 7.6SBA. **Table 2** shows that Mn(salen) catalyst immobilized into the nanopores via propyl sulfonic groups presented higher chemical selectivity and ee value than those of the same catalyst anchored onto the external surface via phenyl sulfonic groups for the asymmetric epoxidation of styrene. Therefore, the axially rigid and flexible grafting modes and the nanopores or external surface of supports significantly affected the heterogeneous asymmetric epoxidation.

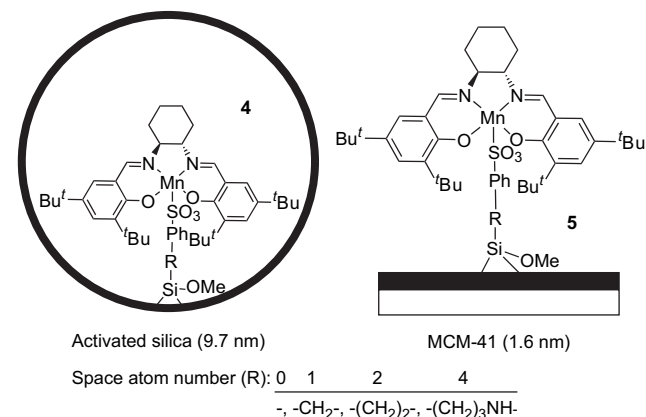
2.3. Polymers as supports

Besides the grafting modes, the types of supports might also affect the heterogeneous asymmetric epoxidation. Polymers have been used as supports to immobilize chiral Mn(salen) catalysts,^{3b,18} which generally gave comparable or lower ee values than the homogeneous counterparts for the asymmetric epoxidation due to the less effective steric restriction in the polymer microenvironment.^{14b} The chiral Mn(salen) complexes were grafted onto insoluble polystyrene resins (PS) via phenoxy groups or phenyl sulfonic groups through axial coordination (**Scheme 3**).¹⁹ These heterogeneous Mn(salen) catalysts showed comparable or even higher enantioselectivities than those of the homogeneous catalysts for the asymmetric epoxidation of unfunctionalized olefins. For example, PS-PhSO₃Mn(salen) (**3**, **Scheme 3**) gave higher ee value than that of the homogeneous catalyst (68.8% vs 25.3% for *cis*-epoxide) for the asymmetric epoxidation of *cis*- β -methylstyrene (entries 1 and 4, **Table 1**). Notably, the catalyst **3** presented lower ee values (for *cis*-epoxide) and cis/trans ratio than those of the same Mn(salen) catalyst immobilized on inorganic material 7.6SBA (entries 2 and 4, **Table 1**). Therefore, the different types of supports obviously affected the reaction performance for the heterogeneous asymmetric epoxidation.

**Scheme 3.** The chiral Mn(salen) catalyst axially immobilized onto the insoluble polystyrene resins via phenyl sulfonic groups.¹⁹

2.4. Grafting using different linkage lengths

The effect of the axial linkage length between the Mn(salen) catalysts and the surface of supports on the heterogeneous asymmetric epoxidation has seldom been investigated.^{3d,e} We have immobilized the chiral Mn(salen) into nanopores of 9.7AS and onto the external surface of 1.6MCM via phenyl sulfonic groups with different linkage lengths (**Scheme 4**).²⁰ One of the representative examples was the heterogeneous asymmetric epoxidation of 1-phenylcyclohexene (see the results shown in **Fig. 1**). The ee values obtained for the reactions catalyzed by **4** increased from 14% to 65% when the number of the space atoms increased from 0 to 4. In contrast, the ee values obtained for the reactions catalyzed by **5** were nearly unaffected by the linkage lengths and remained almost constant at about 45%.

**Scheme 4.** The Mn(salen) catalyst immobilized into the nanopores of 9.7AS (**4**) and on the external surface of 1.6MCM (**5**).²⁰

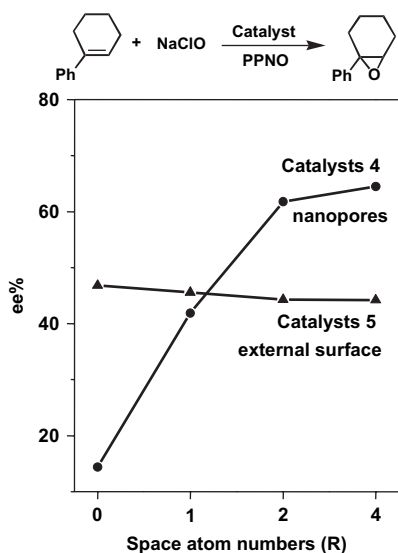


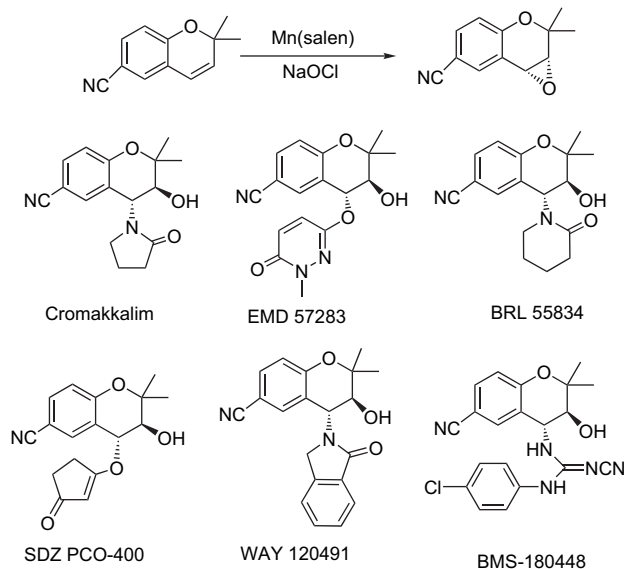
Figure 1. The ee values obtained for the heterogeneous asymmetric epoxidation of 1-phenylcyclohexene catalyzed by catalysts **4** and **5**.²⁰

The effect of PPNO on the heterogeneous asymmetric epoxidation of 1-phenylcyclohexene was also studied. The use of catalyst **5** ($R=0$, Scheme 4) improved the ee values from 13% to 47% after the addition of PPNO (4-phenylpyridine *N*-oxide), whereas the catalyst **4** ($R=0$) gave almost unchanged ee values (14% vs 14%) with or without the axial additive PPNO. This implied that the Mn(salen) catalyst axially immobilized on the open surface of 1.6MCM (**5**) had the interaction with PPNO, but the same catalyst on the concave surface of nanopores of 9.7AS (**4**) had no such interaction. The catalysts **4** and **5** ($R=1$) gave similar ee values due to the enhanced interaction between Mn(salen) and PPNO with increasing linkage length. When the number of the space atoms became 2 or 4 (Fig. 1), the catalyst **4** gave higher ee values than those of the catalyst **5**, which could be due to the fact that the confinement effect originating from the nanopores enhanced the asymmetric induction for the asymmetric epoxidation.

3. Results and discussion

Based on our recent work,^{8f,g,17,20} we conclude that the confinement effect not only alters the cis/trans ratios of epoxides, but also improves the chemical selectivities and enantioselectivities for the asymmetric epoxidation using the catalysts immobilized in mesoporous materials. Among all the factors that contributed to the confinement effect, the nanopores and linkage lengths were found to be the most significant ones for the heterogeneous asymmetric epoxidation. In this work, the chiral Mn(salen) was immobilized on supports with different nanopore sizes via phenoxyl groups or phenyl sulfonic groups with different linkage lengths. To test the catalytic performance of these heterogeneous Mn(salen) catalysts, 6-cyano-2,2-dimethylchromene²¹ was selected as a representative substrate because its corresponding epoxide was an important, biologically active compound.²² Scheme 5 shows a variety of compounds that can be produced from the epoxidation of 6-cyano-2,2-dimethylchromene and these compounds generally exhibit potential antihypertensive

activity by controlling the ATP-sensitive K^+ channels in the cell membrane.²³ In this work, we demonstrated that the optimized heterogeneous Mn(salen) catalysts could give even higher TOF and ee values than their homogeneous counterparts for the asymmetric epoxidation of 6-cyano-2,2-dimethylchromene under the same conditions.

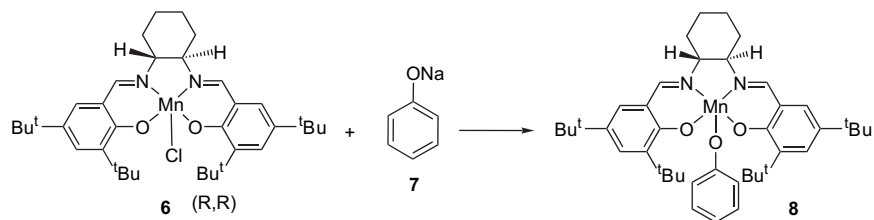


Scheme 5. Benzopyran-based ATP-sensitive potassium channel openers.

3.1. Synthesis and characterization of Mn(salen) catalysts

(*R,R*)-Mn(salen)Cl (**6**) was synthesized and characterized according to the literature.²⁴ Mn(salen)OPh catalyst (**8**) was prepared by ion-exchange of Mn(salen)Cl with PhONa in refluxing ethanol (Scheme 6).^{8g,19} The BET measurement of activated silica showed that the activated silica used in this work has a nanopore size of 9.7 nm with a narrow pore distribution (Fig. 2). The phenyl groups anchored on supports were oxidized to phenoxyl groups with H_2O_2 in the presence of $FeCl_3$ and H_2SO_4 , and then the phenoxyl groups were transformed into their sodium salts (Scheme 7).^{8g,19} The supports modified with sulfonic groups were prepared by a sulfonation of substituted phenyl groups with fuming sulfuric acid and subsequent conversion into their sodium salts (Scheme 7).^{8f,20} Then the chiral Mn(salen) complex was immobilized onto supports according to the methods reported previously (Scheme 8).^{8f,g}

These heterogeneous Mn(salen) catalysts were characterized by FTIR, UV-vis, TEM, and XRD.^{8g,20} The FTIR spectra of the heterogeneous Mn(salen) catalysts confirmed the presence of the phenyl groups (1490 cm^{-1}), alkyl linkage groups (1431 and 1454 cm^{-1}), methyl groups (2979 , 2952 , and 2850 cm^{-1}), and the Mn(salen) complex (characteristic band at 1535 cm^{-1}) on the supports. Mn(salen)Cl and Mn(salen)OPh complexes gave similar peaks at 331 and 446 nm in their UV-vis spectra. After grafting Mn(salen) complex onto the modified supports, the characteristic bands of Mn(salen) complex appeared again in their spectra, but the bands shifted from 331 and 446 nm, respectively, to 430 and 327 nm for 7.6SBA-PhOMn(salen)^{8g} and to 432 and 329 nm for 9.7AS-2-PhSO₃Mn(salen),²⁰ indicating the presence of



Scheme 6. Preparation of homogeneous Mn(salen)OPh catalyst (**8**).

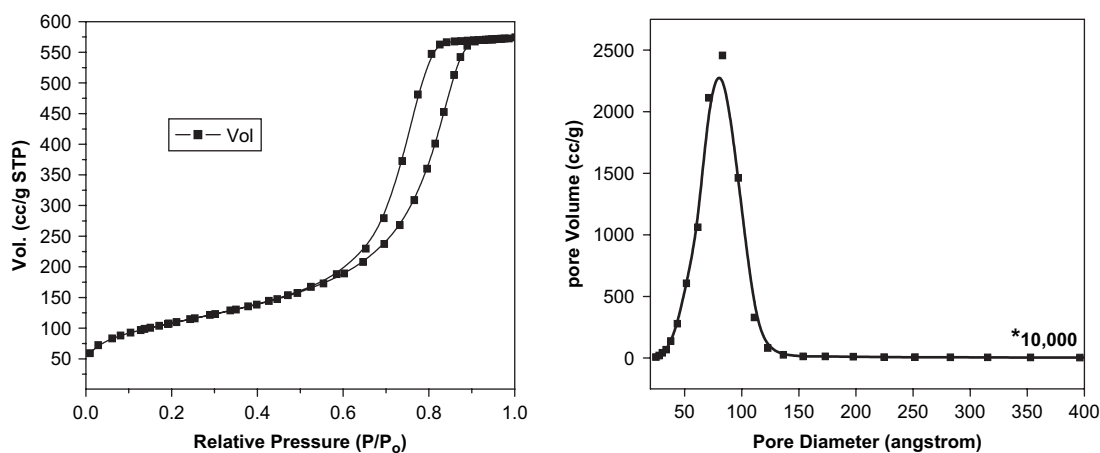
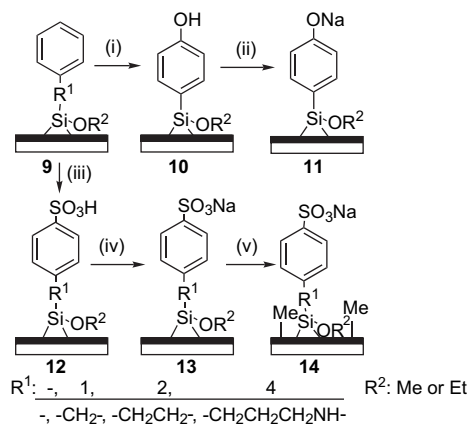


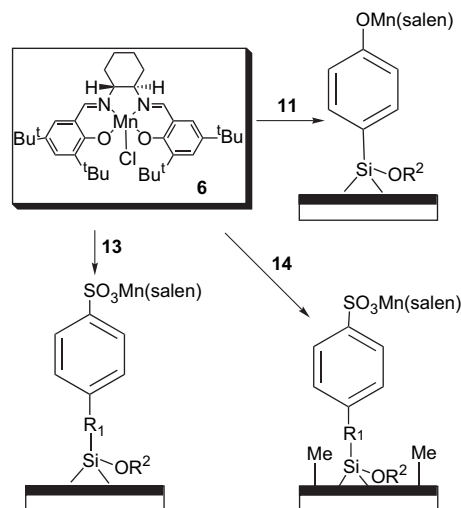
Figure 2. The nitrogen adsorption–desorption isotherms of activated silica (9.7AS) (the left) and pore size distribution curve of 9.7AS calculated from the desorption branch (the right).²⁰

interaction between the immobilized Mn(salen) and the supports. The TEM images and the XRD patterns of the heterogeneous Mn(salen) catalysts showed that the mesoporous supports in the heterogeneous Mn(salen) catalysts still kept good periodic structure after the immobilization of Mn(salen) catalyst onto supports. The amount of Mn(salen) complex immobilized in the heterogeneous catalysts was in the range of 0.01–0.055 mmol/g based on the Mn element analyzed by ICP–AES.

The size of solvated Mn(salen)Cl complex was estimated to be 2.05 nm × 1.61 nm by MM2 based on the minimized energy.^{8g,17,20} The results of nitrogen sorption of the heterogeneous catalysts showed that when the Mn(salen) complex was immobilized on the supports of 2.7MCM, 6.2SBA, 7.6SBA, and 9.7AS, the nanopore sizes, surface areas, and pore volumes all decreased compared to those of the supports before the immobilization.^{17,20} For example, the nanopore size decreased from 7.0 to 6.7 nm, the surface area decreased



Scheme 7. Preparation of the supports modified with phenoxy groups (**11**) and phenyl sulfonic groups with different linkage lengths (**13**, **14**). Mesoporous supports: 9.7AS, 7.6SBA, 6.2SBA, 2.7MCM, and 1.6MCM. Reagents and conditions: (i) H_2O_2 , H_2SO_4 , $\text{FeCl}_3 \cdot 6\text{H}_2\text{O}$, 50 °C, 5 h; (ii) NaOH, rt, 3 h; (iii) 10% fuming sulfuric acid, 40 °C, 2 h; (iv) NaHCO_3 , rt, 3 h; (v) MeSi(OMe)_3 , toluene, reflux.



Scheme 8. The grafting of Mn(salen) catalyst onto various modified supports. Mesoporous supports: 9.7AS, 7.6SBA, 6.2SBA, 2.7MCM, and 1.6MCM.

from 455 to 331 m²/g, and the pore volume decreased from 0.52 to 0.37 cm³/g after the immobilization of Mn(salen) on 7.6SBA–PhSO₃Na. These results clearly suggested that Mn(salen) complex immobilized mainly into the nanopores of supports.^{8b} However, the solvated Mn(salen)Cl complex is too big to be accommodated into the nanopores of 1.6MCM. The results of nitrogen sorption showed that the nanopore sizes (from 1.4 to 1.4 nm), surface areas (from 431 to 403 m²/g), and pore volumes (from 0.26 to 0.27 cm³/g) were almost unchanged after the immobilization of Mn(salen) onto 1.6MCM–PhSO₃Na.^{17,20} Thus Mn(salen) complex was mainly immobilized onto the external surface of 1.6MCM.

3.2. The Mn(salen) catalyst immobilized on mesoporous materials

The results of the asymmetric epoxidation of 6-cyano-2,2-dimethylchromene are compared in Table 3. Homogeneous Mn(salen)Cl catalyst showed almost stoichiometric conversion and 80.1% ee value (entry 1). When the chlorine ion was displayed by phenoxy group, the Mn(salen)OPh catalyst also showed the similar results, indicating that the electronic effect originating from the phenoxy groups did not obviously affect the reaction performance (entry 2). The Mn(salen) catalyst grafted onto the external surface of 1.6MCM gave 49.0% ee for the asymmetric epoxidation of 6-cyano-2,2-dimethylchromene (entry 3). The differences in the catalytic performance between 1.6MCM–PhOMn(salen) and Mn(salen)OPh could be attributed to the axial grafting mode and the influence of support surface, which resulted in the decreased enantioselectivity.

The chiral Mn(salen) catalyst was then immobilized into the nanopores of supports with different nanopore sizes (from 2.7 nm for 2.7MCM to 9.7 nm for 9.7AS). These heterogeneous catalysts had the effect of the axial grafting mode, the effect of support surface, and the confinement effect originating from the nanopores. The reaction results in Table 3 show that the ee values increased from 26.4% for 2.7MCM–PhOMn(salen) to 84.9% for 6.2SBA–PhOMn(salen) under the same reaction conditions (entries 4 and 5). Considering the sizes of Mn(salen), substrate,

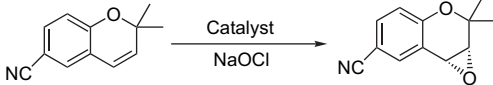
and the nanopore of 2.7MCM, the poor activity and enantioselectivity for 2.7MCM–PhOMn(salen) should be mainly attributed to the spatially overcrowded catalytic microenvironment in the nanopores of 2.7MCM. When the nanopore sizes were increased, the configuration of Mn(salen) in nanopore became free and optimal to adapt the reaction. The ee value of 84.9% obtained for 6.2SBA–PhOMn(salen) was higher than 49.0% for 1.6MCM–PhOMn(salen), which might be mainly due to the confinement effect of the nanopores of 6.2SBA. Although the axial grafting mode and the surface influence decreased the ee values for the asymmetric epoxidation of 6-cyano-2,2-dimethylchromene, the catalyst 6.2SBA–PhOMn(salen) gave 84.9% ee, comparable to the 80.1% ee for the homogeneous catalyst, as a result of the positive confinement effect.

The further increase in nanopore sizes from 6.2 to 7.6 and 9.7 nm resulted in the ee values to decrease slightly from 84.9% to 76.9% and 68.8% (entries 4–7), which were still higher than that for 1.6MCM–PhOMn(salen). It was reported that the chiral restriction did indeed boost the ee values for the asymmetric hydrogenation on the heterogeneous Rh(COD)DED catalyst, in which the influence of spatial constraint was declined in proceeding from the 3.8 nm to the 6.0 nm and then to the 25 nm pore diameter silica.^{15c} For our study on the asymmetric epoxidation of 6-cyano-2,2-dimethylchromene, the confinement effect^{15a} originating from the nanopores improved the asymmetric induction for the heterogeneous asymmetric epoxidation and resulted in higher ee values for the epoxide in nanopores than that on the external surface. And when the nanopore sizes were increased further above 7.6 nm, the confinement effect was weakened, leading to the decrease in ee values.

3.3. The Mn(salen) catalyst immobilized via various linkage lengths

The asymmetric epoxidation of 6-cyano-2,2-dimethylchromene was investigated for the Mn(salen) catalysts immobilized into the nanopores of 9.7AS via phenyl sulfonic groups with different linkage lengths. The linkage lengths between the surface and the phenyl group varied from a single-bond long to five-bonds long (R=0, 1, 2, and 4, Scheme 7). The results of the asymmetric epoxidation are summarized in Table 4. Mn(salen) catalyst immobilized into the nanopores of 9.7AS directly via phenyl sulfonic groups gave a relatively low enantioselectivity, 44.9% ee (entry 2). The enantioselectivities increased with increasing the linkage length between the Mn(salen) catalyst and the pore wall (entries 3–5). The highest ee value of 82.6% could be obtained for the heterogeneous catalyst 9.7AS–4-PhSO₃Mn(salen) with the linkage of five-bonds long (R¹=4, Scheme 7), which was comparable to that of the homogeneous catalyst under the same reaction conditions (entries 1 and 5). The tendency was similar to that of the heterogeneous asymmetric epoxidation of 1-phenylcyclohexene catalyzed by Mn(salen) immobilized into the nanopores of 9.7AS with different linkage lengths (Scheme 4, Fig. 1). When the chiral Mn(salen) catalyst was immobilized into the nanopores of 7.6SBA, the heterogeneous catalysts also showed that the ee values increased with increasing the linkage length for the asymmetric epoxidation of 6-cyano-2,2-dimethylchromene (entries 6 and 7, Table 4). The TOF

Table 3. Asymmetric epoxidation catalyzed by homogeneous Mn(salen) catalyst and Mn(salen) catalyst immobilized via phenoxy groups^a

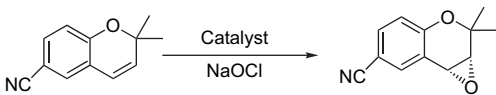


Entry	Catalyst	Pore size (nm)	Time (h)	Conv. (%)	ee (%) ^b
1	Mn(salen)Cl	—	6	97.0	80.1
2	Mn(salen)OPh	—	6	100	84.6
3	1.6MCM–PhOMn(salen)	1.6	24	76.9	49.0
4	2.7MCM–PhOMn(salen)	2.7	24	31.9	26.4
5	6.2SBA–PhOMn(salen)	6.2	24	100	84.9
6	7.6SBA–PhOMn(salen)	7.6	24	72.6	76.9
7	9.7AS–PhOMn(salen)	9.7	24	84.1	68.8

^a Reactions were performed in CH₂Cl₂ (3 ml) with olefin (1.0 mmol), *n*-nonane (1.0 mmol), homogeneous or heterogeneous Mn(salen) catalyst (0.015 mmol, 1.5 mol %), PPNO (0.38 mmol), and NaClO aqueous solution (pH=11.5, 0.55 M, 3.64 ml) at 20 °C.

^b (*R,R*)-Configuration.

Table 4. Asymmetric epoxidation catalyzed by homogeneous Mn(salen) catalyst and Mn(salen) catalyst immobilized via substituted phenyl sulfonic groups^a



Entry	Catalyst	Time (h)	Conv. (%)	ee (%) ^b	TOF (h ⁻¹)
1	Mn(salen)Cl	6	97.0	80.1	10.8
2	9.7AS-PhSO ₃ Mn(salen)	24	26.3	44.9	0.73
3	9.7AS-1-PhSO ₃ Mn(salen)	24	54.0	60.4	1.5
4	9.7AS-2-PhSO ₃ Mn(salen)	24	88.8	78.7	2.47
5	9.7AS-4-PhSO ₃ Mn(salen)	24	87.3	82.6	2.43
6	7.6SBA-2-PhSO ₃ Mn(salen)	24	88.5	84.6	2.46
7	7.6SBA-4-PhSO ₃ Mn(salen)	24	91.0	89.4	2.53
8	1.6MCM-4-PhSO ₃ Mn(salen)	24	76.8	71.1	2.14
9	9.7AS(Me)-2-PhSO ₃ Mn(salen)	6	98.3	86.5	10.9
10	9.7AS(Me)-4-PhSO ₃ Mn(salen)	4.5	100	90.6	14.8

^a Reactions were performed in CH₂Cl₂ (3 ml) with olefin (1.0 mmol), *n*-nonane (1.0 mmol), homogeneous or heterogeneous Mn(salen) catalyst (0.015 mmol, 1.5 mol %), PPNO (0.38 mmol), and NaClO aqueous solution (pH=11.5, 0.55 M, 3.64 ml) at 20 °C.

^b (*R,R*)-Epoxide.

of these heterogeneous catalysts also improved with increasing the linkage length. These results obviously suggested that the longer linkage length could improve the catalytic performance for the epoxidation of 6-cyano-2,2-dimethylchromene.

Mn(salen) catalyst immobilized into the nanopores of 7.6SBA gave higher ee values than that of the same catalyst immobilized into the nanopores of 9.7AS (entries 6 and 7, Table 4). For example, 7.6SBA-4-PhSO₃Mn(salen) gave 89.4% ee, higher than 82.6% ee obtained for 9.7AS-4-PhSO₃Mn(salen) (entries 5 and 7). But 1.6MCM-4-PhSO₃Mn(salen) gave 71.1% ee (entry 8, Table 4), lower than that obtained for the catalysts in the nanopores of 7.6SBA and 9.7AS (entries 7 and 5). This further proved that the confinement effect originating from the nanopores improved the asymmetric induction for the epoxidation.²⁰

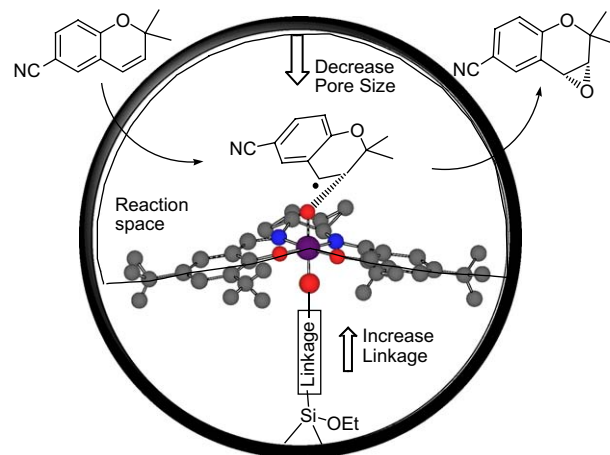
3.4. Mn(salen) catalyst immobilized into the nanopores modified with methyl groups

In order to increase the reaction efficiency, particularly the diffusion of reactants and products in the nanopores, the nanopore of the heterogeneous Mn(salen) catalysts was modified with methyl groups. The results of the asymmetric epoxidation on the methyl-modified catalysts are listed in Table 4 (entries 9 and 10). Similarly, the ee values increased from 86.5% to 90.6% when the linkage lengths were increased from three-bonds long to five-bonds long. And the modified catalysts showed higher ee values than those of the same catalysts without modification (entries 9, 10 and 4, 5).¹⁷ For example, the ee values increased from 82.6% to 90.6% for the catalyst 9.7AS-4-PhSO₃Mn(salen) after the modification of its nanopores with methyl groups (entries 5 and 10), which was also higher than the ee value of 80.1% for the corresponding homogeneous catalyst.

The modification of the nanopores of 9.7AS with methyl groups not only increased the ee values but also greatly

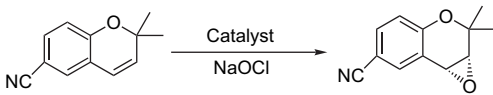
improved the reaction conversion. The catalyst 9.7AS(Me)-2-PhSO₃Mn(salen) could completely convert the substrate into its epoxide within 6 h, with a TOF of 10.9 h⁻¹. The catalyst 9.7AS(Me)-4-PhSO₃Mn(salen) with longer linkage length could completely epoxidize the olefin within 4.5 h with a TOF of 14.8 h⁻¹ (entries 9 and 10), which was higher than the TOF of 10.8 h⁻¹ (entries 1 and 10) obtained for the homogeneous catalyst, as a result of the modified catalytic microenvironment in the nanopore reactors. However, the heterogeneous Mn(salen) catalysts generally gave a lower conversion (or TOF) than that for the homogeneous one due to the lower activity of the immobilized catalysts and/or the difficulty in the diffusion of reactants and products in nanopores.^{3,8f,g,17,20}

The asymmetric epoxidation of 6-cyano-2,2-dimethylchromene was actually performed in the space between the salen plane and the upper wall of nanopores (Scheme 9). When the chiral Mn(salen) catalyst was immobilized in various nanopores of mesoporous materials via phenoxy groups or sulfonic groups, ee values increased with decreasing the nanopore sizes of supports for the heterogeneous asymmetric epoxidation (except for 2.7MCM). When the Mn(salen) catalyst was immobilized into the nanopores of 9.7AS or 7.6SBA via substituted phenyl sulfonic groups, the asymmetric induction enhanced with increasing the linkage length. Both modes led to the same result that the reaction space in nanopores between the salen plan and the upper pore wall was gradually optimized, and accordingly the confinement effect improved the enantioselectivities for the asymmetric epoxidation in the nanopores. Mn(salen) catalysts immobilized into the nanopores of mesoporous supports always gave higher ee values than those obtained on the external surface of 1.6MCM. These results confirmed that the confinement effect originating from nanopores enhanced the asymmetric induction for the heterogeneous asymmetric epoxidation of 6-cyano-2,2-dimethylchromene.



Scheme 9. A schematic description of the heterogeneous asymmetric epoxidation in nanopores of mesoporous supports with decrease in pore sizes and increase in linkage lengths.

Table 5 shows the results of the recycling heterogeneous Mn(salen) catalysts for the asymmetric epoxidation of 6-cyano-2,2-dimethylchromene. The heterogeneous catalysts could be recycled at least three times for the asymmetric

Table 5. The recycles of the heterogeneous Mn(salen) catalysts for the asymmetric epoxidation^a


Catalyst	Run	Time (h)	Conv. (%)	ee (%) ^b
9.7AS–PhOMn(salen)	1st	24	84.1	68.8
	2nd	24	80.1	67.2
	3rd	24	71.3	65.7
9.7AS(Me)–4-PhSO ₃ Mn(salen)	1st	4.5	100	90.6
	2nd	4.5	95.0	87.3
	3rd	6	77.3	83.2

^a Reactions were performed in CH₂Cl₂ (6 ml) with olefin (2.0 mmol), *n*-nonane (2.0 mmol), heterogeneous Mn(salen) catalyst (0.030 mmol, 1.5 mol %), PPNO (0.72 mmol), and NaClO aqueous solution (pH=11.5, 0.55 M, 7.3 ml) at 20 °C.

^b (*R,R*)-Configuration.

epoxidation of 6-cyano-2,2-dimethylchromene without showing dramatic deterioration of the performance.

4. Conclusion

This paper summarized the asymmetric epoxidation of unfunctionalized olefins on Mn(salen) catalysts axially immobilized on inorganic supports or polymers via phenoxy groups and substituted phenyl sulfonic groups. These heterogeneous catalysts usually gave higher ee values and *cis/trans* ratios than those of the homogeneous ones for the asymmetric epoxidation of *cis*- β -methylstyrene. Mn(salen) catalysts immobilized into the nanopores via flexible propyl sulfonic groups generally presented higher ee values and chemical selectivities than those obtained for the catalysts anchored on the external surface via rigid phenyl sulfonic groups for the asymmetric epoxidation of styrene and 1,2-dihydronaphthalene. It was also observed that the ee values increased with increasing the linkage length of Mn(salen) catalysts immobilized into the nanopores for the asymmetric epoxidation. The nanopores and the linkage length were found to be the two most significant factors that influenced the enantioselectivity for the heterogeneous asymmetric epoxidation.

The asymmetric epoxidation of 6-cyano-2,2-dimethylchromene on the Mn(salen) catalysts immobilized into the various nanopores via different linkage lengths was reported for the first time. The Mn(salen) catalyst grafted via phenoxy groups gave the highest ee value of 84.9% when the nanopore sizes of supports were tuned to 6.2 nm, which was also higher than 49.0% ee obtained for the catalyst anchored on the external surface. When the linkage lengths were increased from one single-bond long to five-bonds long, the ee values increased from 44.9% to 82.6% for the Mn(salen) catalyst grafted into the nanopores of 9.7AS via substituted phenyl sulfonic groups. The decrease in nanopores or increase in linkage length strengthened the confinement effect and subsequently enhanced the enantioselectivities for the heterogeneous asymmetric epoxidation. It was also observed that the Mn(salen) catalyst immobilized into the nanopores modified with methyl groups gave higher ee value (90.6% vs 80.1%) and TOF (14.8 h⁻¹ vs 10.8 h⁻¹) than those of the homogeneous catalyst.

5. Experimental

5.1. General

Activated silica (pore size of 9.7 nm with sharp pore distribution, Fig. 2), SBA-15 (pore sizes of 7.6 and 6.2 nm), and MCM-41 (pore sizes 2.7 and 1.6 nm) were used as supports and marked as 9.7AS, 7.6SBA, 6.2SBA, 2.7MCM, and 1.6MCM, respectively. The racemic epoxides were prepared by epoxidation of the olefin with *m*-CPBA in CHCl₃ at 0 °C^{8g} and confirmed by GC–MS (GC6890–MS5973N). Epoxide was analyzed by GC–MS, and the conversions (with *n*-nonane as internal standard) and the ee values were determined by gas chromatography (6890N, Agilent Co.) using a chiral column (HP19091G-B213, Agilent Co.). All FTIR spectra were collected on a Fourier transform infrared spectrometer (Nicolet Nexus 470) with a resolution of 4 cm⁻¹ and 64 scans. IR spectra of the free complexes and the supported complexes were recorded, respectively, by making samples into KBr pellets and self-supporting wafers. NMR spectra were accumulated on a Bruker DRX-400 spectrometer. The UV–vis spectra were recorded on a JASCO V-550 spectrometer. The free Mn(salen) complexes were dissolved in CH₂Cl₂ for UV–vis adsorption with CH₂Cl₂ as reference. Diffuse reflectance UV–vis spectra of the solid samples were recorded in the spectrophotometer with an integrating sphere using BaSO₄ as reference. XRD patterns were recorded on a Rigaku D/Max 3400 powder diffraction system using Cu K α radiation over the range 0.5 $\leq 2\theta < 10^\circ$. The nitrogen sorption experiments were performed at 77 K on ASAP 2000 system in static measurement mode. The samples were degassed at 100 °C for 5 h before the measurement. The pore size distribution curve was obtained from desorption isotherm with BJH method.

5.2. Synthesis of homogeneous Mn(salen)OPh catalysts (8)

Homogeneous Mn(salen)Cl (**6**) was synthesized according to literature²⁴ and their structures were well confirmed by ¹³C NMR, ¹H NMR, FTIR, rotational analysis, and element analysis. Salen: ¹³C NMR (CDCl₃, 400 MHz): δ (ppm)=165.9, 158.1, 139.9, 136.4, 126.7, 126.0, 118.0, 72.4, 35.0, 34.0, 33.2, 31.4, 29.5, 24.3; IR (KBr, cm⁻¹): ν =2952, 1629, 1468, 1434, 1360, 830; $[\alpha]_D^{20} + 300$ (*c* 0.1, CH₂Cl₂); elemental analysis calcd (%) for C₃₆H₅₄N₂O₂: C 79.12, H 9.89, N 5.13; found: C 78.85, H 9.90, N 5.23. Mn(salen)Cl (**6**): IR (KBr, cm⁻¹): ν =2952, 2864, 1609, 1535, 1253, 837; elemental analysis calcd (%) for C₃₆H₅₂ClMnN₂O₂: C 68.13, H 8.20, N 4.41; found: C 70.13, H 8.70, N 4.27.

Phenol (25 g, 0.265 mol) was dissolved in a solution of NaOH (9.54 g, 0.238 mol) in distilled water (10 ml). After stirring for 30 min at room temperature (rt), the mixture was filtrated and washed thoroughly with toluene until no residual phenol could be detected by FeCl₃, then was washed with 3 \times 30 ml of ethanol. The white power PhONa (**7**) was obtained after being dried for 8 h at 80 °C under high vacuum (20.71 g, 75%) and was stored under argon.

Mn(salen)Cl complex (**6**, 0.256 mmol) and PhONa (**7**, 35.9 mg, 0.309 mmol, 1.2 equiv) were added to ethanol (60 ml), and the mixture was refluxed for 3 h at 80 °C

(Scheme 6).^{8g,19} Then ethanol was removed after the mixture was cooled to rt. To this dark solid was added 30 ml of CH₂Cl₂, and the organic phase was washed with 15 ml of distilled water. Samples of the aqueous layer were checked by the HNO₃–AgNO₃ solution until no characteristic white flocc was observed (needed about three times). Then the CH₂Cl₂ solution was washed with 10 ml of saturated NaCl solution, dried over anhydrous Na₂SO₄, and concentrated to give the brown-dark solid Mn(salen)OPh (**8**). IR (KBr, cm⁻¹): ν =2955, 1612, 1535, 1477, 1312, 1253, 1175, 837; elemental analysis calcd (%) for C₄₂H₅₇MnN₂O₃: C 73.26, H 8.28, N 1.16; found: C 74.09, H 8.37, N 1.04.

5.3. Synthesis of modified supports **11**, **13**, and **14**^{8f,g,20}

Pure siliceous support (activated silica, SBA-15 or MCM-41, 9 g) was dehydrated at 125 °C under 0.01 torr for 4 h before the addition of the fresh PhSi(OEt)₃, PhCH₂Si(OEt)₃, PhCH₂CH₂Si(OMe)₃ or PhNHCH₂CH₂CH₂Si(OMe)₃ (21 ml) and dry toluene (450 ml). The resulting mixture was stirred for 1 h at rt, and then refluxed for 18 h at 120 °C under Ar, in which the phenyl groups were grafted on the supports.²⁵ After being cooled, filtrated, and washed with toluene, the solid was dried at 60 °C under reduced pressure overnight to obtain support-R¹-Ph (**9**) as a white powder (Scheme 7).

The supports modified with phenoxy sodium (**11**) were prepared as follows. Support-Ph (5 g) was added to distilled water (90 ml) containing concentrated sulfuric acid (1.3 g) and catalyst FeCl₃·6H₂O (50 mg), and this suspension was stirred at 50 °C for 30 min (Scheme 7).²⁶ Then H₂O₂ (4 ml) was added and the mixture was stirred for an additional 5 h. The solid was filtrated and washed by distilled water till the pH equaled 7 to give support-PhOH (**10**) as a white solid. A solution of NaOH (160 mg, 4 mmol) in distilled water (200 ml) was added to support-PhOH (4 g) and this mixture was stirred for 3 h at rt. The solid was filtrated and washed with distilled water till pH equaled 7 to produce **11** as a white powder (Scheme 7).

The supports modified with sulfonic groups (**13**) were prepared as follows. The support-R¹-Ph (**9**, 3 g) was dehydrated at 125 °C under 0.01 torr for 4 h, then was cooled to 40 °C under Ar atmosphere. Fuming sulfuric acid (10%, 10 ml) was added to the solid and the resulting mixture was stirred for 2 h at 40 °C, in which the phenyl groups were sulfonated to phenyl sulfonic groups (Scheme 7).²⁷ The solid was filtrated under reduced pressure, washed with distilled water till pH near 7, and then washed with 1,4-dioxane for three times, ethanol for three times, and distilled water to obtain support-R¹-PhSO₃H (**12**). To this wet solid **12**, a solution of NaHCO₃ (0.33 g, 3.9 mmol) in distilled water (20 ml) was added to neutralize the PhSO₃H groups and this mixture was stirred for 3 h at rt. The solid was filtrated and washed to neutrality to produce support-R¹-PhSO₃Na as a white powder (**13**).

The 9.7AS–R¹-PhSO₃Na (**13**, 3 g) were dehydrated at 125 °C under 0.01 torr for 4 h and then combined with fresh MeSi(OMe)₃ (3 ml) in dry toluene (50 ml) (Scheme 7). The resulting mixture was stirred for 1 h at rt, and then refluxed for 18 h at 120 °C under Ar, in which the methyl groups were grafted onto the supports. After being cooled, filtrated,

and washed thoroughly with toluene, the solid was dried at 60 °C under reduced pressure overnight to obtain 9.7AS(Me)–R¹-PhSO₃Na (**14**) as a white powder.

5.4. Synthesis of heterogeneous Mn(salen) catalysts

The grafting of Mn(salen) complexes on the supports was performed by refluxing the mixture of Mn(salen)Cl (**6**, 1.0 mmol) and **11**, **13** or **14** (1.0 g) in ethanol (60 ml) for 5 h (Scheme 8).^{8d,g} Then the solid was filtrated and washed thoroughly with ethanol, and then with CH₂Cl₂ in order to eliminate all the Mn(salen) complexes adsorbed on the supports. The CH₂Cl₂ filtrates were detected by UV–vis spectra until no characteristic peaks of Mn(salen) could be detected (CH₂Cl₂ as reference). After being dried, the three kinds of heterogeneous Mn(salen) catalysts were obtained as brown powder: support-PhOMn(salen), support-R¹-PhSO₃Mn(salen), and 9.7AS(Me)–R¹-PhSO₃Mn(salen) (Scheme 8).

5.5. Asymmetric epoxidation of 6-cyano-2,2-dimethylchromene^{8d,g}

In order to quantitatively compare the catalytic performance, the amount of heterogeneous catalysts was normalized based on the same amount of Mn(salen) active center. Dichloromethane was used as the optimal solvent. *n*-Nonane was used as internal standard due to its stability, inertia, and easy handling (bp 151 °C). A typical epoxidation^{8g} was processed in a stirred solution of olefin (1 mmol) in CH₂Cl₂ (3 ml) containing *n*-nonane (1.0 mmol), PPNO as axial additive (0.38 mmol), homogeneous or heterogeneous Mn(salen) catalyst (0.015 mmol, 1.5 mol%, based on Mn element), and NaClO aqueous solution (pH=11.5, 0.55 M, 3.64 ml, 2 equiv) at 20 °C. After the reaction, the organic layer was concentrated and purified by flash chromatography for the homogeneous systems or filtered to remove catalysts for the heterogeneous systems. The recycling experiments were carried out following the same procedure but the amounts of all the components were doubled. After a reaction, the solid catalysts were filtrated and washed thoroughly with distilled water, ethanol, and dichloromethane for the next cycle.

Acknowledgements

The financial support from the National Natural Science Foundation of China (NSFC, Grant No. 20321303) is gratefully acknowledged. We would like to thank Dr. Jianliang Xiao at the University of Liverpool, UK, for helpful discussion.

References and notes

- Blaser, H. U.; Spindler, F.; Studer, M. *Appl. Catal., A* **2001**, *221*, 119.
- (a) Zhang, W.; Loebach, J. L.; Wilson, S. R.; Jacobsen, E. N. *J. Am. Chem. Soc.* **1990**, *112*, 2801; (b) Irie, R.; Noda, K.; Ito, Y.; Matsumoto, N.; Katsuki, T. *Tetrahedron Lett.* **1990**, *31*, 7345.
- For recent reviews on heterogeneous chiral catalysis, see: (a) Bianchini, C.; Barbaro, P. *Top. Catal.* **2002**, *19*, 17; (b) Fan, Q. H.; Li, Y. M.; Chan, A. S. C. *Chem. Rev.* **2002**, *102*, 3385; (c) Song, C.-E.; Lee, S.-G. *Chem. Rev.* **2002**,

- 102, 3495; (d) McMorn, P.; Hutchings, G. J. *Chem. Soc. Rev.* **2004**, *33*, 108; (e) Li, C. *Catal. Rev.—Sci. Eng.* **2004**, *46*, 419.
4. (a) Davis, M. E. *Nature* **2002**, *417*, 813; (b) Trong, O. D.; Desplandier-Giscard, D.; Danumah, C.; Kaliaguine, S. *Appl. Catal. A* **2003**, *253*, 545.
5. Frunza, L.; Kosslick, H.; Landmesser, H.; Hoft, E.; Fricke, R. *J. Mol. Catal. A: Chem* **1997**, *123*, 179.
6. Sabatier, M. J.; Corma, A.; Domenech, A.; Fornes, V.; Garcia, H. *Chem. Commun.* **1997**, 1285.
7. Reger, T. S.; Janda, K. D. *J. Am. Chem. Soc.* **2000**, *122*, 6929.
8. For covalent grafting of Mn(salen) on mesoporous materials, see: (a) Zhou, X.-G.; Yu, X.-Q.; Huang, J.-S.; Li, S.-G.; Li, L.-S.; Che, C.-M. *Chem. Commun.* **1999**, 1789; (b) Kim, G.-J.; Shin, J.-H. *Tetrahedron Lett.* **1999**, *40*, 6827; (c) Kim, G.-J.; Kim, S.-H. *Catal. Lett.* **1999**, *57*, 139; (d) Xiang, S.; Zhang, Y. L.; Xin, Q.; Li, C. *Chem. Commun.* **2002**, 2696; (e) Ayala, V.; Corma, A.; Iglesias, M.; Rincón, J. A.; Sánchez, F. *J. Catal.* **2004**, *224*, 170; (f) Zhang, H. D.; Xiang, S.; Li, C. *Chem. Commun.* **2005**, 1209; (g) Zhang, H. D.; Xiang, S.; Xiao, J. L.; Li, C. *J. Mol. Catal. A: Chem.* **2005**, *238*, 175; (h) Kureshy, R. I.; Ahmad, I.; Khan, N. H.; Abdi, S. H. R.; Singh, S.; Pandia, P. H.; Jasram, R. V. *J. Catal.* **2005**, *235*, 28.
9. Baleizão, C.; Gigante, B.; Garcia, H.; Corma, A. *J. Catal.* **2004**, *221*, 77.
10. For ion-exchange of Mn(salen) into layered double hydroxides, see: (a) Fraille, J. M.; Garcia, J. I.; Massam, J.; Mayoral, J. A. *J. Mol. Catal. A: Chem.* **1998**, *136*, 47; (b) Kureshy, R. I.; Khan, N. H.; Abdi, S. H. R.; Ahmael, I.; Singh, S.; Jasra, R. V. *J. Catal.* **2004**, *221*, 234; (c) Bhattacharjee, S.; Anderson, J. A. *Chem. Commun.* **2004**, 554; (d) Bhattacharjee, S.; Dines, T. J.; Anderson, J. A. *J. Catal.* **2004**, *225*, 398.
11. (a) Piaggio, P.; Langham, C.; McMorn, P.; Bathell, D.; Page, P. C. B.; Hancock, F. E.; Sly, C.; Hutchings, G. J. *J. Chem. Soc., Perkin Trans. 2* **2000**, 143; (b) Piaggio, P.; McMorn, P.; Murphy, D.; Bathell, D.; Page, P. C. B.; Hancock, F. E.; Sly, C.; Kerton, O. J.; Hutchings, G. J. *J. Chem. Soc., Perkin Trans. 2* **2000**, 2008.
12. Schuster, C.; Möllmann, E.; Tompos, A.; Hölderich, W. F. *Catal. Lett.* **2001**, *74*, 69.
13. (a) Baleizão, C.; Gigante, B.; Das, D.; Alvaro, M.; Garcia, H.; Corma, A. *Chem. Commun.* **2003**, 1860; (b) Baleizão, C.; Gigante, B.; Das, D.; Alvaro, M.; Garcia, H.; Corma, A. *J. Catal.* **2004**, *223*, 106.
14. (a) Srinivasan, K.; Michaud, P.; Kochi, J. K. *J. Am. Chem. Soc.* **1986**, *108*, 2309; (b) Canali, L.; Cowan, E.; Deleuze, H.; Gibson, C. L.; Sherrington, D. C. *Chem. Commun.* **1998**, 2561.
15. For J. M. Thomas' work about the confinement effect, see: (a) Thomas, J. M.; Maschmeyer, T.; Johnson, B. F. G.; Shephard, D. S. *J. Mol. Catal. A: Chem.* **1999**, *141*, 139; (b) Jones, M. D.; Raja, R.; Thomas, J. M.; Johnson, B. F. G.; Lewis, D. W.; Rouzaud, J.; Harris, K. D. M. *Angew. Chem. Int. Ed.* **2003**, *42*, 4326; (c) Raja, R.; Thomas, J. M.; Jones, M. D.; Johnson, B. F. G.; Vaughan, D. E. W. *J. Am. Chem. Soc.* **2003**, *125*, 14982.
16. For Hutchings' work about the confinement effect, see: (a) Taylor, S.; Gullick, J.; McMorn, P.; Bethell, D.; Page, P. C. B.; Hancock, F. E.; King, F.; Hutchings, G. J. *J. Chem. Soc., Perkin Trans. 2* **2001**, 1714; (b) Caplan, N. A.; Hancock, F. E.; Page, P. C. B.; Hutchings, G. J. *Angew. Chem. Int. Ed.* **2004**, *43*, 1685.
17. Zhang, H. D.; Zhang, Y. M.; Li, C., unpublished.
18. For recent reviews on polymer-immobilized Mn(salen) catalysts, see: (a) Clapham, B.; Reger, T. S.; Janda, K. D. *Tetrahedron* **2001**, *57*, 4637; (b) Dhal, P. K.; De, B. B.; Sivaram, S. *J. Mol. Catal. A: Chem.* **2001**, *177*, 71; (c) Sherrington, D. C. *Catal. Today* **2000**, *57*, 87; (d) Canali, L.; Sherrington, D. C. *Chem. Soc. Rev.* **1999**, *28*, 85.
19. Zhang, H. D.; Zhang, Y. M.; Li, C. *Tetrahedron: Asymmetry* **2005**, *16*, 2417.
20. Zhang, H. D.; Zhang, Y. M.; Li, C. *J. Catal.* **2006**, *238*, 369.
21. (a) North, J. T.; Kronenthal, D. R.; Pullockaran, A. J.; Real, S. D.; Chen, H. Y. *J. Org. Chem.* **1995**, *60*, 3397; (b) Page, P. C. B.; Buckley, B. R.; Heaney, H.; Blacker, A. J. *Org. Lett.* **2005**, *7*, 375.
22. Lee, N. H.; Muci, A. R.; Jacobsen, E. N. *Tetrahedron Lett.* **1991**, *32*, 5055.
23. For the antihypertensive active compounds with chromene skeleton, see: (a) Cho, H.; Katoh, S.; Sayama, S.; Murakami, K.; Nakanishi, H.; Kajimoto, Y.; Ueno, H.; Kawasaki, H.; Aisaka, K.; Uchida, I. *J. Med. Chem.* **1996**, *39*, 3797; (b) Bogaert-Alvarez, R. J.; Demena, P.; Kodersha, G.; Polomski, R. E.; Soundararajan, N.; Wang, S. S. Y. *Org. Process Res. Dev.* **2001**, *5*, 636; (c) Bergmann, R.; Eiermann, V.; Gericke, R. *J. Med. Chem.* **1990**, *33*, 2759.
24. For the synthesis of Mn(salen) catalysts, see: (a) Zhang, W.; Jacobsen, E. N. *J. Org. Chem.* **1991**, *56*, 2296; (b) Larrow, J. F.; Jacobsen, E. N. *J. Org. Chem.* **1994**, *59*, 1939.
25. Hecker, A.; Seebach, D. *Helv. Chim. Acta* **2002**, *85*, 913.
26. (a) Bianchi, D.; Bortolo, R.; Tassinari, R.; Ricci, M.; Vignola, R. *Angew. Chem., Int. Ed.* **2000**, *39*, 4321; (b) Peng, J.; Shi, F.; Gu, Y.; Deng, Y. *Green Chem.* **2003**, *5*, 224.
27. Jones, C. W.; Tsuji, K.; Davis, M. E. *Nature* **1998**, *393*, 52.

Indirect catalytic epoxidation with hydrogen peroxide electrogenerated in ionic liquids

Kam-Piu Ho,^{a,b} Kwok-Yin Wong^{a,b,*} and Tak Hang Chan^{a,b,*}

^aDepartment of Applied Biology and Chemical Technology, The Hong Kong Polytechnic University, Hung Hom, Kowloon, Hong Kong, PR China

^bThe Institute of Molecular Technology for Drug Synthesis and Discovery, The Hong Kong Polytechnic University, Hung Hom, Kowloon, Hong Kong, PR China

Received 11 November 2005; revised 5 December 2005; accepted 7 December 2005

Available online 22 May 2006

Abstract—Hydrogen peroxide was generated in room temperature ionic liquids by electrolysis, which was then used for the epoxidation of lipophilic alkenes under a carbon dioxide-saturated environment and in the presence of catalytic amount of manganese salt. ¹³C NMR showed that the active peroxy monocarbonate (HCO_4^-) was generated from the mixture of H_2O_2 , CO_2 , and water in the ionic liquids. Most lipophilic alkenes were selectively epoxidized within 4–5 h. The ionic liquids can be recovered and reused without any deterioration in the performance. © 2006 Elsevier Ltd. All rights reserved.

1. Introduction

Epoxides are useful chemicals in the manufacture of a range of important commercial products.¹ They can easily be modified to other functionalized compounds or conjugated to other building blocks. For many years, epoxides are produced from alkenes and chlorine treated with alkali via chlorohydrins.² This process has a high efficiency, but consumes chlorine and caustic, and produces NaCl as the by-product.² With the development of new industrial applications using epoxides as intermediates, the demand for epoxides has been increasing. There is therefore a pressing need to develop ‘greener’ routes for epoxide production, especially epoxidation.

Hydrogen peroxide (H_2O_2) is considered as an environmentally benign oxidant for epoxidation because only water is produced as the by-product. Many metal-based catalytic systems including tungsten,^{3–5} titanium,^{6–8} manganese,^{9–11} rhenium,^{12–14} and iron^{15–17} have been reported using H_2O_2 as the terminal oxidant. H_2O_2 is produced by the anthraquinone process (AQ process) in industry. This process requires the use of toxic organic solvents (e.g., trimethylbenzene) for catalyst recycle and is thus not totally green.¹⁸ Moreover, the hazards associated with the storage and transportation of concentrated H_2O_2 contribute significantly to its cost.¹⁹ Thus it is desirable to have an alternative yet environmentally

benign way for on-site generation of hydrogen peroxide in the chemical plant. In industry, an alternative way to produce low strength H_2O_2 is by electrochemical reduction of O_2 .²⁰ This simple and waste-free route uses air or oxygen gas as feedstock and electrons as the reducing agent.

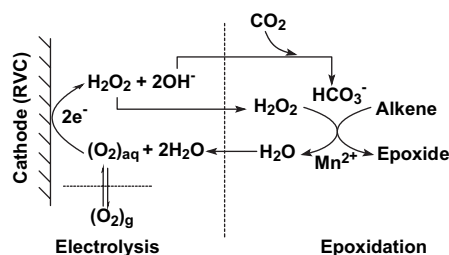
Solvents are the most ubiquitous class of chemicals used as reaction media and in the separation and extraction of products from reaction mixtures. Many of them are volatile organic compounds (VOCs) and they are often used in large-scale in industrial plants. These volatile organic solvents are harmful to human health and cause environmental problems.²¹ Room temperature ionic liquids (ILs) are considered as ‘green’ alternatives to replace volatile organic solvents because of their low vapor pressures, high thermal stabilities, and good solubility for a broad spectrum of chemicals.²² Reports on their use as solvents in extraction,^{23,24} as electrolytes in solar cells,^{25,26} as reaction media for various catalytic processes,^{27,28} and as solvents/electrolytes in electrosyntheses^{29–31} are now available in literature.

Electrogeneration of H_2O_2 in aqueous^{32–35} and biphasic systems^{36,37} has been extensively reported. Recently, we have reported the electrogeneration of H_2O_2 in the ionic liquid 3-butyl-1-methylimidazolium tetrafluoroborate ([bmim][BF₄]) and demonstrated that the H_2O_2 could be used in situ for the epoxidation of electrophilic alkenes in alkaline medium.³⁸ As this system is only applicable to the epoxidation of electrophilic alkenes such as α,β -unsaturated ketones, it would be of interest if we can widen the scope and extend its application to other classes of alkenes. We have therefore investigated the coupling of the electrogeneration

Keywords: Hydrogen peroxide; Oxygen reduction; Electrogeneration; Manganese/bicarbonate-catalyzed epoxidation; Ionic liquids.

* Corresponding authors. Tel.: +86 852 2766 5644; fax: +86 852 2364 9932; e-mail addresses: bckywong@polyu.edu.hk; bcchanth@polyu.edu.hk

of H_2O_2 in ionic liquid (IL) with the environmentally benign manganese/bicarbonate-activated epoxidation system³⁹ (Scheme 1). Carbon dioxide gas (CO_2) was used to generate the bicarbonate (HCO_3^-) and the active peroxymonocarbonate species (HCO_4^-) in situ in the H_2O_2 /ionic liquid/ $\text{NaOH}_{(\text{aq})}$ mixture because it is relatively inexpensive, and provides a convenient means to neutralize the NaOH in the ionic liquid electrolyte, that is, required for the electrogeneration of H_2O_2 , and brings down the pH to the optimal range for epoxidation.



Scheme 1. Electrogeneration of H_2O_2 for the epoxidation of lipophilic alkenes with active species generated in situ in $[\text{bdmim}][\text{BF}_4]/\text{NaOH}_{(\text{aq})}$ mixture.

2. Results and discussion

2.1. Electrogeneration of hydrogen peroxide in $[\text{bdmim}][\text{BF}_4]$



We carried out the electrogeneration of H_2O_2 using an electrochemical cell with reticulated vitreous carbon (RVC) as the cathode and a platinum-coated titanium plate as the anode. The cyclic voltammograms of O_2 reduction in the ionic liquid 1-butyl-2,3-dimethylimidazolium tetrafluoroborate ($[\text{bdmim}][\text{BF}_4]$) are shown in Figure 1. In the absence of water, a reversible couple at -0.75 V versus SCE was observed, which can be assigned to the reduction of O_2 to O_2^- as previously reported by AlNashef and co-workers (Eq. 1).^{40,41} The addition of water to the ionic liquid leads to an enhancement of the reduction, which is accompanied by an anodic shift of the reduction peak potential (Fig. 1). This can be attributed to the activation of O_2^- by water leading to the further reduction to H_2O_2 or HO_2^- (Eq. 2).⁴²

When a constant current was applied to the electrochemical cell, H_2O_2 was electrogenerated at a steady rate and its concentration in the electrolyte increased with time. The current efficiency, however, shows a clear correlation with the water content in the ionic liquid (Fig. 2). When the water concentration is less than 20% (v/v), H_2O_2 production is relatively slow and a higher cell potential is required to drive the reaction at fixed current density (Table 1). When the water content is increased to 20% (v/v) or above, the production of H_2O_2 occurs at a relatively fast rate. However, too high a water content will lead to a drop in the current efficiency of H_2O_2 production due to the lower solubility of O_2 as well

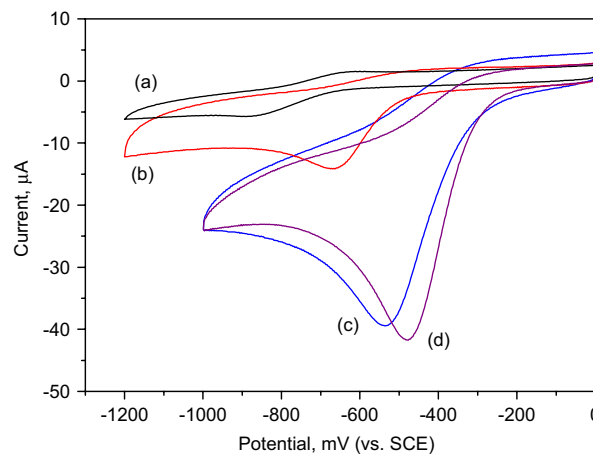


Figure 1. Cyclic voltammograms of oxygen reduction in $[\text{bdmim}][\text{BF}_4]$. (a) $[\text{bdmim}][\text{BF}_4]$ only, (b) $[\text{bdmim}][\text{BF}_4]/\text{water}$ (9:1 v/v) mixture, (c) $[\text{bdmim}][\text{BF}_4]/\text{water}$ (4:1 v/v) mixture, and (d) $([\text{bdmim}][\text{BF}_4]/\text{water}$ (4:1 v/v))/0.006 M NaOH mixture. All are saturated with O_2 . Working electrode: 0.196 cm^2 . Scan rate: 100 mV s^{-1} .

as side reactions such as the electrolysis of water. As a result, 20% (v/v) of water was selected as the optimal water content to drive the production of H_2O_2 effectively in the $[\text{bdmim}][\text{BF}_4]/\text{NaOH}_{(\text{aq})}$ mixture in subsequent experiments.

In the H_2O_2 electrogeneration, O_2 is electrochemically reduced to H_2O_2 in the form of HO_2^- with OH^- produced concurrently (Eq. 2) in the $[\text{bdmim}][\text{BF}_4]/\text{NaOH}_{(\text{aq})}$ (4:1 v/v) mixture (catholyte). When the same electrolyte was used as the anolyte, precipitates (NaOH) appeared in the catholyte upon continuous electrolysis and the cell potential increased with the charge consumption (Table 2). Experimentally, the maximum concentration of NaOH in $[\text{bdmim}][\text{BF}_4]/\text{water}$ (4:1 v/v) mixture was found to be ~ 0.044 M. When the concentration exceeds this value, it precipitates out quickly.

In the electrochemical cell, the cation-selective nafion membrane allows cations to move between the anode and cathode compartments. The permeation selectivity depends on the size ($\text{H}^+ < \text{Na}^+ < \text{bdmim}$ ion) and concentration of cations.

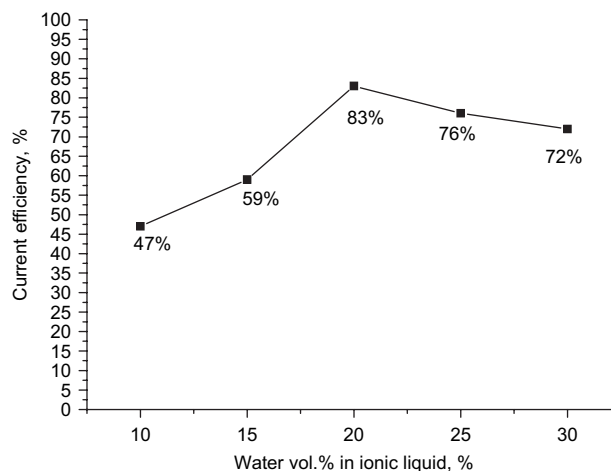


Figure 2. The effect of water content on the current efficiency of H_2O_2 electrogeneration in $[\text{bdmim}][\text{BF}_4]/\text{NaOH}_{(\text{aq})}$ mixture. Current density: 0.38 mA cm^{-2} . Catholyte: $[\text{bdmim}][\text{BF}_4]/0.006 \text{ M NaOH}_{(\text{aq})}$ mixture. Anolyte: $[\text{bdmim}][\text{BF}_4]/4 \text{ M H}_2\text{SO}_{4(\text{aq})}$ mixture.

Table 1. Electrogeneration of H₂O₂ in [bdmim][BF₄]/NaOH_(aq) mixture with different water contents

Water content, vol % in [bdmim][BF ₄]	Cell potential, V	Concentration of H ₂ O ₂ , mM	Current efficiency, %
10	3.53	21	47
15	3.37	23	59
20	2.94	37	83
25	3.02	33	76
30	3.17	31	72

Current density: 0.38 mA cm⁻². Catholyte: [bdmim][BF₄]/0.006 M NaOH_(aq) mixture. Cathode: 60 ppi RVC. Cathode surface area: 156 cm². Anolyte: [bdmim][BF₄]/4 M H₂SO_{4(aq)} mixture. Volumes of catholyte and anolyte: 25 ml. Electrolysis time: 1 h.

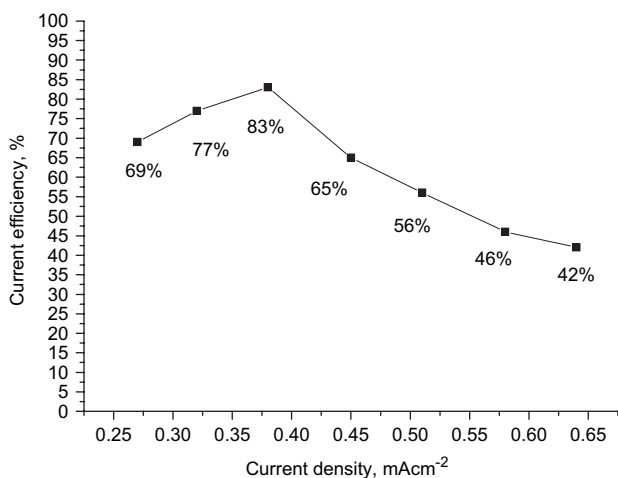
Table 2. Effect of anolyte composition on the current efficiency of H₂O₂ electrogeneration

Anolyte	Cell potential, V	Concentration of H ₂ O ₂ , mM	Current efficiency, %
[bdmim][BF ₄]/4 M H ₂ SO _{4(aq)} (4:1 v/v)	2.94	37	83
[bdmim][BF ₄]/0.006 M NaOH _(aq) (4:1 v/v)	3.12–3.57	32	71

Catholyte: [bdmim][BF₄]/0.006 M NaOH_(aq) mixture. Cathode: 60 ppi RVC. Cathode surface area: 156 cm². Volumes of catholyte and anolyte: 25 ml. Current density: 0.38 mA cm⁻². Electrolysis time: 1 h.

When an acidic mixture ([bdmim][BF₄]/H₂SO_{4(aq)} (4:1 v/v)) was used as the anolyte, H⁺ diffused to the cathodic side through the nafion during electrolysis to balance the charge consumption. Those OH⁻ generated at the cathode were simply neutralized, and the alkalinity was maintained (Table 2).

The favorable current density range for H₂O₂ production lies from 0.27 to 0.38 mA cm⁻² (Fig. 3). There is only a small change in cell potential at this current density range. At a current density of 0.38 mA cm⁻², the current efficiency reaches 83%. The current efficiency drops at current density higher than 0.45 mA cm⁻². Side reaction such as the reduction of O₂ to H₂O or the formation of H₂ may occur at such high current densities.⁴³

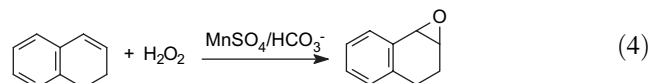
**Figure 3.** The effect of current density on the current efficiency of H₂O₂ electrogeneration in [bdmim][BF₄]/NaOH_(aq) mixture. Catholyte: [bdmim][BF₄]/0.006 M NaOH_(aq) mixture. Anolyte: [bdmim][BF₄]/4 M H₂SO_{4(aq)} mixture. Cathode: 60 ppi RVC. Cathode surface area: 156 cm². Current density: 0.38 mA cm⁻². Electrolysis time: 1 h.

2.2. In situ generation of peroxymonocarbonate by purging CO₂ gas into the [bdmim][BF₄]/NaOH_(aq)/HO₂⁻ mixture

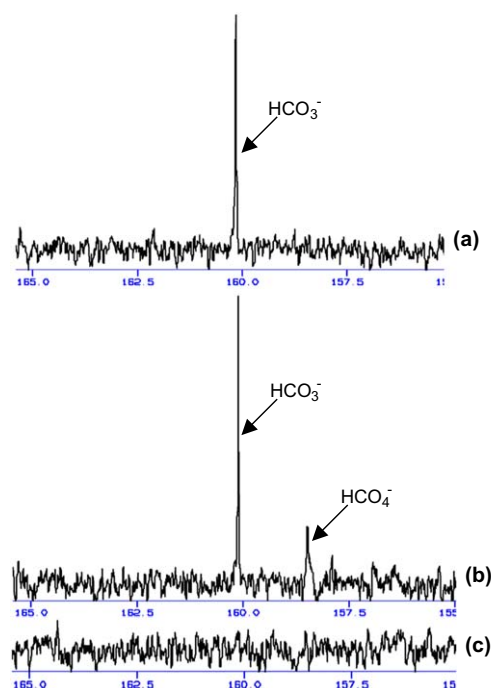
After HO₂⁻ has been generated by electrolysis, we purged the [bdmim][BF₄]/NaOH_(aq)/HO₂⁻ mixture with CO_{2(g)}. In the epoxidation of alkenes with the H₂O₂/HCO₃⁻/Mn²⁺ system, the active species corresponding to the epoxidation is believed to be a peroxymonocarbonate anion, HCO₄⁻, which is generated in situ by the reaction of HO₂⁻ with CO_{2(g)} (Eq. 3).³⁹ In our study, we were able to demonstrate that HCO₄⁻ existed in equilibrium with HCO₃⁻ by ¹³C NMR at the reaction mixture (Fig. 4). In the absence of CO_{2(g)}, no ¹³C NMR signal was observed in the range from 150 to 170 ppm. When CO_{2(g)} was continuously purged into the mixture for 5 min, two ¹³C NMR signals were observed at 158.3 and 160.3 ppm, which correspond to HCO₄⁻ and HCO₃⁻, respectively.^{39,44}



2.3. The effect of catalyst loading on the efficiency of alkene epoxidation



In this study, the H₂O₂ electrogeneration in an [bdmim][BF₄]/NaOH_(aq) mixture is in the form of HO₂⁻. Epoxidation was carried out in a separate step by transferring the [bdmim][BF₄]/NaOH_(aq)/HO₂⁻ mixture into a reaction vessel and then purged with CO₂ gas to generate the reactive HCO₄⁻ species (Fig. 5). 1,2-Dihydronaphthalene was used as

**Figure 4.** ¹³C NMR spectra. (a) [bdmim][BF₄]/NaOH_(aq)/CO_{2(g)} mixture, (b) [bdmim][BF₄]/NaOH_(aq)/0.1 M HO₂⁻/CO_{2(g)} mixture, and (c) [bdmim][BF₄]/NaOH_(aq)/0.1 M HO₂⁻ mixture.

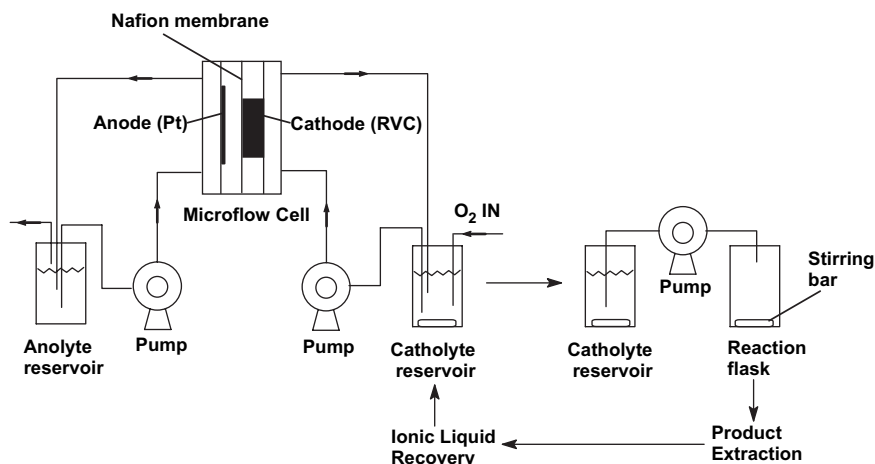


Figure 5. Schematic diagram of H_2O_2 electrogeneration in ionic liquid for catalytic epoxidation.

the standard substrate for optimizing the reaction conditions because of its high solubility and reactivity in the IL/ H_2O_2 / $\text{Mn}^{2+}/\text{HCO}_3^-$ system (Eq. 4).⁴⁴

MnSO_4 is the catalyst for the epoxidation of alkenes with H_2O_2 in the presence of bicarbonate ion. A set of experiments was carried out to test for the optimal loading of Mn^{2+} in the IL system. **Figure 6** indicates that the extent of conversion of the alkene to epoxide was comparable when 0.41–0.74 mol % of MnSO_4 (relative to that of the alkene substrate) was used. When the amount of MnSO_4 was less than 0.08 mol %, the conversion efficiency dropped significantly.

A comparison of conversion efficiency using different CO_2 sources is shown in **Table 3**. When the reaction temperature was maintained at 5°C , there was no significant difference on the product yield whether dry ice (solid CO_2) (entry 4) or CO_2 gas (entry 2) was used to generate HCO_3^- and HCO_4^- , and good yields of epoxide (>80%) were obtained.⁴⁵ By comparison, when the temperature was controlled at 22°C , only moderate yields were obtained in both cases (entries 1 and 3). The use of air (0.04% CO_2) as control

Table 3. The effect of CO_2 source and temperature on the epoxide yield

Entry	CO_2 source	Reaction temperature, $^\circ\text{C}$	Epoxide yield, %
1	$\text{CO}_{2(\text{g})}$	22	61
2	$\text{CO}_{2(\text{g})}$	5	80
3	$\text{CO}_{2(\text{s})}$ (dry ice)	22	70
4	$\text{CO}_{2(\text{s})}$ (dry ice)	5	83
5	$\text{CO}_{2(\text{g})}$ (air)	22	0
6	$\text{CO}_{2(\text{g})}$ (air)	5	0

Substrate: 1,2-dihydronaphthalene (0.13 mmol). [H_2O_2]: 0.08 M (electro-generated in 25 ml [bdmim][BF_4]/ $\text{NaOH}_{(\text{aq})}$ mixture).

indicates that no epoxide product could be obtained (entries 5 and 6).

2.4. Catalytic epoxidation of alkenes

The alkene was mixed with a solution of MnSO_4 in the reaction flask prior to charge with $\text{CO}_{2(\text{g})}$. When 0.08 M H_2O_2 (15 equiv) in [bdmim][BF_4]/ $\text{NaOH}_{(\text{aq})}$ mixture was added all at once, gas bubble was observed and only moderate yield of the epoxide (36%) was obtained. This showed that H_2O_2 decomposition had occurred in the presence of Mn^{2+} .^{46,47} On the other hand, when the H_2O_2 was added slowly to the alkene substrate solution over a period of 1 h at 5°C , decomposition of H_2O_2 was minimized. The epoxidation reaction then proceeded smoothly to give the epoxides in good yield.

The optimal amount of electrogenerated H_2O_2 in the [bdmim][BF_4]/ $\text{NaOH}_{(\text{aq})}$ mixture was tested. **Figure 7** indicates that the epoxide yield was the highest when 15–16 equiv of H_2O_2 were used. This value is comparable to our previous report using 10 equiv of H_2O_2 for epoxidation with the $\text{HCO}_3^-/\text{Mn}^{2+}/[\text{bmim}][\text{BF}_4]$ system.⁴⁴ It should be noted that the concentration of H_2O_2 (~ 0.08 M) prepared by electrogeneration in this study is much lower than the 35 wt % H_2O_2 (~ 11.7 M) used in our previous study.⁴⁴ Thus the hazards associated with the handling of concentrated H_2O_2 are greatly reduced.

After optimizing the catalytic process, a number of lipophilic alkenes were epoxidized under similar conditions (**Table 4**). In general, good to excellent yields of the epoxides

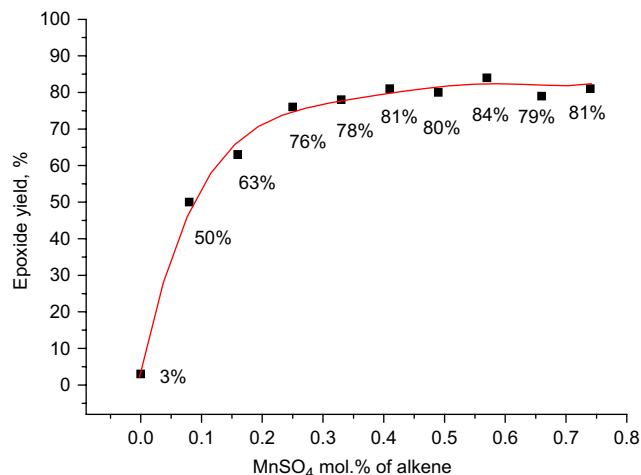


Figure 6. The effect of MnSO_4 concentration on the efficiency of epoxide formation. Substrate: 1,2-dihydronaphthalene (0.13 mmol). [H_2O_2]: 0.08 M (electro-generated in 25 ml [bdmim][BF_4]/ $\text{NaOH}_{(\text{aq})}$ mixture).

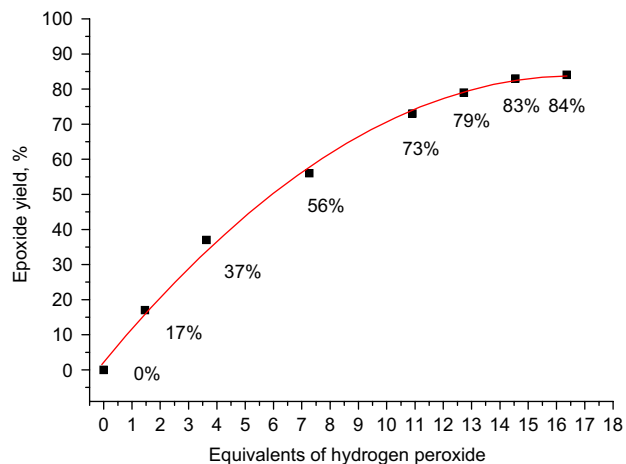
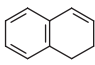
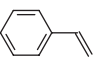
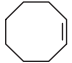
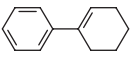
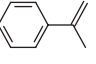
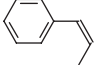
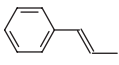
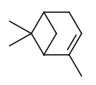
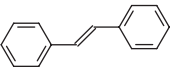
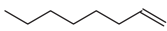


Figure 7. Optimization of alkene/H₂O₂ stoichiometry. Substrate: 1,2-dihydronaphthalene (0.13 mmol). MnSO₄: 0.41 mol %.

Table 4. Epoxidation of various lipophilic alkenes

Entry	Substrate	Reaction time, h	Conversion, %	Yield, %
1	1,2-dihydronaphthalene 	4	>99	83
2	Styrene 	4	>99	84
3	Cyclooctene 	4	>99	80
4	1-phenyl-1-cyclohexene 	5	>99	90
5	α -methyl styrene 	5	95	83
6	<i>cis</i> - β -methyl styrene 	5	87	76 ^a
7	<i>trans</i> - β -methyl styrene 	5	81	71 ^b
8	α -pinene 	5	75	62
9	<i>trans</i> -stilbene ^c 	5	44	42
10	1-octene 	5	0	0

Substrate: 0.13 mmol. MnSO₄: 0.41 mol %. [H₂O₂]: 0.08 M (electrogenerated in 25 ml [bdmim][BF₄]/NaOH_(aq) mixture). Yields were calculated on the basis of converted alkenes and determined by GC–MS versus an internal standard.

^a Only *cis*-epoxide was produced.

^b Only *trans*-epoxide was produced.

^c [odmim][BF₄] was used in place of [bdmim][BF₄].

could be obtained. The styryl and cyclic alkenes (entries 1–8) were easily oxidized to give epoxides in good yields. For *trans*-stilbene (entry 9), 3-octyl-1,2-dimethylimidazolium tetrafluoroborate ([odmim][BF₄]) was used to enhance its solubility of *trans*-stilbene in the IL mixture and moderate yield was obtained. 1-Octene (entry 10) was not epoxidized, which is in agreement with the fact that the Mn²⁺/HCO₃[−]/H₂O₂ system is not effective in the epoxidation of aliphatic terminal alkenes.⁴⁸

2.5. Recycling of the ionic liquid

Because the IL ([bdmim][BF₄]) is likely to be the most expensive component of the reaction system, it is important to demonstrate that the IL can be recovered and reused. After product extraction, water, MnSO₄, and NaHCO₃ were retained in the yellowish IL mixture. Attempts to use the crude IL mixture for H₂O₂ electrogeneration indicated that

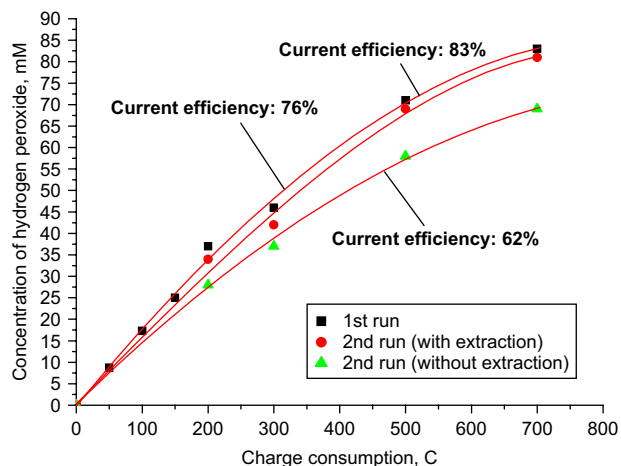


Figure 8. Effect of ionic liquid purity on H_2O_2 electrogeneration.

the current efficiency dropped to 62% (Fig. 8). Presumably, the Mn^{2+} salt interfered with the H_2O_2 production through catalytic decomposition. Attempts were therefore made to remove the Mn^{2+} before the IL mixture was reused for H_2O_2 electrogeneration.

Literature report indicates that ILs can be purified through extraction and separation into different phases.⁴⁹ In this study, 1 M $\text{Na}_2\text{CO}_3(\text{aq})$ was used for extraction and purification of the IL mixture (Fig. 9). It was found that two immiscible phases were formed without the assistance of any pressurized equipment. One liquid phase was rich in IL and water, while the other was mainly water, Na_2CO_3 , and Mn^{2+} . This interesting biphasic behavior allows us to separate most MnSO_4 from the IL mixture in a convenient manner.

Attempts to use 1 M or saturated $\text{NaOH}(\text{aq})$ for extraction of MnSO_4 from the IL mixture indicated that it is impossible to form two clear separate phases in the extraction. This is probably because of the higher solubility of NaOH than Na_2CO_3 in the IL/water (4:1 v/v) mixture (the solubility of Na_2CO_3 and NaOH are 0.016 M and 0.044 M, respectively).

The IL mixture was thus extracted with 1 M $\text{Na}_2\text{CO}_3(\text{aq})$ solution (2×15 ml). After each extraction, 85–90% of the $[\text{bdmim}][\text{BF}_4]$ was recovered and the aqueous phases were combined for further recycling. In the IL phase, the water content was always less than 20% by volume. After purification, an appropriate amount of $[\text{bdmim}][\text{BF}_4]$ or water

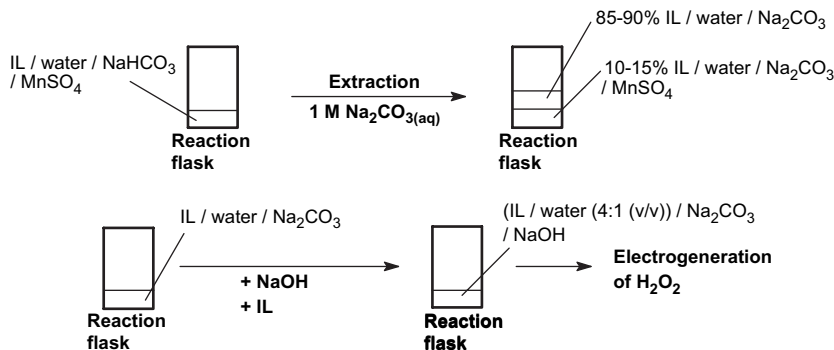


Figure 9. Ionic liquid purification before re-usage for H_2O_2 electrogeneration.

Table 5. Recovery and reuse of $[\text{bdmim}][\text{BF}_4]$ for 1,2-dihydronaphthalene epoxidation

Cycle	1	2	3	4	5
Epoxide yield, %	83	86	87	84	85

Substrate: 0.13 mmol. MnSO_4 : 0.41 mol %. $[\text{H}_2\text{O}_2]$: 0.08 M electrogenerated in 25 ml $[\text{bdmim}][\text{BF}_4]/\text{NaOH}(\text{aq})$ mixture. Yields were calculated on the basis of converted alkenes and determined by GC–MS versus an internal standard.

was added to the mixture to adjust to the optimal IL/water 8:2 v/v ratio for H_2O_2 electrogeneration. The amount of water in the IL mixture was measured according to the density method as previously reported.³⁸ As noted above, 10–15% of IL was retained in the aqueous phase. Further recovery of IL could be achieved by removing the water under vacuum and further extraction with dichloromethane.

Prior to H_2O_2 electrogeneration, the alkalinity of the recovered IL/water mixture was adjusted to an optimal apparent pH value (\sim pH 9.4) by adding NaOH . The step is important because it provides a sufficiently alkaline media for effective H_2O_2 electrogeneration.

The results of epoxidation with the recovered IL/ H_2O_2 mixture are summarized in Table 5. It can be seen that the IL mixture can be recycled for a number of times without any diminution in the epoxide yield.

3. Conclusions

The electrogeneration of H_2O_2 in ionic liquid ($[\text{bdmim}][\text{BF}_4]$) for epoxidation has been demonstrated. By purging CO_2 gas into the $\text{H}_2\text{O}_2/[\text{bdmim}][\text{BF}_4]/\text{NaOH}(\text{aq})$ mixture, the active peroxymonocarbonate (HCO_4^-) can be generated in situ, and a wide range of alkenes can be epoxidized with a simple Mn^{2+} catalyst. The ionic liquid can be recovered and reused without significant diminution in the current efficiency of H_2O_2 generation and epoxide yield.

4. Experimental

4.1. Synthesis

All chemicals and solvents used were of analytical reagent (A.R.) grade. Alkenes and epoxides were obtained from

commercial sources (Aldrich Co. or Acros Organic), and were used as received unless otherwise noted. Manganese(II) sulfate monohydrate (>99%), sodium hydroxide (98%), and H₂O₂ (35 wt% solution in water) were purchased from Aldrich Co. Oxygen (>99.7%) and argon (>99.995%) were obtained from Hong Kong Oxygen Co. Double deionized water was purified by passing through an ion-exchange resin purification train (Millipore).

4.1.1. 1-Butyl-2,3-dimethylimidazolium tetrafluoroborate ([bdmim][BF₄]).⁵⁰ A solution of 1-bromobutane (119 ml, 1.1 equiv) was added slowly and cautiously to 1,2-dimethylimidazole (96.1 g, 1 mol) in 500 ml acetone. The mixture was gently heated at reflux under argon for 24 h. After cooling to room temperature, a white solid precipitated out and the yellowish solvent was decanted. The white solid (1-butyl-2,3-dimethylimidazolium bromide, [bdmim]Br) was washed thoroughly with acetone (2 × 300 ml) and ether (2 × 300 ml). A 2 l round bottle flask was then charged with 1.5 l acetonitrile, [bdmim]Br, and sodium tetrafluoroborate (120 g, 1.1 equiv). The mixture was allowed to stand at room temperature for three days with stirring. The precipitate (NaBr) that appeared was filtered off and the filtrate was concentrated under vacuum to give a colorless liquid. Further precipitation of NaBr was achieved upon the addition of dichloromethane (1 l). The crude IL was purified on a silica column using dichloromethane as eluent to give a colorless liquid. Yield: 201.6 g (84%). ¹H NMR (CDCl₃, δ ppm): 7.32 (dd, 2H), 4.07 (t, 2H), 3.80 (s, 3H), 2.61 (s, 3H), 1.76 (m, 2H), 1.37 (m, 2H), 0.93 (t, 3H).

4.1.2. 3-Octyl-1,2-dimethylimidazolium tetrafluoroborate ([odmim][BF₄]). The preparation was similar to that of [bdmim][BF₄] except that 1-bromooctane (190 ml, 1.1 equiv) was used. Yield: 228.0 g (77%). ¹H NMR (CDCl₃, δ ppm): 7.33 (dd, 2H), 4.07 (t, 2H), 3.80 (s, 3H), 2.61 (s, 3H), 1.76 (m, 2H), 1.77 (m, 10H), 0.86 (t, 3H).

4.2. Instrumentation

The electrochemical cell was purchased from ElectroCell AB, Sweden. A 33 mm × 27 mm × 5 mm reticulated vitreous carbon (60 pores per inch (ppi)) was used as the cathode. The anode was a platinum-coated titanium plate. A Nafion 424 cation permeable membrane was used to separate the cathode and anode compartments. It was connected to the peristaltic pumps and Teflon tubings (Fig. 10). The gas and electrolyte flow rates were monitored by flowmeters purchased from Gilmont Instruments. The electrolysis was carried out at controlled current mode using an EG&G Princeton Applied Research Potential/Galvanostat (Model 273A).

For voltammetric measurements, glassy carbon and platinum electrodes were polished with 0.05 μm α-alumina (Buehler) on a microcloth, rinsed with double deionized water, and then sonicated for 5 min in water before used. Cyclic voltammetry (CV) was measured by a Bioanalytical Systems (BAS) model 100 W electrochemical analyzer and carried out in a conventional two-compartment cell with a sintered glass separated the two compartments. A platinum wire was used as the counter electrode, whereas the reference electrode was a saturated calomel electrode (SCE).

¹H and ¹³C NMR spectra were recorded on a Bruker DPX-400 MHz NMR spectrometer. A Hewlett-Packard 8900 GC-MS equipped with ECTM-1 or ECTM-WAX columns (Alltech Associate, Inc.) was used for analyzing volatile chemicals. DMSO and tetradecane were used as internal standards for ¹H NMR and GC-MS quantitative measurements, respectively.

4.3. Electrogeneration and determination of H₂O₂ in reaction mixture

The apparatus for the electrogeneration of H₂O₂ is shown in Figure 10. The two reservoirs were charged with 25 ml

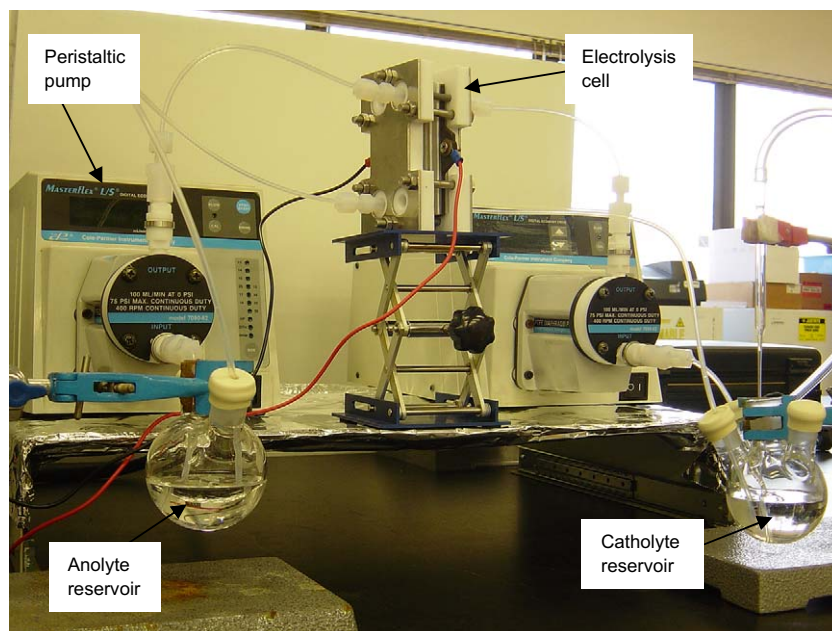


Figure 10. Apparatus for the electrogeneration of hydrogen peroxide.

solutions of anolyte (IL/H₂SO_{4(aq)}) and catholyte (IL/NaOH_(aq)), respectively. Electrolysis was carried out under circulation mode at a flow rate of 135 ml min⁻¹. O₂ was continuously purged into the catholyte throughout the process at 45 ml min⁻¹ for the electrogeneration of H₂O₂.

The H₂O₂ concentration was determined using permanganate titration. At regular time intervals during electrolysis, 0.1 ml catholyte was withdrawn and diluted with 0.5 M H₂SO_{4(aq)} (5 ml) for the titration.

4.4. Epoxidation of lipophilic alkenes with H₂O₂

Epoxidation of alkenes was achieved by using the H₂O₂ electrogenerated in IL/NaOH_(aq) mixture (Fig. 5). This mixture was added dropwisely into a flask pre-charged with alkene substrate and MnSO₄ at 2 ml min⁻¹. Meanwhile, CO_{2(g)} was continuously purging at 10 ml min⁻¹. Alternatively, dry ice (solid CO₂) was added in small portions. Throughout the mixing process, the flask was kept at 5 °C to reduce the loss of volatile alkene. It was sealed afterwards and allowed to stand at room temperature for another 3–5 h. The product was then extracted by pentane (3×20 ml), and the organic layer was washed with brine (2×10 ml) and dried over sodium sulfate. A portion of the mixture (10 ml) was mixed with the internal standard tetradecane (100 μl of a 0.156 M solution) and analyzed by GC–MS. The other portion was analyzed by ¹H NMR after the solvent had been removed under reduced pressure.

4.5. Recovery and reuse of ionic liquids

Prior to the reuse of ILs for the next H₂O₂ electrogeneration/catalytic epoxidation cycle, removal of Mn²⁺ is necessary to avoid any adverse effects on the electrogeneration of H₂O₂. Na₂CO_{3(aq)} (1 M) (2×15 ml) was used to extract the manganese salt for the electrolyte. After extraction, the mixture was separated into two phases. The IL phase was a mixture of IL/H₂O/NaOH/Na₂CO₃ in which the water content and apparent pH were measured and adjusted before reused for H₂O₂ electrogeneration. Around 10–15% of ILs remained in the aqueous phase, which was recovered by evaporating the water and then extracting with dichloromethane.

Acknowledgements

This work was supported by the Research Grants Council (PolyU 5014/03P) and the Area of Excellence Scheme of the University Grants Committee (AoE/P-10/01).

References and notes

1. Grigoropoulou, G.; Clark, J. H.; Elings, J. A. *Green Chem.* **2003**, *5*, 1–7.
2. Young, R. V.; Sessine, S. *World of Chemistry*; Gale Group: Detroit, 2000.
3. Hannick, S. M.; Kishi, Y. *J. Org. Chem.* **1983**, *48*, 3831–3833.
4. Ishii, Y.; Yamawaki, K.; Ura, T.; Yamada, H.; Yoshida, T.; Ogawa, M. *J. Org. Chem.* **1988**, *53*, 3587–3593.
5. Deng, Y.; Ma, Z.; Wang, K.; Chen, J. *Green Chem.* **1999**, *1*, 275–276.
6. Clerici, M. G.; Ingallina, P. *J. Catal.* **1993**, *140*, 71–83.
7. Sheldon, R. A.; Wallau, M.; Arends, I. W. C. E.; Schuchardt, U. *Acc. Chem. Res.* **1998**, *31*, 485–493.
8. Arends, I. W. C. E.; Sheldon, R. A. *Appl. Catal., A* **2001**, *212*, 175–187.
9. Anelli, P. L.; Banfi, S.; Montanari, F.; Quici, S. *Chem. Commun.* **1989**, 779–780.
10. Hage, R.; Iburg, J. E.; Kerschner, J.; Koek, J. H.; Lempers, E. L. M.; Martens, R. J.; Racherla, U. S.; Russell, S. W.; Swarthoff, T. *Nature* **1991**, *369*, 637–639.
11. De Vos, D. E.; Sels, B. F.; Reynaers, M.; Rao, Y. V. S.; Jacobs, P. A. *Tetrahedron Lett.* **1998**, *39*, 3221–3224.
12. Adolfsson, H.; Coperet, C.; Chiang, J. P.; Yudin, A. K. *J. Org. Chem.* **2000**, *65*, 8651–8658.
13. Yudin, A. K.; Chiang, J. P.; Adolfsson, H.; Coperet, C. *J. Org. Chem.* **2001**, *66*, 4713–4718.
14. Rudolph, J.; Reddy, K. L.; Chiang, J. P.; Sharpless, K. B. *J. Am. Chem. Soc.* **1997**, *119*, 6189–6190.
15. Costas, M.; Tipton, A. K.; Chen, K.; Jo, D. H.; Que, L. *J. Am. Chem. Soc.* **2001**, *123*, 6722–6723.
16. White, M. C.; Doyle, A. G.; Jacobsen, E. N. *J. Am. Chem. Soc.* **2001**, *123*, 7194–7195.
17. Traylor, T. G.; Tsuchiya, S.; Byun, Y. S.; Kim, C. *J. Am. Chem. Soc.* **1993**, *115*, 2775–2781.
18. Huissoud, A.; Tissot, P. *J. Appl. Electrochem.* **1998**, *28*, 653–657.
19. Arends, I.; Sheldon, R. A. *Top. Catal.* **2002**, *19*, 133–141.
20. Pletcher, D. *Industrial Electrochemistry*; Chapman and Hall: London, 1990.
21. Abraham, M. A.; Moens, L. *Clean Solvents: Alternative Media for Chemical Reactions and Processing*; American Chemical Society: Washington, DC, 2002.
22. Welton, T. *Chem. Rev.* **1999**, *99*, 2071–2083.
23. Swatloski, R. P.; Visser, A. E.; Reichert, W. M.; Broker, G. A.; Farina, L. M.; Holbrey, J. D.; Rogers, R. D. *Chem. Commun.* **2001**, 2070–2071.
24. Visser, A. E.; Holbrey, J. D.; Rogers, R. D. *Chem. Commun.* **2001**, 2484–2485.
25. Papageorgiou, N.; Athanassov, Y.; Armand, M.; Bonhote, P.; Pettersson, H.; Azam, A.; Graetzel, M. *J. Electrochem. Soc.* **1996**, *143*, 3099–3108.
26. Hagiwara, R.; Hirashige, T.; Tsuda, T.; Ito, Y. *J. Fluorine Chem.* **1999**, *99*, 1–3.
27. Wheeler, C.; West, K. N.; Eckert, C. A.; Liotta, C. L. *Chem. Commun.* **2001**, 887–888.
28. Song, C. E.; Roh, E. J.; Lee, S. G.; Shim, W. H.; Choi, J. H. *Chem. Commun.* **2001**, 1122–1123.
29. Doherty, A. P.; Brooks, C. A. *Electrochim. Acta* **2004**, *49*, 3821–3826.
30. Barhdadi, R.; Courtinard, C.; Nedelec, J. Y.; Troupel, M. *Chem. Commun.* **2003**, 1434–1435.
31. Picquet, M.; Poinot, D.; Stutzmann, S.; Tkatchenko, I.; Tommasi, I.; Wasserscheid, P.; Zimmermann, J. *Top. Catal.* **2004**, *29*, 139–143.
32. Alcaide, F.; Brillas, E.; Cabot, P. L. *J. Electrochem. Soc.* **1998**, *145*, 3444–3449.
33. Davison, J. B.; Kacsir, J. M.; Peercelanders, P.; Jasinski, R. J. *J. Electrochem. Soc.* **1983**, *130*, 1497–1501.
34. Oloman, C. *J. Electrochem. Soc.* **1979**, *126*, 1885–1892.
35. Oloman, C.; Watkinson, A. P. *J. Appl. Electrochem.* **1979**, *9*, 117–123.
36. Gyenge, E. L.; Oloman, C. W. *J. Appl. Electrochem.* **2003**, *33*, 655–663.

37. Gyenge, E. L.; Oloman, C. W. *J. Appl. Electrochem.* **2003**, *33*, 665–674.
38. Tang, M. C. Y.; Wong, K. Y.; Chan, T. H. *Chem. Commun.* **2005**, 1345–1347.
39. Lane, B. S.; Vogt, M.; DeRose, V. J.; Burgess, K. *J. Am. Chem. Soc.* **2002**, *124*, 11946–11954.
40. AlNashef, I. M.; Leonard, M. L.; Kittle, M. C.; Matthews, M. A.; Weidner, J. W. *Electrochem. Solid-State Lett.* **2001**, *4*, D16–D18.
41. AlNashef, I. M.; Leonard, M. L.; Matthews, M. A.; Weidner, J. W. *Ind. Eng. Chem. Res.* **2002**, *41*, 4475–4478.
42. Sawyer, D. T.; Sobkowiak, A.; Roberts, J. L. *Electrochemistry for Chemists*, 2nd ed.; Wiley Interscience: New York, NY, 1995.
43. Yeager, E. *Electrochim. Acta* **1984**, *29*, 1527–1537.
44. Tong, K. H.; Wong, K. Y.; Chan, T. H. *Org. Lett.* **2003**, *5*, 3423–3425.
45. Espinal, L.; Suib, S. L.; Rusling, J. F. *J. Am. Chem. Soc.* **2004**, *126*, 7676–7682.
46. Wekesa, M.; Ni, Y. H. *Tappi J.* **2003**, *2*, 23–26.
47. Venkatachalapathy, R.; Davila, G. P.; Prakash, J. *Electrochem. Commun.* **1999**, *1*, 614–617.
48. Lane, B. S.; Burgess, K. *Chem. Rev.* **2003**, *103*, 2457–2473.
49. Scurto, A. M.; Aki, S. N. V. K.; Brennecke, J. F. *Chem. Commun.* **2003**, 572–573.
50. Cammarata, L.; Kazarian, S. G.; Salter, P. A.; Welton, T. *Phys. Chem. Chem. Phys.* **2001**, *3*, 5192–5200.



ELSEVIER

Available online at www.sciencedirect.com

SCIENCE @ DIRECT®

Tetrahedron 62 (2006) 6659–6665

Tetrahedron

Comparison of TEMPO and its derivatives as mediators in laccase catalysed oxidation of alcohols

Isabel W. C. E. Arends, Yu-Xin Li, Rina Ausan and Roger A. Sheldon*

Laboratory for Biocatalysis and Organic Chemistry, Department of Biotechnology, Delft University of Technology, Julianalaan 136, 2628 BL, The Netherlands

Received 25 November 2005; accepted 23 December 2005

Available online 5 June 2006

Abstract—A series of TEMPO (2,2',6,6'-tetramethylpiperidiny-1-oxy) derivatives were studied as mediators of laccase (from *Trametes versicolor*) in the oxidation of benzyl alcohol and 1-phenylethyl alcohol. TEMPO (**1**), 4-hydroxy-TEMPO (**2**) and 4-acetylamino-TEMPO (**4**) turned out to be the most active mediators for laccase. In addition, 4-acetylamino-TEMPO and 4-hydroxy-TEMPO were more active in the oxidation of 1-phenylethanol compared to TEMPO. For these mediators kinetic isotope effects in the range of 2.1–3.2 were observed for α -monodeutero-*p*-methylbenzyl alcohol oxidation. These values are consistent with a mechanism involving oxoammonium intermediacy. Competition experiments between benzyl alcohol and 1-phenylethanol showed that TEMPO and its derivatives react faster with primary alcohols than with secondary alcohols, also in line with the proposed mechanism.

© 2006 Elsevier Ltd. All rights reserved.

1. Introduction

The selective oxidation of alcohols is a pivotal reaction in organic synthesis. Recently, much attention has been focused on the development of green, catalytic methods employing dioxygen or hydrogen peroxide as the stoichiometric oxidant.¹ Many examples of aerobic oxidation of alcohols catalysed by transition metals—notably palladium,² platinum³ and ruthenium⁴—have been described in the last few years. Copper compounds are also known to catalyse the aerobic oxidation of alcohols, both *in vitro*^{5,6} and *in vivo*.⁷ A well-known example of the latter is provided by galactose oxidase (EC 1.1.3.9).⁸ Another group of copper-dependant oxidases that has attracted much attention recently comprises the laccases (EC 1.10.3.2).⁹ These enzymes contain four copper centres per protein molecule and catalyse the oxidation of electron rich aromatic substrates, usually phenols or aromatic amines, via four single electron oxidation steps concomitant with the four electron reduction of O₂ to H₂O.^{10–12} Recently few laccases were crystallised and their three-dimensional crystal structures are now available.^{13–16} Its good thermal stability coupled with its lack of substrate inhibition and high rates of oxidation (10–100 fold higher than those of lignin peroxidase or manganese peroxidase) make laccase an ideal candidate for the development of enzymatic oxidation processes.⁹ Envisaged applications¹⁷ are in biobleaching of pulp as a replacement for chlorine, removal of

(poly)phenolic compounds and decolourisation of dyes in wastewater, amperometric biosensors for phenol detection, and many uses in the processing of foods and beverages.

An important role for laccases lies in the delignification of lignocellulose, the major constituent of wood.¹⁸ To that purpose they are secreted by white rot fungi as extracellular glycosylated enzymes. In lignin degradation as well as in most applications, laccase alone, however, is ineffective, since it is too large for a molecule to penetrate the cell walls of wood and react with the lignin. Consequently, so-called mediators, low molecular weight electron transfer agents, are employed to shuttle electrons from the lignin to the enzyme. For example, 3-hydroxy anthranilic acid is produced by the white rot fungus *Pycnoporus cinnabarinus* and is believed to play the role of an electron mediator.¹⁹ 2,2'-Azinobis-(3-ethylbenzothiazoline-6-sulfonic acid) ABTS was the first compound found to be capable of mediating the laccase catalysed oxidation of nonphenolic model compounds, such as the oxidation of veratryl alcohol to the corresponding aldehyde.¹⁸ Subsequently, 1-hydroxybenzotriazole²⁰ and other *N*-hydroxy compounds such as *N*-hydroxyacetanilide, violuric acid and *N*-hydroxyphthalimide were shown to act as mediators.²¹ A common feature of these mediators appears to be the propensity to form *N*-oxy(nitroxyl) radicals (see Fig. 1).

In 1996 it was shown that by using ABTS as a mediator, laccase from *Trametes versicolor* was able to catalyse the aerobic oxidation of a series of benzylic alcohols to their corresponding benzaldehydes.²² Subsequently, Galli and

Keywords: Laccase; TEMPO; Alcohol oxidation; Nitroxyl radical.

* Corresponding author. Tel.: +31 15 2782683; fax: +31 2781415; e-mail: r.a.sheldon@tudelft.nl

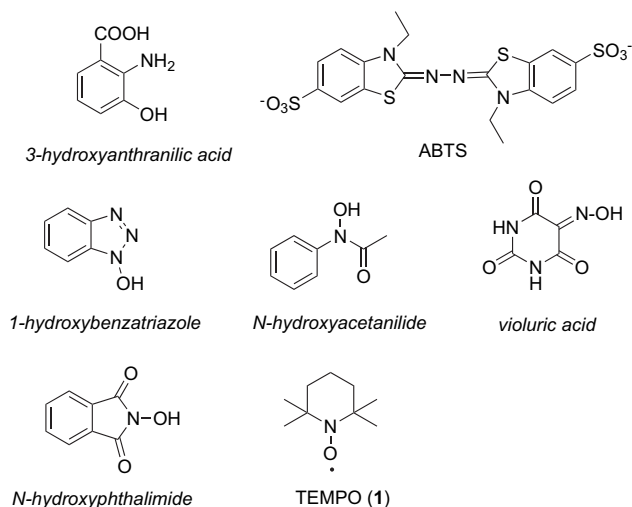


Figure 1. Laccase mediators.

co-workers found that the stable *N*-oxy radical, 2,2',6,6'-tetramethylpiperidyl-1-oxy (TEMPO, **1**, Fig. 1) in combination with laccase from *Trametes villosa*, catalyses the aerobic oxidation of primary benzylic alcohols.²³ The selective oxidation of the primary alcohol moiety in carbohydrates has been previously reported in two patents.²⁴ In a recent publication laccase from *Trametes pubescens* was used to oxidize a water-soluble cellulose sample.²⁵ In a subsequent comparison of various mediators, in the laccase catalysed aerobic oxidation of benzylic alcohols, TEMPO proved to be the most effective.²⁶

The mechanistic details of these laccase/mediator catalysed aerobic oxidations are still a matter of conjecture.^{27–29} However, they are generally believed to involve one electron oxidation of the mediator by the oxidised (cupric) form of the laccase followed by the reaction of oxidised mediator with the substrate, either via electron transfer (ET), e.g., with ABTS, or via hydrogen atom transfer (HAT), e.g., with *N*-hydroxy compounds, which forms *N*-oxy radicals.³⁰ TEMPO and its derivatives form a unique case: one electron oxidation of TEMPO affords the oxoammonium cation (**1a**), which oxidises the alcohol via a heterolytic pathway, giving the carbonyl product and the hydroxylamine **1b** (Fig. 2). The T1 copper centre in fungal laccases has a redox potential of ca. 0.8 V versus NHE (in contrast plant laccases exhibit redox potentials between 0.3 and 0.5 V). Consequently, fungal laccases are able to oxidise TEMPO to the corresponding oxoammonium cation (oxidation of **1a** to **1b**) since the oxidation potential of the latter, which was first measured by

Golubev and co-workers, is 0.75 V.³¹ This value was confirmed recently.³²

There are various alternatives for reoxidising the hydroxylamine (**1b**) back to TEMPO (**1**) to complete the catalytic cycle. It can be oxidised by O₂, O₂/laccase or the oxoammonium cation (**1a**). Since it is known that (uncatalysed) reoxidation of **1b** is slow under acidic conditions,³³ we suppose that regeneration of **1** takes place via the laccase/O₂ route.

The active oxidant (**1a**) is the same as that in the TEMPO catalysed oxidation of alcohols with hypochlorite (or other single oxygen donors), a method that is widely used in the oxidation of a broad range of alcohols using low catalyst loadings (1 mol % or less).³⁴ In contrast, the laccase/TEMPO catalysed aerobic oxidations of alcohols require high loadings of TEMPO (typically 30 mol % on substrate), which militates against commercial viability.²³ The aim of this study was to obtain mechanistic information regarding the laccase/TEMPO catalysed aerobic oxidations of alcohols, by studying the isotope effect in water as well as in biphasic mixtures. Furthermore, we wanted to investigate whether the use of other, including more water-soluble, TEMPO-derivatives could increase the performance of the catalyst. Previously, hydroxy-TEMPO and acetylamino-TEMPO were also shown to be active in the laccase/TEMPO catalysed oxidation of benzylic alcohol. However, in this case the reaction was pursued up to 100% conversion in all cases, so that no differences in reactivity could be observed.²⁶

2. Results and discussion

For the sake of convenience, TEMPO-like nitroxyl radicals are referred to as mediators (Med) and alcohols as substrates (Sub), although strictly speaking the nitroxyl is the substrate of the laccase according to the proposed mechanism (Fig. 2). The stable nitroxyl radicals shown in Figure 3 were tested as mediators. They are easily synthesised and/or commercially available.^{35,36}

First the performance of these TEMPO-derivatives was tested under typical reaction conditions. These conditions were largely similar to those previously used,²³ except for the amount of TEMPO, which was only 10 mol % relative to substrate in the present case. In all experiments 0.1 M acetate buffer (AB) at pH 4.5 was used and the reactions were carried out at room temperature under an oxygen atmosphere. The conversion of benzyl alcohol in the presence of laccase and various mediators obtained after 24 h is given in Table 1. In all cases, selectivity to the aldehyde is >95%.

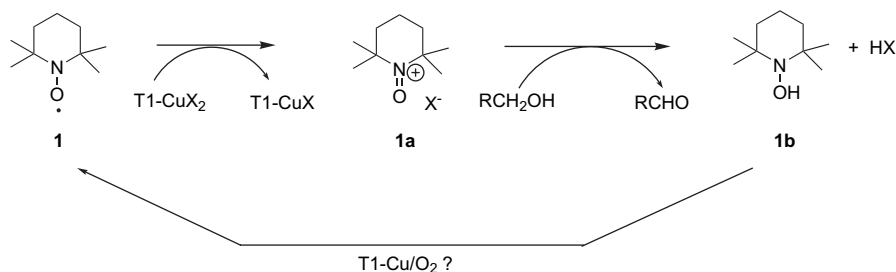


Figure 2. Pathway of laccase/TEMPO catalysed oxidation. T1 refers to Type I copper site.

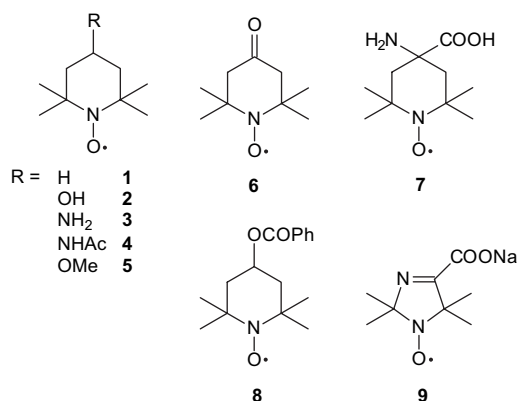


Figure 3. TEMPO and its derivatives used in this study.

Table 1. Aerobic oxidation of benzyl alcohol catalysed by laccase and nitroxyl radicals

Nitroxyl radical	Conv (%)
1	100
2	100
4	95.7
5	26
7	20.4
3	6.5
6	2.7
8	<1
9	<1

Conditions: [Sub]₀: 140 mM, Lac: 3.5 U/ml, [Med]: 14 mM, 24 h, rt, 1 atm O₂.

Among the nitroxyl radicals tested, oxo-TEMPO (**6**), amino-TEMPO (**3**), 4-hydroxy-TEMPO benzoate (**8**) and 2,2,5,5-tetramethyl-3-imidazoline-1-oxo-carboxylic acid sodium salt (**9**) showed very low activity. Methoxy-TEMPO (**5**) and 4-amino-4-carboxy-TEMPO (**7**) were moderately active. The conversion of benzyl alcohol was complete after 24 h in the systems mediated by TEMPO (**1**), hydroxy-TEMPO (**2**) and acetylamino-TEMPO (**4**). It was surprising that **8** showed no activity. This could be due to a high K_m of this mediator with the laccase.

The differences observed in **Table 1** cannot be explained simply on the basis of redox potential (E^0). In **Table 2** some published values of E^0 of TEMPO-derivatives are given.^{31,37–39} The data in **Table 2** were taken from different sources, and obtained under different conditions. Therefore, these values cannot be compared directly. We believe that the E^0 of TEMPO-derivatives generally lies around 0.75 V, which was the value obtained by Golubev and co-workers (see above) and thus all the E^0 values of the nitroxyl radicals (**Table 2**) are comparable to the E^0 of TvL. Only amino-TEMPO (**3**) exhibits a value, which is somewhat higher

Table 2. Redox potential of some nitroxyl radicals and laccase

Nitroxyl radical	E^0 (V) versus NHE	Ref. ^a
1	0.75, 0.74	31,37
2	0.80	37
3	0.89	37
6	0.78	38
TvL	0.78	11,39

^a Values in Ref. 37 measured by CV at pH 5 in citrate buffer. Values at pH 7.4 for **1**, **2** and **3**, amount to 0.74, 0.80 and 0.82, respectively.

(0.89 V), but strongly pH-dependent.³⁷ We can state, however, that TvL has sufficient oxidation potential to oxidise the nitroxyl radicals and forms the corresponding oxoammonium ions as proposed in **Figure 2**.

The oxoammonium salt of **6** was previously shown to be unstable in weakly acidic and basic medium.⁴⁰ Cyclic voltammetry revealed that it decomposed irreversibly into nonradical species at pH above 3.5. The low stability of **6**, in the presence of acids such as trichloroacetic acid, was also observed by Abakunov and Tikhonov.⁴¹ A mixture of the corresponding hydroxylamine and a ring-opened nitroso compound was formed (**Fig. 4**). Presumably this involves initial disproportionation of the nitroxyl radical to the hydroxylamine and oxoammonium cation. The latter then undergoes ring opening to form the nitroso compound.

In our system, **6** is presumably oxidised by laccase to form its oxoammonium ion, and the latter undergoes ring cleavage to form a $-N=O$ compound (**Fig. 5**), thus losing its oxidising ability. In acetate buffer, the oxoammonium cation can be coupled with the acetate anion leading to decomposition via the mechanism shown in **Figure 5**. Decomposition of **1a** under basic aqueous conditions was previously described by Golubev and co-workers³¹ leading to similar nitroso compounds. In the end as a result of intra- and intermolecular processes, about 2/3 of the cation **1a** was reduced under basic conditions to the radical and the rest was transformed into a mixture of nitrones and their condensation products.

In this context, the higher reactivity of **1** and **2** is probably a result of the higher stability of their oxoammonium ions. In the case of **3**, the situation is more complicated. Under acidic conditions, first **3** will be converted into the corresponding oxoammonium cation either by disproportionation (compare **Fig. 4**) or by laccase oxidation. The amino group, either in the nitroxyl radical structure or in the oxoammonium cation, can then be oxidised by the oxoammonium cation. In addition, it is reported that amines can react easily with nitroxyl radicals in an acid medium.^{42,43} This is confirmed by the results of Nakatsuji co-workers,⁴⁴ who reported that **3** is more readily oxidised than **1** and **2**. They found by cyclic voltammetry that **1** and **2** showed only one oxidation potential corresponding to nitroxyl radical, while **3** showed two oxidation potentials related to the oxidation of the amino group and the nitroxyl radical, respectively.

We studied the stability of **3** spectrometrically in acidic medium. When **3** was incubated in acetate buffer at pH 4.5, the absorbance maximum at 430 nm increased (**Fig. 6a**). This could be due to the formation of the $-N=O$ group (unfortunately we could not isolate the product). On the other hand, there was no absorbance change observed for **1** under the same conditions (**Fig. 6b**). Another possibility is oxidation of the amine to the imine. In this case, a similar

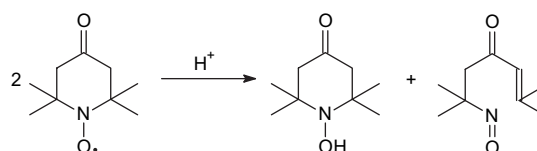


Figure 4. Interaction of **6** with acid.

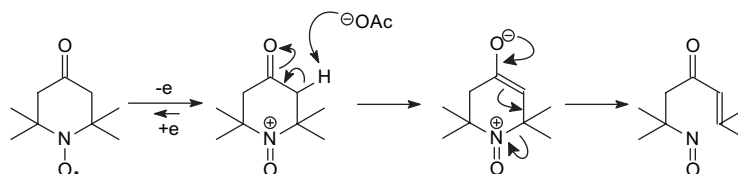


Figure 5. Postulated route for decomposition of **6** in acidic medium.

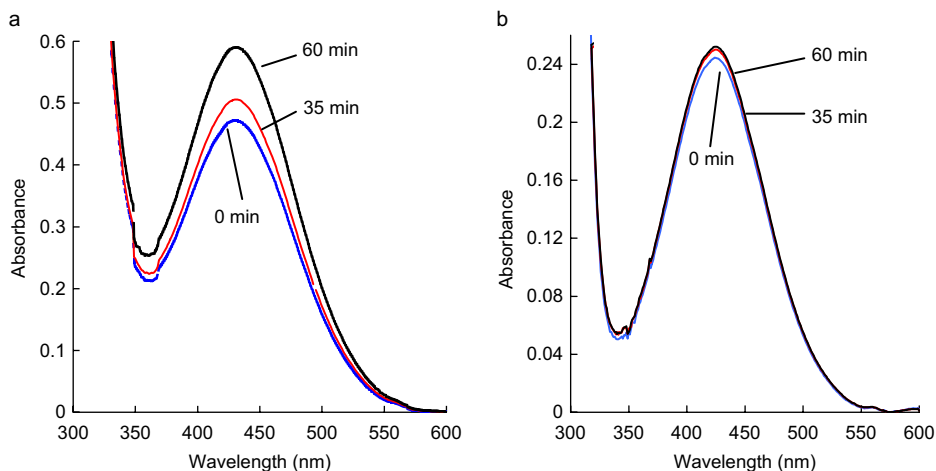


Figure 6. Absorption as a function of time of **3** (a) and **1** (b) in acetate buffer at pH 4.5.

instability as observed for oxo-TEMPO (see above) can be anticipated.

When the amino group in **3** is protected with an acetyl group, the resulting amide moiety is stable towards oxidation. Hence, **4** was an efficient mediator. It is not clear why **5** and **7** display intermediate activities. Especially the cation of **5** is known to be a good oxidant.^{45,46} We suggest that decomposition of the cation of **5**, is probably faster than that of **1a**, leading to lower activities.

For a better comparison of mediators **1**, **2** and **4**, the reaction was followed in time. Figure 7 shows that **2** and **4** display similar activity in the oxidation of benzyl alcohol, whereas **1** is more active. In case of **1**, already 87% conversion was observed after 7 h, while for **2** and **4**, the conversion only amounted to 56 and 44% at this point. In all cases the reaction was completed after 24 h.

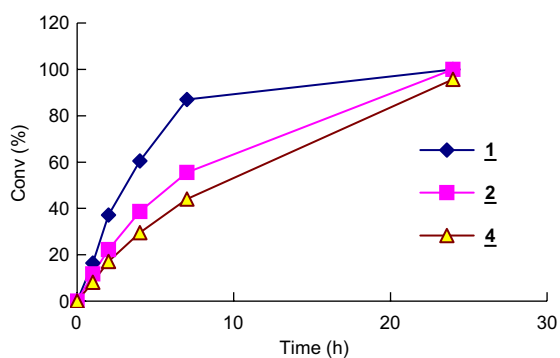


Figure 7. Comparison of nitroxyl radicals in the laccase catalysed aerobic oxidation of benzyl alcohol. [Sub]₀: 125 mM, Lac/Sub: 5.9 U/ml, [Med] 19 mM, rt, 1 atm O₂.

In Table 3, an overview of the reactivities of various TEMPO-derivatives with the secondary alcohol 1-phenylethanol is given. Surprisingly, in this case **2** and **4** displayed higher activity than **1**. The difference was more pronounced in water (pH 4.5)/toluene (W/T=1/1) mixtures than in aqueous buffer. Again, no activity was observed for **3**. It was expected that by adding more organic solvent to the system (the alcohols themselves already form a separate phase) the whole oxoammonium reaction could be moved from the aqueous layer to the organic layer and the reaction rate could be improved. However, it transpired that by adding toluene to the system, the reaction rate is retarded considerably. This could be due to a lower activity of the enzyme at the interphase layer.

Table 3. Conversion of 1-phenylethanol by laccase-nitroxyl radicals catalysed aerobic oxidation

Mediator	Acetate buffer ^a	W/T (1/1) ^{b,c}
1	66.8	27.6 (44.0)
2	76.8	60.7 (80.8)
4	78.5	81.7
5	2.4	—
3	2.4	—
9	—	3.9 (4.2)

Conditions: [Sub]₀: 125 mM, Lac: 5.9 U/ml, [Med]: 19 mM, rt, 1 atm O₂.

^a Reaction time: 5.5 h.

^b Reaction time: 24 h.

^c Data in parentheses were obtained after 48 h.

To confirm the difference in overall reactivities between **1**, **2** and **4** for benzyl alcohol and 1-phenylethanol, respectively, competition experiments were performed in which both substrates were present. In Table 4, the conversions of benzylic alcohol and 1-phenylethanol as well as the ratio of the overall rate constants are denoted. The overall rates were denoted

Table 4. Competition reaction of benzyl alcohol and 1-phenylethanol

Mediator	AB (5 h)		W/T (1/1) (23 h)	
	Conv ₁ /Conv ₂	<i>k</i> ₁ / <i>k</i> ₂	Conv ₁ /Conv ₂	<i>k</i> ₁ / <i>k</i> ₂
1	76.8/35.2	3.4	96.5/21.9	13.6
2	40.6/32.1	1.3	98.9/68.9	3.9
4	51.6/31.8	1.9	97.4/50.5	5.2

Conditions: equimolar amounts of benzyl alcohol and 1-phenylethanol were applied, [Sub]₀ 62.5 mM, Lac: 2.9 U/ml, [Med]: 9.3 mM. The ratio *k*₁/*k*₂ was calculated according to $k_1/k_2 = \ln(1 - \text{Conv}_1) / \ln(1 - \text{Conv}_2)$.

as *k*₁ and *k*₂ for benzylic alcohol and 1-phenylethanol, respectively.

The observations made in separate experiments were confirmed. In all cases benzyl alcohol was converted 1–3 times faster than 1-phenylethanol. When toluene was added to the medium, this difference was even larger.

2.1. Kinetic isotope effects

Further evidence for the alcohol oxidation mechanism was sought in kinetic isotope effects. Therefore, the primary kinetic isotope effects (*k*_H/*k*_D) were measured in the laccase-nitroxyl radical catalysed oxidation of α -monodeutero-*p*-methylbenzyl alcohol. We used this technique previously to unravel the mechanism of Ru/TEMPO⁴⁷ and Cu/TEMPO⁴⁸ catalysed oxidation of alcohols. A *k*_H/*k*_D value for the room temperature oxidation of α -monodeutero-*p*-methylbenzyl alcohol is 2.05, which was measured in acetate buffer at pH 4.5 (Table 5). Under biphasic conditions, using a mixture of toluene and water as solvent the *k*_H/*k*_D value was slightly higher and amounted to 2.32. These values are much lower than those obtained for laccase/violuric acid, laccase/1-hydroxybenzotriazole and laccase/*N*-hydroxyphthalimide reactions. In these cases *k*_H/*k*_D values of 6.2–6.4 were observed, which is in line with a radical hydrogen atom transfer route of oxidation.⁴⁹

Table 5. Kinetic isotope effect (*k*_H/*k*_D) in the laccase/TEMPO/O₂ catalysed oxidation of α -monodeutero-*p*-methylbenzyl alcohol

Entry	Catalyst	AB (pH 4.5)	W/T (1/1)
1	Laccase/TEMPO	2.05	2.32
2	TEMPO ⁺ -ClO ₄ ⁻	3.58	2.97
3	Laccase/4-hydroxy-TEMPO	2.54	2.61
4	Laccase/4-acetylamino-TEMPO	2.51	3.19

Substrate: 125 mM, [Med]: 18.8 mM, Lac: 5.9 U/ml, TEMPO⁺-ClO₄⁻: 1 equiv, 24 h; AB: acetate buffer pH 4.5; W/T: water/toluene (1/1).

We thus observed that the *k*_H/*k*_D ratio of benzylic alcohol oxidation by TEMPO and laccase is in the range expected for oxoammonium ions. Usually these values lie between 1.7 and 2.3⁵⁰ under basic conditions, and 3.1⁵¹ under acidic conditions. This low kinetic isotope effect is in accordance with a transition state of the process in which first

oxoammonium forms a complex with the alcohol, after which intramolecular transfer of hydrogen takes place, as illustrated in Figure 8.³⁴ The exact value for *k*_H/*k*_D is dependent on solvent, pH and the counterion. For that reason we also measured the *k*_H/*k*_D value for α -monodeutero-*p*-methylbenzyl alcohol, using separately prepared TEMPO⁺-ClO₄⁻ under identical conditions (see entry 2, Table 5). In acetic buffer, as well as under biphasic conditions using a mixture of toluene and water, slightly higher values were obtained using TEMPO⁺-ClO₄⁻ (3.6 and 3.0, respectively). We think that the nature of the counterion is essential in determining the *k*_H/*k*_D value. The counterion in the case of our laccase/TEMPO system has not been established, but it seems most likely that acetate ions function as counterion. For the sake of completeness, data using other TEMPO-derivatives were also measured. The use of 4-hydroxy-TEMPO and 4-acetylamino-TEMPO leads to kinetic isotope effects, which are identical in acetate buffer (2.54 and 2.51, respectively) and even higher under biphasic conditions, 2.61 and 3.19, respectively.

3. Conclusions

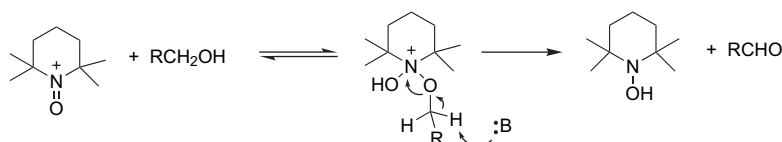
A number of stable TEMPO-like nitroxyl radicals were tested as mediators in the laccase catalysed aerobic oxidation of alcohols. Among them TEMPO (**1**) itself, as well as its hydroxy (**2**) and acetylamino (**4**) derivative are the most effective mediators, both in pH 4.5 buffered media as well as in buffer/toluene mixtures. The stability of the *N*-oxy radical and/or its resulting oxoammonium ions at pH 4.5 is limited for derivatives such as oxo-TEMPO and amino-TEMPO, resulting in very low conversion of alcohols. Kinetic isotope effect studies for **1**, **2** and **4** were performed for a primary benzylic alcohol, and values range from 2.1–3.2 in various media. These *k*_H/*k*_D values are characteristic of the ionic mechanism known in literature for alcohol oxidations with oxoammonium ions, and were verified in separate experiments under the current reaction conditions.

Competition studies indicate that, for all mediators, the primary alcohol reacts faster than the secondary alcohol. Also this observation is in line with literature data.³⁴ The overall reaction kinetics cannot be fully understood at this point because the concentration of the oxoammonium ions will depend on both the interaction with laccase as well as on its rate of regeneration by laccase (or otherwise). Future studies will be directed towards determining the rate constants of the individual steps.

4. Experimental

4.1. Enzymes and chemicals

Laccase from *T. versicolor* (TvL) was purchased from Juelich Fine Chemicals as a lyophilised powder. The content

**Figure 8.** Mechanism for oxoammonium catalysed oxidation of alcohols under acidic conditions.

of the protein is 8.8 mg/g solid (data from the enzyme supplier). TEMPO was obtained from BASF, Germany. The other nitroxyl radicals were purchased from Acros. 2,2'-Azinobis-(3-ethylbenzothiazoline-6-sulfonic acid) (ABTS) was purchased from Fluka. 1-Phenylethanol and benzyl alcohol were distilled before use. Other chemicals were purchased from Aldrich or Acros and used as received. Acetate buffer (0.1 M) at pH 4.5 was used for preparing solutions for the activity assay and as oxidation reaction medium unless otherwise specified.

4.2. Preparation of TEMPO⁺-ClO₄⁻⁵²

To a suspension of TEMPO (3.95 g, 25.3 mmol) in water (20 ml) was added dropwise a solution of 70% HClO₄ (3.66 g, 25.6 mmol) in water (5 ml) under ice-cooled conditions in 15 min, followed by addition of 15% NaOCl solution (6.4 g, 12.8 mmol) with ice-cooling in 10 min. The slurry of the reaction mixture was stirred for further 1 h at below 4 °C, and then the yellow precipitate was filtered and washed with 5% NaHCO₃ solution, ice-water and ether. The solid was dried under vacuum overnight to give the product TEMPO⁺-ClO₄⁻ 3.0 g (yield 46.4%). Mp 148–149 °C.

4.3. Laccase activity assay

The laccase activity was determined spectroscopically at 25 °C using ABTS as substrate. To an UV cuvette, a certain amount of ABTS (4.3–9.6 mg) was added to 2.0 ml of 0.1 M acetate buffer (pH 4.5) containing 2.0–7.0 μg of laccase. The absorbance change at 420 nm was recorded for 5 min ($\epsilon_{420}=36,000 \text{ M}^{-1} \text{ cm}^{-1}$).⁵³ One unit (U) of the enzyme was defined as 1 μmol ABTS oxidised per minute under the stated assay conditions.

4.4. Typical procedure for alcohol oxidation by laccase-nitroxyl radical

A mixture of benzyl alcohol (54 mg, 0.5 mmol), dodecane (34 mg, internal standard), laccase (24.5 mg, 47 U) and TEMPO (11.7 mg, 0.075 mmol) in acetate buffer (pH 4.5, 4 ml) was placed in a 10 ml glass vial. The vial was connected with an oxygen source to keep the system under atmospheric pressure of oxygen. The mixture was stirred at room temperature for a certain time. After reaction, the mixture was washed with diethyl ether (2×4 ml). The organic solution was dried with anhydrous sodium sulfate, centrifuged and analysed with GC.

4.5. Kinetic isotope effect studies

Intramolecular kinetic isotope effect (k_H/k_D): α -monodeuterio-*p*-methylbenzyl alcohol (125 mM) was used as the substrate in the above procedure. TEMPO 18.8 mM; laccase 47 U/mmol. After complete conversion of alcohol to aldehyde (monitored with TLC after 24 h), the reaction mixture was quenched with MTBE and dried over Na₂SO₄. Removal of the solvent under vacuum gave a mixture of TEMPO and *p*-methylbenzaldehyde. Both labelled and unlabelled aldehydes were isolated and purified by column chromatography using petroleum/CH₂Cl₂ (5/5). The k_H/k_D was determined by ¹H NMR by measuring the intensity of the α -proton.

4.6. Analysis methods

Alcohol conversion was analysed by GC with column WAX 52 CB (on Varian 3400 CX) or Sil 5 CB (on Varian STAR 3400). FID detector and temperature program (70 °C for 9 min, then increased at a rate of 10 °C/min to 250 °C for 6 min) were used on either column. Dodecane or hexadecane was used as an internal standard. The products were characterised by GCMS.

References and notes

- Sheldon, R. A.; Arends, I. W. C. E.; Dijkstra, A. *Catal. Today* **2000**, *57*, 157–166; Sheldon, R. A.; van Bekkum, H. *Fine Chemicals Through Heterogeneous Catalysis*; Wiley-VCH: Weinheim, 2001; Sheldon, R. A.; Arends, I. W. C. E.; ten Brink, G. J.; Dijkstra, A. *Acc. Chem. Res.* **2002**, *35*, 774–781.
- For recent reviews see: Muzart, J. *Tetrahedron* **2003**, *59*, 5789–5816; Stahl, S. S. *Angew. Chem., Int. Ed.* **2004**, *43*, 3400–3420.
- Anderson, R.; Griffin, K.; Johnston, P.; Alsters, P. L. *Adv. Synth. Catal.* **2003**, *345*, 517–523 and references cited therein; Besson, M.; Gallezot, P. *Catal. Today* **2000**, *57*, 127–141.
- For leading references see: Yamaguchi, K.; Mizuno, N. *Chem.—Eur. J.* **2003**, *9*, 4353–4361 and references cited therein.
- Markó, I. E.; Giles, P. R.; Tsukazaki, M.; Brown, S. M.; Urch, C. J. *Science* **1996**, *274*, 2044–2046; Markó, I. E.; Gautier, A.; Dumeinier, R.; Doda, K.; Philippart, F.; Brown, S. M.; Urch, C. J. *Angew. Chem., Int. Ed.* **2004**, *43*, 1588–1591.
- Gamez, P.; Arends, I. W. C. E.; Reedijk, J.; Sheldon, R. A. *Chem. Commun.* **2003**, 2414–2415.
- Kroutil, W.; Mang, H.; Edegger, K.; Faber, K. *Adv. Synth. Catal.* **2004**, *346*, 125–142.
- Hamilton, G. A. *Copper Proteins*; Spiro, T. G., Ed.; Wiley: New York, NY, 1981; pp 193–218; Whittaker, J. W. *Chem. Rev.* **2003**, *103*, 2347–2363.
- Call, H. P.; Mucke, I. *J. Biotechnol.* **1997**, *53*, 163–202; Gianfreda, L.; Xu, F.; Bollag, J. M. *Biorem. J.* **1999**, *3*, 1–25.
- Have, R. ten.; Teunissen, P. J. M. *Chem. Rev.* **2001**, *101*, 3397–3413.
- Multi-Copper Oxidases*; Messerschmidt, A., Ed.; World Scientific: Singapore, 1997.
- Solomon, E. I.; Sundaram, U. M.; Machonkin, T. *Chem. Rev.* **1996**, *96*, 2563–2605.
- Ducros, V.; Brzozowski, A. M.; Wilson, K. S.; Brown, S. H.; Østergaard, P.; Schneider, P.; Yaver, S.; Petersen, A. H.; Davies, G. J. *Nat. Struct. Biol.* **1998**, *5*, 310–316.
- Hakulinen, N.; Kiiskinen, L.-L.; Kruus, K.; Saloheimo, M.; Paananen, A.; Koivula, A.; Rouvinen, J. *Nat. Struct. Biol.* **2002**, *9*, 601–605.
- Bertrand, T.; Jolival, C.; Briozzo, P.; Caminade, E.; Joly, N.; Madzak, C.; Mouglin, C. *Biochemistry* **2002**, *41*, 7325–7333.
- Piontek, K.; Antorini, M.; Choinowski, T. *J. Biol. Chem.* **2002**, *277*, 37663–37669.
- Duran, N.; Rosa, M. A.; Annibale, A. D.; Gianfreda, L. *Enzyme Microb. Technol.* **2002**, *31*, 907–931; Mayer, A. M.; Staples, R. C. *Phytochemistry* **2002**, *60*, 551–565.
- Bourbonnais, R.; Paice, M. G. *FEBS Lett.* **1990**, *267*, 99–102; Rochefort, D.; Leech, D.; Bourbonnais, R. *Green Chem.* **2004**, *6*, 14–24.
- Eggert, C. B.; Temp, U.; Eriksson, K. E. *FEBS Lett.* **1996**, *391*, 144–148.

20. Srebotnik, E.; Hammel, K. E. *J. Biotechnol.* **2000**, *81*, 179–188; Sealey, J.; Ragauskas, A. J. *J. Wood Chem. Technol.* **1998**, *18*, 403–416.
21. Xu, F.; Kulyas, J. J.; Duke, K.; Li, K.; Krikstopaitis, K.; Deussen, H. J. W.; Abbate, E.; Galinyte, V.; Schneider, P. *Appl. Environ. Microbiol.* **2000**, *66*, 2052–2056.
22. Potthast, A.; Rosenau, T.; Chen, C. L.; Gratzl, J. S. *J. Mol. Catal. A: Chem.* **1996**, *108*, 5–9.
23. Fabbrini, M.; Galli, C.; Gentili, P.; Macchitella, D. *Tetrahedron Lett.* **2001**, *42*, 7551–7553.
24. Viikari, L.; Niku-Paavola, M. L.; Buchert, J.; Forssell, P.; Teleman, A.; Kruus, K. WO 9923240, 1999; Jetten, J. M.; van den Dool, R. T. M.; van Hartingsveldt, W.; van Wandelen, M. T. R. WO 00/50621, 2000.
25. Marzorati, M.; Danieli, B.; Haltrich, D.; Riva, S. *Green Chem.* **2005**, *7*, 310–315.
26. Fabbrini, M.; Galli, C.; Gentili, P. *J. Mol. Catal. B: Enzym.* **2002**, *16*, 231–240.
27. d'Acunzo, F.; Baiocco, P.; Fabbrini, M.; Galli, C.; Gentili, P. *Eur. J. Org. Chem.* **2002**, 4195–4201; Cantarella, G.; Galli, C.; Gentili, P. *J. Mol. Catal. B: Enzym.* **2003**, *22*, 135–144.
28. Crestini, C.; Jurasek, L.; Argyropoulos, D. S. *Chem.—Eur. J.* **2003**, *9*, 5371–5378.
29. Marjasvaara, A.; Torvinen, M.; Vainiotalo, P. *J. Mass Spectrom.* **2004**, *39*, 1139–1146.
30. Baiocco, P.; Barreca, A. M.; Fabbrini, M.; Galli, C.; Gentili, P. *Org. Biomol. Chem.* **2003**, *1*, 191–197.
31. Golubev, V. A.; Rudijk, T. S.; Sen, V. D.; Aleksandrov, A. L. *Izv. Akad. Nauk. SSSR Ser. Khim.* **1976**, *4*, 763–771; *Bull. Acad. Sci. USSR Div. Chem. Sci.* **1976**, *4*, 744–750; Golubev, V. A.; Kozlov, Y. N.; Petrov, A. N.; Purmal, A. P. *Bioactive Spin Labels*; Zhdanov, R. I., Ed.; Springer: Berlin, 1992; pp 119–140.
32. Goldstein, S.; Merenyi, G.; Russo, A.; Samuni, A. *J. Am. Chem. Soc.* **2001**, *125*, 789–795.
33. Ben-Daniel, R.; Alsters, P.; Neumann, R. *J. Org. Chem.* **2001**, *66*, 8650–8653.
34. de Nooy, A. E. J.; Besemer, A. C.; van Bekkum, H. *Synthesis* **1996**, 1153–1174.
35. Rozantsev, E. G.; Sholle, V. D. *Synthesis* **1971**, 190–202.
36. Sosnovsky, G.; Konieczny, K. *Synthesis* **1976**, 735–736.
37. Limoges, B.; Degrand, C. *J. Electroanal. Chem.* **1997**, *422*, 7–12.
38. Grimshaw, J. *Electrochemical Reactions and Mechanisms in Organic Chemistry*; Elsevier: Amsterdam, 2000; p 262.
39. Reinhammar, B. Laccase. In *Copper Proteins and Copper Enzymes*; Lonhe, R., Ed.; CRC: Boca Raton, 1984; Chapter 1.
40. Thomas, G.; Mohanty, J. G. *Indian J. Chem.* **1982**, *21A*, 451–455.
41. Abakunov, G. A.; Tikhonov, V. D. *Bull. Acad. Sci. U.S.S.R., Div. Chem. Sci.* **1969**, 724–727.
42. Neiman, M. B.; Medzhidov, A. A.; Rozantsev, E. G.; Skripko, L. A. *Dokl. Akad. Nauk SSSR* **1964**, *154*, 387.
43. Medzhidov, A. A.; Rozantsev, E. G.; Neiman, M. B. *Dokl. Akad. Nauk SSSR* **1966**, *168*, 348.
44. Nakatsujii, S.; Takai, A.; Nishikawa, K.; Morimoto, Y.; Yasuoka, N.; Suzuki, K.; Enoki, T.; Anzai, H. *J. Mater. Chem.* **1999**, *9*, 1747–1754.
45. Anelli, P. L.; Biffi, C.; Montanari, F.; Quici, S. *J. Org. Chem.* **1987**, *52*, 2559–2562.
46. Miyazawa, T.; Endo, T.; Shiihashi, S.; Okawara, M. *J. Org. Chem.* **1985**, *50*, 1332–1334.
47. Dijkman, A.; Arends, I. W. C. E.; Sheldon, R. A. *J. Am. Chem. Soc.* **2001**, *123*, 6826–6833.
48. Dijkman, A.; Arends, I. W. C. E.; Sheldon, R. A. *Org. Biomol. Chem.* **2003**, *1*, 3231–3237.
49. Galli, C.; Gentili, P. *J. Phys. Org. Chem.* **2004**, *17*, 973–977.
50. Semmelhack, M. F.; Schmid, C. R.; Cortés, D. A. *Tetrahedron Lett.* **1986**, *27*, 1119–1122.
51. Golubev, V. A.; Borislavskii, V. N.; Aleksandrov, A. L. *Izv. Akad. Nauk SSSR, Ser. Khim.* **1977**, 2025–2034; *Bull. Acad. Sci. USSR, Div. Chem. Sci.* **1977**, 1874–1881.
52. Bobbitt, J. M. *J. Org. Chem.* **1998**, *63*, 9367–9374.
53. Childs, R. E.; Bradseley, W. G. *Biochem. J.* **1975**, *145*, 93–103.

Efficient chemoselective alcohol oxidation using oxygen as oxidant. Superior performance of gold over palladium catalysts

Alberto Abad, Carles Almela, Avelino Corma* and Hermenegildo García*

Instituto de Tecnología Química CSIC-UPV, Universidad Politécnica de Valencia, Av. De los Naranjos s/n, 46022 Valencia, Spain

Received 3 November 2005; revised 12 January 2006; accepted 18 January 2006

Available online 30 May 2006

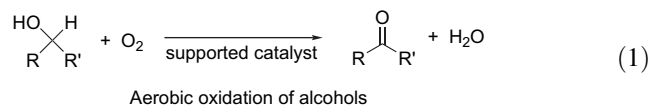
Abstract—Gold nanoparticles supported on nanocrystalline ceria (Au/CeO₂) is a general, air- and moisture-stable, commercial catalyst for the atmospheric pressure, solventless oxidation of aromatic, primary and secondary alcohols to the corresponding benzaldehyde or ketone compound. Aliphatic primary alcohols are oxidized to the corresponding alkyl ester and aliphatic secondary alcohols are oxidized to ketones. Conversions and product yields are in most of the cases excellent. The oxidizing reagent and the experimental conditions are almost ideal from the environmental point of view. Comparison with analogous ceria supported and hydroxyapatite-supported palladium catalysts, Au/CeO₂ clearly shows the superior performance of Au/CeO₂ in terms of higher chemoselectivity. In contrast to palladium catalysts that promote C=C double isomerization, Au/CeO₂ oxidizes selectively allylic alcohols to conjugated ketones.

© 2006 Elsevier Ltd. All rights reserved.

1. Introduction

Oxidation of alcohols to carbonyl compounds is one of the simplest and most useful transformations in Organic Chemistry that is at the core of many synthetic routes. This essential reaction has attracted the attention of considerable fundamental and applied research since the beginning of Organic Chemistry as a Science. However, in spite of this intensive research effort, alcohol oxidation processes are still far from being ideal from the environmental point of view and requires much improvement. The use of conventional transition metal or halogen oxo, salts such as permanganate, chromate, bromate or other stoichiometric oxidants generates an intolerably high amount of (toxic) wastes and violates at least three of the Green Chemistry principles.¹ Other alternative processes, like the Swern or Meerwein–Verley–Pondorf oxidations, also use noxious reagents, Lewis acid catalysts and organic solvents, producing a large amount of waste.^{2,3} As a summary of the present status, it can be said that most of the currently used alcohol oxidation processes are not sustainable and suitable green alternatives need to be developed. The processes to be developed have to be general in scope for aliphatic primary and secondary alcohols, selective towards the corresponding carbonylic compound and compatible with the presence of other functional groups in the molecule, particularly allylic C=C double bonds.

There is no doubt that from the *green* point of view molecular dioxygen is the ideal oxidizing reagent, water being the only by-product of the process (Eq. 1). The use of oxygen as oxidant is very challenging from the catalytic point of view, since the general problem of thermal or photochemical oxygen oxidations is their lack of selectivity with the formation of complex reaction mixtures. Also, explosion hazard has to be taken into account when alcohols in organic solvents are mixed with oxygen under high pressure. For safety and experimental reasons, it would be convenient to use oxygen at atmospheric pressure when performing alcohol oxidations.



The problem of atmospheric pressure, oxygen oxidations was that until a few years ago, no active and general catalysts were known. This situation is about to change drastically, since recently highly active metallic catalysts have been reported to produce the aerobic, atmospheric-pressure oxidation of alcohols with high-turnover numbers, selectivity, and reusability. Currently there is a concurrence between ruthenium, platinum, palladium, and gold catalysts to become the most active and general catalyst for the aerobic oxidation of alcohols.^{4–7}

As a continuation of our on-going work in the finding of oxygen-based oxidation catalysts,^{8,9} we report here that

* Corresponding authors. Tel.: +34 96 387 7800; fax: +34 96 387 7809; e-mail: acorma@itq.upv.es

ceria-supported gold catalyst exhibits a superior performance than analogous palladium catalysts for this process, approaching almost the status of being the perfect catalyst for aerobic alcohol oxidation. We will show that the supported gold catalyst is quite general for aliphatic and aryl alcohols and the process is chemoselective for allylic hydroxyl groups.

2. Results and discussion

2.1. Catalysts

The activity of a series of three supported palladium and gold catalysts for the oxidation of alcohols has been compared in the present work. Two of them used ceria nanoparticles as support. Ceria nanoparticles were obtained following a reported procedure consisting in the controlled aging in acid aqueous media of $\text{Ce}(\text{NO}_3)_3$. It is known that particle size reduced down to 3–8 nm makes considerable defects on ceria. These defects consist in the presence of lattice oxygen defective sites and in the presence of a considerable population of Ce(III) sites in addition to the normal Ce(IV) sites. These special defective properties are only encountered when sufficiently small particles are obtained and arise from the high external versus total atomic ratio characteristic of nanoparticles.

These ceria nanoparticles were prepared and used as support to deposit palladium and gold nanoparticles.¹⁰ Gold supported on ceria (Au/CeO_2) was obtained by stirring a colloidal suspension of ceria nanoparticles in water containing a soluble gold(III) salt and adjusting the pH to 10. Under these basic conditions, gold hydroxides precipitate over the ceria. The preparation of palladium supported on ceria (Pd/CeO_2) follows an analogous procedure to that reported by Kaneda and co-workers for hydroxyapatite-supported palladium ($\text{Pd}/\text{apatite}$). Basically the procedure consists of dissolving in an organic solvent a soluble palladium complex and adsorbing it on the inorganic support by stirring the suspension. From these solids, the active form of these catalysts was obtained by reducing them to form noble metal particles. In contrast to the rest of noble metals such as

platinum, palladium, etc., gold was considered until recently as not exhibiting interesting catalytic properties. However, Haruta reported that when the particle size is sufficiently small in the nanometer scale, gold can exhibit exceedingly good catalytic properties for the aerobic oxidation of CO.¹¹ Then gold on supported catalyst has shown to be active for different oxidation, reduction, and C–C forming bond reactions.^{12–17}

The particle size distribution, the noble metal and ceria domains, and the particle morphology can be observed by transmission electron microscopy. Figures 1–4 show selected images and particle size distribution for the supported catalysts used in this work. As it can be seen there, the particle size of the noble metal is about 1–10 nm and the colloidal ceria particles have similar dimensions, being both spheroidal particles in shape.

The catalyst series was completed with a third catalyst consisting of palladium nanoparticles supported on hydroxyapatite ($\text{Pd}/\text{apatite}$). This catalyst has been recently reported by Kaneda and co-workers¹⁸ as one of the most active for the aerobic oxidation of alcohols exhibiting turnover numbers of 250,000. This means that on average a palladium atom is able to form 250,000 molecules of ketone, or that $\text{Pd}/\text{apatite}$ is active at molar ratios below 0.0004 mol %. $\text{Pd}/\text{apatite}$ is analogous to Pd/CeO_2 except that the support has a composition of CaHPO_4 and is obtained synthetically by precipitating phosphate with calcium under controlled pH conditions.

2.2. Catalytic activity

It has been reported that $\text{Pd}/\text{apatite}$ is an extremely active heterogeneous catalyst for the oxidation of 1-phenylethanol. In the first stage of our work we have performed preliminary studies in the solventless aerobic oxidation of this alcohol, being able to reproduce the activity reported by Kaneda et al.

Aerobic oxidation of 1-phenylethanol was performed at atmospheric pressure by bubbling oxygen through 1-phenylethanol in the absence of solvent using a Dean–Stark apparatus to remove the water formed in the process.

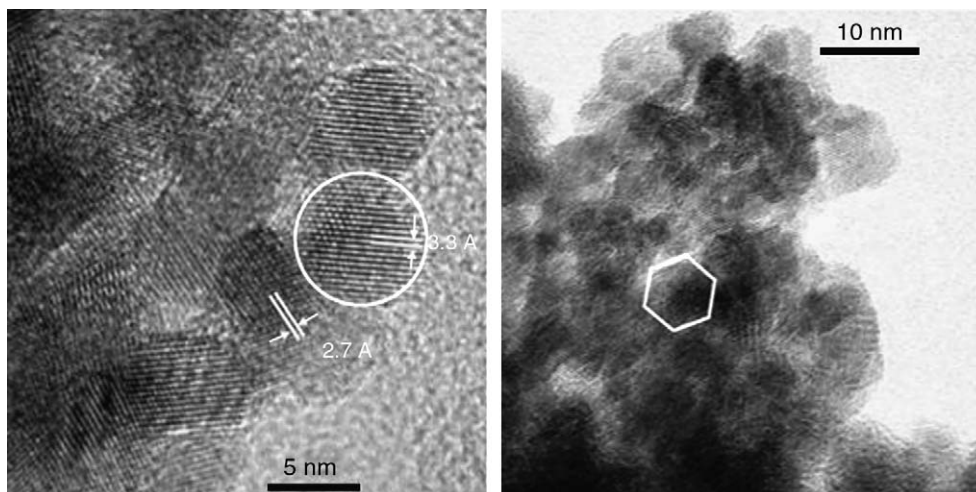


Figure 1. Left: High resolution TEM of the Au/CeO_2 sample, the white lines correspond to the (202) (3.3 Å) Ce_2O_3 and the (200) CeO_2 (2.7 Å) lattice spacing. Right: A hexagonal faceted (111) Au crystal is circled.

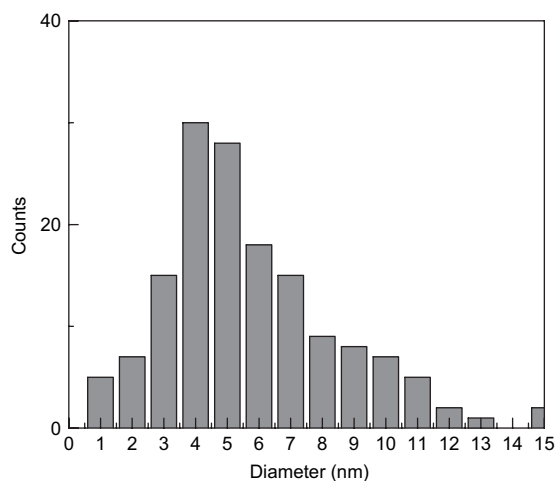


Figure 2. Au particle size distribution determined by statistical analysis of Au/CeO₂.

According to Eq. 1, as the oxidation progresses significant volumes of water are formed and they were separated from the reaction mixture with the Dean–Stark apparatus. This

experimental procedure has the additional advantage of avoiding the use of any solvent, thus conforming the eighth principle of Green Chemistry. Two reaction temperatures (over the 100 °C necessary for the operation of the Dean–Stark apparatus) were studied. Complete conversions with high selectivity towards acetophenone were obtained when the reaction was conducted at 160 °C for Pd catalysts (see Table 1). For catalysts that exhibit almost quantitative conversion and selectivity, a way to rank their activity is to consider the turnover frequency (TOF) that is calculated by dividing the initial reaction rate to the number of catalytic sites. Initial reaction rates can be obtained from the slope of the time–conversion plot at zero time. Figure 5 shows the aerobic oxidation of 1-phenylethanol and 3-octanol as a function of time in the presence of the series of catalysts used. The estimated TOF values are also given in Table 1.

It can be seen in Figure 5 and Table 1 that both supported palladium catalysts are more active than Au/CeO₂ when the reaction is carried out at 160 °C. However, the reverse behavior is observed at 120 °C where Au/CeO₂ becomes the most active catalyst and the activity of palladium catalysts was significantly lower.

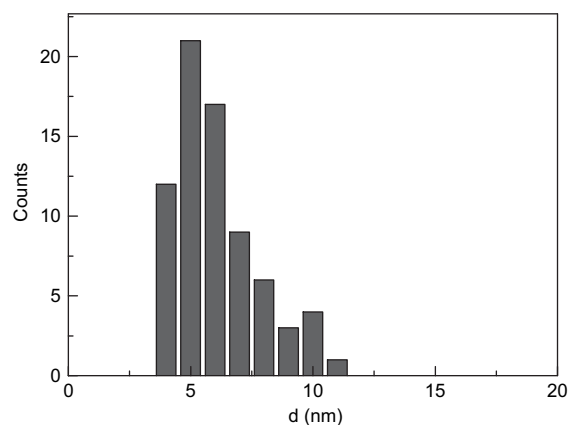
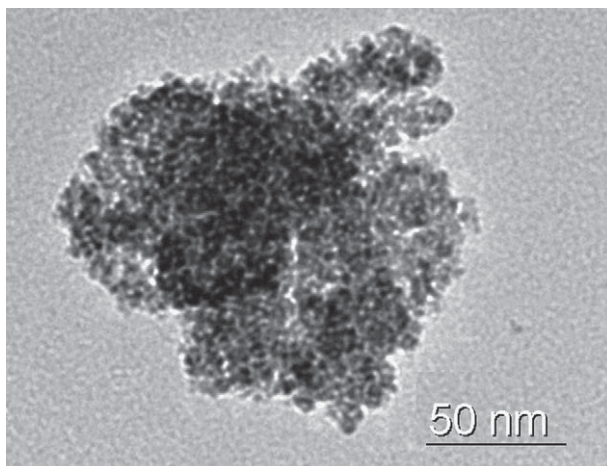


Figure 3. Left: High resolution TEM image of the Pd/CeO₂ catalyst. Darker spots correspond to palladium nanoparticles. Right: Pd particle size distribution determined by statistical analysis of the left image.

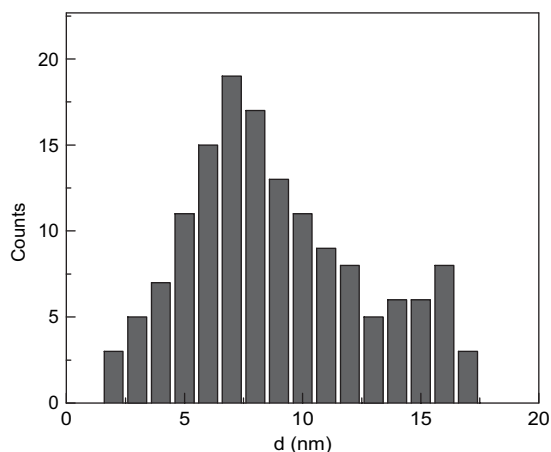
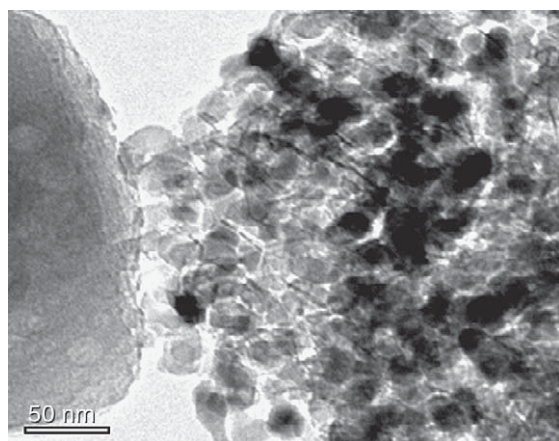


Figure 4. Left: High resolution TEM image of the Pd/apatite catalyst. Right: Pd particle size distribution determined by statistical analysis of Pd/apatite.

Table 1. Results of the solventless, atmospheric-pressure aerobic oxidation of two secondary alcohols using a Dean–Stark apparatus in the presence of heterogeneous gold or palladium catalyst

Substrate	<i>T</i> (°C)	Catalyst	Ketone yield (%)	TOF (h ⁻¹)
1-Phenylethanol	160	Au/CeO ₂ ^a	33	12,480
		Pd/CeO ₂ ^a	>95	32,558
		Pd/apatite ^a	>95	33,223
	120	Au/CeO ₂	>95	1511
		Pd/CeO ₂	91	645
		Pd/apatite	90	1127
3-Octanol	120	Au/CeO ₂	>95	2337
		Pd/CeO ₂	3	63
		Pd/apatite	45	379

Reaction conditions: 12.5 mmol of alcohol, 0.154 mol % (substrate to catalyst ratio), and PO₂ 1 atm (35 mL min⁻¹ flow).

^a Substrate to catalyst ratio is 0.0004%.

Moreover, aliphatic secondary alcohols, such as 3-octanol, can also be equally well oxidized at 120 °C in almost quantitative yield by oxygen at atmospheric pressure in the absence of solvent using supported gold as heterogeneous catalyst. Working at temperatures of 120 °C or below, the activity of Au/CeO₂ was higher than that of analogous supported palladium catalysts, for which the yield of ketone for palladium catalysts was unsatisfactory under the substrate to catalyst ratio and conditions studied. The TOF values of Au/CeO₂ were correspondingly considerably much higher than those of the supported palladium catalysts.

In order to demonstrate the generality of ceria-supported gold as catalyst for the aerobic oxidation of alcohols and its higher performance compared to analogous palladium

catalyst, we studied under the same experimental conditions, the oxidations of three other substrates, namely, a primary benzylic alcohol, a primary aliphatic alcohol, and an allylic alcohol. In all the cases the reaction product was the corresponding aldehyde or ketone, except in the case of 3-phenyl-1-propanol that gives the ester 3-phenylpropyl 3-phenyl-1-propanoate as the reaction product. The results of conversion, selectivity, and TOF values are tabulated in Table 2.

As it can be seen in Table 2, Au/CeO₂ exhibits high activity and selectivity for the alcohols studied, being considerably more active than the analogous supported palladium catalysts. There are also some distinctive features that deserve some comments. Thus, the presence of reduction products (see footnotes a and b in Table 2) was observed in minor quantities using supported palladium catalysts, but were absent using Au/CeO₂. Also allylic alcohol 1-octen-3-ol undergoes a chemoselective oxidation in the presence of Au/CeO₂ to the corresponding ketone without oxidizing or isomerizing the C=C double bond. In contrast to this, palladium catalysts promote a considerable degree of C=C double bond isomerization with the formation of 3-octanone as the final product.

Also benzylic alcohols can be oxidized selectively by oxygen to the corresponding benzaldehydes in the presence of Au/CeO₂ as catalyst. Again, the activity of Pd/CeO₂ was significantly lower and, moreover, exhibited less selectivity towards the corresponding benzaldehyde.

Aliphatic primary alcohols can also be oxidized by oxygen using Au/CeO₂ as catalyst. In this case, however, the product was the corresponding esters rather than aldehydes. The presence of minor quantities of the corresponding carboxylic acid was also observed. This indicates that under the experimental conditions used, the carboxylic acid must be the predominant oxidation product and as the reaction progresses it

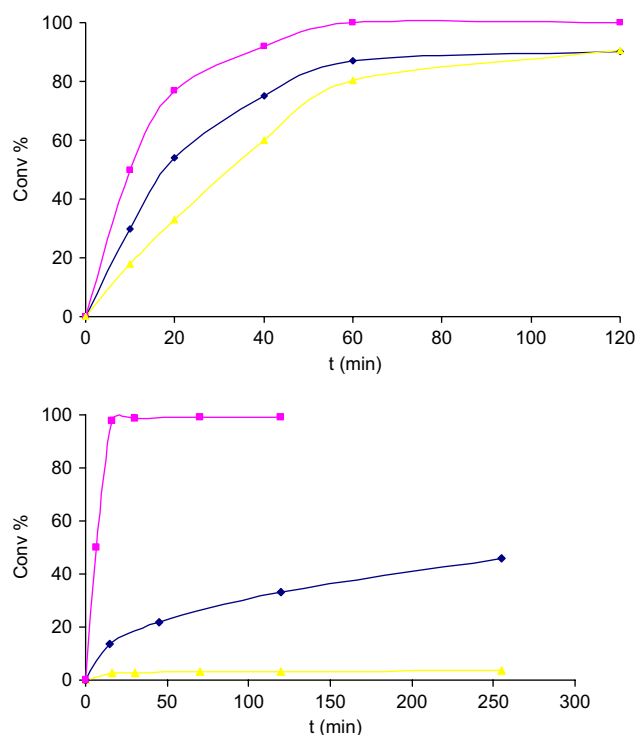


Figure 5. Comparison of the catalytic activity of Pd/CeO₂ ▲, Au/CeO₂ ■, and Pd/apatite ◆ for the aerobic alcohol oxidation at 120 °C (substrate to catalyst ratio 0.154 mol %). Top: 1-phenylethanol. Bottom: 3-octanol.

Table 2. Results of the solventless, atmospheric-pressure aerobic oxidation of alcohols at 120 °C using a Dean–Stark apparatus in the presence of heterogeneous gold or palladium catalyst

Substrate	Time (h)	Catalyst	Conversion (%)	Selectivity (%)
1-Phenylethanol	2	Au/CeO ₂	>99	>99
		Pd/CeO ₂	91 ^a	>99
		Pd/apatite	91 ^a	93
3-Octanol	4.5	Au/CeO ₂	99	>99
		Pd/CeO ₂	3	>99
		Pd/apatite	45	>99
1-Octen-3-ol	3	Au/CeO ₂	>99	93
		Pd/CeO ₂	>99	58
		Pd/apatite	>99	23
3,4-Dimethoxybenzyl alcohol	5	Au/CeO ₂	>99	83
		Pd/CeO ₂	>99	47 ^b
3-Phenyl-1-propanol ^{c,d}	7	Au/CeO ₂	>99	88
		Pd/CeO ₂	79	69

Reaction conditions: 12.5 mmol of alcohol, 0.154 mol % (substrate to catalyst ratio), PO₂ 1 atm (35 mL min⁻¹ flow), and *T* at 120 °C.

^a Ethylbenzene was also formed as product.

^b 3,4-Dimethoxytoluene was also formed as product.

^c The reaction temperature was 160 °C.

^d The reaction product was 3-phenylpropyl 3-phenyl-1-propanoate.

undergoes esterification with the alcohol to give the ester. As in the previous cases, also for primary aliphatic alcohols the activity of the palladium catalysts was considerably lower than that of gold.

The above reactions were carried out under solventless conditions. It is evident that this procedure is greener and convenient for the oxidation of alcohols in large volumes. However, it is obvious that this cannot be applied for the oxidation of high melting point, solid alcohols. Also, this procedure may be less suitable for the oxidation of small amounts of alcohol. It is frequent situation in Organic synthesis that the amount of alcohol available as intermediate in a synthetic route is not large enough to allow solventless processes.

For this reason, we have also tested the activity of the ceria-supported catalyst in other solvents. There is an increasing interest in developing organic reactions in water, that is considered the greenest solvent. Water in the presence of base at reflux temperature is also a suitable reaction medium to perform aerobic oxidation catalyzed by supported gold. The main peculiarity of water as solvent is, however, that primary alcohol such as 1-hexanol undergoes oxidation to the corresponding carboxylic acid (>95% yield) rather than to aldehyde, although the selectivity to carboxylic acid can also be very high. We notice that as it has been indicated in the footnotes of Table 2, also in solventless conditions 3-phenyl-1-propanol undergoes oxidation to ester rather than to aldehyde.

Water, even at high reaction temperatures, has the limitation of its low solubility for most alcohols. For this reason, we are currently studying aerobic alcohol oxidation in other solvents that while still being environmentally benign can be of more general use in Organic Chemistry. In this context we have performed some preliminary tests using imidazolium ionic liquid as medium. Although aerobic oxidation of alcohols can also be performed in 1-butyl-3-methylimidazolium hexafluorophosphate, the catalyst becomes strongly

deactivated over the course of the reaction and the conversion suddenly stops before complete disappearance of the alcohols. For this reason, 3,4-dimethoxybenzyl alcohol gives only 45% of the corresponding benzaldehyde when the reaction is carried out in imidazolium ionic liquid.

One important issue when testing a heterogeneous catalyst is to determine its reusability. We have found that for the solventless alcohol oxidation, once the reaction has finished and the solid recovered, it can be reused by washing it with copious basic water (pH 10), drying in an oven for 2 h with only a marginal decrease in its catalytic activity. We have determined that carboxylic acids act as poisons of Au/CeO₂. Most probably they strongly coordinate to positive gold species reducing their ability to bind with alcohols forming the gold-alcoholate intermediate. Poisoning by carboxylic acid is the most probable cause of the catalyst deactivation under our solvent-less conditions.

Concerning the reaction mechanism of the aerobic oxidation, Figure 6 shows the most reasonable mechanism that accounts for the known facts. The process will start with oxygen physisorption at the oxygen defective sites on the ceria surface that initiates oxygen activation. Upon physisorption, the interaction between defective cerium(III) and oxygen can be understood as forming a metal peroxy radical such as Ce^{iv}-O-O[•]. On the other hand the presence of positive gold atoms at the interface between gold and ceria has been demonstrated and will be ready to form a gold-alcoholate species. The combination of surface bound peroxy radicals and metal alcoholate will end-up in the ketone and metal hydroperoxide. This cerium peroxide will decompose by the action of gold. Although it is clear that many details of the mechanism are still to be unveiled, the key point concerning the excellent activity of the Au/CeO₂ solid for the aerobic oxidation is the presence of surface oxygen vacancies, a structural feature that arises from the nanometric size of ceria, and the presence of positive gold species in a cluster that contains many gold(0) atoms. The presence of positive gold species also arises from the high interfacial contact

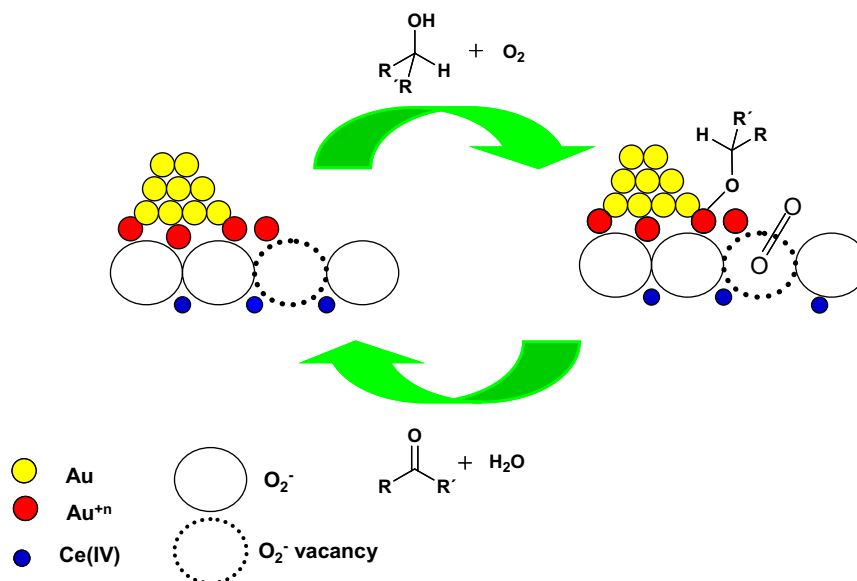


Figure 6. Reasonable mechanism for aerobic alcohol oxidation on Au/CeO₂ catalyst.

between gold and ceria that at the end is also the result of the nanometric size of the particles.

3. Conclusions

Contrary to the general belief in Organic synthesis, homogeneous and heterogeneous catalysis have been developing excellent systems to effect the aerobic oxidation of alcohols using molecular oxygen as oxidant. This process has been regarded by Organic chemists as being limited and specific for large-scale industrial oxidation processes. But, currently there are several noble metal catalysts that exhibit a general activity to oxidize any hydroxyl group to the corresponding carbonyl compound. Among this extremely active catalysts, we have shown in the present work that commercially available, air- and moisture-stable Au/CeO₂ shows a wide generality for the oxidation of primary and secondary, aliphatic and benzylic hydroxy groups, thus, making aerobic oxidation amenable to general Organic Chemistry. The current work in this area is focused in further expanding the solvents that can be used, determining compatibility with substrate functional groups and the reusability of the gold catalyst.

4. Experimental

4.1. General

HAuCl₄, (NH₄)₂HPO₄, Mg(CH₃COO)₂·4H₂O, NH₃ (25%), Ca(NO₃)₂·4H₂O, and Ce(NO₃)₄ were purchased from Sigma–Aldrich Chemical Co. PdCl₂(PhCN)₂ was purchased from ABCR GmbH Co. All reagents were used without further purification. All solvents and acids used were reagent grade, purchased from Sigma–Aldrich Chemical Co., and used as received. All the experiments were performed using mQ water.

4.2. Catalysts

4.2.1. Synthesis of nanoparticulated ceria. A colloidal dispersion of CeO₂ nanoparticles was prepared by thermolysis of an acidified Ce(NO₃)₄ solution followed by re-dispersion. The dispersion was purified and concentrated using an ultrafiltration cell equipped with a 3KD membrane. The purification was monitored by the residual acidity of the dispersion, determined by an acid titration of the supernatant after ultra-centrifugation at 50,000 rpm for 6 h. The resulting cerium oxide has, owing to the small size of the nanoparticles, a very high surface area (180 m² g⁻¹) as determined by isothermal nitrogen adsorption.

4.2.2. Synthesis of hydroxyapatite. Hydroxyapatite was prepared using a method as described in the literature. A solution of (NH₄)₂HPO₄ (40.0 mmol) in deionized water (150 mL) was set at pH 11 with aqueous NH₃ solution. This solution was added dropwise over 30 min to a solution of Ca(NO₃)₂·4H₂O (66.7 mmol) in deionized water (120 mL) adjusted to pH 11 with aqueous NH₃ solution. Vigorous stirring at room temperature was maintained during the addition process. The resulting milky solution was heated at 90 °C for 10 min. The precipitate was filtered, washed with deionized

water, and dried at 110 °C giving a solid with the stoichiometry of Ca₁₀(PO₄)₆(OH)₂ corresponding to hydroxyapatite.

4.2.3. Preparation of Au/CeO₂ catalyst. Au was deposited on the nanoparticulated ceria by the following procedure: a solution of HAuCl₄·3H₂O (296 mg) in 60 mL of deionized water was brought to pH 10 by addition of a solution of NaOH 0.2 M. Once the pH value was stable the solution was added to a gel containing of colloidal CeO₂ (4.01 g) in H₂O (50 mL). After adjusting the pH of the slurry to a value of 10 by addition of a solution of NaOH 0.2 M, the slurry was left under vigorous stirring for 18 h at room temperature. The Au/CeO₂ solid was then filtrated and exhaustively washed with distilled water until no traces of chlorides were detected by the AgNO₃ test. The catalyst was dried at vacuum at room temperature for 1 h. Then 3.5 g of the supported catalyst was added over 30 g of 1-phenylethanol at 160 °C and the mixture was allowed for reduction during 20 min. The catalyst was filtered, washed, with acetone and water, and dried under vacuum at room temperature. The total Au content of the final catalyst Au/CeO₂ was 1.54 wt % as determined by chemical analysis. This catalyst Au/CeO₂ is commercially available at www.upv.es/itq.

4.2.4. Preparation of Pd supported catalysts. Colloidal ceria or hydroxyapatite (4 g) was stirred at room temperature for 3 h in 400 mL of acetone solution of PdCl₂(PhCN)₂ (1.5×10⁻³ M). The obtained mixture was filtered, washed with acetone, and dried under vacuum at room temperature. Then 3.5 g of the supported catalyst was added over 30 g of 1-phenylethanol at 160 °C and the mixture was allowed for reduction during 20 min. The catalysts were filtered, washed, with acetone and water, and dried under vacuum at room temperature. The total Pd content of the final catalyst as determined by chemical analysis was 1.57 and 1.44% for Pd/CeO₂ and Pd/apatite, respectively.

4.2.5. Catalyst characterization. For crystal analysis and indexation, the samples were examined by bright- and dark-field electron microscopy in a Jeol 2200 HRTEM operated at an accelerating voltage of 200 kV. Dark field consists on observing the image produced by diffracted electrons corresponding to a determined lattice spacing leaving the rest dark.

Chemical analyses of gold and palladium metals in the catalysts were carried out after dissolving the solids by attack with a 2:1 mixture of HNO₃/HF on a Varian-10 Plus Atomic Absorption Spectrometer or directly of the solids using on a Philips MiniPal 25 fm Analytic X-ray apparatus and a calibration plot. Analysis of reaction products was carried out by GC on an HP–Agilent 5973 with a 6980N mass selective detector.

4.3. Typical procedure for the aerobic solventless oxidation of alcohols

All alcohols provided by Aldrich were used without further purification. The corresponding alcohol (12.5 mmol) was added over Au/CeO₂ catalyst (0.252 g), molecular oxygen was bubbled continuously through the suspension (35 mL m⁻¹). The resulting mixture was then heated at 120 °C. After the reaction, acetone was added and the

catalyst was separated by centrifugation. The products in the solution were analyzed by GC–MS and conversion and selectivity were determined by GC using undecane as external standard. Supported catalyst was washed with 1 M aqueous solution of NaOH, and dried in vacuum before reuse.

Acknowledgements

Financial support by the Spanish Ministry of Science and Education (Projects MAT03-) and Generalidad Valenciana (grupos03-020) is gratefully acknowledged. A.A. and C.A. thank the Spanish Ministry of Science and Education and ITQ for a postgraduate scholarship.

References and notes

1. Corma, A.; García, H. *Chem. Rev.* **2002**, *102*, 3837–3892.
2. Corma, A.; Domine, M. E.; Nemeth, L.; Valencia, S. *J. Am. Chem. Soc.* **2002**, *124*, 3194–3195.
3. Corma, A.; Domine, M. E.; Valencia, S. *J. Catal.* **2003**, *215*, 294–304.
4. Yamaguchi, K.; Mizuno, N. *Angew. Chem., Int. Ed.* **2002**, *41*, 4538–4542.
5. Mallat, T.; Baiker, A. *Catal. Today* **1994**, *19*, 247–283.
6. Matsumoto, M.; Watanabe, N. *J. Org. Chem.* **1984**, *49*, 3435–3436.
7. Nishimura, T.; Kakiuchi, N.; Inoue, M.; Uemura, S. *Chem. Commun.* **2000**, 1245–1246.
8. Abad, A.; Concepcion, P.; Corma, A.; Garcia, H. *Angew. Chem., Int. Ed.* **2005**, *44*, 4066–4069.
9. Corma, A.; Domine, M. E. *Chem. Commun. (Cambridge)* **2005**, 4042–4044.
10. Carretin, S.; Concepcion, P.; Corma, A.; Lopez Nieto, J. M. *Angew. Chem.* **2004**, *43*, 2538–2540.
11. Haruta, M. *Catal. Today* **1997**, *36*, 153–166.
12. Hutchings, G. J. *Gold Bull. (London)* **2004**, *37*, 3–11.
13. Saltsburg, Q. F. H.; Stephanopoulos, M. *Science* **2003**, *301*, 935–938.
14. Guzman, J.; Gates, B. C. *J. Am. Chem. Soc.* **2004**, *126*, 2672–2673.
15. Guzman, J.; Carretin, S.; Fierro-Gonzalez, J. C.; Hao, Y.; Gates, B. C.; Corma, A. *Angew. Chem., Int. Ed.* **2005**, *44*, 4778–4781.
16. Carretin, S.; Guzman, J.; Corma, A. *Angew. Chem., Int. Ed.* **2005**, *44*, 2242–2245.
17. Guzman, J.; Carretin, S.; Corma, A. *J. Am. Chem. Soc.* **2005**, *127*, 3286–3287.
18. Mori, K.; Hara, T.; Mizugaki, T.; Ebitani, K.; Kaneda, K. *J. Am. Chem. Soc.* **2004**, *126*, 10657–10666.

One-pot conversion of activated alcohols into 1,1-dibromoalkenes and terminal alkynes using tandem oxidation processes with manganese dioxide

Ernesto Quesada, Steven A. Raw, Mark Reid, Estelle Roman and Richard J. K. Taylor*

Department of Chemistry, University of York, Heslington, York YO10 5DD, UK

Received 29 October 2005; revised 22 December 2005; accepted 23 December 2005

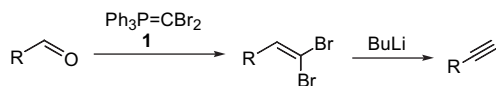
Available online 6 June 2006

Abstract—Approaches to the preparation of C₁-homologated dibromoalkenes and terminal alkynes from activated alcohols using one-pot tandem oxidation processes (TOPs) with manganese dioxide are outlined. The conversion of alcohols into dibromoalkenes is described using dibromomethyltriphenylphosphonium bromide and the formation of terminal alkynes was achieved via a sequential one-pot, two-step process utilising the Bestmann–Ohira reagent.

© 2006 Elsevier Ltd. All rights reserved.

1. Introduction

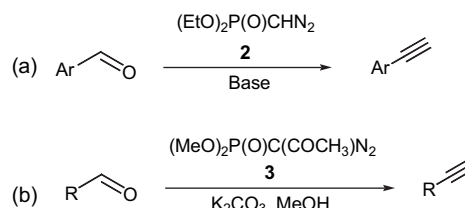
Terminal alkynes are of great industrial and academic importance, both as versatile synthetic building blocks and as commercial products. Some time ago, Corey and Fuchs demonstrated that terminal alkynes can be prepared from the corresponding dibromoalkenes through treatment with *n*-butyllithium.¹ The dibromoalkenes can themselves be obtained by a C₁-homologation reaction of aldehydes (via the Ramirez procedure² using dibromomethylenephosphorane **1**), thus offering a convenient and simple route to the homologated terminal alkyne products from aldehydes (Scheme 1). However, the need for strong bases to dehydrohalogenate the intermediate 1,1-dibromoalkenes can limit the generality of the Corey–Fuchs procedure.



Scheme 1.

More recently, diazoalkyl phosphonate reagents have been introduced for the conversion of aldehydes into terminal alkynes.^{3–9} These reagents have gained rapid acceptance⁹ due to their accessibility, the one-step nature of the transformation and the mild nature of the reaction conditions. Seyferth and Gilbert³ and Colvin⁴ first showed that aldehydes

could be converted into terminal alkynes using dialkyl diazomethylphosphonates (e.g., **2**, Scheme 2a). After deprotonation, a Horner–Wadsworth–Emmons-type olefination generates an unstable diazoalkene, which after thermal loss of nitrogen gives an alkylidene carbene, which then undergoes 1,2-rearrangement to provide the product alkyne.⁵



Scheme 2.

More recently, the groups of Ohira⁶ and Bestmann⁷ reported a valuable modification to the original Seyferth–Gilbert procedure, utilising dimethyl 1-diazo-2-oxopropylphosphonate **3** (Bestmann–Ohira reagent, Scheme 2b), a stable reagent readily prepared from commercially available precursors.⁸ This method represents a significant improvement as alkynes can be directly synthesised at rt from the Bestmann–Ohira reagent in MeOH/K₂CO₃ via the in situ generation of **2**. It is noteworthy that, while previously only aromatic aldehydes could be used as substrates in this reaction, the development of **3** allowed the extension of the methodology to a range of alkyl aldehydes.

We recently initiated a programme to develop novel one-pot manganese dioxide-mediated tandem oxidation processes (TOPs), leading directly from primary alcohols to a range

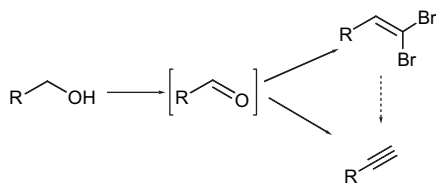
Keywords: Oxidation; One-pot transformations; Tandem reactions; Alkynes; Bestmann–Ohira; TOPs; Dibromoalkenes.

* Corresponding author. Tel.: +44(0) 1904 432606; fax: +44(0) 1904 434523; e-mail: rjktl@york.ac.uk

of synthetically useful functionalities (alkenes, imines, etc.) via in situ trapping of the intermediate aldehydes.¹⁰ One-pot reaction sequences are of great importance to organic chemistry and offer many practical advantages over conventional stepwise transformations. These one-pot tandem reactions have significant cost/time benefits (reducing solvent waste, etc.). In addition, one-pot methodologies can also be used to access volatile, toxic or unstable intermediates, which can be elaborated in situ, thus avoiding problematic isolations. Furthermore, given the fact that there are many more commercially available alcohols than aldehydes,¹¹ TOPs are becoming an increasingly important tool for the synthetic organic chemist.¹⁰

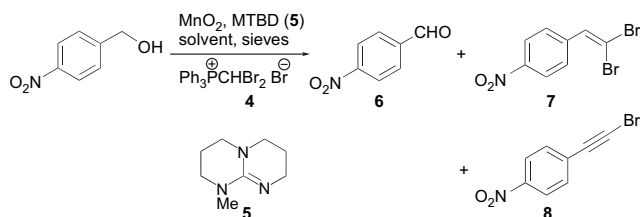
2. Results and discussion

With the above factors in mind, we embarked on an investigation to develop TOPs which provide the C₁-homologation of alcohols to give the corresponding dibromoalkenes and alkynes (Scheme 3).



Scheme 3.

We commenced this investigation by studying the direct conversion of alcohols into dibromoalkenes.¹² Dibromoalkenes are usually prepared by treating aldehydes with phosphorane **1**, generated from the reaction of triphenylphosphine and carbon tetrabromide² or, as in the method developed by Dolhem et al.,^{13a} using phosphonium salt **4** and a base.¹³ As we have previously developed TOPs utilising phosphonium salts with added bases,¹⁴ and as phosphonium salt **4** can be stored on the bench for several months without decomposition, its use was investigated first (Scheme 4, Table 1). We chose to initially investigate the homologation of the electron-deficient aromatic alcohol, *p*-nitrobenzyl alcohol, and chose 1-methyl-1,5,7-triazabicyclo[4.4.0]dec-5-ene (MTBD, **5**)¹⁵ as the in situ base as we had previously shown its efficiency in manganese dioxide TOP–Wittig reactions.¹⁴ Thus, stirring *p*-nitrobenzyl alcohol (1 equiv), active MnO₂ (10 equiv), phosphonium salt **4** (3.0 equiv), MTBD **5** (2.3 equiv) and 4 Å mol sieves in THF at reflux for 15 h, afforded the desired dibromoalkene **7**, but in a disappointing 24% yield (Table 1, entry i). Interestingly, however, bromoalkyne **8** was also isolated in 10% yield indicating that MTBD may be basic enough to also carry out the elimination



Scheme 4.

Table 1. Optimisation of the conversion of *p*-nitrobenzyl alcohol into dibromoalkene **7**

Entry	Conditions	6 (%)	7 (%)	8 (%)
i	THF, 2.3 equiv MTBD, 3.0 equiv 4 , reflux, 15 h	0	24	10
ii	CH ₂ Cl ₂ , 1.5 equiv MTBD, 2.2 equiv 4 , reflux, 14 h	ca. 50	30	0
iii	CH ₂ Cl ₂ , 1.5 equiv MTBD, 3.0 equiv 4 , reflux, 14.5 h	Trace	80	0
iv	CH ₂ Cl ₂ , 1.5 equiv MTBD, 3.5 equiv 4 , reflux, 16 h	0	86	0
v	CHCl ₃ , 1.5 equiv MTBD, 3.5 equiv 4 , reflux, 15 h	0	56	0

of HBr and thus form bromoalkynes in a one-pot, 3-step sequence from activated alcohols (see later discussion).

In an attempt to optimise the yield of dibromoalkene **7**, the reaction was then repeated by reducing the amounts of MTBD **5** and Wittig salt **4** to 1.5 and 2.2 equiv, respectively (entry ii). Dichloromethane was then found to be the solvent of choice to circumvent solubility issues and increase ease of work-up. Gratifyingly, this resulted in an improved yield of 30% of dibromoalkene **7** with no bromoalkyne **8** detected. However, *p*-nitrobenzaldehyde **6** was also recovered and therefore further optimisation of the stoichiometries was investigated. Increasing the amounts of Wittig salt **4** used to 3.0 equiv resulted in a marked increase in the yield of dibromoalkene **7** (80%) with only a trace of aldehyde **6** remaining (entry iii). Finally, increasing the amounts of Wittig salt further to 3.5 equiv resulted in complete consumption of intermediate *p*-nitrobenzaldehyde and an isolated yield of 86% of the desired dibromoalkene **7** (entry iv). In an attempt to reduce the reaction time, the use of chloroform as a reaction solvent was also investigated; dibromoalkene **7** was isolated in a respectable yield but the dichloromethane procedure was preferred for *p*-nitrobenzyl alcohol (entry v). However, in most other examples, chloroform was the preferred solvent.

The scope and limitations of this procedure leading to dibromoalkenes was next investigated using a range of alcohols (Table 2).

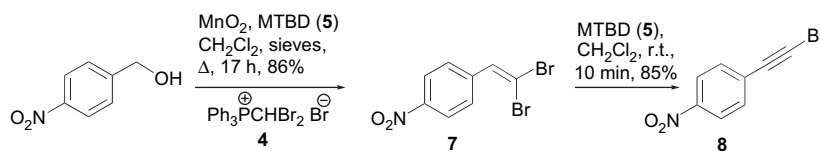
Table 2 shows that moderate to excellent yields of the dibromoalkenes were obtained directly from a range of activated alcohols including electron-neutral, electron-deficient and electron-rich aromatic examples (entries i–iii). Aromatic diols have proved to be versatile substrates as two directional building blocks and 4-hydroxymethylbenzyl alcohol gave an excellent 86% yield over the four-step, one-pot process (entry iv).¹⁶ Heterocyclic (entries v and vi) and allylic and propargylic examples (entries vii and viii) have also been carried out in good to excellent yield, further demonstrating the scope of the procedure. An aliphatic example was also studied but the reaction was slow and low yielding, indicating a limitation to this methodology (entry ix). However, the synthetic utility of this one-pot method is emphasised by the fact that comparable, or indeed better (entries iv¹⁷ and vi¹⁸), yields can be obtained directly from the substrate alcohol when compared to those previously reported in the literature for the conversion from the aldehyde. The low yield obtained from *p*-methoxybenzyl alcohol (entry iii) deserves comment, however. This is presumably due to the reduced

Table 2. Investigation of the scope and limitations of the oxidation-dibromoalkene synthesis^a

Entry	Alcohol	Product	Reaction time (h)	Isolated yield (%) ^a
i			18	73
ii			17	86 ^b
iii			18	46 (64) ^c
iv			20	86
v			18	60
vi			17	84 ^d
vii			17	84
viii			3.5	65 ^c
ix			36	14

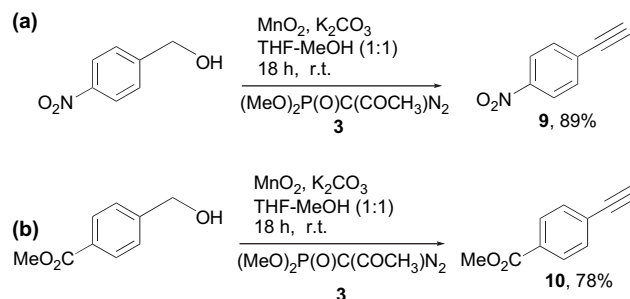
^a Reaction carried out in refluxing chloroform unless otherwise stated.^b In CH₂Cl₂ (56% in CHCl₃).^c Yield calculated with respect to recovered *p*-methoxybenzaldehyde.^d In CH₂Cl₂ (28% in CHCl₃).^e 1-Bromo-3-phenylprop-1-yne also formed (5%).

electrophilicity of the intermediate *p*-methoxybenzaldehyde. Also, it should be pointed out that with the electron-deficient example (entry ii), much higher yields were achieved by carrying out the reaction in refluxing dichloromethane rather than chloroform; the lower temperature presumably minimises side-reactions of the reactive electron-deficient dibromoalkene product. It should be noted that dibromoalkenes are of increasing importance¹⁹ being readily converted into *Z*-bromoalkenes,²⁰ *E*-bromoalkenes,²¹ trisubstituted alkenes,²² bromoalkynes,²³ disubstituted alkynes,²² amidines and carboxylic acid derivatives:²⁴ we feel that this TOP sequence should provide a useful new procedure for obtaining these valuable synthetic intermediates.

**Scheme 5.**

With a successful protocol for the preparation of a range of C₁-homologated dibromoalkenes from activated alcohols in hand, we moved on to investigate modifications to the procedure, which would give access to bromoalkynes (and possibly alkynes, as in the Corey–Fuchs procedure). Initially, we concentrated on the reaction of *p*-nitrobenzyl alcohol described earlier (Scheme 4), which produced 1-bromoalkyne **8** in 10% yield (Table 1, entry i). However, despite investigating a range of conditions, attempts to increase the yield of bromoalkyne **8** to an acceptable level, via a one-pot procedure, proved disappointing (maximum yield, 35%). Nevertheless, a two-step process was developed in which dibromoalkene **7** was first isolated and purified after the TOP sequence and then treated with MTBD (1.5 equiv at rt) to furnish the desired bromoalkyne **8** in 85% yield, 73% overall from *p*-nitrobenzyl alcohol (Scheme 5).

This inability to develop a one-pot procedure to C₁-homologated terminal alkynes from alcohols via a modified Corey–Fuchs approach encouraged us to investigate the in situ use of diazophosphonate reagents.²⁵ Initial studies using the Seyferth–Gilbert dialkyl diazomethylphosphonate reagent **2** in a TOP sequence were unsuccessful. We therefore moved on to study the use of the Bestmann–Ohira reagent **3** in TOP sequences. We first developed an improved procedure for preparing the Bestmann–Ohira reagent **3**, which utilised commercially available dimethyl (2-oxopropyl)phosphonate and proceeded under mild conditions in high yield (97% on a 5–10 g scale) using Koskinen’s diazo-transfer procedure.²⁶

**Scheme 6.**

We initially explored the TOP sequence illustrated in Scheme 6, in which the alcohol, MnO₂ and the Bestmann–Ohira reagent **3** were mixed together so that the intermediate aldehyde would be trapped as soon as it was generated. Using *p*-nitrobenzyl alcohol (1 equiv), MnO₂ (5 equiv), Bestmann–Ohira reagent **3** (1.2 equiv) and K₂CO₃ (2 equiv) in a mixture of THF/MeOH (1:1) at rt for 18 h we were delighted to find that the desired terminal alkyne **9** was obtained in 89% isolated yield (Scheme 6a). Remarkably, this transformation proceeds smoothly without rigorously anhydrous solvents, although an inert atmosphere is used to prevent terminal alkyne dimerisation. We also established that the presence of an excess of methanol, which deacetylates the

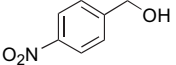
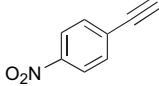
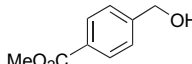
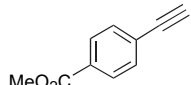
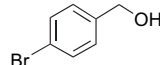
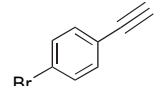
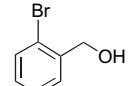
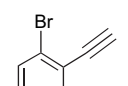
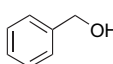
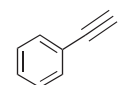
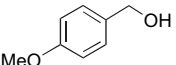
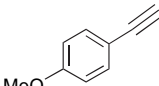
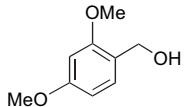
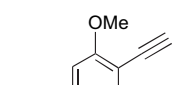
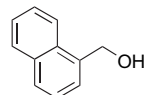
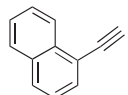
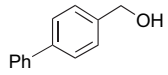
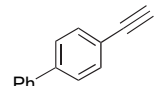
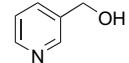
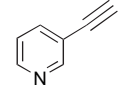
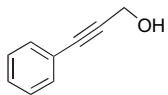
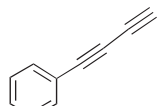
Bestmann–Ohira reagent, is crucial for success — reactions in THF alone failed to generate any alkyne. In addition, attempts to replace MeOH by other alcohols failed; when *iso*-propanol was employed as co-solvent the *p*-nitrobenzyl alcohol was acetylated by the Bestmann–Ohira reagent.

We therefore moved on to investigate the scope of this procedure, and first studied other benzylic alcohols. Unfortunately, the presence of methanol reduces the activity of the manganese dioxide and we quickly demonstrated that this precludes the efficient oxidation of many alcohols to the intermediate aldehydes. For this reason, the only other satisfactory substrate for this TOP sequence was found to be 4-carbomethoxybenzyl alcohol, which gave alkyne **10** in 78% yield (Scheme 6b). Other benzyl alcohol derivatives with electron-withdrawing substituents such as *p*-bromobenzyl alcohol reacted only partially, while benzyl alcohol itself, and derivatives containing electron-donating substituents, did not give any observable alkyne product. Attempts to modify the reaction conditions proved fruitless. Interestingly, when forcing conditions were employed (large excess of MnO₂ in refluxing solvent), methyl esters were isolated as the main reaction products in moderate yields (e.g., methyl *p*-bromobenzoate from *p*-bromobenzyl alcohol in 35% yield); however, we have previously described a TOP procedure using MnO₂/NaCN/MeOH, which can be employed to convert benzyl alcohols directly in the corresponding methyl esters rather more efficiently.²⁷

Given the above observations, we decided to investigate a sequential one-pot procedure in which the oxidation was carried out using MnO₂/THF prior to addition of the Bestmann–Ohira reagent in methanol. This modification produced a procedure that was more generally applicable (Table 3). Thus, the oxidations were accomplished using 5 equiv of MnO₂ in THF at rt and once all of the alcohol had been converted into the intermediate aldehyde (TLC monitoring, 3–24 h), methanol was added followed by K₂CO₃ (2 equiv) and the Bestmann–Ohira reagent (1.2 equiv). After stirring for a further 12–17 h, the terminal alkynes were obtained in good to excellent yield. It must be noted that the Bestmann–Ohira alkylation proceeds smoothly in the presence of the unreacted MnO₂.

The results in Table 3 clearly show that the one-pot, two-step sequence proceeds efficiently (56–99% isolated yields) and that it is a widely applicable general procedure with activated alcohols. Electron-withdrawing functional groups increase activity towards oxidation of the benzylic alcohols, leading to the highest yields of alkyne (entries i–iv). Good to excellent yields were also obtained using benzylic alcohols bearing electron-donating groups (entries vi and vii), and benzyl alcohol itself (entry v). Success was also achieved using naphthalene-1-methanol (entry viii), 4-phenylbenzyl alcohol (entry ix) and a heteroaromatic example, pyridine 3-methanol (entry x). Entries i and ii were noteworthy cases as the reactions were so efficient that products were isolated analytically pure (by NMR spectroscopy) in high yield after a simple extractive work-up and further chromatographic purification was not required. Purification by chromatography was difficult when the terminal alkyne products were volatile, particularly when benzyl alcohol was employed (entry v); in this case phenylacetylene was isolated in 87%

Table 3. Sequential one-pot MnO₂ oxidation/Bestmann–Ohira alkylation procedure^a

Entry	Alcohol	Product	Isolated yield (%) ^a
	$\text{Ar-CH}_2\text{-OH} \xrightarrow[\text{ii. (MeO)}_2\text{P(O)C(COCH}_3\text{)N}_2 \text{ 3, MeOH, K}_2\text{CO}_3, 12 \text{ h, rt}]{\text{i. MnO}_2, \text{ THF, 4-24 h, rt}} \text{Ar-C}\equiv\text{C-H}$		
i			99 ^b
ii			97 ^b
iii			85
iv			94
v			87 ^c
vi			56
vii			59 ^d
viii			89
ix			92
x			68 ^d
xi			59 ^d

^a Carried out on a 0.15–0.50 mmol scale, unless stated otherwise. The oxidation was left for 4 h (unless stated otherwise), the alkylation overnight (12–17 h). Yields refer to isolated products. Spectroscopic/analytical data of alkynes are in agreement with those reported.

^b Chromatographic purification not required; product essentially pure after extractive work-up.

^c Carried out in a 10 mmol scale and the alkyne purified by distillation.

^d Longer oxidation times required; 8 h for entry vii, 10 h for entry x and 24 h for entry xi.

yield by direct distillation from the crude mixture, although this procedure needed to be carried out on a 10 mmol scale. Reaction times for the oxidation step with aromatic substrates varied from 3 to 10 h, with 2,4-dimethoxybenzyl alcohol and pyridine 2-methanol taking the longest (8 and 10 h, respectively). On the other hand, this transformation does not appear to be over-sensitive to steric factors as hindered *ortho*-substituted alcohols underwent oxidation–alkynylation in good to excellent yields (entries iv, vii and viii). The efficient preparation of 4-bromo- and 2-bromo-phenylacetylene (entries iii and iv) are noteworthy. These and related compounds are commonly prepared through transition metal-mediated cross-coupling transformations (i.e., Sonogashira–Hagihara, Negishi, alkynyl Grignard, etc.)²⁸ with the requirement for anhydrous solvents and inert atmospheres, expensive catalysts, and the need for alkyne protection to prevent homocoupling.

Finally, it should be noted that, according to the literature,⁷ allylic alcohols cannot be employed in this methodology because methanol adds to the intermediate α,β -unsaturated aldehydes. Unactivated alcohols are also unreactive under these conditions, but 3-phenylpropargyl alcohol was successfully converted into 1-phenylidyne in 59% yield, although a long oxidation time (24 h) was required (entry xi).

In conclusion, we have developed simple and practical TOP sequences for the one-pot preparation of synthetically important 1,1-dibromoalkenes from activated alcohols, MnO₂, phosphonium salt **4** and MTBD **5**. Furthermore, we have developed a very mild and straightforward sequential one-pot method for the conversion of a variety of benzylic, heterocyclic and propargylic alcohols into their corresponding homologated terminal alkynes in good to excellent yield using MnO₂ and the Bestmann–Ohira reagent **3**. In addition, a TOP has been developed for the conversion of benzyl alcohols substituted by highly electron-withdrawing groups (nitro, ester) on the aromatic ring into the corresponding terminal alkynes. We are currently applying these procedures in target molecule synthesis.

3. Experimental

3.1. General

NMR spectra were recorded on JEOL EX-270 or EX-400 spectrometers using CDCl₃ as solvent unless otherwise stated. Tetramethylsilane or residual CHCl₃ were used as the internal standard. IR spectra were recorded on an ATI Mattson Genesis FTIR or ThermoNicolet IR 100 spectrometer. Low-resolution electron impact (EI) spectra were obtained on a Kratos MS 25 spectrometer. Chemical ionisation (CI) and high-resolution mass spectra were recorded on a Micromass Autospec spectrometer. Melting points were determined on a Gallenkamp melting point apparatus and are uncorrected. Flash column chromatography was carried out using silica gel 35–70 mesh, which was purchased from Fluka. All reagents were purchased from commercial sources and were used without further purification unless stated in the text. Activated manganese dioxide was obtained from Aldrich, catalogue number 21,764-6. PE is petroleum ether (bp 40–60 °C). Dibromomethyltriphenylphosphonium bromide **4** was prepared using the published^{13a} procedure.

3.2. General procedure for synthesis of dibromoalkenes from alcohols

To a suspension of activated manganese dioxide (867 mg, 9.97 mmol), phosphonium salt **4** (1.805 g, 3.50 mmol) and ground 4 Å molecular sieves (100 mg) in solvent (CH₂Cl₂ or chloroform) (10 mL) was added MTBD **5** (0.22 mL, 1.50 mmol). The reaction mixture was heated at reflux for 30 min, cooled to rt, then a solution of alcohol (1 mmol) in solvent (5 mL) added. The reaction mixture was then heated at reflux for the time specified, cooled to rt and filtered through Celite[®]. The resulting filtrate was then pre-loaded on to silica and the dibromoalkenes were purified by silica chromatography, eluting with EtOAc/PE.

3.2.1. 1,1-Dibromostyrene (Table 2, entry i). Reaction time of 18 h in CHCl₃; chromatography (10% EtOAc/PE) afforded the title compound (191 mg, 73%) as a pale yellow oil; *R_f* 0.61 (20% EtOAc/PE); ¹H NMR data consistent with those published.²⁴

3.2.2. 1,1-Dibromo-2-(4-nitrophenyl)ethene 7 (Table 2, entry ii). Reaction time of 17 h in CH₂Cl₂; chromatography (10% EtOAc/PE) afforded the title compound **7** (264 mg, 86%) as a pale yellow solid; mp 103–104 °C (lit.²⁴ 104–105 °C); *R_f* 0.58 (10% EtOAc/PE); ¹H NMR data consistent with those published.²⁴

3.2.3. 1-(2,2-Dibromo-vinyl)-4-methoxy-benzene (Table 2, entry iii). Reaction time of 18 h in CHCl₃; chromatography (10% EtOAc/PE) afforded the title compound (187 mg, 46%, 64% based on recovered *p*-methoxybenzaldehyde) as a pale yellow solid; mp 39–40 °C (lit.²⁴ 39–40 °C); *R_f* 0.56 (20% EtOAc/PE); ¹H NMR data consistent with those reported in the literature.²⁴

3.2.4. 1,4-Bis-(2,2-dibromovinyl)benzene (Table 2, entry iv). Reaction time of 20 h in CHCl₃; chromatography (10% EtOAc/PE) afforded the title compound (383 mg, 86%) as a pale yellow solid; mp 97 °C (lit.²⁹ 98–99 °C); *R_f* 0.67 (20% EtOAc/PE); ¹H NMR data consistent with those reported in the literature.²⁹

3.2.5. 3-(2,2-Dibromoethenyl)thiophene (Table 2, entry v). Reaction time of 18 h in CHCl₃; chromatography (10% EtOAc/PE) afforded the title compound (161 mg, 60%) as a pale yellow oil; *R_f* 0.58 (20% EtOAc/PE); ¹H NMR data consistent with those reported in the literature.³⁰

3.2.6. 3-(2,2-Dibromoethenyl)pyridine (Table 2, entry vi). Reaction time of 17 h in CHCl₃; chromatography (40% EtOAc/PE) afforded the title compound (221 mg, 84%) as a pale yellow solid; mp 55–57 °C (lit.¹⁸ 57–59 °C); *R_f* 0.23 (40% EtOAc/PE); ¹H NMR data was consistent with those reported in the literature.¹⁸

3.2.7. (4,4-Dibromo-buta-1,3-dienyl)benzene (Table 2, entry vii). Reaction time of 17 h in CH₂Cl₂; chromatography (10% EtOAc/PE) afforded the title compound (242 mg, 84%) as a pale yellow solid; mp 45 °C (lit.³¹ 55–56 °C); *R_f* 0.63 (20% EtOAc/PE); ¹H NMR data consistent with those reported in the literature.³¹

3.2.8. (4,4-Dibromo-but-3-en-1-yl)benzene (Table 2, entry viii). Reaction time of 3.5 h in CHCl_3 ; chromatography (eluting with 10% EtOAc/PE) afforded the title compound (186 mg, 65%) as a pale yellow oil; R_f 0.62 (20% EtOAc/PE); ^1H NMR data consistent with those reported in the literature.³²

3.2.9. (3,3-Dibromoprop-2-enyl)benzene (Table 2, entry ix). Reaction time of 36 h in CHCl_3 ; chromatography (10% EtOAc/PE) afforded the title compound (39 mg, 14%) as a pale yellow oil; R_f 0.56 (20% EtOAc/PE); ^1H NMR data consistent with those reported in the literature.³³

3.2.10. 1-Bromo-2-(4-nitrophenyl)ethyne 8. To a solution of 1,1-dibromo-2-(4-nitrophenyl)ethene **7** (40 mg, 0.13 mmol) in dichloromethane (2 mL), MTBD **5** (28 μL , 0.20 mmol) was added dropwise. The reaction was stirred for 10 min and then diluted with saturated aq NH_4Cl (5 mL). The resulting mixture was extracted with dichloromethane (3×10 mL) and the combined organic extracts were dried over Na_2SO_4 and concentrated in vacuo to give a crude orange solid that was purified by silica chromatography (eluting with 5% EtOAc/PE) to afford the title compound (25 mg, 85%) as a white solid; mp 168–169 °C (lit.³⁴ 172 °C); R_f 0.28 (5% EtOAc/PE); ^1H NMR data consistent with those reported in the literature.²⁴

3.2.11. Bestmann–Ohira reagent 3. Dimethyl (2-oxopropyl)phosphonate (Lancaster, 97%, 5 g, 30 mmol) was dissolved in dry CH_3CN (50 mL) and cooled to 0 °C (ice-bath) under argon. K_2CO_3 (4.58 g, 33 mmol) and then tosyl azide (6.53 g, 33 mmol) [Caution: highly toxic and explosive; handle in a well ventilated fume cupboard wearing protective gloves] were added sequentially in single portions and the resulting mixture was stirred at rt for 3 h. The solvent was eliminated in vacuo and the crude redissolved in dichloromethane (50 mL) and washed with water (50 mL). The organic layer was washed additionally with brine (50 mL), dried over MgSO_4 , filtered and the solvent removed in vacuo. After purification by chromatography on silica gel (EtOAc/PE, 7:3), the Bestmann–Ohira reagent **3** was isolated as a yellow oil (5.58 g, 29 mmol, 97%); R_f 0.28 (EtOAc). Spectroscopic and analytical data were consistent with those reported.⁸

3.2.12. 1-Ethynyl-4-nitrobenzene 9 by tandem procedure. *p*-Nitrobenzyl alcohol (50 mg, 0.33 mmol) was dissolved in dry THF (3 mL). Anhydrous MeOH (3 mL) was added followed by activated MnO_2 (142 mg, 1.6 mmol), dry K_2CO_3 (90 mg, 0.66 mmol) and Bestmann–Ohira reagent **3** (75 mg, 0.4 mmol). The heterogeneous mixture was stirred at rt for 18 h under argon. The crude mixture was filtered through a short Celite[®] pad (dichloromethane eluent). The volatiles were removed in vacuo, the residue redissolved in dichloromethane (10 mL) and then washed with 5% aq NaHCO_3 solution (10 mL) and brine. The organic layer was dried over anhydrous MgSO_4 , filtered and the solvent removed under reduced pressure. The residue was purified by chromatography on silica gel (EtOAc/PE, 1:9) giving title compound as a white solid (43 mg, 89%); mp 150–151 °C (lit.³⁵ 150–150.5 °C); R_f 0.7 (50% EtOAc/PE); spectroscopic data consistent with those reported in the literature.³⁵

3.2.13. 1-Ethynyl-4-carbomethoxybenzene 10 by tandem procedure. *p*-Carboxymethoxy benzyl alcohol (77 mg, 0.46 mmol) was dissolved in dry THF (5 mL). Anhydrous MeOH (2 mL) was added to the homogeneous solution, followed by activated MnO_2 (201 mg, 2.3 mmol), dry K_2CO_3 (128 mg, 0.9 mmol) and finally Bestmann–Ohira reagent **3** (125 mg, 0.65 mmol). The mixture was efficiently stirred at rt for 18 h under argon. MnO_2 was removed by filtration through a short Celite[®] pad (dichloromethane eluent). The volatiles were removed under reduced pressure, the residue redissolved in dichloromethane (10 mL) and washed with 5% aq NaHCO_3 solution (20 mL) and brine. The organic layer was dried over anhydrous MgSO_4 , filtered and the solvent was eliminated in vacuo. The residue was purified by chromatography on silica gel (EtOAc/PE, 1:9). The title compound was obtained as a white solid (57 mg, 78%); mp 94 °C; lit.³⁶ 93–95 °C; R_f 0.68 (50% EtOAc/PE); spectroscopic data consistent with those reported in the literature.³⁷

3.3. General procedure for the synthesis of terminal alkynes from activated alcohols by sequential, one-pot method

Activated alcohol (0.15–0.50 mmol) was dissolved in dry THF (6 mL) and activated MnO_2 (142 mg, 1.6 mmol, 5 equiv) was added. The heterogeneous mixture was efficiently stirred at rt for the time specified (4–24 h). Anhydrous MeOH (6 mL) was added, followed by dry K_2CO_3 (84 mg, 0.6 mmol) and Bestmann–Ohira reagent **3** (70 mg, 0.36 mmol). The reaction was stirred overnight (12–17 h) at rt under argon and the crude mixture filtered through a short Celite[®] pad using dichloromethane eluent. The organic solvent was removed in vacuo, the residue redissolved in dichloromethane (10 mL) and then washed with 5% aq NaHCO_3 (10 mL) and then brine. The organic layer was dried over anhydrous MgSO_4 , filtered and the solvent was removed under reduced pressure to give the product alkyne. If necessary, the alkyne could be purified further by silica chromatography, eluting with EtOAc/PE. In the case of phenylacetylene, the reaction was carried out on a 10 mmol scale and purification was carried by direct distillation of the crude reaction mixture (see later).

3.3.1. 1-Ethynyl-4-nitrobenzene (Table 3, entry i). 0.15 mmol scale, oxidation time of 4 h; chromatography was not required; title compound obtained as a white solid (22 mg, 99%); mp 150–151 °C (lit.³⁵ 150–150.5 °C); R_f 0.7 (50% EtOAc/PE); spectroscopic data consistent with those reported in the literature.³⁵

3.3.2. 1-Ethynyl-4-carbomethoxybenzene (Table 3, entry ii). 0.15 mmol scale, oxidation time of 4 h; chromatography was not required; title compound obtained as a white solid (23 mg, 97%); mp 94 °C (lit.³⁶ 93–95 °C); R_f 0.68 (50% EtOAc/PE); spectroscopic data consistent with those reported in the literature.³⁷

3.3.3. 1-Ethynyl-4-bromobenzene (Table 3, entry iii). 0.30 mmol scale, oxidation time of 4 h; chromatography (10% EtOAc/PE) afforded the title compound (46 mg, 85%) as a white wax; R_f 0.73 (50% EtOAc/PE); spectroscopic data consistent with those reported in the literature.²⁸

3.3.4. 1-Ethynyl-2-bromobenzene (Table 3, entry iv). 0.30 mmol scale, oxidation time of 4 h; chromatography (10% EtOAc/PE) afforded the title compound (51 mg, 94%) as a colourless oil; R_f 0.72 (50% EtOAc/PE); spectroscopic data consistent with those reported in the literature.³⁸

3.3.5. Phenylacetylene (Table 3, entry v). 10 mmol scale, oxidation time of 4 h; distillation from the crude reaction mixture gave the title compound (890 mg, 87%) as a colourless oil; spectroscopic data consistent with those reported in the literature.³⁹

3.3.6. 1-Ethynyl-4-methoxybenzene (Table 3, entry vi). 0.36 mmol scale, oxidation time of 4 h; chromatography (10% EtOAc/PE) gave the title compound (27 mg, 56%) as a white waxy solid; R_f 0.76 (50% EtOAc/PE); spectroscopic data consistent with those reported in the literature.⁴⁰

3.3.7. 1-Ethynyl-2,4-dimethoxybenzene (Table 3, entry vii). 0.33 mmol scale, oxidation time of 8 h; chromatography (10% EtOAc/PE) gave the title compound (31 mg, 59%) as a colourless oil; R_f 0.6 (50% EtOAc/PE); spectroscopic data consistent with those reported in the literature.⁴¹

3.3.8. 1-Naphthylacetylene (Table 3, entry viii). 0.23 mmol scale, oxidation time of 4 h; chromatography (10% EtOAc/PE) gave the title compound (31 mg, 89%) as a colourless oil; R_f 0.65 (50% EtOAc/PE); spectroscopic data consistent with those reported in the literature.⁴²

3.3.9. 1-Ethynyl-4-phenylbenzene (Table 3, entry ix). 0.20 mmol scale, oxidation time of 4 h; chromatography (10% EtOAc/PE) gave the title compound (33 mg, 92%) as a colourless oil; R_f 0.6 (50% EtOAc/PE); spectroscopic data consistent with those reported in the literature.⁴³

3.3.10. 3-Ethynyl pyridine (Table 3, entry x). 0.50 mmol scale, oxidation time of 10 h; chromatography (10% EtOAc/PE) gave the title compound (35 mg, 68%) as a white waxy solid; R_f 0.5 (EtOAc); spectroscopic data consistent with those reported in the literature.⁴⁴

3.3.11. Buta-1,3-diynyl-benzene (Table 3, entry xi). 0.50 mmol scale, oxidation time of 24 h; chromatography (10% EtOAc/PE) gave the title compound (37 mg, 59%) as a colourless liquid; R_f 0.75 (EtOAc); spectroscopic data consistent with those reported in the literature.⁴⁵

Acknowledgements

We are grateful to the EPSRC for postdoctoral support (ROPA Fellowship, S.A.R.), to the EPSRC, Oxford Chemicals and The Gen Foundation for studentship support (M.R.), and to ENSIACET, Toulouse for exchange support (E.R.).

References and notes

- Corey, E. J.; Fuchs, P. L. *Tetrahedron Lett.* **1972**, *13*, 3769–3772.
- Ramirez, F.; Desai, N. B.; McKelvie, N. *J. Am. Chem. Soc.* **1962**, *84*, 1745–1747.
- (a) Seyferth, D.; Marmor, R. S.; Hilbert, P. *J. Org. Chem.* **1971**, *36*, 1379–1386; (b) Gilbert, J. C.; Weerasooriya, U. *J. Org. Chem.* **1982**, *47*, 1837–1845.
- Colvin, E. W.; Hamill, B. J. *J. Chem. Soc., Perkin Trans. 1* **1977**, 869–874.
- Brown, D. G.; Velthuisen, E. J.; Commerford, J. R.; Brisbois, R. G.; Hoye, T. R. *J. Org. Chem.* **1996**, *61*, 2540–2541.
- Ohira, S. *Synth. Commun.* **1989**, *19*, 561–564.
- Roth, G. J.; Liepold, B.; Müller, S. G.; Bestmann, H. J. *Synlett* **1996**, 521–522.
- (a) Callant, P.; D'Haenens, L.; Vandewalle, M. *Synth. Commun.* **1984**, *14*, 155–161; (b) Ghosh, A. K.; Bischoff, A.; Cappiello, J. *Eur. J. Org. Chem.* **2003**, 821–832.
- Dixon, D. J.; Ley, S. V.; Reynolds, D. J. *Chem.—Eur. J.* **2002**, *8*, 1621–1636; Goundry, W. R. F.; Baldwin, J. E.; Lee, V. *Tetrahedron* **2003**, *59*, 1719–1729; Xu, Z.; Peng, Y.; Ye, T. *Org. Lett.* **2003**, *5*, 2821–2824; Marshall, J. A.; Schaaf, G. M. *J. Org. Chem.* **2003**, *68*, 7428–7432; Maehr, H.; Uskokovic, M. R. *Eur. J. Org. Chem.* **2004**, 1703–1713.
- For a review of the use of MnO₂ in tandem oxidation processes see: Taylor, R. J. K.; Reid, M.; Foot, J.; Raw, S. A. *Acc. Chem. Res.* **2005**, *38*, 851–869 and references therein; see also Refs. **12**, **14**, **25** and **27** and McAllister, G. D.; Oswald, M. F.; Paxton, R. J.; Raw, S. A.; Taylor, R. J. K. *Tetrahedron* **2006**, *62*, doi:10.1016/j.tet.2005.12.078.
- Baxendale, I. R.; Ley, S. V.; Sneddon, H. F. *Synlett* **2002**, 775–777.
- Preliminary communication: Raw, S. A.; Reid, M.; Roman, E.; Taylor, R. J. K. *Synlett* **2004**, 819–822.
- (a) Dolhem, F.; Lièvre, C.; Demailly, G. *Tetrahedron Lett.* **2002**, *43*, 1847–1849; (b) Patrick, M.; Gennet, D.; Rassat, A. *Tetrahedron Lett.* **1999**, *40*, 8575–8578.
- Blackburn, L.; Pei, C.; Taylor, R. J. K. *Synlett* **2002**, 215–218; Reid, M.; Rowe, D. J.; Taylor, R. J. K. *Chem. Commun.* **2003**, 2284–2285.
- Simoni, D.; Rossi, M.; Rondanin, R.; Mazzani, A.; Baruchello, C.; Malagutti, C.; Roberti, M.; Indiviata, F. P. *Org. Lett.* **2000**, *2*, 3765–3768.
- Magnuson, S. R. *Tetrahedron* **1995**, *51*, 2167–2213; for recent examples of two directional synthesis using TOPs see: Wei, X.; Taylor, R. J. K. *J. Org. Chem.* **2000**, *65*, 616–620; Frederico, D.; Donate, P. M.; Constantino, M. G.; Bronze, E. S.; Sairre, M. I. *J. Org. Chem.* **2003**, *68*, 9126–9128; McDermott, P. J.; Stockman, R. A. *Org. Lett.* **2005**, *7*, 27–29.
- Bestmann, H. J.; Frey, H. *Liebigs Ann. Chem.* **1980**, *12*, 2061–2071.
- Lok, W. N.; Ward, A. D. *Aust. J. Chem.* **1978**, *31*, 617–625.
- For some noteworthy recent examples in natural product synthesis see: Roush, W. R.; Brown, B. B. *J. Org. Chem.* **1993**, *58*, 2162–2172; Myers, A. G.; Hogan, P. C.; Hurd, A. R.; Goldberg, S. D. *Angew. Chem., Int. Ed.* **2002**, *41*, 1062–1067; Evans, D. A.; Starr, J. T. *Angew. Chem., Int. Ed.* **2002**, *41*, 1787–1790; Mergott, D. J.; Frank, S. A.; Roush, W. R. *Org. Lett.* **2002**, *4*, 3157–3160.
- Uenishi, J.; Kawahama, R.; Yonemitsu, O. *J. Org. Chem.* **1998**, *63*, 8965–8975.
- Kuang, C.; Senboku, H.; Tokuda, M. *Tetrahedron* **2002**, *58*, 1491–1496.
- Lee, H. B.; Huh, D. H.; Oh, J. S.; Min, G.-H.; Kim, B. H.; Lee, D. H.; Hwang, J. K.; Kim, Y. G. *Tetrahedron* **2001**, *57*, 8283–8290.
- Lin, S.-T.; Lee, C.-C.; Liang, D. W. *Tetrahedron* **2000**, *56*, 9619–9623.
- Huh, D. H.; Jeong, J. S.; Lee, H. B.; Ryu, H.; Kim, Y. G. *Tetrahedron* **2002**, *58*, 9925–9932.

25. Preliminary communication: Quesada, E.; Taylor, R. J. K. *Tetrahedron Lett.* **2005**, *46*, 6473–6476.
26. Koskinen, A. M. P.; Muñoz, L. *J. Chem. Soc., Chem. Commun.* **1990**, 652–653.
27. Foot, J. S.; Kanno, H.; Giblin, G. M. P.; Taylor, R. J. K. *Synthesis* **2003**, 1055–1064.
28. Kamikawa, T.; Hayashi, T. *J. Org. Chem.* **1998**, *63*, 8922–8925 and references therein.
29. Hwang, G. T.; Son, H. S.; Ku, J. K.; Kim, B. H. *J. Am. Chem. Soc.* **2003**, *125*, 11241–11248.
30. Beny, J.-P.; Dhawan, S. N.; Kagan, J.; Sundlass, S. *J. Org. Chem.* **1982**, *47*, 2201–2204.
31. Torrado, A.; López, S.; Alvarez, R.; de Lera, A. R. *Synthesis* **1995**, 285–293.
32. Uenishi, J.; Kawahama, R.; Yonemitsu, O. *J. Org. Chem.* **1996**, *61*, 5716–5717.
33. Korotchenko, V. N.; Shastin, A. V.; Nenajdenko, V. G.; Balenkova, E. S. *Org. Biomol. Chem.* **2003**, *1*, 1906–1908.
34. Beltrame, P.; Cattania, M. G.; Simonetta, M. *J. Chem. Soc., Perkin Trans. 2* **1973**, 63–66.
35. Serwinski, P. R.; Lahti, P. M. *Org. Lett.* **2003**, *5*, 2099–2102.
36. Kataoka, H.; Nakagawa, M. *Bull. Chem. Soc. Jpn.* **1963**, *36*, 799–806.
37. Li, Q.; Rukavishnikov, A. V.; Petukhov, P. A.; Zaikova, T. O.; Jin, C.; Keana, J. F. W. *J. Org. Chem.* **2003**, *68*, 4862–4869.
38. Van Meurs, P. J.; Janssen, R. A. *J. Org. Chem.* **2000**, *65*, 5712–5719.
39. Ibrahim, Y. A.; Al-Awadi, N. A.; Kaul, K. *Tetrahedron* **2001**, *57*, 7377–7381.
40. Kundu, N. G.; Khan, M. W. *Tetrahedron* **2000**, *56*, 4777–4792.
41. Nielsen, S. F.; Kharazmi, A.; Christensen, S. B. *Bioorg. Med. Chem.* **1998**, *6*, 937–942.
42. John, J. A.; Tour, J. M. *Tetrahedron* **1997**, *53*, 15515–15534.
43. Barrett, A. G. M.; Hopkins, B. T.; Love, A. C.; Tedeschi, L. *Org. Lett.* **2004**, *6*, 835–837.
44. Rodríguez, J. G.; Martín-Villamil, R.; Cano, H. F.; Fonseca, I. *J. Chem. Soc., Perkin Trans. 1* **1997**, 709–714.
45. Jiang, M. X.-W.; Rawat, M.; Wulff, W. D. *J. Am. Chem. Soc.* **2004**, *126*, 5970–5971.

The direct preparation of functionalised cyclopropanes from allylic alcohols or α -hydroxyketones using tandem oxidation processes

Graeme D. McAllister, Magalie F. Oswald, Richard J. Paxton,
Steven A. Raw and Richard J. K. Taylor*

Department of Chemistry, University of York, Heslington, York YO10 5DD, UK

Received 29 October 2005; revised 22 December 2005; accepted 23 December 2005

Available online 6 June 2006

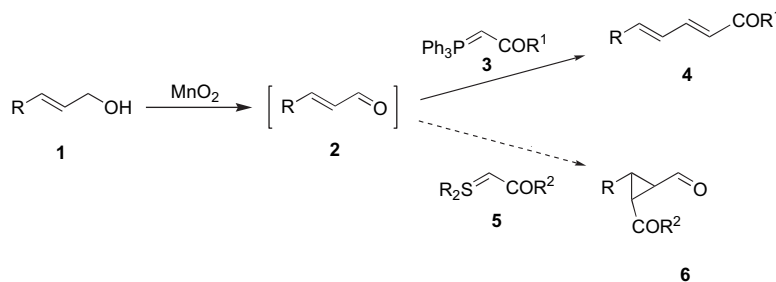
Abstract—New manganese dioxide-mediated tandem oxidation processes (TOPs) have been developed, which facilitate the direct conversion of allylic alcohols and α -hydroxyketones into polysubstituted functionalised cyclopropanes. In the simplest version, the oxidation of an allylic alcohol is carried out in the presence of a stabilised sulfurane, and the intermediate α,β -unsaturated carbonyl compound undergoes in situ cyclopropanation. By using a combination of stabilised phosphorane and sulfurane, the direct conversion of allylic alcohols or α -hydroxyketones into functionalised cyclopropanes is achieved, with in situ cyclopropanation being followed by Wittig olefination, or vice versa. The application of these methods to a formal synthesis of the lignan (\pm)-picropodophyllone, and to novel analogues of the insecticide allethrin II, is described.

© 2006 Elsevier Ltd. All rights reserved.

1. Introduction

We have recently developed a range of manganese dioxide-mediated tandem oxidation processes (TOPs) in which primary alcohols are oxidised and the intermediate aldehydes are trapped in situ to give alkenes, imines, oximes, amines, nitriles, esters, amides and heterocyclic systems via one-pot procedures.¹ These TOP sequences offer a number of advantages to the organic chemist: they are operationally straightforward, the MnO_2 and its by-products being removed by a simple filtration; they result in a reduced number of operations, giving significant time–cost benefits; and they

allow the use of ‘difficult’ carbonyl intermediates (i.e., those that are volatile, toxic or noxious) as they are prepared and elaborated in situ. The initial studies referred to above concentrated on 1,2-additions to the intermediate carbonyl compounds, as illustrated in **Scheme 1** for the oxidation–Wittig reaction of allylic alcohols **1** in which the intermediate conjugated aldehydes **2** are trapped by a stabilised phosphorane **3** giving the product dienes **4**. However, since the seminal research of Corey and Chaykovsky and others,² it is well known that sulfuranes undergo 1,4-addition to α,β -unsaturated carbonyl compounds to produce the corresponding cyclopropanes. Cyclopropanes are widespread in natural products



Scheme 1.

Keywords: Oxidation; One-pot transformations; Tandem reactions; TOPs; Cyclopropanes; Picropodophyllone; Allethrin analogues.

* Corresponding author. Tel.: +44 (0)1904 432606; fax: +44 (0)1904 434523; e-mail: rjkt1@york.ac.uk

and biologically active analogues, and are valuable synthetic intermediates.³ We therefore decided to investigate whether a manganese dioxide-mediated TOP sequence could be carried out using stabilised sulfuranes **5** to produce a one-pot procedure for converting allylic alcohols into polysubstituted cyclopropanes **6** (Scheme 1). Herein, we describe detailed results concerning TOP sequences involving oxidation–cyclopropanation and their applications in target molecule synthesis.⁴

2. Tandem oxidation–cyclopropanation reactions

In order to determine the viability of an oxidation–cyclopropanation sequence, we first examined the reaction of 2-methyl-2-propen-1-ol **1a** with activated MnO₂ in the presence of (carbethoxymethylene)dimethylsulfurane **5a**, prepared from the commercially available sulfonium salt,^{2d} and powdered 4 Å molecular sieves in benzene at reflux (Scheme 2). We were delighted to observe the formation of the desired cyclopropanecarboxaldehyde **6a** in 37% yield, indicating that sulfurane **5a** is compatible with manganese dioxide. We quickly established that the use of dichloromethane as solvent gave the optimum yield of **6a**, 78% as a mixture of trans/cis-isomers (~2:1).

With this result in hand, we then moved on to establish the scope of the TOP–cyclopropanation methodology, with respect to the alcohol and sulfurane; the results are shown in Table 1. With 2-methyl-2-propen-1-ol **1a**, we first established that (benzoylmethylene)dimethylsulfurane **5b**, again prepared from the commercially available sulfonium salt,^{2e} was also successful, producing cyclopropane **6b** in 53% yield (entry ii). Allyl alcohol **1b** also gave the desired cyclopropane **6c** on treatment with MnO₂ and sulfurane **5a** (entry

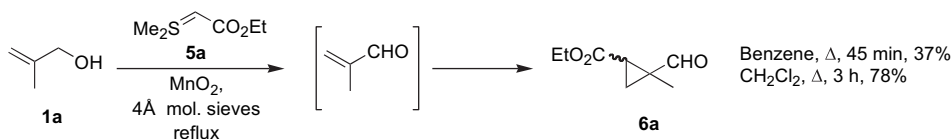
iii), although the yield was low (36%), presumably due to the volatility of the product (bp 97 °C).^{3q} By changing to sulfurane **5b**, however, adduct **6d** was obtained in an improved yield of 77% (entry iv).

Next we explored the use of the functionalised allylic alcohol **1c** (entries v and vi). This proved to be a viable substrate with both sulfuranes **5a** and **5b**, giving the expected cyclopropanes **6e** and **6f**, respectively. Cyclopropane **6e** (entry v) is a particularly interesting example as it is trisubstituted, with each substituent being in a different oxidation state (i.e., alkoxy, aldehyde and carboxylate), offering the possibility of further functionalisation in a selective manner. Cyclopropane **6f** (entry iv) has similar potential (i.e., alkoxy, aldehyde and ketone substituents).

We then proceeded to investigate the use of secondary alcohols with a range of 1-substituted propen-1-ols (entries vii–xi); these also gave good yields and complete trans-selectivity about the cyclopropane.

Divinylmethanol **1f** was studied next and, with both sulfuranes **5a** and **5b**, oxidation and double-cyclopropanation occurred, giving **6j** and **6k** in 60% and 69% yield, respectively; each product was obtained as a mixture of isomers (~1:1 as determined by ¹H NMR spectroscopy), but again with trans-orientation about the cyclopropanes (entries x and xi).

The trends in stereochemistry seen with 1- and 2-substituted propen-1-ols are consistent with the reaction mechanism proposed by Curley and DeLuca involving equilibration of initial adducts.⁵ With 1-substituted propen-1-ols (entries vii–xi), the increased size of the substituent in the intermediate (ketone vs aldehyde) results in an equilibrium giving solely the trans-cyclopropane products. Thus (Fig. 1), the



Scheme 2.

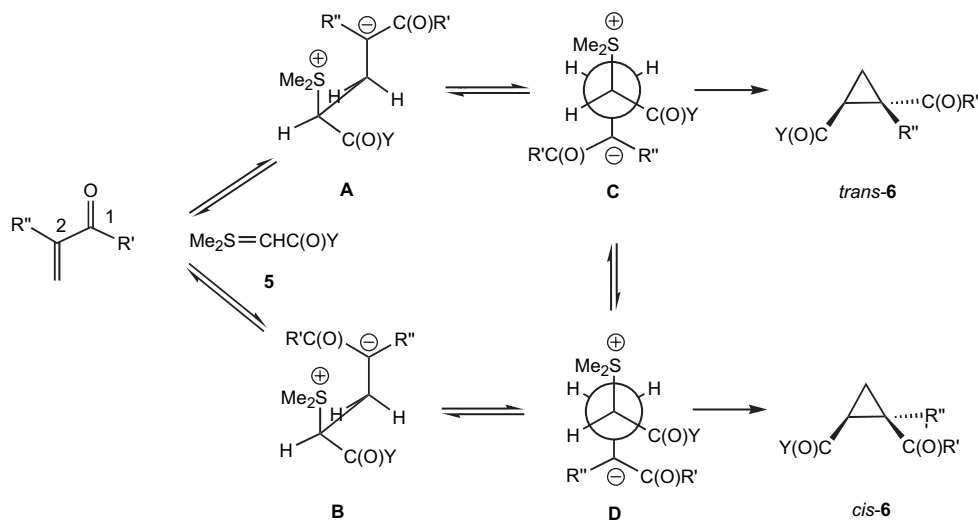
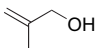
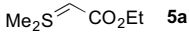

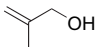
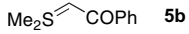

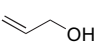
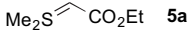

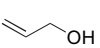
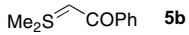

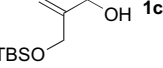
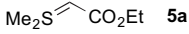
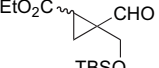
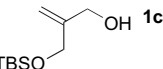
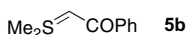
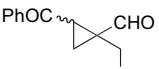
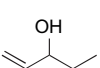

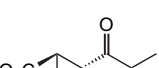
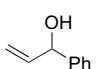
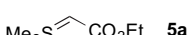

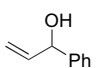
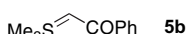
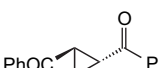
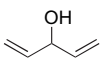
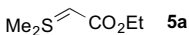
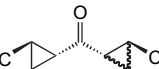
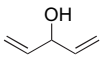
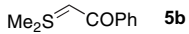
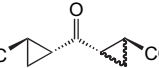
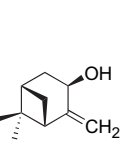

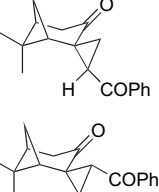
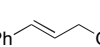
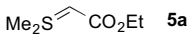
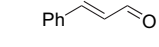
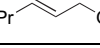
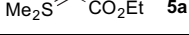
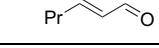


Figure 1.

Table 1. MnO₂-mediated TOP methodology for the preparation of cyclopropanes

Entry	Alcohol	Sulfurane	Product	Ratio (trans/cis)	Isolated yield (reaction time)
i	 1a	 5a	 6a	~2:1	78% (3 h)
ii	 1a	 5b	 6b	~4.2:1	53% (2 h)
iii	 1b	 5a	 6c	~3:1	36% ^a (6 h)
iv	 1b	 5b	 6d	~3:1	77% (3 h)
v	 1c	 5a	 6e	~3.6:1	74% (14 h)
vi	 1c	 5b	 6f	~2:1	73% (4.5 h)
vii	 1d	 5a	 6g	All trans	67% (18 h)
viii	 1e	 5a	 6h	All trans	100% (17 h)
ix	 1e	 5b	 6i	All trans	78% (2 h)
x	 1f	 5a	 6j	All trans	60% (4 h)
xi	 1f	 5b	 6k	All trans	69% (2 h)
xii	 1g	 5b	 6l	5:1 ^b	76% (16 h)
xiii	 1h	 5a		—	(quant.) ^c
xiv	 1i	 5a		—	(quant.) ^c

^a It is probable that the low yield for this example is due in part to the volatility of **6c** (bp 97 °C).^{3q}

^b Of a possible four isomers, a mixture of just two (ca. 5:1) was isolated: the stereochemistry of these diastereoisomers has not been allocated with certainty.

^c Based on ¹H NMR analysis of the unpurified reaction mixture, which showed only the aldehyde and sulfurane **5a**.

first ‘kinetic’ intermediates **A/B** (stabilised by electrostatic interactions) collapse to the cyclopropanes via the anti-conformers **C/D**. A solvent of low dielectric constant, such as CH₂Cl₂, retards this rotation and collapse due to the higher energy of the charge-separated intermediates. This allows greater equilibration of **A** and **B** and, hence, **C** and **D**, presumably driven by steric demands in the intermediates. In 2-substituted propen-1-ols, there is a balance between the aldehyde (R′=H) and R″ interacting with COY, resulting in

isomeric mixtures. In 1-substituted propen-1-ols (R″=H), this is now a balance between a proton and a ketone (R′=alkyl, etc.) interacting with COY, making **A** and **C** highly favoured and resulting solely in trans-cyclopropane.

The more complex (–)-trans-pinocarveol **1g** also worked well in this methodology, giving the spirocyclopropane **6l** in 76% yield (entry xii). This product was isolated as a mixture of just two of the four possible isomers (~5:1). We also

investigated the use of 3-substituted 2-propen-1-ols (entries xiii–xiv) but unfortunately no cyclopropanation was observed with **1h** and **1i**, despite complete oxidation occurring. The low reactivity of terminally substituted conjugated carbonyl compounds to stabilised sulfuranes has been well documented.²

Next, we went on to explore the use of disubstituted 2-propen-1-ols **1j–m** which, on oxidation, give chalcones which are known⁶ to be good substrates for cyclopropanation with stabilised sulfuranes (Scheme 3). The results are summarised in Table 2 (no all-cis isomers were observed). For these alcohols, the choice of solvent was crucial, with each example being carried out in CH₂Cl₂, THF and 1,2-dichloroethane (DCE). The optimum solvent for each reaction is indicated in Table 2.

With sulfurane **5a** and electron-rich, electron-deficient, and ‘electron-neutral’ alcohols, the yields are good to excellent (entries i and iii–v, 51–90%). Sulfurane **5b** was also utilised in a reaction with alcohol **1j**, again in excellent yield (entry ii). The observed erosion of the original trans-double bond stereochemistry can be understood by the equilibration of reaction intermediates, as discussed earlier (Fig. 1).

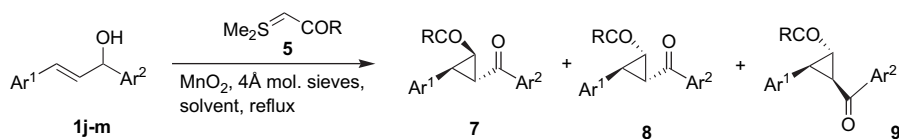
3. Tandem oxidation–cyclopropanation–Wittig reactions

We were intrigued by the possibility that the cyclopropane-carboxaldehyde products **6** could be exploited in further in

situ transformations. We decided to first examine the tandem oxidation–cyclopropanation–Wittig sequence, as we have already established the compatibility of phosphoranones with MnO₂.¹ We hoped to tune the reaction conditions so that both sulfuranes and phosphoranones could be used in situ, in the presence of MnO₂, to allow first oxidation, followed by sulfurane-mediated cyclopropanation, and finally phosphorane-induced olefination.

We first examined the reaction of 2-methylprop-2-en-1-ol **1a** with sulfurane **5a**, phosphorane **3a** and activated MnO₂. We were delighted to observe, in the first attempt, the formation of the desired cyclopropane **10a** as a ~1.4:1 mixture of cis/trans-isomers (about the cyclopropane) in a yield of 62% (Scheme 4). Cyclopropane **10a** was accompanied by a small amount (8%) of dienolate **11**. A brief optimisation study was then carried out, varying temperature and equivalents of ylides **3a** and **5a**. It was quickly established that use of a two-fold excess of sulfurane **5a** and carrying out the reaction at reflux gave the best yield of **10a**, 81%, with no dienolate **5a** being observed.

The optimum reaction stoichiometry indicates that the major reaction sequence involves oxidation, then cyclopropanation and then olefination. This is supported by the following observations: (i) TLC analysis indicates significant oxidation–cyclopropanation, giving cyclopropyl aldehyde **6a**, before major amounts of adduct **10a** are observed; (ii) when isolated dienolate **11** was exposed to sulfurane **5a** under similar conditions, only ~50% conversion to **10a** was observed after 16 h.

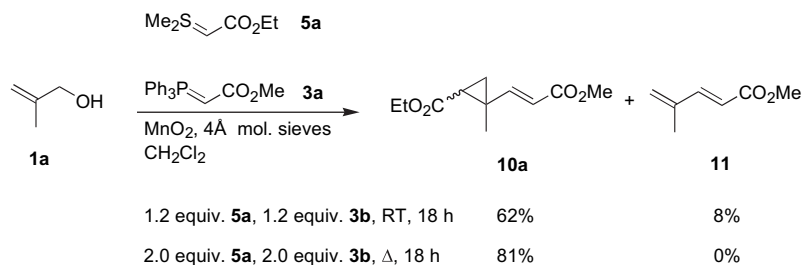


Scheme 3.

Table 2. Disubstituted 2-propen-1-ols in MnO₂-mediated TOP–cyclopropanation

Entry	Alcohol	Ylide/solvent	Product	Ratio (7:8:9)	Yield (reaction time)
i		5a THF		7a:8a:9a =5.0:1.0:3.0	70% (10 h)
ii		5b THF		(7b+9b):8b =2.6:1 ^a	75% (17 h)
iii		5a CH ₂ Cl ₂		7c:8c:9c =3.9:1.0:2.8	80% (19 h)
iv		5a CH ₂ Cl ₂		7d:8d:9d =4.5:1.0:2.8	51% (17 h)
v		5a CH ₂ Cl ₂		7e:8e:9e =4.0:1.0:1.6	90% (14 h)

^a Compounds **7b** and **9b** are enantiomers.



Scheme 4.

Table 3. TOP-cyclopropanation–olefination methodology

Entry	Alcohol	Sulfurane/phosphorane ^a	Product	2,3- <i>trans/cis</i> ^b	Yield (reaction time)
i		5a, 3a		~3.5:1	81% ^c (18 h)
ii		5b, 3a		~3.0:1	66% (14 h)
iii		5a, 3b		— ^d	88% (23 h)
iv		5a, 3a		~6.5:1	61% (5 h)
v		5b, 3a		~3.5:1	74% (14 h)
vi		5a, 3c		~7.0:1	56% ^c (18 h)
vii		5a, 3a		~1.8:1	64% (18 h)

^a **3a** = $\text{Ph}_3\text{P}=\text{CHCO}_2\text{Me}$; **3b** = $\text{Ph}_3\text{P}=\text{CHCN}$; **3c** = $\text{Ph}_3\text{P}=\text{C}(\text{Me})\text{CO}_2\text{Me}$.

^b Ratio determined by integration of ^1H NMR spectra.

^c With $\text{Ph}_3\text{P}=\text{CHCO}_2\text{Bu}^t$ the corresponding *tert*-butyl ester was obtained in 56% yield (*trans/cis* = 1.8:1).

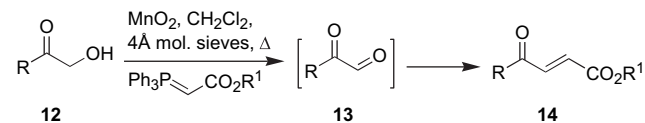
^d Alkene also showed *E*- and *Z*-isomers. *trans/E:cis/E:trans/Z:cis/Z* ~8.5:4.4:3.6:1.0.

^e The use of microwave irradiation reduced the reaction time to 1 h but the yield was reduced (45%); in both cases only the *E*-product was observed.

The optimum conditions illustrated in Scheme 4 were then applied to a range of alcohols **1**, sulfuranes **5** and phosphoranes **3**. The results are summarised in Table 3. As can be seen, good to excellent (56–88%) yields were obtained with the three allylic alcohols **1a–c** undergoing oxidation–elaboration with combinations of the sulfuranes **5a,b** and the phosphoranes **3a–c**, although the degree of stereocontrol in relation to the *cis/trans*-ratio of the 2,3-cyclopropane substituents was variable.

4. Tandem oxidation–Wittig–cyclopropanation reactions

We have previously described the manganese dioxide tandem oxidation–olefination of α -hydroxyketones **12** leading, by way of intermediate α -keto aldehydes **13**, to γ -ketocrotonates **14** in synthetically useful yields (Scheme 5).⁷

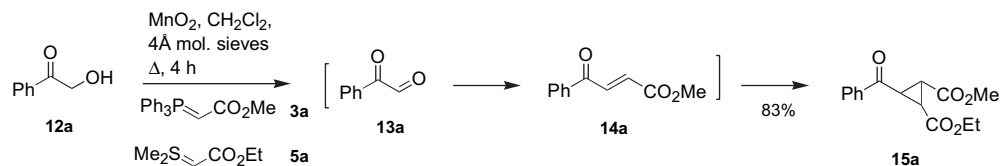


Scheme 5.

In the current study, we envisaged a complementary oxidation–olefination–cyclopropanation sequence, in which the alcohol is treated with MnO_2 , phosphorane and sulfurane but, of course, in this case, olefination has to occur first, followed by in situ cyclopropanation of the intermediate γ -ketocrotonate (Scheme 6). As shown, this idea was tested out using hydroxyacetophenone **12a** and we were delighted to obtain an excellent 83% yield of the 1,2,3-trisubstituted cyclopropane **15a** from this one-pot, three-step tandem sequence.

These conditions were then applied to a variety of α -hydroxyketones **12**, phosphoranes **3** and sulfuranes **5** to give substituted cyclopropanes **15b–h** in good to excellent (50–81%) yields (Table 4).

To demonstrate the applicability of this technology to complex, multifunctional substrates, hydrocortisone **12f** was employed as the α -hydroxyketone, giving the desired cyclopropane **15i** in 78% yield (Scheme 7). Moreover, NMR spectroscopy indicates that just one diastereoisomer (yet to be determined) of the product **15i** greatly predominates,



Scheme 6.

Table 4. TOP–olefination–cyclopropanation methodology^a

Entry	Alcohol	Phosphorane/sulfurane ^b	Product ^c	Yield (diastereoisomer ratio)
i		12a 3a, 5a		15a 83% (3.2:1)
ii		12a 3b, 5a		15b 80% (3.8:1)
iii		12a 3d, 5a		15c 50% (2.2:1)
iv		12a 3e, 5b		15d 81% (1.2:1)
v		12b 3a, 5b		15e 70% ^d
vi		12c 3e, 5b		15f 60% ^e (2.7:1)
vii		12d 3a, 5a		15g 78% ^f
viii		12e 3a, 5a		15h 51% ^g

^a Reaction times 1.5–15 h (see Section 6 for exact time); traces of a third diastereoisomer were observed (NMR) in entries i–iii.

^b **3a** = Ph₃P=CHCO₂Me; **3b** = Ph₃P=CHCN; **3d** = Ph₃P=CHCON(Me)OMe; **3e** = Ph₃P=CHCO₂Et.

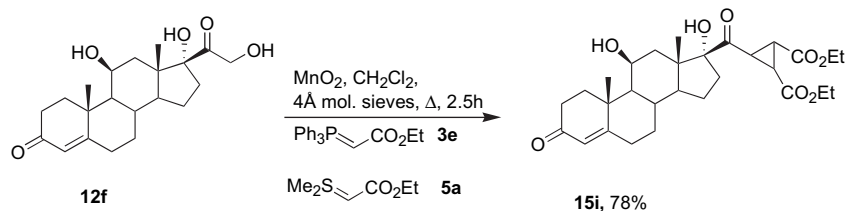
^c Isolated as a mixture of isomers about the cyclopropane.

^d The structures of individual diastereoisomers were not assigned.

^e When sulfurane **5a** was used, the corresponding cyclopropane was isolated in 54% yield.

^f When sulfurane **5a** was used, the corresponding cyclopropane was isolated in 55% yield.

^g One major diastereoisomer with only traces of minor isomers.



Scheme 7.

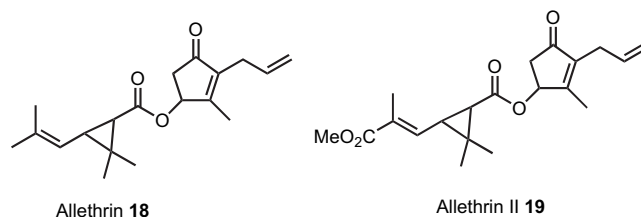
implying substrate-induced regio- and stereoselectivity in the in situ cyclopropanation step.

5. Applications in target molecule synthesis

In order to validate the TOP–cyclopropanation methodology, we decided to examine applications in target molecule synthesis. In the first example (Scheme 8), we prepared cyclopropane **17**, which was utilised by Murphy and Wattanasin as a late-stage intermediate in their synthesis of (\pm)-picropodophyllone⁸ which, along with related lignan lactones, is of interest as a cancer chemotherapeutic agent. Allylic alcohol **16** was treated with MnO₂ and sulfurane **5a** in DCE at reflux. We were delighted to find that this procedure produced cyclopropane **17** as a mixture of three diastereoisomers (ca. 3.6:2.9:1.0) in 80% combined yield. This result is noteworthy as allylic alcohol **16** is particularly electron-rich, and in our experience, this slows oxidation by MnO₂. Cyclopropane **17**, also as a mixture of diastereoisomers,⁸ has been converted into (\pm)-picropodophyllone in four steps;⁸ the sequence shown in Scheme 8 therefore represents a formal synthesis of this simple natural product.

Pyrethroids have proved extremely valuable as naturally occurring, non-toxic and biodegradable insecticides and insect repellants.⁹ Allethrin **18** and allethrin II **19** are typical synthetic pyrethroids, and **18** is widely used against houseflies and mosquitoes.^{3c,10} In order to showcase the TOP–cyclopropanation methodology, we prepared novel allethrin analogues as shown in Scheme 9. Cyclopentenone **20** is commercially available (Salor) and readily prepared.¹¹ Conversion into the ester **21**, salt **22** and then to sulfurane **22** was straightforward (although attempts to go directly from the bromide corresponding to **21** to a sulfonium salt such as **22** by treatment with dimethyl sulfide were unsuccessful). Then, treatment of allyl alcohol **1b**, sulfurane **22** and phosphorane **3c** with MnO₂ gave allethrin II analogue **24** in 57% yield via the one-pot TOP sequence illustrated in Scheme 9. Examination of the ¹H and ¹³C NMR spectra of **24** indicated that only two diastereoisomers were present (ca. 3:1 as an inseparable mixture). Extensive NOE studies indicated that both diastereoisomers possessed *E*-configured trisubstituted alkenes. Coupling constant analysis showed that both major and minor components are *trans*-

cyclopropane isomers, with no *cis*-isomers observed. Thus, coupling constants across the cyclopropane ring (*J* 8.5 Hz in both diastereomers) are in accordance with literature values.¹³ Also, in the ¹³C NMR spectrum, the chemical shifts of the ring carbons [δ_C 16.7 (CH₂), 22.3 (CH) and 22.4 (CH) ppm] are consistent with those of closely related *trans*-disubstituted cyclopropanes.¹⁴ Other allethrin analogues should be readily available by similar processes.

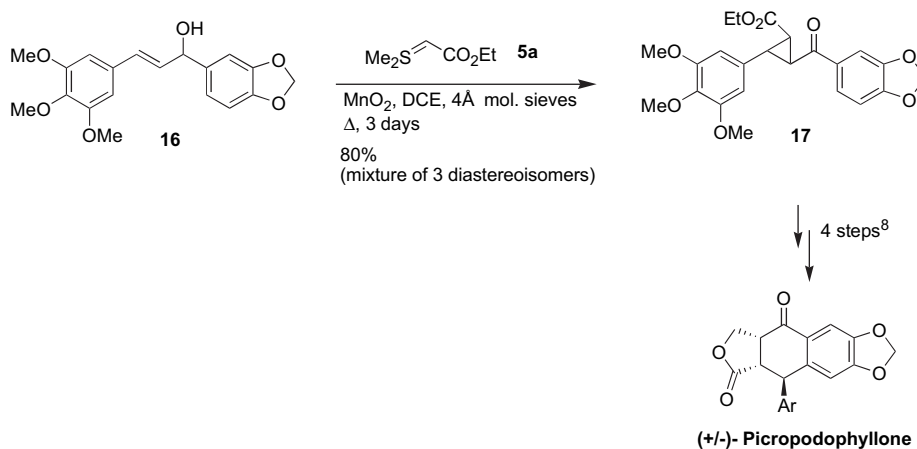


In summary, a number of different one-pot MnO₂-mediated TOP methodologies have been developed, which allow straightforward access to a range of functionalised cyclopropanes. Applications of the methodology in target molecule synthesis have been described, and further examples are currently under investigation.

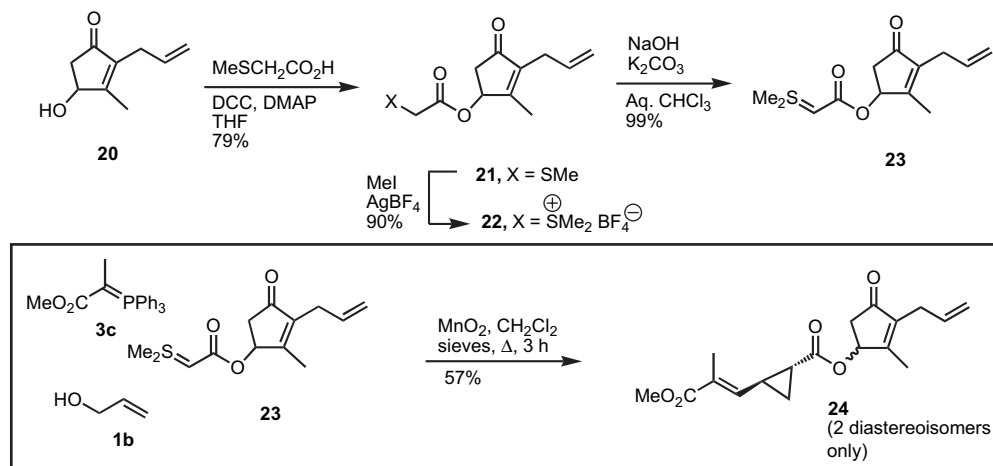
6. Experimental

6.1. General details

NMR spectra were recorded on Jeol EX-270 and ECX-400 spectrometers. Diastereomer ratios were obtained by ¹H NMR integration. Chemical shifts (δ) are given in parts per million (ppm), using the residual solvent as reference (CDCl₃ unless otherwise stated), and coupling constants are given in Hertz (Hz). IR spectra were recorded on ThermoNicolet IR100 or ATI Mattson Genesis FTIR spectrometers, as thin films between NaCl plates. Mass spectra were recorded on a Fisons analytical autospec instrument in either chemical ionisation (CI), electron ionisation (EI), or fast atom bombardment (FAB) modes. Melting points were measured on a Gallenkamp instrument in open capillary tubes, and are uncorrected. Flash chromatography was performed on Fluorochem silica gel (35–70 μ m) using the eluent specified. Thin layer chromatography (TLC) was



Scheme 8.



Scheme 9.

carried out using Merck silica gel 60F₂₅₄ pre-coated aluminium foil plates with a thickness of 250 μm , and visualised with UV light (254 nm), and KMnO₄/vanillin solutions. All reagents were purchased from commercial sources, and used without further purification, unless specified. Activated manganese(IV) dioxide was purchased from Aldrich (cat. no. 21,764; <5 μm , activated, 85%). Tetrahydrofuran, diethyl ether and dichloromethane were either dried using standard distillation procedures, or with an MBraun Solvent Purification System (SPS), immediately prior to use. Petrol is the fraction with boiling range 40–60 °C. Alcohol **1b** was obtained from the corresponding ketone¹² by standard reduction with NaBH₄/CsBr. Sulfuranes **5a** and **5b** were prepared from the commercially available (Aldrich) sulfonium salts using published procedures.^{2d,e}

Compounds **6a**,^{3n,q} **6c**,^{3m} **6d**,³ⁱ **6g**,^{3r} **6h**,^{3p} **6i**,^{3o} **7a**,^{2g} **7b**,^{3h} **7d**^{3k} and **17**⁸ are known compounds and the data correspond with those reported in the literature.

6.2. Tandem oxidation–cyclopropanation reactions

6.2.1. 2-Benzoyl-1-methylcyclopropanecarboxaldehyde 6b: representative procedure. To a solution of 2-methyl-2-propen-1-ol **1a** (36 mg, 0.50 mmol) in dichloromethane (5 mL) was added powdered 4 Å molecular sieves (0.50 g), (benzoylmethylene)dimethylsulfurane **5b** (108 mg, 0.60 mmol) and manganese dioxide (435 mg, 5.0 mmol). The mixture was heated at reflux for 2 h, and then cooled to rt. The crude mixture was then filtered through Celite[®] and the residue washed with dichloromethane (50 mL) giving a pale yellow solution. After removal of the solvent in vacuo, the residue was purified by flash column chromatography (petrol–EtOAc, 19:1 to 4:1) to give the *title compound* **6b** (50 mg, 53%) as an inseparable mixture (~4.2:1 *trans/cis*) as a colourless oil, *R_f* 0.31 (petrol–EtOAc, 4:1); ν_{max} (film) 2935, 1712, 1665, 1596, 1449, 1379, 1305, 1225 cm^{-1} ; δ_{H} (400 MHz, CDCl₃) *trans*: 1.26 (3H, s), 1.59 (1H, dd, *J* 4.9 and 8.2 Hz), 1.91 (1H, dd, *J* 4.9 and 7.0 Hz), 3.20 (1H, dd, *J* 8.2 and 7.0 Hz), 7.47 (2H, dd (app t), *J* 7.6 Hz), 7.58 (1H, dd (app t), *J* 7.6 Hz), 7.90 (2H, d, *J* 7.6 Hz), 9.09 (1H, s); *cis*: δ_{H} 1.44 (3H, s), 1.54 (1H, dd, *J* 4.9 and 7.6 Hz), 2.39 (1H, dd, *J* 4.9 and 7.0 Hz), 3.01 (1H, dd, *J* 7.6 and 7.0 Hz), 7.47 (2H, dd (app t), *J* 7.6 Hz), 7.58 (1H, dd (app t),

J 7.6 Hz), 7.93 (2H, d, *J* 7.6 Hz), 9.11 (1H, s); δ_{C} (100 MHz, CDCl₃) *trans*: 10.3 (CH₃), 18.6 (CH₂), 29.9 (CH), 37.4 (C), 128.3 (CH), 128.9 (CH), 133.6 (CH), 137.8 (C), 194.9 (C), 200.0 (C); *cis*: 17.5 (CH₃), 21.2 (CH₂), 35.0 (CH), 37.8 (C), 128.4 (CH), 128.9 (CH), 133.7 (CH), 137.2 (C), 195.6 (C), 200.4 (C); *m/z* (CI) 189 (MH⁺); HRMS (CI) [MH⁺], found 189.0912. C₁₂H₁₃O₂ requires 189.0916 (2.1 ppm error).

6.2.2. Ethyl 2-(*tert*-butyldimethylsilyloxymethyl)-2-formyl-cyclopropanecarboxylate 6e. Using the above procedure for **6b** (but with sulfurane **5a** and for 14 h), the *title compound* **6e** was prepared in 74% yield as an inseparable mixture (*trans/cis* ~3.6:1) as a colourless oil, *R_f* 0.33 (petrol–EtOAc, 12:1); ν_{max} (film) 2953, 2931, 2856, 1732, 1704, 1257, 1176, 1097, 839, 779 cm^{-1} ; δ_{H} (270 MHz, CDCl₃) *trans*: δ_{H} 0.02 (3H, s), 0.05 (3H, s); 0.84 (9H, s), 1.23–1.28 (3H, m), 1.45 (1H, dd, *J* 4.5 and 8.5 Hz), 1.53 (1H, dd, *J* 4.5 and 6.7 Hz), 2.31 (1H, dd, *J* 8.5 and 6.7 Hz), 3.86 (1H, d, *J* 11.1 Hz), 4.03–4.20 (2H, m), 4.32 (1H, d, *J* 11.1 Hz), 9.52 (1H, s); *cis*: δ_{H} 0.02 (3H, s), 0.05 (3H, s); 0.84 (9H, s), 1.23–1.28 (3H, m), 1.63 (1H, dd, *J* 4.8 and 8.2 Hz), 1.91 (1H, dd, *J* 4.8 and 6.7 Hz), 2.33 (1H, dd, *J* 8.2 and 6.7 Hz), 3.93 (2H, s), 4.03–4.20 (2H, m), 9.38 (1H, s); δ_{C} (67.5 MHz, CDCl₃) *trans*: –5.5 (CH₃), –5.4 (CH₃), 14.3 (CH₃), 18.3 (C), 18.9 (CH), 25.8 (CH₃), 26.4 (CH), 40.6 (C), 59.4 (CH₂), 61.3 (CH₂), 170.1 (C), 200.2 (C); *cis*: δ_{C} –5.5 (CH₃), –5.4 (CH₃), 14.3 (CH₃), 16.1 (CH₂), 18.3 (C), 25.2 (CH), 25.8 (CH₃), 40.3 (C), 59.1 (CH₂), 61.5 (CH₂), 171.0 (C), 200.4 (C); *m/z* (CI) 287 (MH⁺); HRMS (CI) [MH⁺], found: 287.1681. C₁₄H₂₇O₄Si requires 287.1679 (0.2 ppm error).

6.2.3. 2-Benzoyl-1-(*tert*-butyldimethylsilyloxymethyl)-cyclopropanecarboxaldehyde 6f. Using the above procedure for **6b** (for 14 h), the *title compound* **6f** was prepared in 73% yield as an inseparable mixture (*trans/cis* ~2:1) as a colourless oil, *R_f* 0.51 (petrol–EtOAc, 4:1); ν_{max} (film) 2954, 2929, 2857, 1716, 1675, 1451, 1255, 1223, 1090 cm^{-1} ; δ_{H} (400 MHz, CDCl₃) *trans*: –0.29 (3H, s), –0.09 (3H, s), 0.62 (9H, s), 1.49 (1H, dd, *J* 4.1 and 7.9 Hz), 1.91 (1H, dd, *J* 4.1 and 6.7 Hz), 3.35 (1H, dd, *J* 7.9 and 6.7 Hz), 3.58 (1H, d, *J* 11.3 Hz), 4.35 (1H, d, *J* 11.3 Hz), 7.39–7.49 (2H, m), 7.50–7.62 (2H, m), 7.94 (1H,

d, J 7.3 Hz), 9.76 (1H, s); *cis*: 0.11 (3H, s), 0.12 (3H, s), 0.92 (9H, s), 1.68 (1H, dd, J 4.6 and 7.6 Hz), 2.27 (1H, dd, J 4.6 and 6.7 Hz), 3.35 (1H, dd, J 7.6 and 6.7 Hz), 3.79 (1H, d, J 10.8 Hz), 4.30 (1H, d, J 10.8 Hz), 7.39–7.49 (2H, m), 7.50–7.62 (2H, m), 8.03 (1H, d, J 7.6 Hz), 9.12 (1H, s); δ_{C} (100 MHz, CDCl_3) *trans*: –6.0 (CH_3), –5.8 (CH_3), 18.1 (C), 18.6 (CH_2), 25.6 (CH_3), 30.2 (CH), 43.7 (C), 59.2 (CH_2), 128.5 (CH), 128.6 (CH), 133.2 (CH), 137.7 (C), 194.9 (C), 200.7 (C); *cis*: –5.4 (CH_3), –5.3 (CH_3), 16.6 (CH_2), 18.4 (C), 25.9 (CH_3), 30.1 (CH), 42.8 (C), 60.3 (CH_2), 128.6 (CH), 128.8 (CH), 133.6 (CH), 137.3 (C), 195.9 (C), 199.4 (C); m/z (CI) 319 (MH^+); HRMS (CI) [MH^+], found: 319.1730. $\text{C}_{18}\text{H}_{27}\text{O}_3\text{Si}$ requires 319.1729 (0.1 ppm error).

6.2.4. Diethyl 2,2'-carbonyldicyclopropanecarboxylate 6j. Using the above procedure for **6b** (but with sulfurane **5a** and for 4 h), the *title compound 6j* was prepared in 60% yield as a wax: R_f 0.32 (petrol–EtOAc, 4:1); ν_{max} (film) 2983, 1731, 1692, 1369, 1334, 1186 cm^{-1} ; δ_{H} (270 MHz, CDCl_3) 1.26 (6H, t, J 7.0 Hz), 1.40–1.46 (4H, m), 2.16–2.23 (2H, m), 2.58–2.65 (2H, m), 4.14 (4H, q, J 7.0 Hz); δ_{C} (67.5 MHz, CDCl_3) 14.3 (CH_3), 17.8 (CH), 24.9 (CH), 29.9 (CH_2), 61.3 (CH_2), 171.9 (C), 204.7 (C); m/z (CI) 255 (MH^+) 272 (MNH_4^+); HRMS (CI) [MNH_4^+], found: 272.1500. $\text{C}_{13}\text{H}_{22}\text{NO}_5$ requires 272.1498 (0.7 ppm error).

6.2.5. {2-[(2-Benzoylcyclopropyl)carbonyl]cyclopropyl}(phenyl)methan-one 6k. Using the above procedure for **6b** (also for 2 h), the *title compound 6k* was prepared in 69% yield as a white solid, mp 148–150 °C; R_f 0.35 (petrol–EtOAc, 4:1); ν_{max} (film) 1660, 1349, 1225 cm^{-1} ; δ_{H} (400 MHz, CDCl_3) 1.58–1.78 (4H, m), 2.84–2.97 (2H, m), 3.23–3.38 (2H, m), 7.38–7.51 (4H, m), 7.52–7.64 (2H, m), 7.91–8.06 (4H, m); δ_{C} (100 MHz, CDCl_3) 20.2/20.3 (CH_2), 28.4/28.5 (CH), 32.3/32.4 (CH), 128.3/128.4 (CH), 128.7/128.8 (CH), 133.4/133.5 (CH), 136.9 (C), 196.9 (C), 205.8 (C); m/z (CI) 319 (MH^+) 336 (MNH_4^+); HRMS (CI) [MH^+], found: 319.1330. $\text{C}_{21}\text{H}_{19}\text{O}_3$ requires 319.1334 (1.3 ppm error).

6.2.6. (1R,3R,6S,8S)-1-Benzoyl-7,7-dimethyl-6,8-methylene-spiro[2.5]octan-4-one and (1S,3S,6S,8S)-isomer 6l. Using the above procedure for **6b** (but for 16 h), the *title compound 6l* was prepared in 76% yield as an inseparable mixture (*trans/cis* ~5:1) as a colourless oil, R_f 0.54 (petrol–EtOAc, 4:1); ν_{max} (film) 2924, 1703, 1664, 1597, 1449, 1385, 1326, 1289, 1220, 1033 cm^{-1} ; δ_{C} (400 MHz, CDCl_3) *major*: 0.94 (3H, s), 1.01 (1H, d, J 10.7 Hz), 1.28 (3H, s), 1.65 (1H, dd, J 6.4 and 3.4 Hz), 1.72 (1H, dd, J 7.9 and 3.4 Hz), 1.93 (1H, t, J 6.7 Hz), 2.10–2.19 (1H, m), 2.30–2.39 (1H, m), 2.56 (1H, dd, J 19.2 and 2.5 Hz), 2.71 (1H, dt, J 19.2 and 2.5 Hz), 3.27 (1H, t, J 7.3 Hz), 7.39–7.45 (2H, m), 7.49–7.55 (2H, m), 7.91 (1H, d, J 7.6 Hz); *minor*: δ_{H} 0.56 (3H, s), 1.13 (3H, s), 1.37 (1H, d, J 10.5 Hz), 1.52–1.59 (2H, m), 1.93 (1H, obscured), 2.10–2.19 (2H, m), 2.54 (1H, dd, J 19.3 and 2.8 Hz), 2.65 (1H, dt, J 19.3 and 2.8 Hz), 3.56 (1H, t, J 7.3 Hz), 7.39–7.45 (2H, m), 7.49–7.55 (2H, m), 7.93 (1H, d, J 7.3 Hz); δ_{C} (100 MHz, CDCl_3) *major*: 21.1 (CH_3), 22.5 (CH_2), 26.2 (CH_3), 32.2 (CH), 32.6 (CH_2), 38.6 (CH), 40.3 (CH), 40.4 (C), 43.5 (CH_2), 45.3 (CH), 128.2 (CH), 128.6 (CH), 133.2 (CH), 137.9 (C), 195.8 (C),

210.5 (C); *minor*: 21.4 (CH_3), 22.1 (CH_2), 25.9 (CH_3), 32.6 (CH_2), 33.4 (CH), 38.7 (CH), 39.5 (C), 40.0 (CH), 43.4 (CH_2), 45.6 (C), 128.4 (CH), 128.6 (CH), 133.1 (CH), 137.8 (C), 195.8 (C), 210.4 (C); m/z (CI) 269 (MH^+); HRMS (CI) [MH^+], found: 269.1537. $\text{C}_{18}\text{H}_{21}\text{O}_2$ requires 269.1542 (1.7 ppm error).

6.2.7. Ethyl 2-benzoyl-3-(4-chlorophenyl)cyclopropanecarboxylate 7c. Using the above procedure for **6b** (but with sulfurane **5a** and for 10 h), the *title compound 7c* was prepared in 80% yield as a mixture of isomers, partially separable by chromatography (petrol–EtOAc, 10:1). The first eluting and major product **7c** was obtained as a colourless oil, R_f 0.52 (petrol–EtOAc, 10:1); ν_{max} (film) 2980, 1730, 1680, 1494, 1450, 1372, 1191, 1014 cm^{-1} ; δ_{H} (270 MHz, CDCl_3) 1.11 (3H, t, J 7.2 Hz), 2.82 (1H, dd, J 4.8 and 10.0 Hz), 3.21 (1H, dd, J 6.3 and 10.0 Hz), 3.80 (1H, dd, J 4.8 and 6.3 Hz), 4.01 (2H, q, J 7.2 Hz), 7.27 (4H, br s), 7.48–7.56 (2H, m), 7.61–7.67 (1H, m), 8.10 (2H, d, J 7.2 Hz); δ_{C} (67.5 MHz, CDCl_3) 14.3 (CH_3), 29.8 (CH), 32.3 (CH), 34.3 (CH), 61.3 (CH_2), 128.6 (CH), 128.7 (CH), 130.4 (CH), 132.2 (CH), 133.3 (CH), 133.4 (C), 133.8 (C), 137.0 (C), 168.8 (C), 196.5 (C); m/z (CI) 328 (MH^+); HRMS (CI) [MH^+], found 329.0947. $\text{C}_{19}\text{H}_{18}\text{O}_3^{35}\text{Cl}$ requires 329.0944 (0.8 ppm error).

6.2.8. Ethyl 2-benzoyl-3-(4-nitrophenyl)cyclopropanecarboxylate 7e. Using the above procedure for **6b** (but for 17 h), the *title compound 7e* was prepared in 90% yield as a mixture of isomers, partially separable by chromatography (petrol–EtOAc, 5:1). The first eluting and major product **7e** was obtained as a pale yellow oil, R_f 0.54 (petrol–EtOAc, 5:1); ν_{max} (film) 3390, 2923, 2852, 1597, 1515, 1344, 1010 cm^{-1} ; δ_{H} (270 MHz, CDCl_3) 1.12 (3H, t, J 7.1 Hz), 2.88 (1H, dd, J 4.8 and 10.0 Hz), 3.32 (1H, dd, J 6.3 and 9.7 Hz), 3.88 (1H, dd, J 4.8 and 6.3 Hz), 4.02 (2H, q, J 7.1 Hz), 7.45–7.58 (4H, m), 7.60–7.69 (1H, m), 8.07–8.12 (2H, m), 8.13–8.20 (2H, m); δ_{C} (67.5 MHz, CDCl_3) 14.2 (CH_3), 29.9 (CH), 32.4 (CH), 33.9 (CH), 61.5 (CH_2), 123.5 (CH), 128.5 (CH), 129.0 (CH), 130.0 (CH), 134.0 (CH), 136.7 (C), 142.5 (C), 147.3 (C), 168.5 (C), 195.9 (C); m/z (CI) 240 (MH^+) 257 (MNH_4^+); HRMS (CI) [MNH_4^+], found: 357.1448. $\text{C}_{19}\text{H}_{21}\text{N}_2\text{O}_5$ requires 357.1450 (0.2 ppm error).

6.3. Tandem oxidation–cyclopropanation–Wittig reactions

6.3.1. Ethyl 2-(2-cyanoethenyl)-2-methyl-cyclopropanecarboxylate 10c: representative procedure. To a solution of 2-methyl-2-propen-1-ol **1a** (36 μL , 0.50 mmol) in CH_2Cl_2 (5.0 mL) was added powdered 4 Å molecular sieves (0.50 g), (carboethoxymethylene)dimethylsulfurane **5a** (0.148 g, 1.00 mmol), (cyanomethylene)triphenylphosphorane **3b** (0.181 g, 0.60 mmol) and manganese dioxide (0.435 g, 5.0 mmol). The mixture was heated at reflux for 23 h, and then cooled to rt. The crude mixture was filtered through Celite® and the residue washed with CH_2Cl_2 . After removal of the solvent, the resulting yellow oil was purified by flash column chromatography (petrol–EtOAc, 19:1 to 4:1) to give the *title compound 10c* (0.079 g, 88%) as an inseparable mixture of *cis/trans* cyclopropane isomers and *E/Z* alkene isomers (*trans/E:cis/E:trans/Z:cis/Z* ~8.5:4.4:3.6:1) as a colourless oil, R_f 0.35 (petrol–EtOAc, 4:1); ν_{max} (film) 2983,

2222, 1726, 1626, 1448, 1406, 1383, 1223, 1184, 1097, 1073, 1024, 980 cm^{-1} ; δ_{H} (400 MHz, CDCl_3) 1.20–1.28 (m, $\text{CO}_2\text{CH}_2\text{CH}_3$, all isomers), 1.30 (s, Me, *trans*-cyclopropanes), 1.33–1.39 (m), 1.42–1.50 (m), 1.51 (s, Me, *cis*-cyclopropanes), 1.56 (dd (app t), J 5.5 Hz, *trans/E*), 1.66–1.76 (m), 1.86–1.98 (m), 4.04–4.22 (m, $\text{CO}_2\text{CH}_2\text{CH}_3$, all isomers), 5.27 (d, J 11.9 Hz, *trans/Z*), 5.31 (d, J 16.2 Hz, *trans/E*), 5.33 (d, J 16.5 Hz, *cis/E*), 5.35 (d, J 11.6 Hz, *cis/Z*), 5.98 (d, J 11.9 Hz, *trans/Z*), 6.14 (d, J 16.2 Hz, *trans/E*) 6.44 (d, J 11.6 Hz, *cis/Z*), 6.85 (d, J 16.5 Hz, *cis/E*); δ_{C} (100 MHz, CDCl_3) [though it was not possible to assign signals to a given isomer, all are cited] 13.3 (CH_3), 14.1 (CH_3), 14.2 (CH_3), 14.2 (CH_3), 14.3 (CH_3), 14.3 (CH_3), 14.3 (CH_3), 15.4 (CH_3), 21.6 (CH_2), 21.9 (CH_2), 23.6 (CH_2), 23.8 (CH_2), 27.8 (C), 27.9 (C), 28.1 (CH), 28.4 (CH), 28.6 (CH), 30.0 (C), 30.5 (CH), 31.7 (C), 61.0 (CH_2), 61.1 (CH_2), 61.4 (CH_2), 61.5 (CH_2), 97.3 (CH), 97.4 (CH), 98.1 (CH), 99.2 (CH), 116.1 (C), 117.5 (C), 117.5 (C), 117.8 (C), 153.9 (CH), 156.3 (CH), 157.3 (CH), 160.4 (CH), 170.1 (C), 170.4 (C), 170.7 (C), 170.8 (C); m/z (CI) 197 (MNH_4^+); HRMS (CI) [MNH_4^+], found: 197.1291. $\text{C}_{10}\text{H}_{17}\text{N}_2\text{O}_2$ requires 197.1290 (0.6 ppm error).

6.3.2. 2-((*E*)-2-Methoxycarbonyl-vinyl)-2-methyl-cyclopropanecarboxylic acid ethyl ester 10a. Using the above procedure for **10c** (but with phosphorane **3a** for 18 h), the *title compound 10a* was prepared in 81% yield as a colourless oil as a mixture (*trans/cis* \sim 3.5:1), which was separated by column chromatography (petrol–EtOAc, 19:1 to 4:1): *major isomer*: R_f 0.41 (petrol–EtOAc, 4:1); ν_{max} (film) 2934, 1723, 1646, 1437, 1405, 1384, 1317, 1272, 1228, 1172, 1019 cm^{-1} ; δ_{H} (400 MHz, CDCl_3) 1.22–1.26 (4H, m), 1.33 (3H, s), 1.46 (1H, dd, J 5.2 and 6.4 Hz), 1.90 (1H, dd, J 6.4 and 8.5 Hz), 3.70 (3H, s), 4.12 (2H, q, J 7.0 Hz), 5.83 (1H, d, J 15.6 Hz), 6.43 (1H, d, J 15.6 Hz); δ_{C} (100 MHz, CDCl_3) 14.1 (CH_3), 14.4 (CH_3), 21.8 (CH_2), 27.2 (C), 28.7 (CH), 51.6 (CH_3), 60.9 (CH_2), 118.4 (CH), 154.7 (CH), 167.1 (C), 170.7 (C); m/z (CI) 213 (MH^+) 230 (MNH_4^+); HRMS (CI) [MH^+], found: 213.1125. $\text{C}_{11}\text{H}_{17}\text{O}_4$ requires 213.1127 (0.9 ppm error). *Minor isomer*: R_f 0.35 (petrol–EtOAc, 3:1); ν_{max} (film) 2951, 1727, 1644, 1437, 1407, 1382, 1304, 1273, 1228, 1170, 1019 cm^{-1} ; δ_{H} (400 MHz, CDCl_3) 1.23–1.26 (4H, m), 1.30 (3H, s), 1.60 (1H, dd, J 4.9 and 76.59 Hz), 1.92 (1H, dd, J 6.5 and 7.9 Hz), 3.71 (3H, s), 4.12 (2H, m), 5.88 (1H, d, J 15.9 Hz), 7.08 (1H, d, J 15.9 Hz); δ_{C} (100 MHz, CDCl_3) 14.3 (CH_3), 21.8 (CH_3), 23.5 (CH_2), 27.6 (C), 30.5 (CH), 51.6 (CH_3), 61.0 (CH_2), 120.0 (CH), 150.3 (CH), 167.0 (C), 171.0 (C); m/z (CI) 213 (MH^+) 230 (MNH_4^+); HRMS (CI) [MH^+], found: 213.1125. $\text{C}_{11}\text{H}_{17}\text{O}_4$ requires 213.1127 (0.9 ppm error).

6.3.3. (*E*)-3-(2-Benzoyl-1-methyl-cyclopropyl)-acrylic acid methyl ester 10b. Using the above procedure for **10c** (but with sulfurane **5b** and phosphorane **3a** for 14 h), the *title compound 10b* was prepared in 66% yield as a pale yellow oil as a mixture (*trans/cis* \sim 3:1), which was separated by column chromatography (petrol–EtOAc, 19:1 to 9:1): *major isomer*: R_f 0.34 (petrol–EtOAc, 9:1); ν_{max} (film) 2950, 1721, 1673, 1643, 1450, 1386, 1317, 1273, 1225, 1173, 987 cm^{-1} ; δ_{H} (400 MHz, CDCl_3) 1.18 (3H, s), 1.33 (1H, dd, J 4.8 and 8.0 Hz), 1.87 (1H, dd, J 4.8 and 6.5 Hz), 2.85 (1H, dd, J 6.5 and 8.0 Hz), 3.75 (3H, s), 5.92 (1H, d, J 15.6 Hz), 6.68 (1H, d, J 15.6 Hz), 7.41–7.57 (3H, m), 7.85–7.88 (2H, m);

δ_{C} (100 MHz, CDCl_3) 13.6 (CH_3), 21.3 (CH_2), 30.1 (CH), 33.5 (CH), 51.6 (CH_3), 118.6 (CH), 128.0 (CH), 128.6 (CH), 133.0 (CH), 138.1 (C), 154.6 (CH), 167.0 (C), 195.9 (C); m/z (CI) 245 (MH^+) 262 (MNH_4^+); HRMS (CI) [MH^+], found: 245.1178. $\text{C}_{15}\text{H}_{17}\text{O}_3$ requires 245.1174 (1.4 ppm error). *Minor isomer*: R_f 0.22 (petrol–EtOAc, 9:1); ν_{max} (film) 2950, 1721, 1669, 1643, 1449, 1395, 1326, 1273, 1222, 1172, 992 cm^{-1} ; δ_{H} (400 MHz, CDCl_3) 1.25 (3H, s), 1.38 (1H, dd, J 4.5 and 7.4 Hz), 2.02 (1H, dd, J 4.5 and 6.3 Hz), 2.92 (1H, dd, J 6.3 and 7.4 Hz), 3.66 (3H, s), 5.86 (1H, d, J 15.6 Hz), 6.85 (1H, d, J 15.6 Hz), 7.92–8.12 (3H, m), 8.13–8.15 (2H, m); δ_{C} (125 MHz, CDCl_3) 21.9 (CH_3), 23.3 (CH_2), 30.7 (C), 35.4 (CH), 51.4 (CH_3), 120.0 (CH), 128.1 (CH), 128.5 (CH), 132.9 (CH), 138.0 (C), 149.1 (CH), 166.6 (C), 196.0 (C); m/z (CI) 245 (MH^+), 262 (MNH_4^+); HRMS (CI) [MH^+], found: 245.1178. $\text{C}_{15}\text{H}_{17}\text{O}_3$ requires 245.1174 (1.4 ppm error).

6.3.4. 2-((*E*)-2-Methoxycarbonyl-vinyl)-cyclopropanecarboxylic acid ethyl ester 10d. Using the above procedure for **10c** (but with phosphorane **3a** for 5 h), the *title compound 10d* was prepared in 61% yield as a colourless oil as a mixture (*trans/cis* \sim 6.5:1), which was not separated: ν_{max} (film) 2978, 2950, 1721, 1655, 1438, 1410, 1261, 1197, 1180, 1148, 1032 cm^{-1} ; *major isomer*: R_f 0.36 (petrol–EtOAc, 3:1); δ_{H} (400 MHz, CDCl_3) 1.11 (1H, ddd, J 4.3, 5.8 and 10.4 Hz), 1.24 (3H, t, J 7.0 Hz), 1.51 (1H, app td, J 5.5 and 10.4 Hz), 1.82 (1H, ddd, J 4.3, 5.5 and 8.9 Hz), 2.12 (1H, m), 3.69 (3H, s), 4.12 (2H, q, J 7.0 Hz), 5.94 (1H, d, J 15.6 Hz), 6.39 (1H, dd, J 10.1 and 15.6 Hz); δ_{C} (100 MHz, CDCl_3) 14.3 (CH_3), 16.5 (CH_2), 23.0 (CH), 24.4 (CH), 51.6 (CH_3), 61.0 (CH_2), 120.7 (CH), 149.0 (CH), 166.7 (C), 172.5 (C). *Minor isomer*: R_f 0.33 (petrol–EtOAc, 3:1); δ_{H} (400 MHz, CDCl_3) 1.31–1.44 (1H, m), 1.95–2.06 (1H, m), 3.68 (3H, s), 5.98 (1H, d, J 15.0 Hz), 6.91 (1H, dd, J 9.8 and 15.0 Hz) (*the remaining signals were obscured by the major isomer*); δ_{C} (100 MHz, CDCl_3) 14.3 (CH_3), 15.4 (CH_2), 22.3 (CH), 23.4 (CH), 51.5 (CH_3), 61.0 (CH_2), 120.0 (CH), 146.6 (CH), 166.5 (C), 171.2 (C); m/z (CI) 199 (MH^+), 216 (MNH_4^+); HRMS (CI) [MNH_4^+], found: 216.1236. $\text{C}_{10}\text{H}_{18}\text{NO}_4$ requires 216.1235 (0.2 ppm error).

6.3.5. (*E*)-3-(2-Benzoyl-cyclopropyl)-acrylic acid methyl ester 10e. Using the above procedure for **10c** (but with sulfurane **5a** and phosphorane **3a** for 14 h), the *title compound 10e* was prepared in 74% yield as an off-white solid as a mixture (*trans/cis* \sim 3.5:1), which was separated by column chromatography (petrol–EtOAc, 19:1 to 9:1): *major isomer*: mp 85–87 °C; R_f 0.15 (petrol–EtOAc, 9:1); ν_{max} (film) 2960, 1710, 1661, 1580, 1450, 1434, 1399, 1261, 1211, 1152, 1023, 919 cm^{-1} ; δ_{H} (400 MHz, CDCl_3) 1.31 (1H, ddd, J 4.3, 5.8 and 10.0 Hz), 1.82 (1H, ddd, J 4.3, 6.0 and 9.0 Hz), 2.30 (1H, ddd, J 3.7, 6.0 and 10.0 Hz), 2.88 (1H, ddd, J 3.7, 5.8 and 9.0 Hz), 3.71 (3H, s), 5.98 (1H, d, J 15.6 Hz), 6.56 (1H, dd, J 10.0 and 15.6 Hz), 7.43–7.59 (3H, m), 7.95–7.97 (2H, m); δ_{C} (100 MHz, CDCl_3) 18.7 (CH_2), 26.9 (CH), 27.6 (CH), 51.5 (CH_3), 120.5 (CH), 128.0 (CH), 128.6 (CH), 133.1 (CH), 137.2 (CH), 149.2 (CH), 166.6 (C), 197.4 (C); m/z (CI) 231 (MH^+) 248 (MNH_4^+); HRMS (CI) [MH^+], found: 231.1018. $\text{C}_{14}\text{H}_{15}\text{O}_3$ requires 231.1021 (1.2 ppm error). *Minor isomer*: mp 86–87 °C; R_f 0.10 (petrol–EtOAc, 9:1); ν_{max} (film) 2955, 1708, 1661, 1646, 1450, 1432, 1258, 1195, 1150, 1016, 985 cm^{-1} ; δ_{H} (400 MHz,

CDCl₃) 1.49 (1H, app dt, *J* 4.5 and 8.2 Hz), 1.83 (1H, app dt, *J* 4.5 and 7.0 Hz), 2.30 (1H, dddd, *J* 7.0, 8.2, 10.4 and 11.0 Hz), 3.13 (1H, ddd, *J* 4.5, 7.0 and 11.0 Hz), 3.66 (3H, s), 5.98 (1H, d, *J* 15.6 Hz), 6.79 (1H, dd, *J* 10.4 and 15.6 Hz), 7.42–7.59 (3H, m), 7.95–7.99 (2H, m); δ_{C} (100 MHz, CDCl₃) 15.6 (CH₂), 26.5 (CH), 26.6 (CH), 51.4 (CH₃), 121.9 (CH), 128.1 (CH), 128.6 (CH), 133.0 (CH), 138.0 (CH), 146.0 (CH), 166.1 (C), 196.0 (C); *m/z* (CI) 231 (MH⁺) 248 (MNH₄⁺); HRMS (CI) [MH⁺], found: 231.1016. C₁₄H₁₅O₃ requires 231.1021 (1.6 ppm error).

6.3.6. 2-((E)-2-Methoxycarbonyl-propenyl)-cyclopropane-carboxylic acid ethyl 10f. Using the above procedure for **10c** (but with phosphorane **3c** for 18 h), the *title compound* **10f** was prepared in 56% yield as a colourless oil as an inseparable mixture (trans/cis ~7:1), *R_f* 0.34 (petrol–Et₂O, 3:1); ν_{max} (film) 2950, 1719, 1710, 1648, 1437, 1412, 1349, 1311, 1263, 1252, 1200, 1180, 1104, 1037 cm⁻¹; δ_{H} (400 MHz, CDCl₃) 1.05 (1H, ddd, *J* 4.3, 5.8 and 9.0 Hz), 1.22 (3H, d, *J* 7.0 Hz), 1.49 (1H, ddd, *J* 4.3, 5.5 and 9.4 Hz), 1.77 (1H, ddd, *J* 3.7, 5.5 and 9.0 Hz), 1.90 (3H, d, *J* 1.5 Hz), 2.15 (1H, dddd, *J* 3.7, 5.8, 9.4 and 11.0 Hz), 3.67 (3H, s), 4.10 (2H, *J* 7.0 Hz), 6.06 (1H, dd, *J* 1.5 and 11.0 Hz); δ_{C} (100 MHz, CDCl₃) 12.6 (CH₃), 14.1 (CH₃), 16.3 (CH₂), 21.9 (CH), 22.6 (CH), 51.6 (CH₃), 60.8 (CH₂), 127.8 (C), 142.0 (CH), 168.0 (C), 172.7 (C); *m/z* (CI) 213 (MH⁺) 230 (MNH₄⁺); HRMS (CI) [MH⁺], found: 230.1392. C₁₁H₂₀NO₄ requires 230.1391 (0.2 ppm error).

6.3.7. Ethyl 2-(tert-butylidimethylsilyloxymethyl)-2-(2-methoxycarbonylethenyl)-cyclopropanecarboxylate 10g. Using the above procedure for **10c** (but with phosphorane **3a** for 18 h), the *title compound* **10g** was prepared in 64% yield as a colourless oil as an inseparable mixture of cis/trans cyclopropane isomers (trans/*E*:cis/*E* ~1.8:1), *R_f* 0.40 (petrol–EtOAc, 4:1); ν_{max} (film) 2954, 2931, 2858, 1727, 1650, 1259, 1213, 1178, 1094, 838, 778 cm⁻¹; δ_{H} (400 MHz, CDCl₃) *trans*: 0.00 (3H, s, SiMe), 0.04 (3H, s, SiMe), 0.83 (9H, s, SiCMe₃), 1.21–1.26 (3H, m, CO₂CH₂CH₃), 1.26–1.30 (1H, m), 1.48–1.53 (1H, m), 1.94 (1H, dd, *J* 8.0 and 6.4 Hz), 3.71 (3H, s, OMe), 3.75 (1H, d, *J* 11.0 Hz), 4.02 (1H, d, *J* 11.0 Hz), 4.04–4.20 (2H, m, CO₂CH₂CH₃), 5.97 (1H, d, *J* 15.6 Hz), 6.63 (1H, d, *J* 15.6 Hz); *cis*: 0.04 (3H, s, SiMe), 0.05 (3H, s, SiMe), 0.85 (9H, s, SiCMe₃), 1.26–1.30 (3H, m, CO₂CH₂CH₃), 1.42 (1H, dd, *J* 4.0 and 8.2 Hz), 1.41–1.50 (1H, m), 2.14 (1H, dd, *J* 8.2 and 5.2 Hz), 3.70 (3H, s, OMe), 3.72 (1H, d, *J* 10.4 Hz), 3.82 (1H, d, *J* 10.4 Hz), 4.04–4.20 (2H, m, CO₂CH₂CH₃), 5.89 (1H, d, *J* 16.5 Hz), 6.63 (1H, d, *J* 16.5 Hz); δ_{C} (100 MHz, CDCl₃) *trans*: -5.4 (CH₃), 14.3 (CH₃), 18.2 (C), 18.3 (CH), 25.9 (CH₃), 26.0 (CH), 33.6 (C), 51.6 (CH₃), 61.0 (CH₂), 61.6 (CH₂), 119.3 (CH), 151.2 (CH), 167.2 (C), 170.6 (C); *cis*: -5.4 (CH₃), -5.3 (CH₃), 14.3 (CH₃), 18.3 (C), 19.9 (CH₂), 25.8 (CH), 25.9 (CH₃), 32.3 (C), 51.6 (CH₃), 61.0 (CH₂), 63.4 (CH₂), 120.5 (CH), 147.2 (CH), 166.9 (C), 171.2 (C); *m/z* (CI) 343 (MH⁺); HRMS (CI) [MH⁺], found: 343.1940. C₁₇H₃₁O₅Si requires 343.1941 (0.1 ppm error).

6.3.8. 3-Benzoyl-cyclopropane-1,2-dicarboxylic acid 1-ethyl ester 2-methyl ester 15a. Using the above procedure for **10c** (but with phosphorane **3a** for 4 h), the *title compound* **15a** was prepared in 83% yield as a colourless oil as an

inseparable mixture of cyclopropane isomers (3.2:1), *R_f* 0.21 (petrol–EtOAc, 6:1); ν_{max} (film) 2980, 2954, 1735, 1679, 1597, 1449, 1372, 1353, 1302, 1211, 1175, 1059, 1020 cm⁻¹; *major isomer*: δ_{H} (400 MHz, CDCl₃) 1.28 (3H, t, *J* 7.3 Hz), 1.30–1.32 (1H, m), 2.72 (1H, d, *J* 5.8 Hz), 3.75 (3H, s), 3.77–3.78 (1H, m), 4.19–4.24 (2H, m), 7.48–7.53 (3H, m), 8.09–8.12 (2H, m); *minor isomer*: δ_{H} (400 MHz, CDCl₃) 2.78 (1H, dd, *J* 5.2 and 9.8 Hz), 3.00 (1H, app t, *J* 5.5 Hz), 3.28 (1H, dd, *J* 5.5 and 9.8 Hz), 3.58 (3H, s), 7.51–7.60 (3H, m), 7.92–7.97 (2H, m) (*the remaining signals were obscured by the major isomer*); δ_{C} (100 MHz, CDCl₃) 14.1 (CH₃), 29.1 (CH), 29.9 (CH), 30.0 (CH), 52.5 (CH₃), 61.6 (CH₂), 128.4 (CH), 128.7 (CH), 133.8 (CH), 136.3 (C), 168.0 (C), 168.4 (C), 194.9 (C); *m/z* (CI) 277 (MH⁺); HRMS (CI) [MH⁺], found: 277.1077. C₁₅H₁₇O₅ requires 277.1076 (-0.5 ppm error).

6.3.9. 2-Benzoyl-3-cyano-cyclopropanecarboxylic acid ethyl ester 15b. Using the above procedure for **10c** (but for 3 h), the *title compound* **15b** was prepared in 80% yield as a yellow oil as a mixture of cyclopropane isomers (3.8:1), *m/z* (CI) 261 (MNH₄⁺); HRMS (CI) [MH⁺], found: 261.1240. C₁₄H₁₇N₂O₃ requires 261.1239 (-0.1 ppm error). These isomers could be partially separated by chromatography (petrol–EtOAc, 4:1) giving *major isomer*: *R_f* 0.21 (petrol–EtOAc, 4:1); ν_{max} (film) 3062, 2984, 2247, 1734, 1678, 1597, 1450, 1372, 1346, 1295, 1201, 1186, 1014 cm⁻¹; δ_{H} (400 MHz, CDCl₃) 1.33 (3H, t, *J* 7.0 Hz), 2.56 (1H, dd, *J* 5.5 and 8.9 Hz), 2.66 (1H, dd, *J* 5.5 and 8.9 Hz), 3.74 (1H, app t, *J* 5.5 Hz), 4.30 (2H, q, *J* 7.0 Hz), 7.51–7.55 (2H, m), 7.65–7.68 (1H, m), 8.01–8.03 (2H, m); δ_{C} (100 MHz, CDCl₃) 14.1 (CH₃), 28.4 (CH), 28.5 (CH), 29.3 (CH), 62.4 (CH₂), 115.8 (C), 128.6 (CH), 129.0 (CH), 134.5 (CH), 135.5 (C), 167.0 (C), 192.6 (C); *minor isomer*: *R_f* 0.18 (petrol–EtOAc, 4:1); ν_{max} (film) 3050, 2983, 2246, 1729, 1672, 1596, 1449, 1368, 1350, 1296, 1199, 1180, 1011 cm⁻¹; δ_{H} (400 MHz, CDCl₃) 1.32 (3H, t, *J* 7.3 Hz), 2.55 (1H, dd, *J* 5.5 and 8.8 Hz), 3.03 (1H, app t, *J* 5.5 Hz), 3.52 (1H, dd, *J* 5.5 and 8.8 Hz), 4.22–4.29 (2H, m), 7.52–7.66 (3H, m), 8.04–8.05 (2H, m); δ_{C} (100 MHz, CDCl₃) 14.0 (CH₃), 27.4 (CH), 29.2 (CH), 29.3 (CH), 62.4 (CH₂), 115.3 (C), 128.6 (CH), 129.1 (CH), 134.3 (CH), 135.9 (C), 168.7 (C), 190.9 (C).

6.3.10. 2-Benzoyl-3-(methoxy-methyl-carbamoyl)-cyclopropanecarboxylic acid ethyl ester 15c. Using the above procedure for **10c** (but with phosphorane **3d** for 4 h), the *title compound* **15c** was prepared in 50% yield as a yellow oil as an inseparable mixture of cyclopropane isomers (2.2:1), *R_f* 0.26 (petrol–EtOAc, 3:2); ν_{max} (film) 2980, 2940, 1732, 1686, 1655, 1597, 1449, 1411, 1381, 1335, 1277, 1220, 1183, 1010 cm⁻¹; δ_{H} (400 MHz, CDCl₃) *major isomer*: 1.07 (3H, t, *J* 7.0 Hz), 2.79 (1H, dd, *J* 5.5 and 10.0 Hz), 3.03 (1H, app t, *J* 5.5 Hz), 3.25 (3H, s), 3.29 (1H, dd, *J* 5.5 and 10.0 Hz), 3.83 (3H, s), 4.02 (2H, q, *J* 7.0 Hz), 7.45–7.50 (3H, m), 7.95–8.00 (2H, m); *minor isomer*: 1.30 (3H, t, *J* 7.0 Hz), 3.21 (3H, s), 3.71 (3H, s), 4.22 (2H, q, *J* 7.0 Hz), 7.56–7.58 (3H, m), 8.06–8.11 (2H, m) (*the remaining signals were obscured by the major isomer*); δ_{C} (100 MHz, CDCl₃) *major isomer* 13.9 (CH₃), 23.2 (CH), 29.9 (CH), 32.6 (CH), 32.7 (CH₃), 61.2 (CH₂), 62.1 (CH₃), 128.4 (CH), 128.7 (CH), 133.5 (CH), 136.4 (C), 168.2 (C), 169.7 (C), 192.8 (C); *minor isomer* 14.1 (CH₃), 25.4 (CH),

30.3 (CH), 30.4 (CH), 32.6 (CH₃), 61.5 (CH₂), 62.1 (CH₃), 128.4 (CH), 128.7 (CH), 133.3 (CH), 136.6 (C), 170.4 (C), 171.4 (C), 192.6 (C); *m/z* (CI) 306 (MH⁺); HRMS (CI) [MH⁺], found: 306.1342. C₁₆H₂₀NO₅ requires 306.1341 (−0.1 ppm error).

6.3.11. Ethyl 2,3-dibenzoylcyclopropanecarboxylate 15d.

Using the above procedure for **10c** (but with sulfurane **5b** and phosphorane **3e** for 1.5 h), the *title compound 15d* was prepared in 81% yield as a colourless oil as a mixture of cyclopropane isomers (1.2:1), which were not separated, *R_f* 0.30/0.25 (petrol–EtOAc, 4:1); *ν_{max}* (film) 3062, 2984, 1731, 1673, 1449, 1326, 1216, 1020, 738 cm^{−1}; *δ_H* *major* (2,3-*trans*): 1.07 (3H, t, *J* 7.3 Hz), 2.98 (1H, dd, *J* 9.8 and 5.2 Hz), 3.43 (1H, dd, *J* 9.8 and 5.8 Hz), 3.98–4.15 (3H, m), 7.35–7.60 (6H, m), 8.04 (2H, d, *J* 7.3 Hz), 8.12 (2H, d, *J* 7.3 Hz); *minor* (2,3-*cis*): 1.30 (3H, t, *J* 7.0 Hz), 3.22 (1H, t, *J* 5.5 Hz), 3.56 (1H, d, *J* 5.5 Hz), 4.23 (2H, q, *J* 7.0 Hz), 7.35–7.60 (6H, m), 8.04 (4H, d, *J* 7.3 Hz); *δ_C* (100 MHz, CDCl₃) *major* (2,3-*trans*): 13.9 (CH₃), 29.1 (CH), 31.6 (CH), 34.8 (CH), 61.4 (CH₂), 128.5 (CH), 128.6 (CH), 128.7 (CH), 128.8 (CH), 133.7 (CH), 133.8 (CH), 136.3 (C), 136.5 (C), 168.0 (C), 192.5 (C), 195.4 (C); *minor* (2,3-*cis*): 14.2 (CH₃), 26.6 (CH), 34.6 (CH), 61.7 (CH₂), 128.4 (CH), 128.6 (CH), 133.5 (CH), 136.5 (C), 171.1 (C), 192.4 (C); (no *all-syn-isomer* was detected); *m/z* (CI) 323 (MH⁺); HRMS (CI) [MH⁺], found: 323.1280. C₂₀H₁₉O₄ requires 323.1283 (1.2 ppm error).

6.3.12. 2-Benzoyl-3-(furan-2-carbonyl)-cyclopropanecarboxylic acid ethyl ester 15e.

Using the above procedure for **10c** (but with sulfurane **5b** and phosphorane **3a** for 15 h), the *title compound 15e* was prepared in 70% yield as an orange oil as an inseparable mixture of cyclopropane isomers (1.2:1), *R_f* 0.14 (petrol–EtOAc, 3:1); *ν_{max}* (film) 2950, 1735, 1667, 1468, 1323, 1207, 1015, 731 cm^{−1}; *major isomer*: *δ_H* (400 MHz, CDCl₃) 2.92 (1H, dd, *J* 5.5 and 9.5 Hz), 3.44 (1H, dd, *J* 5.8 and 9.5 Hz), 3.69 (3H, s), 3.98 (1H, dd, *J* 5.5 and 5.8 Hz), 6.56–6.57 (1H, m), 7.30 (1H, d, *J* 3.6 Hz), 7.45–7.52 (3H, m), 7.63 (1H, br s), 8.10 (2H, d, *J* 8.0 Hz); *minor isomer*: *δ_H* (400 MHz, CDCl₃) 2.96 (1H, dd, *J* 5.5 and 9.5 Hz), 3.46 (1H, dd, *J* 5.5 and 9.5 Hz), 3.61 (3H, s), 3.86 (1H, t, *J* 5.5 Hz), 6.60–6.61 (1H, m), 7.43 (1H, d, *J* 3.4 Hz), 7.57–7.61 (3H, m), 7.69 (1H, br s), 8.02 (2H, d, *J* 7.9 Hz); *δ_C* (100 MHz, CDCl₃) (there was difficulty in assigning signals to a given isomer, but the following were observed) 28.5 (CH), 28.7 (CH), 30.6 (CH), 31.1 (CH), 32.8 (CH), 33.5 (CH), 51.9 (CH₃), 52.0 (CH₃), 112.3 (CH), 112.5 (CH), 128.3 (CH), 128.5 (CH), 128.6 (CH), 128.7 (CH), 133.6 (CH), 133.8 (CH), 136.1 (C), 136.2 (C), 147.2 (CH), 147.2 (CH), 147.7 (CH), 147.7 (CH), 152.1 (C), 152.3 (C), 168.2 (C), 168.4 (C), 181.6 (C), 183.7 (C), 192.6 (C), 195.5 (C); *m/z* (CI) 299 (MH⁺); HRMS (CI) [MH⁺], found: 299.0917. C₁₇H₁₅O₅ requires 299.0919 (0.7 ppm error).

6.3.13. 2-Acetyl-3-benzoyl-cyclopropanecarboxylic acid ethyl ester 15f. Using the above procedure for **10c** (but with sulfurane **5b** and phosphorane **3e** for 2.5 h), the *title compound 15f* was prepared in 60% yield as an orange oil as a mixture of cyclopropane isomers (2.7:1), *ν_{max}* (film) 2955, 1735, 1709, 1685, 1597, 1450, 1372, 1359, 1301, 1191, 1003 cm^{−1}; *m/z* (CI) 261 (MH⁺); HRMS (CI)

[MH⁺], found: 261.1127. C₁₅H₁₇O₄ requires 261.1125 (0.7 ppm error). This mixture could be partially separated by chromatography (petrol–EtOAc, 4:1) giving *major isomer*: *R_f* 0.16 (petrol–EtOAc, 4:1); *δ_H* (400 MHz, CDCl₃) 1.03 (3H, t, *J* 7.0 Hz), 1.22–1.29 (1H, m), 2.40 (3H, s), 2.72–2.76 (1H, m), 3.21–3.28 (1H, m), 3.97 (2H, q, *J* 7.0 Hz), 7.39–7.55 (3H, m), 7.89–7.96 (2H, m); *δ_C* (100 MHz, CDCl₃) 13.8 (CH₃), 31.2 (CH₃), 31.6 (CH), 31.9 (CH), 34.5 (CH), 61.2 (CH₂), 128.3 (CH), 128.6 (CH), 133.5 (CH), 136.0 (C), 167.7 (C), 192.0 (C), 204.1 (C); *minor isomer*: *R_f* 0.11 (petrol–EtOAc, 4:1); *δ_H* (400 MHz, CDCl₃) 2.31 (3H, s), 2.93–2.98 (1H, m), 3.33 (1H, d, *J* 5.5 and 10.0 Hz), 3.78 (1H, dd, *J* 4.3 and 5.5 Hz), 4.13–4.21 (2H, m), 7.97–8.03 (2H, m) (*the remaining signals were obscured by the major isomer*); *δ_C* (100 MHz, CDCl₃) 14.1 (CH₃), 29.3 (CH₃), 30.6 (CH), 34.2 (CH), 36.9 (CH), 61.5 (CH₂), 128.6 (CH), 128.7 (CH), 136.2 (CH), 136.3 (C), 1707.7 (C), 195.1 (C), 201.2 (C).

6.3.14. Cyclopropane-3-(cyclohexanecarbonyl)-1,2-dicarboxylic acid 1-ethyl ester 2-methyl ester 15g.

Using the above procedure for **10c** (but with phosphorane **3a** for 15 h), the *title compound 15g* was prepared in 78% yield as essentially a single diastereomer as a clear oil; *R_f* 0.28 (petrol–EtOAc, 3:1); *ν_{max}* (film) 2934, 2854, 1735, 1703, 1450, 1373, 1294, 1174 cm^{−1}; *δ_H* (400 MHz, CDCl₃) 1.24 (3H, t, *J* 7.0 Hz), 1.28–1.34 (4H, m), 1.63–1.78 (4H, m), 1.93–1.95 (2H, m), 2.46 (2H, d, *J* 5.5 Hz), 2.52–2.58 (1H, m), 3.07 (1H, t, *J* 5.5 Hz), 3.70 (3H, s), 4.15 (2H, q, *J* 7.0 Hz); *δ_C* (100 MHz, CDCl₃) 13.7 (CH₃), 25.2 (CH₂), 25.5 (CH₂), 27.5 (CH₂), 29.2 (CH), 29.4 (CH), 30.2 (CH), 51.5 (CH), 52.3 (CH₃), 61.4 (CH₂), 168.5 (C), 168.9 (C), 209.0 (C); *m/z* (CI) 283 (MH⁺); HRMS (CI) [MH⁺], found: 283.1546. C₁₅H₂₃O₅ requires 283.1545 (−0.4 ppm error).

6.3.15. 2-Benzoyl-3-(3-phenyl-propionyl)-cyclopropanecarboxylic acid ethyl ester 15h.

Using the above procedure for **10c** (but with phosphorane **3a** for 15 h), the *title compound 15h* was prepared as essentially a single diastereomer in 51% yield as a colourless oil; *R_f* 0.24 (petrol–EtOAc, 3:1); *ν_{max}* (film) 2909, 1735, 1710, 1454, 1373, 1304, 1197, 912, 732 cm^{−1}; *δ_H* (400 MHz, CDCl₃) 1.24 (3H, t, *J* 7.0 Hz), 2.49 (2H, d, *J* 5.5 Hz), 2.92–2.94 (3H, m), 3.00 (2H, d, *J* 5.5 Hz), 3.69 (3H, s), 4.14 (2H, q, *J* 7.0 Hz), 7.16–7.17 (1H, m), 7.19–7.20 (2H, m), 7.26–7.27 (1H, m), 7.28–7.29 (1H, m); *δ_C* (100 MHz, CDCl₃) 13.4 (CH₃), 28.9 (CH₂), 29.1 (CH), 29.3 (CH), 31.1 (CH), 45.2 (CH₂), 52.0 (CH₃), 61.1 (CH₂), 126.2 (CH), 128.2 (CH), 128.5 (CH), 140.3 (C), 167.9 (C), 168.4 (C), 205.1 (C); *m/z* (CI) 305 (MH⁺); HRMS (CI) [MH⁺], found: 305.1386. C₁₇H₂₁O₅ requires 305.1389 (1.0 ppm error).

6.3.16. Diethyl 3-(11,17-dihydroxy-10,13-dimethyl-3-oxo-2,3,6,7,8,9,10,11,12,13,14,15,16,17-tetradecahydro-1*H*-cyclopenta[*a*]phenanthrene-17-carbonyl)-cyclopropane-1,2-dicarboxylate 15i.

Using the above procedure for **10c** (but with phosphorane **3e** for 2.5 h), the *title compound 15i* was prepared in 78% yield as a colourless oil as an inseparable mixture (5:1) of cyclopropane isomers with one major, *R_f* 0.34 (petrol–EtOAc, 4:1); *ν_{max}* (film) cm^{−1}; *δ_H* (400 MHz, CDCl₃) 0.91 (3H, s), 0.95–1.02 (1H, m), 1.17–1.31 (7H, m), 1.32–1.55 (5H, m), 1.66–1.88 (4H, m), 1.92–2.37 (4H, m), 1.98 (3H, s), 2.37–2.51 (3H, m),

2.68–2.84 (2H, m), 3.43 (1H, dd (app t), J 5.5 Hz), 4.03–4.15 (5H, m), 4.41 (1H, br s), 5.62 (1H, s); δ_C (100 MHz, CDCl₃) 14.1 (CH₃), 14.2 (CH₃), 18.0 (CH₃), 21.0 (CH₃), 23.9 (CH₂), 29.2 (CH), 30.0 (CH), 31.4 (CH), 31.7 (CH), 32.1 (CH₂), 32.8 (CH₂), 33.1 (CH₂), 33.8 (CH₂), 34.9 (CH₂), 39.3 (C), 40.0 (CH₂), 47.6 (C), 51.8 (CH), 56.0 (CH), 61.6 (CH₂), 61.7 (CH₂), 68.3 (CH), 90.0 (C), 122.3 (CH), 167.8 (C), 168.3 (C), 172.7 (C), 199.9 (C), 207.4; m/z (CI) 517 (MH⁺); HRMS (CI) [MH⁺], found: 517.2794. C₂₉H₄₁O₈ requires 517.2801 (1.5 ppm error).

6.3.17. Methylsulfanyl-acetic acid 3-allyl-2-methyl-4-oxo-cyclopent-2-enyl ester 21. Dicyclohexylcarbodiimide (3.31 g, 16.0 mmol) in THF (20 mL) was added to a solution of alcohol **20**¹¹ (2.03 g, 13.4 mmol), (methylthio)acetic acid (1.28 mL, 14.7 mmol), and DMAP (163 mg, 1.3 mmol) in THF (90 mL) at rt under a nitrogen atmosphere. Precipitation of DCU was observed after a few minutes. After 2 h, the reaction was filtered through Celite® washing with EtOAc, and then the filtrate concentrated in vacuo. Purification by flash column chromatography (petrol–EtOAc, 4:1) gave the *title compound 21* (2.52 g, 79%) as a yellow oil; R_f 0.48 (petrol–EtOAc, 3:1); ν_{\max} (film) 2953, 1734, 1710, 1655, 1638, 1385, 1268, 1130, 1001 cm⁻¹; δ_H (400 MHz, C₆D₆) 1.57 (3H, s), 1.81 (3H, s), 2.07 (1H, dd, J 1.9 and 18.5 Hz), 2.49 (1H, dd, J 6.0 and 18.5 Hz), 2.66 (2H, s), 2.80 (2H, t, J 5.6 Hz), 4.88–4.97 (2H, m), 5.34 (1H, br d, J 6.0 Hz), 5.70 (1H, ddt, J 6.3, 10.0 and 16.7 Hz); δ_C (100 MHz, C₆D₆) 12.8 (CH₃), 15.4 (CH₃), 30.3 (CH₂), 34.6 (CH₂), 40.7 (CH₂), 73.0 (CH), 115.2 (CH₂), 127.6 (C), 133.4 (CH), 141.1 (C), 163.2 (C), 169.0 (C); m/z (CI) 241 (MH⁺), 258 (MNH₄⁺); HRMS (CI) [MNH₄⁺], found: 241.0894. C₁₂H₁₇O₃S requires 241.0898 (2.0 ppm error).

6.3.18. (3-Allyl-2-methyl-4-oxo-cyclopent-2-enyloxycarbonylmethyl)-dimethylsulfonium tetrafluoroborate 22. Ester **21** (661 mg, 2.75 mmol) was dissolved in iodomethane (15 mL). Silver tetrafluoroborate (574 mg, 2.95 mmol) was added in one portion and the reaction stirred in the dark for 3 h at rt, after which time stirring was stopped and the precipitate allowed to settle. The supernatant was decanted carefully and the residue dried in vacuo before being extracted with MeOH (three times). Filtration and removal of the MeOH in vacuo (water bath <35 °C) gave the *title compound 22* (848 mg, 90%) as a yellow oil; ν_{\max} (film) 3033, 2944, 1736, 1709, 1655, 1638, 1432, 1388, 1312, 1194, 1064, 922 cm⁻¹; δ_H (400 MHz, CD₃OD) 2.10 (3H, s), 2.44 (1H, dd, J 1.6 and 18.6 Hz), 2.91 (1H, dd, J 6.1 and 18.6 Hz), 2.99–3.02 (8H, m), 4.50 and 4.57 (2H, AB q, J 16.5 Hz), 4.98–5.04 (2H, m), 5.77 (1H, ddt, J 6.3, 10.0 and 16.7 Hz), 5.86 (1H, d, J 6.1 Hz); δ_C (100 MHz, CD₃OD) 14.0 (CH₃), 25.7 (CH₃), 27.8 (CH₂), 41.9 (CH₂), 46.4 (CH₂), 77.6 (CH), 116.4 (CH₂), 134.7 (CH), 143.2 (C), 166.0 (C), 166.7 (C), 205.3 (C); m/z (FAB) 255 (M⁺), 597 (2 M⁺+BF₄⁻); HRMS (FAB) [M⁺], found: 255.1062. C₁₃H₁₉O₃S requires 255.1055 (–3.0 ppm error).

6.3.19. (Dimethyl- λ^4 -sulfanylidene)-acetic acid 3-allyl-2-methyl-4-oxo-cyclopent-2-enyl ester 23. Salt **22** (836 mg, 2.44 mmol) was suspended in CHCl₃ (4 mL), and to this was added a suspension of powdered NaOH (98 mg, 2.44 mmol) in satd aq K₂CO₃ (2 mL). The biphasic solution was stirred at rt for 20 min before being filtered through

Celite®, and washed with CH₂Cl₂. The filtrate was dried (MgSO₄) and concentrated in vacuo to give the *title compound 23* (617 mg, 99%) as a pale yellow oil, which was used immediately; ν_{\max} (film) 2981, 2923, 1703, 1647, 1636, 1616, 1431, 1383, 1366, 1317, 1190, 1129, 1055, 1031, 996, 916 cm⁻¹; δ_H (400 MHz, CDCl₃) 1.99 (3H, s), 2.26 (1H, dd, J 1.8 and 18.6 Hz), 2.73 (6H, s), 2.76 (1H, dd, J 6.1 and 18.6 Hz), 2.92 (2H, d, J 6.4 Hz), 2.95 (1H, br s), 4.93–4.99 (2H, m), 5.66–5.78 (2H, m); δ_C (100 MHz, CDCl₃) 14.0 (CH₃), 27.0 (CH₂), 30.5 (CH₃), 30.6 (CH₃), 32.8 (CH), 42.3 (CH₂), 70.2 (CH), 115.5 (CH₂), 133.9 (CH), 140.0 (C), 168.5 (C), 169.3 (C), 205.1 (C).

6.3.20. 2-((E)-2-Methoxycarbonyl-propenyl)-cyclopropanecarboxylic acid 3-allyl-2-methyl-4-oxo-cyclopent-2-enyl ester 24. To a solution of allyl alcohol **1b** (77 μ L, 1.13 mmol) in CH₂Cl₂ (7 mL) was added powdered 4 Å molecular sieves (1.13 g), dimethylsulfurane **23** (573 mg, 2.26 mmol) in CH₂Cl₂ (3 mL), (carbomethoxyethylene)triphenylphosphorane **3c** (471 mg, 1.35 mmol) and manganese dioxide (981 mg, 11.3 mmol). The mixture was heated at reflux for 3 h, and then cooled to rt. The crude mixture was filtered through Celite® and the residue washed with CH₂Cl₂. After removal of the solvent, the resulting yellow oil was purified by flash column chromatography (petrol–Et₂O, 2:1) to give the *title compound 24* (206 mg, 57%) as a mixture of cyclopropane isomers (~3.1:1) as a colourless oil, R_f 0.21 (petrol–Et₂O, 2:1); ν_{\max} (film) 2922, 1716, 1655, 1437, 1409, 1386, 1255, 1173, 916, 734 cm⁻¹; m/z (CI) 319 (MH⁺), 336 (MNH₄⁺); HRMS (CI) [MH⁺], found 319.1545. C₁₈H₂₃O₅ requires 319.1546 (0.2 ppm error). *NMR data for major isomer only:* δ_H (500 MHz, CDCl₃) 1.12–1.15 (1H, m), 1.57 (1H, ddd, J 5.1, 10.1, 14.5 Hz), 1.83 (1H, dd, J 5.1, 8.5 Hz), 1.94 (3H, d, J 5.0 Hz), 2.01 (3H, s), 2.19–2.29 (2H, m), 2.85 (1H, dd, J 6.3, 18.6 Hz), 2.97 (2H, d, J 6.3 Hz), 3.70 (3H, s), 4.98–5.01 (2H, m), 5.70–5.73 (1H, m), 5.76 (1H, tdd, J 6.3, 9.5, 13.0 Hz), 6.09 (1H, app t, J 9.0 Hz); δ_C (125 MHz, CDCl₃) 12.7 (CH₃), 13.8 (CH₃), 16.7 (CH₂), 22.3 (CH), 22.4 (CH), 27.1 (CH₂), 41.5 (CH₂), 51.8 (CH₃), 73.4 (CH), 116.0 (CH₂), 128.4 (C), 133.4 (CH), 141.3 (CH), 141.7 (C), 165.2 (C), 168.0 (C), 172.6 (C), 203.3 (C).

Acknowledgements

We are grateful to the EPSRC for support (ROPA Fellowship, S.A.R. and studentship, R.J.P.), to the École Normale Supérieure de Lyon and Université Claude Bernard Lyon 1 for ERASMUS exchange support (M.O.).

References and notes

- For a review of the use of MnO₂ in tandem oxidation processes see: Taylor, R. J. K.; Reid, M.; Foot, J. S.; Raw, S. A. *Acc. Chem. Res.* **2005**, *38*, 851–869 and references therein; see also Refs. **4** and **7** and: Quesada, E.; Raw, S. A.; Reid, M.; Roman, E.; Taylor, R. J. K. *Tetrahedron*, in this issue, please see doi:10.1016/j.tet.2005.12.077.
- (a) Corey, E. J.; Chaykovsky, M. *J. Am. Chem. Soc.* **1962**, *84*, 867–868; (b) Corey, E. J.; Chaykovsky, M. *J. Am. Chem. Soc.* **1962**, *84*, 3782–3783; (c) Truce, W. E.; Badiger, V. V. *J. Org.*

- Chem.* **1964**, *29*, 3277–3280; (d) Payne, G. B. *J. Org. Chem.* **1967**, *32*, 3351–3355; (e) Quintana, J.; Torres, M.; Serratosa, F. *Tetrahedron* **1973**, *29*, 2065–2076; (f) Johnson, C. R.; Schroeck, C. W.; Shanklin, J. R. *J. Am. Chem. Soc.* **1973**, *95*, 7424–7431; (g) Aggarwal, V. K.; Smith, H. W.; Hynd, G.; Jones, R. V. H.; Fieldhouse, R.; Spey, S. E. *J. Chem. Soc., Perkin Trans. 1* **2000**, 3267–3276.
3. (a) For reviews see: Wessjohann, L. A.; Brandt, W.; Thiemann, T. *Chem. Rev.* **2003**, *103*, 1625–1647; Reissig, H.-U.; Zimmer, R. *Chem. Rev.* **2003**, *103*, 1151–1196; Pietruszka, J. *Chem. Rev.* **2003**, *103*, 1051–1070; Lebel, H.; Marcoux, J.-F.; Molinaro, C.; Charette, A. B. *Chem. Rev.* **2003**, *103*, 977–1050 and references therein; (b) For recent references see: Zheng, J.-C.; Liao, W.-W.; Tang, Y.; Sun, X.-L.; Dai, L.-X. *J. Am. Chem. Soc.* **2005**, *127*, 12222–12223 and references therein; (c) Ningsanont, N.; Black, D. S. C.; Chanphen, R.; Thebtaranonth, Y. *J. Med. Chem.* **2003**, *46*, 2397–2403; (d) Wipf, P.; Reeves, J. T.; Balachandran, R.; Day, B. W. *J. Med. Chem.* **2002**, *45*, 1901–1917; (e) Rugutt, J. K.; Henry, C. W.; Franzblau, S. G.; Warner, I. M. *J. Agric. Food Chem.* **1999**, *47*, 3402–3410; (f) Han, S.-Y.; Cho, S.-H.; Kim, S.-Y.; Seo, J.-T.; Moon, S.-J.; Jhon, G.-J. *Bioorg. Med. Chem. Lett.* **1999**, *9*, 59–64; (g) Barrett, A. G. M.; Doubleday, W. W.; Hamprecht, D.; Kasdorf, K.; Tustin, G. J.; White, A. J. P.; Williams, D. J. *Chem. Commun.* **1997**, 1693–1700; (h) Matano, Y. *J. Chem. Soc., Perkin Trans. 1* **1994**, 2703–2709; (i) Wu, P.-L.; Wang, W.-S. *J. Org. Chem.* **1994**, *59*, 622–627; (j) Bucsh, R. A.; Domagala, J. M.; Laborde, E.; Sesnie, J. C. *J. Med. Chem.* **1993**, *36*, 4139–4151; (k) Rai, K. M. L.; Anjanamurthy, C.; Radhakrishna, P. M. *Synth. Commun.* **1990**, *20*, 1273–1277; (l) Martinez, G. R.; Hirschfeld, D. R.; Maloney, P. J.; Yang, D. S.; Rosenkranz, R. P.; Walker, K. A. M. *J. Med. Chem.* **1989**, *32*, 890–897; (m) Boland, W.; Niedermeyer, U. *Synthesis* **1987**, 28–32; (n) Curley, R. W., Jr.; DeLuca, H. F. *J. Org. Chem.* **1984**, *49*, 1941–1944; (o) Duhamel, P.; Poirier, J.-M.; Hennequin, L. *Tetrahedron Lett.* **1984**, *25*, 1471–1474; (p) Doyle, M. P.; Dorow, R. L.; Tambllyn, W. H. *J. Org. Chem.* **1982**, *47*, 4059–4068; (q) Kusuyama, Y.; Ikeda, Y. *Bull. Chem. Soc. Jpn.* **1977**, *50*, 1784–1787; (r) Hammerschmidt, F.; Zbiral, E. *Liebigs Ann. Chem.* **1977**, 1026–1038; (s) Adams, J.; Hoffman, L., Jr.; Trost, B. M. *J. Org. Chem.* **1970**, *35*, 1600–1604.
4. For preliminary communications see: (a) Oswald, M. F.; Raw, S. A.; Taylor, R. J. K. *Org. Lett.* **2004**, *6*, 3997–4000; (b) Oswald, M. F.; Raw, S. A.; Taylor, R. J. K. *Chem. Commun.* **2005**, 2253–2255.
5. Curley, R. W., Jr.; DeLuca, H. F. *J. Org. Chem.* **1984**, *49*, 1944–1946.
6. Murphy, W. S.; Wattanasin, S. *J. Chem. Soc., Perkin Trans. 1* **1982**, 1029–1035.
7. Runcie, K. A.; Taylor, R. J. K. *Chem. Commun.* **2002**, 974–975.
8. Murphy, W. S.; Wattanasin, S. *J. Chem. Soc., Perkin Trans. 1* **1982**, 271–276.
9. For reviews see: Jeanmart, S. *Aust. J. Chem.* **2003**, *56*, 559–566; Crombie, L. *Pestic. Sci.* **1980**, *11*, 102–118.
10. Matsui, M.; Meguro, H. *Agric. Biol. Chem.* **1964**, *28*, 27–31; Kobayashi, A.; Yamashita, K.; Ohshima, K.; Yamamoto, I. *Agric. Biol. Chem.* **1971**, *35*, 1961–1965.
11. Farkas, J.; Komrsová, H.; Krupicka, J.; Novák, J. J. K. *Collect. Czech. Chem. Commun.* **1960**, *25*, 1824–1836; for improved preparation of the precursors see: Chattopadhyay, S. K.; Pattenden, G. *J. Chem. Soc., Perkin Trans. 1* **2000**, 2429–2454; Kato, T.; Mochizuki, M.; Okano, S.; Matsuo, N. *Synth. Commun.* **2003**, *33*, 3977–3982.
12. Wattanasin, S.; Murphy, W. S. *Synthesis* **1980**, 647–650.
13. Bramwell, A. F.; Crombie, L.; Hemesley, P.; Pattenden, G.; Elliott, M.; Janes, N. F. *Tetrahedron* **1969**, *25*, 1727–1741.
14. (a) McDonald, W. S.; Verbicky, C. A.; Zercher, C. K. *J. Org. Chem.* **1997**, *62*, 1215–1222; (b) Fritschi, H.; Leutenegger, U.; Pfaltz, A. *Helv. Chim. Acta* **1988**, *71*, 1553–1565.



ELSEVIER

Aerobic oxidation of trimethylbenzenes catalyzed by *N,N',N''*-trihydroxyisocyanuric acid (THICA) as a key catalyst

Naruhisa Hirai, Yoshinobu Tatsukawa, Michiko Kameda,
Satoshi Sakaguchi and Yasutaka Ishii*

Department of Applied Chemistry and High Technology Research Center, Faculty of Engineering,
Kansai University, Suita, Osaka 564-8680, Japan

Received 31 October 2005; revised 20 December 2005; accepted 23 December 2005

Available online 26 May 2006

Abstract—The oxidation of trimethylbenzenes was examined with air or O₂ using *N,N',N''*-trihydroxyisocyanuric acid (THICA) as a key catalyst. Thus, 1,2,3-, 1,2,4-, and 1,3,5-trimethylbenzenes under air (20 atm) in the presence of THICA (5 mol %), Co(OAc)₂ (0.5 mol %), Mn(OAc)₂, and ZrO(OAc)₂ at 150 °C were oxidized to the corresponding benzenetricarboxylic acids in good yields (81–97%). In the aerobic oxidation of 1,2,4-trimethylbenzene by the THICA/Co(II)/Mn(II) system, remarkable acceleration was observed by adding a very small amount of ZrO(OAc)₂ to the reaction system to form 1,2,4-benzenetricarboxylic acid in excellent yield (97%). In contrast, no considerable addition effect was observed in the oxidation of 1,3,5-trimethylbenzene. This aerobic oxidation by the present catalytic system provides an economical and environmentally benign direct method to benzenetricarboxylic acids, which are very important polymer materials. © 2006 Elsevier Ltd. All rights reserved.

1. Introduction

Aromatic tricarboxylic acids like 1,2,3-benzenetricarboxylic acid (hemimellitic acid), 1,2,4-benzenetricarboxylic acid (trimellitic acid), and 1,3,5-benzenetricarboxylic acid (trimesic acid), which are converted into their anhydrides are of industrial importance. These anhydrides are used to make plasticizers for polyvinyl chloride and are also used as monomer materials for polyester and polyimide resins having high thermal resistance. These polycarboxylic acids are produced in large scale by aerobic oxidation of the corresponding trimethylbenzenes or by oxidation with dilute nitric acid (ca. 7%), which is known as the Amoco method¹ or the Bergwerksverband method,² respectively. An alternative process for trimellitic acid involves carboxylation of *m*-xylene followed by aerobic oxidation in the presence of MnBr₂/HBr.^{1e,3} The aerobic oxidation is usually carried out under the influence of a small amount of cobalt and manganese salts in the presence of bromine.^{1,4} However, the autoxidation of polymethylbenzenes must be carried out under harsh conditions (higher pressure and temperature). In addition, the need of the corrosive bromide ion as a promoter calls for the use of reactors made of titanium alloy. Fortunately, we have recently developed an innovative halogen-free catalytic method for aerobic oxidation of alkanes using *N*-hydroxyphthalimide (NHPI), which serves as a

carbon radical producing catalyst (CRPC) from alkanes.⁵ Thus, alkanes like ethane, isobutene, cyclohexane, and alkylbenzenes can be efficiently oxidized with dioxygen to oxygen-containing compounds like alcohols, ketones, and carboxylic acids under mild conditions. In the aerobic oxidation of alkenes by NHPI combined with Co(II), the key step in sequential reactions is the generation of a phthalimide-*N*-oxyl (PINO) radical by the hydrogen abstraction from the NHPI by oxygen or a cobalt(III)-oxygen complex generated in situ from Co(II) and molecular oxygen. The resulting PINO abstracts the hydrogen atom from the C–H bond of alkanes to lead to alkyl radicals that are readily trapped by O₂ to give eventually oxygen-containing products through the redox decomposition of alkylhydroperoxides by metal ions. The catalysis of NHPI as the CRPC is very unique and deserves attention as a new catalyst for generation of carbon radicals by hydrogen abstraction from various C–H bonds like alkanes, alkenes, alkynes, alcohols, and ethers, etc. In the oxidation of alkylbenzenes like *p*-xylene, which are susceptible to autoxidation, however, the NHPI was found to be converted into an inactive species like phthalimide in the course of the oxidation owing to a violent chain reaction. Hence, the oxidation must be carried out in the presence of a large amount of NHPI (20 mol %) to obtain terephthalic acid in higher yield. In the course of our study to develop an NHPI analogue, which can be stable at higher temperature, we have found *N,N',N''*-trihydroxyisocyanuric acid (THICA), which serves as a good CRPC from alkylbenzenes.⁶ In this paper, we wish to report the aerobic oxidation of trimethylbenzenes by THICA as a key catalyst.

* Corresponding author. Tel.: +81 6 6368 0793; fax: +81 6 6339 4026; e-mail: ishii@ipcku.kansai-u.ac.jp

2. Results and discussion

The aerobic oxidation of 1,2,4-trimethylbenzene (pseudocumene) (**1**) by THICA in acetic acid under several reaction conditions was first examined (Table 1).

The oxidation of **1** under air (20 atm) in the presence of THICA (5 mol %), Co(OAc)₂ (0.5 mol %), and Mn(OAc)₂ (0.5 mol %) at 120 °C for 6 h afforded a mixture of mono, di, and tricarboxylic acids, **2**, **3**, and **4**, in 10%, 66%, and 7% yields, respectively (entry 1). Although the reaction time was prolonged to 14 h, the yield of desired 1,2,4-benzenetricarboxylic acid (trimellitic acid) **4** was slightly increased (24%) (entry 2). When the amount of Co(OAc)₂ and Mn(OAc)₂ was increased to 2 mol % under these conditions, it was found that the oxidation was considerably accelerated by these metal ions and the main product in the oxidation became trimellitic acid **4** (54%) rather than **3** (31%) (entry 3). The oxidation at higher temperature (150 °C) afforded **4** in high yield (70%) along with **3** (19%) (entry 4), although the oxidation using NHPI is difficult to carry out at 150 °C because of decomposition under such circumstances. It is interesting to note that a small amount of ZrO(OAc)₂ (0.5 mol %) was added to the catalytic system to lead to **4** in an almost quantitative yield (97%) (entry 5). The acceleration effect of the Zr additive on the Co-catalyzed autoxidation has appeared in a patent by Ichikawa.^{4a} Subsequently, the effect of a Zr species on the Co/Mn/Br system was studied in detail by Partenheimer^{4b} who pointed out the importance of Lewis acidity of the Zr species in the oxidation of *p*-xylene. There is no systematic study on the aerobic oxidation of **1** in the literature except for several patent works. In these patents, the aerobic oxidations of **1** by the Co/Mn/Br/Zr system was carried out under 10–27 atm of air at 160–210 °C to lead to trimellitic acid **4** in about 90% yield.^{4c} Therefore, it is

Table 1. Aerobic oxidation of 1,2,4-trimethylbenzene (**1**) by THICA under selected conditions^a

Entry	Co(II)/Mn(II) (mol %)	Temp (°C)	Time (h)	Yield (%) ^b		
				2	3	4
1	0.5/0.5	120	6	10	66	7
2	0.5/0.5	120	14	Trace	68	24
3	2/2	120	6	n.d.	31	54
4	2/2	150	6	n.d.	19	70
5 ^c	0.5/0.5	150	6	n.d.	n.d.	97

^a Compound **1** (1 mmol) was oxidized under air (20 atm) in the presence of THICA (5 mol %), Co(OAc)₂·4H₂O, and Mn(OAc)₂·4H₂O in AcOH (2.5 mL).

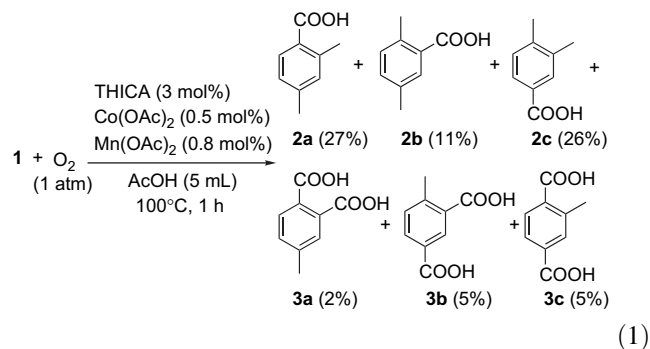
^b Conversion of **1** was over 99% in each run.

^c ZrO(OAc)₂ (0.5 mol %) was added.

important to note that the oxidation of **1**, which has been difficult to carry out up to now, in the absence of bromine, can be first performed by a bromine-free condition to lead to **4** in the highest yield. Our oxidation provides the best result of trimellitic acid **4** from **1** by a bromine-free catalytic system.

Since it is possible to form three positional isomers of mono and dicarboxylic acids, **2** and **3**, in the oxidation of **1**, it is interesting to clarify which methyl group in **1** is preferentially oxidized.

Thus, we examined the oxidation of **1** under mild conditions at 100 °C for 1 h under atmospheric dioxygen and obtained 2,4-dimethylbenzoic acid (**2a**) (27%), 2,5-dimethylbenzoic acid (**2b**) (11%), and 3,4-dimethylbenzoic acid (**2c**) (26%) as well as dicarboxylic acids consisting of **3a** (2%), **3b** (5%), and **3c** (5%) (Eq. 1). The amounts of these mono and dicarboxylic acids were confirmed as their methyl esters by esterification of the resulting carboxylic acids with diazomethane. From consideration of the electron-donating effect of the methyl groups and their steric effect, it is reasonable that **2a** and **2c** are preferentially formed rather than **2b**. On the other hand, in the oxidation of a 1:1:1 mixture of **2a**, **2b**, and **2c** under the same conditions as Eq. 1, the conversion of **2a**, **2b**, and **2c** was 17%, 32%, and 24%, respectively. These results indicate that **2b** is the most subject to autoxidation among dimethylbenzoic acids.



It is interesting to compare the catalytic performance of THICA with that of NHPI for the oxidation of **1**. Thus, the oxidation of **1** with O₂ (1 atm) by THICA (10 mol %) in the presence of Co(OAc)₂ (2 mol %) and Mn(OAc)₂ (0.5 mol %) at 100 °C was compared with that by NHPI (20 mol %) under these conditions. The time-dependence curves of products, **2**, **3**, and **4** for the oxidation of **1** by NHPI and THICA are shown in Figure 1a and b, respectively.

By the NHPI catalyst, **1** was found to be rapidly oxidized to monocarboxylic acid **2** in over 90% yield within 2 h. However, dicarboxylic acid **3** was rarely formed at the stage of 2 h and then gradually increased up to 35%, while no trimellitic acid **4** was observed throughout the reaction. That there was no oxidation of **3** to **4** is believed to be due to the deactivation by the decomposition of NHPI and/or the adduct formation of the resulting radical species with the phthalimide-*N*-oxyl (PINO) radical because of the slow diffusion of oxygen into the liquid phase from the gaseous phase at the early stage of the reaction.⁷ On the other hand, oxidation of **1** to **2** by THICA proceeded more slowly than that by NHPI, since THICA is less active but more

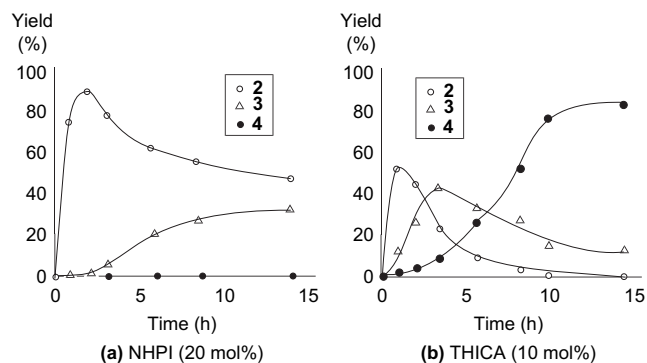
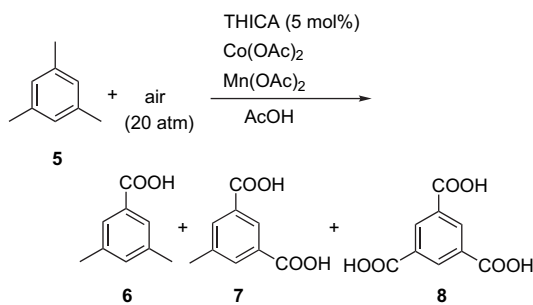


Figure 1. Time-dependence curves for the oxidation of **1** by THICA or NHPI; reaction conditions: **1** (1 mmol), THICA (10 mol %) or NHPI (20 mol %), $\text{Co}(\text{OAc})_2$ (2 mol %), $\text{Mn}(\text{OAc})_2$ (0.5 mol %), AcOH (2.5 mL), O_2 (1 atm), and 100 °C.

stable than NHPI. As a result, THICA is not decomposed during the reaction and can oxidize **1** to **4**. These results indicate that THICA served as a more efficient catalyst than NHPI for the oxidation of reactive trimethylbenzenes to benzenetricarboxylic acids.

We next tried the aerobic oxidation of 1,3,5-trimethylbenzene (mesitylene) (**5**) under air (20 atm) by THICA in the presence of $\text{Co}(\text{OAc})_2$ and $\text{Mn}(\text{OAc})_2$ (Table 2). To our knowledge, there has been no study on the aerobic oxidation of **5** except for several patent works.⁸ 1,3,5-Benzenetricarboxylic acid (trimesic acid) (**8**) is known to be used as a cross-linking agent for polymers, plasticizers etc.⁹

Table 2. Aerobic oxidation of 1,3,5-trimethylbenzene (**5**) by THICA under selected conditions^a



Entry	Co(II)/Mn(II) (mol %)	Temp (°C)	Time (h)	Yield (%) ^b		
				6	7	8
1	0.5/0.5	120	6	n.d.	41	48
2	0.5/0.5	150	6	n.d.	9	82
3	2/0.5	120	6	n.d.	6	85
4 ^c	0.5/0.5	120	6	n.d.	25	65

^a Compound **5** (1 mmol) was oxidized under air (20 atm) in the presence of THICA (5 mol %), $\text{Co}(\text{OAc})_2 \cdot 4\text{H}_2\text{O}$, and $\text{Mn}(\text{OAc})_2 \cdot 4\text{H}_2\text{O}$ in AcOH (2.5 mL) at 120 or 150 °C for 6 h.

^b Conversion was over 99% in each run.

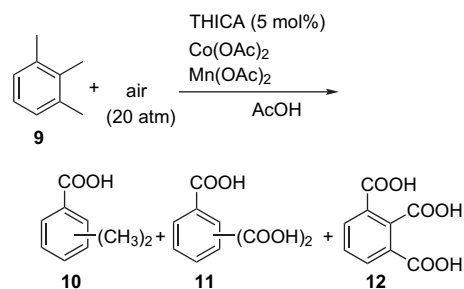
^c $\text{ZrO}(\text{OAc})_2$ (0.5 mol %) was added.

The oxidation of **5** by THICA (5 mol %) in the presence of $\text{Co}(\text{OAc})_2$ (0.5 mol %) and $\text{Mn}(\text{OAc})_2$ (0.5 mol %) at 120 °C for 6 h afforded dicarboxylic acid (**7**) (41%) and trimesic acid **8** (48%), but 3,5-dimethylbenzoic acid (**6**) was not detected (entry 1). The reaction was carried out at 150 °C

under these conditions giving **8** in 82% yield (entry 2). When the amount of $\text{Co}(\text{OAc})_2$ was increased to 2 mol %, trimesic acid **8** was obtained in high yield (85%) even at 120 °C (entry 3). It was found that a moderate effect of $\text{ZrO}(\text{OAc})_2$ was observed in the oxidation of **5** different from that of **1** (entry 4). In patent works on the oxidation of **5**, the best result of **8** is 88% yield when **5** was oxidized by a Co/Mn/Br system under 20 atm of air at 220 °C.^{4d} It is important to note that the present oxidation by THICA can be carried out even at 120 °C to give **8** in comparable yield with that by the Co/Mn/Br system, while the oxidation by the Co/Mn/Br system is carried out at higher temperature (220 °C).

The oxidation of 1,2,3-trimethylbenzene (hemimellitene) (**9**) was examined under the same conditions as in Table 2 (Table 3).

Table 3. Aerobic oxidation of 1,2,3-trimethylbenzene (**9**) by THICA under selected conditions^a



Entry	Co(II)/Mn(II) (mol %)	Temp (°C)	Conv. (%)	Yield (%) ^b		
				10	11	12
1	0.5/0.5	120	6	14	16	14
2	2/2	120	6	2	11	40
3 ^c	0.5/0.5	120	6	5	29	41
4	0.5/0.5	150	6	5	21	29
5 ^c	0.5/0.5	150	6	n.d.	5	81

^a Compound **9** (1 mmol) was oxidized under air (20 atm) in the presence of THICA (5 mol %), $\text{Co}(\text{OAc})_2 \cdot 4\text{H}_2\text{O}$, and $\text{Mn}(\text{OAc})_2 \cdot 4\text{H}_2\text{O}$ in AcOH (2.5 mL) at 120 or 150 °C for 6 h.

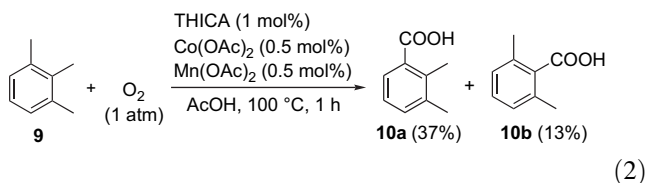
^b Conversion was over 99% in each run.

^c $\text{ZrO}(\text{OAc})_2$ (0.5 mol %) was added.

The oxidation of **9** was difficult to carry out selectively at 120 °C different from that of **1** or **5**, and about a 1:1:1 mixture of mono, di, and tricarboxylic acids, **10**, **11**, and **12**, was obtained in low yields (entry 1). When the amount of $\text{Co}(\text{OAc})_2$ and $\text{Mn}(\text{OAc})_2$ was increased to 2 mol %, hemimellitonic acid **12** was obtained in 40% yield. By adding $\text{ZrO}(\text{OAc})_2$ (0.5 mol %) to the THICA/ $\text{Co}(\text{OAc})_2$ / $\text{Mn}(\text{OAc})_2$ system, the oxidation of **9** at 120 °C for 6 h led to **10** (5%), **11** (29%), and **12** (41%) (entry 3). A similar tendency was observed in the oxidation at 150 °C. When **9** was oxidized at 150 °C, **10**, **11**, and **12** were obtained in 5, 21, and 29% yields, respectively (entry 4). However, in the presence of $\text{ZrO}(\text{OAc})_2$ (0.5 mol %) under these conditions, the oxidation resulted in **12** in high yield (81%) (entry 5). In the oxidation of **9**, a remarkable addition effect of $\text{ZrO}(\text{OAc})_2$ was observed. In order to obtain information on the formation of mono and dicarboxylic acids, **9** was oxidized at low temperature (100 °C).

The oxidation of **9** by THICA/ $\text{Co}(\text{OAc})_2$ / $\text{Mn}(\text{OAc})_2$ at 100 °C for 1 h afforded 2,3-dimethylbenzoic acid (**10a**)

(37%) in preference to 2,6-dimethylbenzoic acid (**10b**) (13%) (Eq. 2).



In the oxidation of **9** at 100 °C, no di and tricarboxylic acids were formed. The preferential formation of **10a** over **10b** indicates that the steric effect of the methyl group is a more important factor than the electron-donating effect.

In conclusion, we have carried out the first systematic study on the aerobic oxidation of trimethylbenzenes and developed an efficient halogen-free route to 1,2,4-benzenetricarboxylic acid **4**, which is an important polymer material, using THICA as a key catalyst.

3. Experimental

3.1. General procedure

Starting materials and catalysts were purchased from commercial sources and used without further treatment. Yields were estimated from the peak areas based on the internal standard technique by using GC. GC analysis was performed with a flame ionization detector using a 0.2 mm×30 m capillary column (OV-17). ¹H and ¹³C NMR spectra were measured at 270 and 400 MHz, respectively, in chloroform-*d* with Me₄Si as the internal standard. Infrared (IR) spectra were measured using NaCl or KBr pellets. GC–MS were obtained at ionization energy of 70 eV. All products were identified by comparison of the isolated products with authentic samples.

3.2. Preparation of *N,N',N''*-trihydroxyisocyanuric acid (THICA)

THICA was prepared by a modified literature procedure.¹⁰ 1,1'-Carbonyldiimidazole (165 mmol) was added to a pyridine (250 mL) solution of *O*-benzylhydroxylamine (150 mmol) under Ar. The mixture was stirred for 1 h at room temperature, and the temperature was raised to 60 °C for 6 h, and 90 °C for 5 h. After the reaction, the solvent was removed under reduced pressure until the mixture was 100 g. Water (500 mL) was added slowly to the mixture to give a white precipitate. The precipitate was filtered and washed with water (50 mL), AcOH (40 mL), and *n*-hexane (40 mL). The solid was recrystallized from AcOH (80 mL) and AcOEt (70 mL) and dried under vacuum to give tribenzoyloxy-1,3,5-triazine-2,4,6-(1*H*,3*H*,5*H*)-trione (TBTA) (5.1 g) in 23% yield.

TBTA (5 mmol) in 100 mL of dioxane was hydrogenated on 10 wt % Pd/C (0.5 g) under normal pressure of hydrogen at room temperature overnight. After removal of the catalyst by filtration, the filtrate was evaporated under reduced pressure to afford THICA, which was recrystallized from acetone,

in 90% yield. The X-ray analysis of THICA indicates that three OH groups are situated at the same plane.

TBTA: ¹H NMR δ 7.52 (m, 2H), 7.42 (m, 3H), 5.1 (s, 2H); ¹³C NMR δ 144.83, 133.47, 129.52, 129.04, 128.35, 78.482; IR (KBr) 1740s, 1401s, 1197m, 1001s, 750s, 696s cm⁻¹.

THICA: ¹H NMR δ 11.03 (s, 3H); ¹³C NMR δ 146.65; IR (KBr) 3539s, 3166s, 2827s, 1720s, 1433s, 1211m, 1010s, 701s cm⁻¹.

3.3. Procedure for oxidation of substituted toluenes under dioxygen atmosphere

An acetic acid solution (5 mL) of substrate (3 mmol), THICA, Co(OAc)₂ (0.5 mol %) was placed in a 50-mL pear-shaped flask with a balloon filled with O₂. The mixture was stirred at 100 °C for 6 h. After the reaction, the solvent was removed under reduced pressure, and the products were purified by column chromatography on silica gel to give the corresponding oxygenated products. The products were identified through comparison of the isolated products with authentic samples.

Acknowledgements

This work was supported by a Grant-in-Aid for Scientific Research on Priority Areas 'Advanced Molecular Transformations of Carbon Resources' from the Ministry of Education, Culture, Sports, Science, and Technology, Japan.

References and notes

- (a) Ockerbloom, N. E. *Hydrocarbon Process.* **1972**, *51*, 114; (b) Partenheimer, W. *Catal. Today* **1995**, *23*, 69; (c) Pershall, G. W.; Ittel, S. D. *Homogeneous Catalysis*, 2nd ed; Wiley: New York, NY, 1992; (d) Suresh, A. K.; Sharma, M. M.; Sridhar, T. *Ind. Eng. Chem. Res.* **2000**, *39*, 3958; (e) Weissmehl, K.; Arpe, H.-J. *Industrial Organic Chemistry*, 4th ed; Wiley-VCH: Weinheim, 2003.
- (a) Bergwerksverband. *Hydrocarbon Process.* **1971**, *50*, 214; (b) Handrick, K.; Benning, A.; George, D.; Curland, E. GB Patent 1,149,321, 1969.
- Tanaka, T.; Hataya, M.; Tanaka, K. EP Patent 83,224, 1983.
- (a) Ichikawa, I. U.S. Patent 3,299,125, 1967; (b) Partenheimer, W. *J. Mol. Catal. A: Chem.* **2003**, *206*, 105 and 131; (c) Partenheimer, W.; Schammel, W. P. U.S. Patent 4,786,753, 1988; (d) Reeve, A. C. U.S. Patent 5,107,020, 1992.
- (a) Ishii, Y.; Sakaguchi, S. *Oxidation Methods*; Bäckvall, J.-E., Ed.; Wiley-VCH: Weinheim, 2003; Chapter 5; (b) Ishii, Y.; Sakaguchi, S.; Iwahama, T. *Adv. Synth. Catal.* **2001**, *343*, 393.
- (a) Hirai, N.; Sawatari, N.; Nakamura, N.; Sakaguchi, S.; Ishii, Y. *J. Org. Chem.* **2003**, *68*, 6587; (b) Hirai, N.; Kagayama, T.; Tatsukawa, Y.; Sakaguchi, S.; Ishii, Y. *Tetrahedron Lett.* **2004**, *45*, 8277.
- In the previous papers, we have shown that the NHPI catalyst decomposed gradually to inert phthalimide and phthalic

- anhydride during the oxidation.⁵ Tashiro, Y.; Sakaguchi, S.; Iwahama, T.; Ishii, Y. *Adv. Synth. Catal.* **2001**, *343*, 220.
8. (a) Garcia-Verdugo, E.; Venardou, E.; Thomas, W. B.; Whiston, K.; Partenheimer, W.; Hamley, P. A.; Poliakoffa, M. *Adv. Synth. Catal.* **2004**, *346*, 307; (b) Saffer, A.; Barker, R. S. U.S. Patent 3,089,906, 1963; (c) Reeve, A. C. U.S. Patent 5,107,020, 1992.
 9. West, R. C.; Diurovich, P. I. U.S. Patent 4,602,050, 1986.
 10. Butula, I.; Takac, M. J.-M. *Croat. Chem. Acta* **2000**, *73*, 569.

Ligand effects in aluminium-catalyzed asymmetric Baeyer–Villiger reactions

Jean-Cédric Frison, Chiara Palazzi and Carsten Bolm*

Institut für Organische Chemie der RWTH Aachen, Landoltweg 1, 52074 Aachen, Germany

Received 1 December 2005; revised 28 December 2005; accepted 29 December 2005

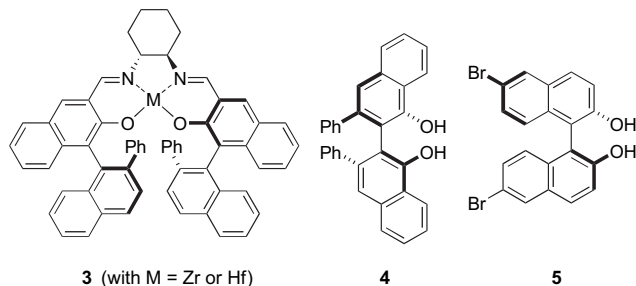
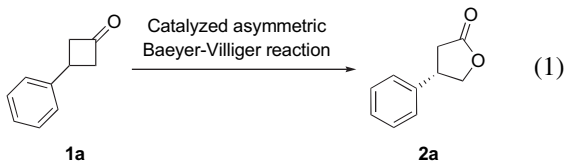
Available online 26 May 2006

Abstract—Asymmetric Baeyer–Villiger oxidations of racemic and prochiral cyclobutanones can be performed with chiral aluminium-based Lewis acids resulting in products with good enantioselectivities in high yields. By employing substituted BINOL derivatives as ligands, remarkable catalyst efficiencies have been achieved and γ -butyrolactones with up to 84% ee were obtained. The relation between the electronic properties of the ligand and the enantioselectivity of the reaction has been investigated, leading to a better understanding of the requirements for achieving a good enantioselectivity in this aluminium-catalyzed oxidative transformation.

© 2006 Elsevier Ltd. All rights reserved.

1. Introduction

The Baeyer–Villiger reaction is a highly useful oxidative transformation in synthetic organic chemistry, which allows the conversion of ketones into esters and lactones.¹ The latter represents core structures of a number of biologically active compounds and, in particular, γ -butyrolactones have proven to be useful intermediates for the synthesis of complex target molecules. Since the first reports on metal-catalyzed asymmetric Baeyer–Villiger reactions in 1994,² numerous chiral catalysts have been developed for this transformation.³ To date, however, only very few of them allow the conversion of simple substrates such as 1-phenylcyclobutanone (**1a**) into the corresponding γ -butyrolactone **2a** with more than



80% ee (Eq. 1). For example, Katsuki utilizes chiral salen metal complexes **3** (with M=Zr or Hf) as catalysts for asymmetric transformations of **1a** (ee_{max}=87%).⁴ Another system stems from our group and is based on chiral BINOL-type ligands in combination with aluminium reagents. For example, we found that VANOL (**4**)⁵ or 6,6'-dibromo-BINOL (**5**)⁶ when treated with equimolar amounts of Me₂AlCl promoted the Baeyer–Villiger oxidation of cyclobutanone **1a** to give lactone **2a** with good enantioselectivity (83 and 77% ee, respectively) in excellent yield.

Several optimization studies have already been conducted and the appropriate choice of reagents and reaction parameters such as the solvent, the oxidant, the aluminium source and the temperature proved to be essential for achieving an efficient catalysis.⁶ In order to further improve the promising result obtained with simple BINOL derivative **5**, we decided to determine the influence of the ligand structure on the catalyst activity and the enantioselectivity in more detail. The results of this study are presented here. Unless noted otherwise, all enantioselectivities and yields mentioned in this article refer to the Baeyer–Villiger reaction of 3-phenylcyclobutanone (**1a**) to give γ -butyrolactone **2a** (Eq. 1), which we used as standard test. In cases, where incomplete reactions are reported, prolongations of the reaction time did not lead to higher conversions. Thus, the indicated reaction time corresponds to the point at which maximum conversion was reached.

2. Results and discussion

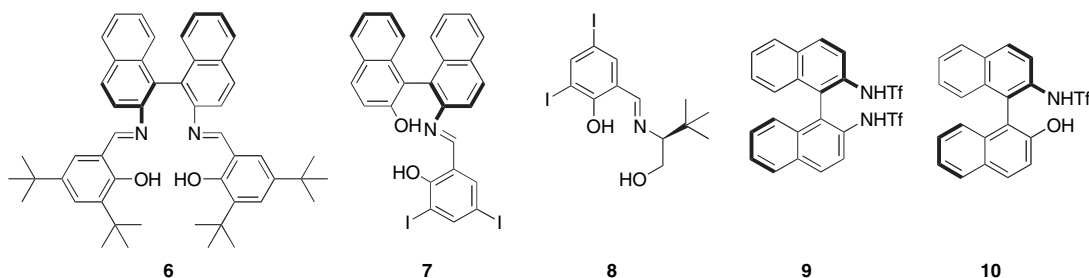
2.1. Effects of substituted ligands

Our previous studies had shown that axially chiral BINOL-type ligands gave high enantioselectivities. However, in the

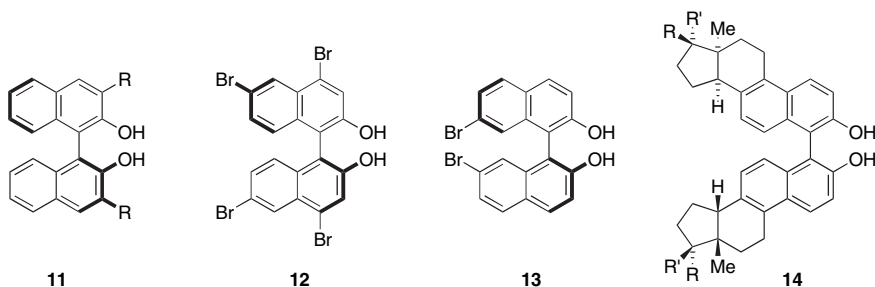
Keywords: Aluminium; Baeyer–Villiger oxidation; BINOL; Catalysis; Oxidation.

* Corresponding author. Tel.: +49 241 8094675; fax: +49 241 8092391; e-mail: carsten.bolm@oc.rwth-aachen.de

light of the successful applications of other chelating molecules in metal-catalyzed oxidations, the current optimization study was started by investigating the effect of Schiff-bases **6**, **7**, **8** and **9** on the transformation shown in Eq. 1. Whereas the former two compounds are axially chiral as **5**, the latter has only a stereogenic centre. Unfortunately, however, the presence of none of these compounds (in combination with Me_2AlCl) allowed the oxidations of **1a** with cumene hydroperoxide (CHP) as oxidant under standard reaction conditions. Since additives such as amines or phosphine oxides can inhibit the oxidation, we hypothesized that the presence of multiple coordination sites in **6–8** was responsible for this low catalyst activity. Consequently, the use of axially chiral *N,N*- and *N,O*-chelates **9**¹⁰ and **10**¹¹ was attempted. Those compounds resemble BINOLs, but distinguish themselves by the presence of one or two triflated amino groups. Also the presence of these compounds had a detrimental effect on the catalyst activity, which was now attributed to the electronic properties of the ligand.



Based on these observations we decided to focus our attention on the use of substituted BINOLs.¹² Previous studies had revealed that BINOLs **11** with substituents at the 3- and 3'-positions were less efficient compared to their 6,6'-disubstituted counterparts (such as **5**) giving lactones with very low enantioselectivity.⁶ To our surprise it was now found that 4,4',6,6'-tetrabromo-BINOL **12**¹³ gave racemic **2a**. BINOL **13** having bromo substituents at the 7,7'-positions¹⁴ afforded **2** in good ee of 64%.



Steroidal BINOLs **14**¹⁵ have previously been applied in various enantioselective metal-catalyzed reactions including the asymmetric oxidation of sulfides.^{15b} There, use of such BINOL derivatives resulted in higher enantioselectivities than with BINOL. In contrast, no major improvement in ee was found, when steroidal BINOLs **14** were applied in the Baeyer–Villiger reaction of **1a**, and out of a range of derivatives only a single compound (**14f**) performed better than BINOL leading to **2a** with 73% ee (Table 1). As revealed by the similar ee-values of products obtained in reactions

Table 1. Application of steroidal BINOLs in Baeyer–Villiger oxidations of **1a**^a

Entry	Ligand ^b	R	R'	Conv. (%) of 1a	Abs config. of 2a	ee (%) of 2a ^c
1	(<i>S</i> _a)- 14a	H	H	100	(+)	67
2	(<i>R</i> _a)- 14a	H	H	100	(–)	68
3	(<i>S</i> _a)- 14b	N–NH ₂		60	(+)	8
4	(<i>R</i> _a)- 14b	N–NH ₂		40		<i>rac</i>
5	(<i>R</i> _a)- 14c	N–NHTos		100	(–)	67
6	(<i>S</i> _a)- 14d	SCH ₂ CH ₂ S		100	(+)	60
7	(<i>R</i> _a)- 14d	SCH ₂ CH ₂ S		100	(–)	68
8	(<i>S</i> _a)- 14e	OH	H	100	(+)	69
9	(<i>R</i> _a)- 14e	OH	H	100	(–)	69
10	(<i>R</i> _a)- 14f	O		100	(–)	73

^a Reaction conditions: **1a** (0.5 mmol), **14** (50 mol %), Me_2AlCl (50 mol %), CHP (1.5 equiv), toluene, –25 °C to rt.

^b Only the axial chirality is indicated. The stereogenic centres relate to the natural steroid skeleton.

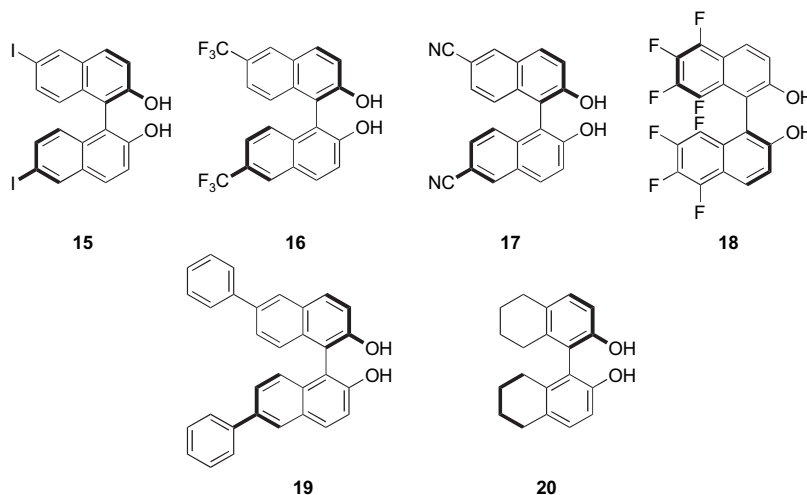
^c Determined by GC using a chiral column: Lipodex B (25×0.25 mm), 60 kPa N₂, at 140 °C; 140 °C, 15 min, 2 °C/min, 160 °C, 50 min; *t*_R=65.0 min (*S*), 66.6 min (*R*).

with diastereomeric ligands, the additional stereogenic centres in the ligand backbone had only a minor influence on the enantioselectivity of the oxygen insertion. Only with the two diastereomeric ligands of **14d** a difference of 8% ee (60 vs 68% ee; entries 6 and 7, respectively) in the formation of product **2a** was detected. In all cases the absolute configuration of lactone **2a** was determined by the chiral axis. Again, the presence of an additional coordinating group (such as the hydrazone moiety in **14b**; Table 1, entries 3

and 4) was detrimental to both catalytic activity and enantioselectivity.

Since at this stage BINOL derivative **5** with two bromo substituents at the 6,6'-positions had led to the best enantioselectivity, this type of substitution pattern was investigated in more detail. Assuming that the bromo substituents exhibited an electronic effect on the ligand, the application of other BINOLs with electronically modified arens was studied. A particular emphasis was put on BINOLs

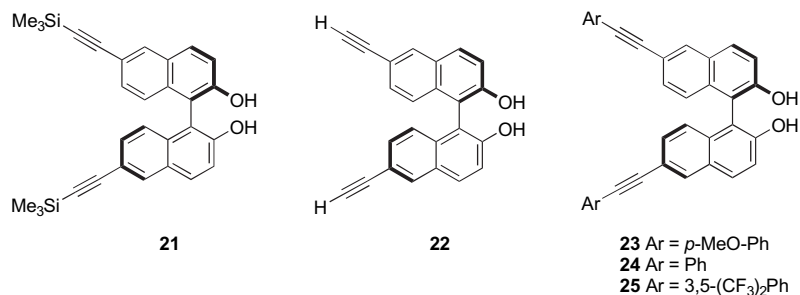
with electron-withdrawing substituents, since those were expected to positively affect the catalytically active metal centre by increasing its Lewis acidity. Starting point was the synthesis and use of **15**, **16**¹⁶ and **17**¹⁷ with iodo, trifluoromethyl and nitrilo substituents, respectively, in the 6- and 6'-positions of the BINOL skeleton. Furthermore, octafluoro derivative **18**¹⁸ was tested.



To our delight we found that Baeyer–Villiger oxidation of **1a** with 10 mol % of a catalyst derived from diiodo BINOL **15** (and equimolar amounts of Me₂AlCl in combination with CHP as oxidant) showed improved properties compared to

substituents at the 6,6'-positions and the sp³ hybridized carbons in the ligand framework, respectively. Presumably, due to these steric effects in combination with the lack of activating substituents the catalysts bearing **19** and **20** showed only a moderate efficiency (with full conversions of **1a** after 24 and 16 h, respectively) affording lactone **2a** with 76 and 73% ee, respectively.

Since Shibasaki had demonstrated that BINOLs with acetylenic substituents in the 6,6'-positions were excellent ligands for Lewis acid catalyzed processes,²¹ we decided to extend our studies on the use of BINOL derivatives **21**–**25**.



the previous systems affording **2a** with 82% ee (at –30 °C). In an attempt to further improve the stereoselectivity, the reaction was conducted at lower temperatures, but unfortunately, only a decrease in activity and enantioselectivity was observed (59% ee at –50 °C and only 54% conversion after 48 h). In contrast to our expectations, however, use of **16**, **17** and **18** led to catalysts with very low activity, and lactone **2a** was formed either as a racemate (as with a catalyst derived from **16**) or with low ee in only small quantities (best result with 10 mol % of the catalyst obtained from **17**: 45% conversion of **1a**, formation of **2a** with 34% ee after 48 h in toluene at –30 °C).

In order to further investigate the impact of the ligand structure on the performance of the catalyst, 6,6'-diphenyl-BINOL **19**¹⁹ and octahydro-BINOL **20**²⁰ were applied in the Baeyer–Villiger reaction of **1** next. Compared to unsubstituted BINOL, **19** and **20** possess a larger torsion angle between the naphthyl moieties induced by the two phenyl

Gratifyingly, BINOL **21** bearing two trimethylsilylalkynyl groups at positions 6 and 6' was also highly efficient in the Baeyer–Villiger reaction, and conversion of **1a** afforded **2a** with 84% ee. Both the catalyst loading (25 mol %) and the temperature (–30 °C) were critical for achieving this enantioselectivity at a reasonable reaction rate. Conducting the reaction with only 5 mol % of the catalyst furnished the lactone with a slightly reduced ee (83%), and the reaction did not go to completion even after 7 days. As with **15**, the enantioselectivity dropped when the catalysis was performed at another temperature (81 and 57% ee at –20 and –50 °C, respectively; in the latter case <10% conversion). Removal of the trimethylsilyl group of **21** to give BINOL **22**¹⁷ proceeded smoothly (K₂CO₃ in MeOH, 98% yield), but unfortunately, use of the resulting catalyst (prepared from BINOL **22** and Me₂AlCl) did not lead to any improvement of the enantioselectivity in the formation of **2a** (82% ee). We therefore concluded that the alkynyl moiety itself and not its terminal substituent were of importance for the catalyst performance

in the Baeyer–Villiger reaction. In order to confirm this hypothesis, BINOLs **23–25** with aryl-substituted alkynyl groups were prepared and applied in the catalysis. Using **22** as starting material all three BINOLs could be obtained by Sonogashira coupling with the corresponding aryl bromides. By selecting the appropriate aryl moiety the electronic properties of the alkynyl group (as well as the entire BINOL) could be varied. Due to the remote position of the electronic modification we did not expect a major impact by the inherent steric alternation. Application of BINOLs **23–25** in the Baeyer–Villiger oxidation of **1a** revealed that the best result was obtained with *p*-methoxy-substituted ligand **23**. In this case, a full conversion of **1a** was observed after 18 h (at $-30\text{ }^{\circ}\text{C}$ in toluene with 20 mol % of **23**, an equimolar amount of Me_2AlCl and CHP as oxidant) leading to lactone **2a** with 82% ee. Bis(trifluoromethyl)-substituted BINOL **25** gave the worst result in this series. Even after 48 h only 54% of ketone **1a** was converted and the resulting product had only 45% ee. After the same period of reaction time the catalysis with phenyl-substituted **24** led to full conversion of **1a** yielding lactone **2a** with 76% ee. These results are remarkable since they indicate that catalysts prepared with these types of BINOLs require electron-rich ligands, which appear to contradict the first assumption that electron-poor BINOLs might be more efficient due to the resulting increased Lewis acidity at the metal centre. Apparently, a well-balanced electronic tuning of the ligand is essential for the success of the reaction, and the background of this key issue will be discussed below taking mechanistic aspects into consideration.

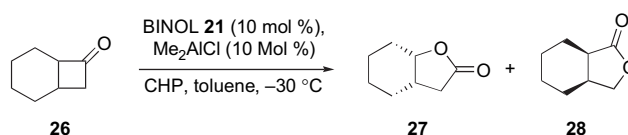
2.2. Substrate scope

Using the catalyst derived from BINOL derivative **21** (in conjunction with 1 equiv of Me_2AlCl), the substrate scope of the asymmetric Baeyer–Villiger oxidation was investigated. Cyclobutanones **1a–e** served as test substrates. The results are summarized in Table 2.

Compared to the (so far best) catalyst derived from VANOL (**4**), the system with **21** as ligand proved about equal or less enantioselective for aryl and alkyl substituted cyclobutanones (Table 2, entries 1–3 vs catalyses with 20 mol % of VANOL, which gave **2a**, **2b** and **2c** with 83, 84 and 69% ee, respectively).⁵ However, the conversion of benzyl-

substituted substrates occurred in a more enantioselective manner (Table 2, entries 4 and 5 vs catalyses with 20 mol % of VANOL, which gave **2d** and **2e** with 41 and 37% ee, respectively).⁵

Finally, the oxidation of racemic ketone **26** was investigated. As in previous studies,³ this cyclobutanone gave two regioisomeric lactones **27** and **28** upon Baeyer–Villiger reaction (83% conversion of **26**). Again, the enantioselectivities (34% ee for **27** and 99% ee for **28**) were better than those obtained before with analogous systems (e.g., BINOL-based ones⁶), albeit the ratio between the two products was similar (**27**:**28**=6.7:1).



Cycloalkanones with larger ring sizes could not be converted with the BINOL **21**/ Me_2AlCl catalyst system.

2.3. Mechanistic considerations

For a rational design and targeted search of new ligands it was considered desirable to get insight into the mechanistic scenario and to identify relevant intermediates. As a first step, we probed the existence of nonlinear effects (NLEs),²² and determined the relationship between the ee of the ligand and the ee of product **2**. At the outset of this investigation, the following observations were made. Upon addition of Me_2AlCl to a solution of BINOL in toluene, the mixture turned into a milky suspension with a white precipitate. This mixture became clearer after the addition of the ketone, which we interpreted as indication for a modification of the catalyst structure. The NLE studies were then done with BINOL derivative **21**. The positive deviation from linearity [(+)-NLE] revealed the presence of nonmonomeric species and their relevance in the stereochemistry-determining step.

Since throughout the catalysis the composition of the reaction media changes with time, we had to ensure that the (enantiomerically enriched) product (here **2a**) as well as the (achiral) ketone (here **1a**) did not affect the ongoing reaction. Therefore a control experiment was performed, which unequivocally showed that the product was formed with the same level of enantioselectivity throughout the entire process. Phenomena such as autocatalysis, auto-amplification or product inhibition/poisoning were thereby excluded.

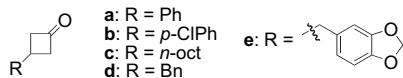
Next, NMR studies were undertaken. A very complex ^1H NMR spectrum was obtained from a 1:1 mixture of BINOL **21** and Me_2AlCl in toluene- d_8 .²³ Upon addition of 5 equiv of 3-phenylcyclobutanone (**1a**) two singlets appeared at 0.24 and 0.33 ppm, replacing the broad coalescent signal corresponding to the TMS groups. Furthermore, clear peaks resulted in the aromatic region. Although a detailed interpretation of (the spectra and) this behaviour is impossible at the present stage, it is hypothesized that the sharpening of the

Table 2. Substrate scope of the asymmetric Baeyer–Villiger reaction (in analogy to Eq. 1)^a

Entry	Substrate	mol % of 21	ee (%) of 2 ^b
1	1a	25	84
2	1b	10	72
3	1c	10	70
4	1d	10	65
5	1e	10	56

^a Reaction conditions: **1** (0.5 mmol), ratio of **21** and Me_2AlCl =1:1, CHP (1.25 equiv), toluene, $-30\text{ }^{\circ}\text{C}$; in all cases the conversion of **1** was complete.

^b Determined by GC using chiral columns.



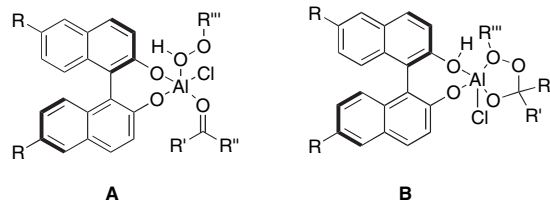
signals indicates a change from oligomeric to more low-molecular associates upon addition of the substrate. Treatment of this mixture with CHP at $-30\text{ }^{\circ}\text{C}$ gave lactone **2a** with 80% ee, which is close to the 84% ee obtained under more diluted conditions.

As demonstrated in other aluminium-catalyzed processes,²⁴ an ageing of the reaction mixture can be crucial for achieving high enantioselectivities, and presumably, this process involves the conversion of multiple (mostly unselective) catalysts into species presenting high enantioselectivities. In the attempt to make use of this effect, a 1:1 mixture of BINOL (**11** with R=H) and $(i\text{-Bu})_2\text{AlCl}$ was stirred at room temperature for 30 min prior to the addition of the ketone. Unfortunately, however, under those conditions both conversion (80%) and enantioselectivity (68% ee) were low. Apparently, the ageing of the catalyst mixture had a negative effect in this case and presumably more oligomeric species were formed, which were neither active nor enantioselective. As a consequence, the conversion of the substrate was slowed down rendering the overall catalysis inefficient.

With the goal to achieve a break-up of the oligomers and to utilize this deoligomerization in the formation of more active low-molecular species, we decided to submit the initial reagent mixture to higher temperatures and, furthermore, to use the Lewis-basic substrate (ketone **1a**) to support this cleavage process. Thus, after BINOL (**11** with R=H) was treated with the aluminium reagent (20 mol % each), the ketone was added, and the resulting mixture was heated at $70\text{ }^{\circ}\text{C}$ for a period of 30 min. After cooling to $-30\text{ }^{\circ}\text{C}$ and addition of the oxidant, the reaction proceeded smoothly to full conversion of **1a** (after 24 h), and lactone **2a** was obtained with remarkable 75% ee. A comparable experiment without this pretreatment at elevated temperature led to product **2a** with only 68% ee. A higher temperature ($90\text{ }^{\circ}\text{C}$) or prolonged heating times (2–16 h) resulted in a lower catalyst activity. The same procedure was applied in a catalysis with **19** as ligand, and also in this case, product **2a** was formed with an improved enantioselectivity (80% ee). Catalysts prepared from VANOL (**4**) and BINOL derivative **21** behaved differently, and no increase in ee was found.

The formation of aggregates might also explain the required electronic fine-tuning of the ligand, which is a key for achieving high activity and enantioselectivity. On one hand, a certain level of Lewis acidity is essential for the conformational fixation and activation of the substrate. Thus, we assume that the ketone is coordinated to the metal site of an intermediately formed chiral aluminium reagent, and upon oxygen transfer and stereoselective rearrangement the observed Baeyer–Villiger product is formed. Such process could proceed via the intermediacy of a pentacoordinated aluminium complex **A**, which would show structural analogies to other known organoaluminium reagents. If, on the other hand, the Lewis acidity is (too) high, two other points become relevant. First, the (spectroscopically observed) aggregates of the chiral aluminium reagent are difficult to break, which slows down the catalysis, and second, the Criegee adduct formed during the reaction might act as bidentate ligand and thereby block turnover of the catalyst

by chelation. Arrangement **B** would then be a critical intermediate, from which the product needs to be liberated for further catalysis. The more Lewis acidic the metal is, the more difficult this step will be, and even a lack of turnover (as observed with catalysts derived from **16** and **18**) can result.



3. Conclusion

In conclusion, we described ligand effects in the aluminium-catalyzed asymmetric Baeyer–Villiger reaction of cyclobutanones. The careful choice of the ligand in combination with appropriate reaction conditions allows the preparation of lactones in excellent yields with enantioselectivities that are among the highest ever obtained in this reaction.

4. Experimental

4.1. General

Details of the asymmetric Baeyer–Villiger reaction protocol as well as the analytical data (including ee determinations) have been reported previously.^{5,6}

4.1.1. (R)-6,6'-Bis-(4-methoxyphenylethynyl)-[1,1']binaphthalenyl-2,2'-diol (23**).** In a Schlenk tube filled with argon were successively added PdCl_2 (9 mg, 0.05 mmol), PPh_3 (55 mg, 0.2 mmol), CuI (11 mg, 0.06 mmol), **22** (334 mg, 1 mmol) and NEt_3 (10 mL). 4-Bromoanisole (470 mg, 2.5 mmol) was then added, and the mixture was heated at $70\text{ }^{\circ}\text{C}$ for 8 h. When the reaction was complete (controlled by TLC), the solution was diluted with ethyl acetate and filtered through Celite. The volatiles were removed and the crude mixture redissolved in ethyl acetate, washed with 1 M HCl, brine and dried (MgSO_4). Column chromatography (silica gel; acetone/pentane 1:4) furnished 498 mg of a yellow solid (91% yield); mp= $147\text{--}149\text{ }^{\circ}\text{C}$; ^1H NMR (400 MHz) δ 7.99 (s, 2H), 7.86 (d, $J=8.8$ Hz, 2H), 7.35–7.25 (m, 8H), 6.98 (d, $J=8.7$ Hz, 2H), 6.80 (d, $J=8.8$ Hz, 2H), 5.06 (br s, 2H), 3.74 (s, 6H); ^{13}C NMR (100 MHz) δ 159.6, 153.3, 133.1, 132.7, 131.6, 131.4, 130.2, 129.2, 124.3, 119.3, 118.5, 115.4, 114.1, 110.9, 89.8, 88.2, 55.4; IR (KBr): $\nu=3000\text{ cm}^{-1}$; MS (EI, 70 eV): m/z 546 (100), 273 (50); Anal. Calcd for $\text{C}_{38}\text{H}_{26}\text{O}_4$: C, 83.50; H, 5.21. Found: C, 83.01; H, 5.14.

4.1.2. (R)-6,6'-Bis-(phenylethynyl)-[1,1']binaphthalenyl-2,2'-diol (24**).**²¹ In analogy to the synthesis of **23** but with bromobenzene (425 mg, 2.5 mmol) instead of 4-bromoanisole. Column chromatography (silica gel; acetone/pentane 1:4) furnished 498 mg of a white solid (91% yield). ^1H NMR (400 MHz) δ 8.04 (d, $J=1.4$ Hz, 2H), 7.88 (d, $J=9.0$ Hz, 2H), 7.51–7.46 (m, 4H), 7.37 (m, 10H), 7.04 (d, $J=8.5$ Hz, 2H), 5.06 (br s, 2H); ^{13}C NMR (100 MHz)

δ 153.4, 132.9, 131.9, 131.6, 131.5, 130.2, 129.1, 128.4, 128.3, 124.3, 123.3, 119.0, 118.6, 110.8, 89.8, 89.3.

4.1.3. (R)-6,6'-Bis-(3,5-bis-trifluoromethylphenyl)ethynyl-[1,1']binaphthalenyl-2,2'-diol (25). In analogy to the synthesis of **23** but with 3,5-bis(trifluoromethyl)-bromobenzene (732 mg, 2.5 mmol) instead of 4-bromoanisole. Column chromatography (silica gel; acetone/pentane 1:4) furnished 728 mg of a yellow solid (96% yield); mp=117–119 °C; ^1H NMR (400 MHz) δ 8.18 (d, $J=1.6$ Hz, 2H), 8.00 (s, 6H), 7.86 (s, 2H), 7.59–7.42 (m, 4H), 7.16 (d, $J=8.6$ Hz, 2H), 4.94 (br s, 2H); ^{13}C NMR (100 MHz) δ 154.0, 133.9, 133.4, 131.8, 131.4, 130.3, 129.0, 127.0, 124.5, 121.5, 119.0, 117.5, 110.9, 93.0, 86.7; IR (KBr): $\nu=3188$ cm^{-1} ; MS (EI, 70 eV): m/z 758.2 (100), 379.2 (22), 351.1 (18); Anal. Calcd for $\text{C}_{40}\text{H}_{20}\text{F}_{12}\text{O}_2$: C, 63.34; H, 2.69. Found: C, 63.21; H, 3.01.

4.1.4. (R)-2,2'-Dihydroxy-[1,1']binaphthalenyl-6,6'-dicarbonitrile (17).²¹ Step 1 (synthesis of (R)-2,2'-bis-methoxymethoxy-[1,1']binaphthalenyl-6,6'-dicarbonitrile): In a Schlenk tube filled with argon were successfully added Pd(dba)₂ (23 mg, 0.04 mmol), DPPF (44 mg, 0.08 mmol), (R)-2,2'-bis-methoxymethoxy-[1,1']binaphthalenyl-6,6'-dibromide (532 mg, 1 mmol), CuCN (540 mg, 5 mmol), *n*-Bu₄I (369 mg, 1 mmol) and dioxane (2 mL). The solution was heated at 100 °C for 3 h, then cooled to rt, diluted with ethyl acetate and filtered through Celite. The organic layer was successively washed with 1 M NaOH, saturated NaHCO₃, brine and dried (Na₂SO₄). The solvents were removed, and the crude product was flash chromatographed with pentane/diethyl ether 1:1 to afford 348 mg of a white solid (82% yield). ^1H NMR (300 MHz) δ 8.20 (d, $J=1.5$ Hz, 2H), 7.95 (d, $J=9.2$ Hz, 2H), 7.64 (d, $J=9.2$ Hz, 2H), 7.28 (dd, $J=1.5$, 8.9 Hz, 2H), 7.07 (d, $J=8.9$ Hz, 2H), 5.06 (d, $J=6.9$ Hz, 2H), 4.97 (d, $J=6.9$ Hz, 2H), 3.11 (s, 6H); ^{13}C NMR (75 MHz) δ 155.2, 135.4, 134.4, 130.6, 128.5, 127.1, 126.2, 119.8, 119.4, 118.0, 107.6, 94.6, 56.1. This product was utilized in the subsequent step without further analysis.

Step 2 (synthesis of (R)-2,2'-dihydroxy-[1,1']binaphthalenyl-6,6'-dicarbonitrile (17)).²¹ To 2,2'-bis-methoxymethoxy-[1,1']binaphthalenyl-6,6'-dicarbonitrile (212 mg, 0.5 mmol) in CH₂Cl₂ (1 mL) was added at 0 °C a saturated methanolic HCl solution (2 mL). The mixture was stirred for 2 h at rt, and then treated with saturated NaHCO₃. Subsequently, the solution was diluted with CH₂Cl₂, extracted with brine and the organic layer dried (Na₂SO₄). After removal of the solvents, the crude product was recrystallized from CH₂Cl₂/pentane to afford 320 mg of **17** as a white solid (95% yield). ^1H NMR (300 MHz) δ 8.15 (s, 2H), 7.94 (d, $J=8.9$ Hz, 2H), 7.42 (d, $J=8.9$ Hz, 2H), 7.31 (d, $J=8.7$ Hz, 2H), 7.05 (d, $J=8.7$ Hz, 2H), 5.93 (br s, 2H); ^{13}C NMR (75 MHz) δ 154.5, 134.4, 133.4, 131.0, 127.2, 127.0, 124.3, 119.0, 118.0, 110.4, 106.1.

Acknowledgements

This work was supported by the Fonds der Chemischen Industrie and the Deutsche Forschungsgemeinschaft (DFG) within the Schwerpunktprogramm 1118. We thank Dr. M. Schneider, Schering AG, Berlin, and Professor Dr.

A. K. Yudin, University of Toronto, for providing samples of BINOL derivatives **14** and **18**, respectively.

References and notes

- (a) Krow, G. R. *Org. React.* **1993**, *43*, 251; (b) Hassal, C. H. *Org. React.* **1957**, *9*, 73; (c) Krow, G. R. *Comprehensive Organic Synthesis*; Trost, B. M., Fleming, I., Eds.; Pergamon: Oxford, 1991; Vol. 7, p 671; (d) Bolm, C. *Advances in Catalytic Processes*; Doyle, M. P., Ed.; JAI: Greenwich, 1997; Vol. 2, p 43; (e) Renz, M.; Meunier, B. *Eur. J. Org. Chem.* **1999**, 737.
- (a) Bolm, C.; Schlinghoff, G.; Weickhardt, K. *Angew. Chem., Int. Ed. Engl.* **1994**, *33*, 1848; (b) Gusso, A.; Baccin, R.; Pinna, F.; Strukul, G. *Organometallics* **1994**, *13*, 3442.
- (a) Bolm, C.; Luong, T. K. K.; Beckmann, O. *Asymmetric Oxidation Reactions*; Katsuki, T., Ed.; University Press: Oxford, 2001; p 147; (b) Bolm, C. *Peroxide Chemistry*; Adam, W., Ed.; Wiley-VCH: Weinheim, 2000; p 494; (c) Kelly, D. R. *Chim. Oggi* **2000**, *18*, 33 and 52; (d) Bolm, C.; Beckmann, O. *Comprehensive Asymmetric Catalysis*; Jacobsen, E. N., Pfaltz, A., Yamamoto, H., Eds.; Springer: Stuttgart, 1999; Vol. 2, p 803; (e) Strukul, G. *Angew. Chem., Int. Ed.* **1998**, *37*, 1199; (f) Bolm, C. *Med. Res. Rev.* **1999**, *19*, 348; (g) ten Brink, G.-J.; Arends, I. W. C. E.; Sheldon, R. A. *Chem. Rev.* **2004**, *104*, 4105; (h) Bolm, C.; Le Paih, J.; Frison, J. C. *Modern Oxidation Methods*; Bäckvall, J. E., Ed.; Wiley-VCH: Weinheim, 2004; p 253; (i) Bolm, C.; Palazzi, C.; Beckmann, O. *Transition Metals for Organic Synthesis*, 2nd ed.; Beller, M., Bolm, C., Eds.; Wiley-VCH: Weinheim, 2004; Vol. 2, p 267.
- (a) With Zr see: Watanabe, A.; Uchida, T.; Ito, K.; Katsuki, T. *Tetrahedron Lett.* **2002**, *43*, 4481; (b) Watanabe, A.; Uchida, T.; Irie, R.; Katsuki, T. *Proc. Natl. Acad. Sci. U.S.A.* **2004**, *101*, 5737; (c) With Hf see: Matsumoto, K.; Watanabe, A.; Uchida, T.; Ogi, K.; Katsuki, T. *Tetrahedron Lett.* **2004**, *45*, 2385.
- Bolm, C.; Frison, J.-C.; Zhang, Y.; Wulff, W. D. *Synlett* **2004**, 1516.
- (a) Bolm, C.; Beckmann, O.; Palazzi, C. *Can. J. Chem.* **2001**, *79*, 1593; (b) Bolm, C.; Beckmann, O.; Kühn, T.; Palazzi, C.; Adam, W.; Rao, P. B.; Saha-Möller, C. R. *Tetrahedron: Asymmetry* **2001**, *12*, 2441.
- For the aluminium complex, see: Evans, D. A.; Janey, J. M.; Magomedov, N.; Tedrow, J. S. *Angew. Chem., Int. Ed.* **2001**, *40*, 1884.
- (a) Yuan, Y.; Li, X.; Sun, J.; Ding, K. *J. Am. Chem. Soc.* **2002**, *124*, 14866; (b) Yuan, Y.; Long, J.; Sun, J.; Ding, K. *Chem.—Eur. J.* **2002**, *8*, 5033 and references therein.
- For successful applications of this ligand in sulfide oxidations, see: (a) Pelotier, B.; Anson, M. S.; Campbell, I. B.; Macdonald, S. J. F.; Priem, G.; Jackson, R. F. W. *Synlett* **2002**, 1055; (b) Legros, J.; Bolm, C. *Angew. Chem., Int. Ed.* **2004**, *43*, 4225; (c) Legros, J.; Bolm, C. *Angew. Chem., Int. Ed.* **2003**, *42*, 5487; (d) Legros, J.; Bolm, C. *Chem.—Eur. J.* **2005**, *11*, 1086.
- Ooi, T.; Ohmatsu, K.; Uraguchi, D.; Maruoka, K. *Tetrahedron Lett.* **2004**, *45*, 4481.
- Belokon, Y. N.; Bespalova, N. B.; Churkina, T. D.; Cisarova, I.; Ezernitskaya, M. G.; Harutyunyan, S. R.; Hrdina, R.; Kagan, H. B.; Kocovsky, P.; Kochetkov, K. A.; Larionov, O. V.; Lyssenko, K. A.; North, M.; Polasek, M.; Peregudov, A. S.; Prisyazhnyuk, V. O. V.; Vyskocil, S. *J. Am. Chem. Soc.* **2003**, *125*, 12860.

12. Chen, Y.; Yekta, S.; Yudin, A. K. *Chem. Rev.* **2003**, *103*, 3155.
13. Gong, L. Z.; Hu, Q. S.; Pu, L. *J. Org. Chem.* **2001**, *66*, 2358.
14. Bandin, M.; Casolari, S.; Cozzi, P. G.; Proni, G.; Schmohel, E.; Spada, G. P.; Tagliavini, E.; Umani-Ronchi, A. *Eur. J. Org. Chem.* **2000**, 491.
15. (a) For the preparation of substituted steroidal BINOL-type ligands, see: Schneider, M. F.; Harre, M.; Pieper, C. *Tetrahedron Lett.* **2002**, *43*, 8751. For applications of such ligands in asymmetric catalyses, see: (b) Enev, V. S.; Mohr, J.; Harre, M.; Nickisch, K. *Tetrahedron: Asymmetry* **1998**, *9*, 2693; (c) Bolm, C.; Dabard, O. *Synlett* **1999**, 360; (d) Kostova, K.; Genov, M.; Philipova, I.; Dimitrov, V. *Tetrahedron: Asymmetry* **2000**, *11*, 3253; (e) Hodgson, D. M.; Stupple, P. A.; Pierard, F. Y. T. M.; Labande, A. H.; Johnstone, C. *Chem.—Eur. J.* **2001**, *7*, 4465.
16. Ishitani, H.; Ueno, M.; Kobayashi, S. *J. Am. Chem. Soc.* **2000**, *122*, 8180.
17. (a) Sasai, H.; Tokunaga, T.; Watanabe, S.; Suzuki, T.; Itoh, N.; Shibasaki, M. *J. Org. Chem.* **1995**, *60*, 7388; (b) For the synthetic method, see: Sakamoto, T.; Ohsawa, K. *J. Chem. Soc., Perkin Trans. 1* **1999**, 2323.
18. Yudin, A. K.; Martyn, L. J. M.; Pandiaraju, S.; Zheng, J.; Lough, A. *Org. Lett.* **2000**, *2*, 41.
19. (a) Chen, R.; Qian, C.; de Vries, J. G. *Tetrahedron Lett.* **2001**, *42*, 6919; (b) Chen, R.; Qian, C.; de Vries, J. G. *Tetrahedron* **2001**, *57*, 9837; (c) Kumaraswamy, G.; Sastry, M. N. V.; Jena, N.; Ravi Kumar, K.; Vairamani, M. *Tetrahedron: Asymmetry* **2003**, *14*, 3797.
20. (a) For a review, see: Au-Yeung, T. T.-L.; Chan, S.-S.; Chan, A. S. C. *Adv. Synth. Catal.* **2003**, *345*, 537; (b) For the use of this ligand with aluminium, see: Lin, Y.-M.; Fu, I.-P.; Uang, B.-J. *Tetrahedron: Asymmetry* **2001**, *12*, 3217.
21. (a) See Ref. 17; (b) Morita, T.; Arai, T.; Sasai, H.; Shibasaki, M. *Tetrahedron: Asymmetry* **1998**, *9*, 1445.
22. (a) Blackmond, D. G. *Proc. Natl. Acad. Sci. U.S.A.* **2004**, *101*, 5732; (b) Kagan, H. B. *Adv. Synth. Catal.* **2001**, *343*, 227; (c) Girard, C.; Kagan, H. B. *Angew. Chem., Int. Ed.* **1998**, *37*, 2922; (d) Kagan, H. B.; Luukas, T. O. *Comprehensive Asymmetric Catalysis*; Jacobsen, E. N., Pfaltz, A., Yamamoto, H., Eds.; Springer: Stuttgart, 1999; Vol. 1, p 101; (e) Bolm, C. *Advanced Asymmetric Catalysis*; Stephenson, G. K., Ed.; Chapman and Hall: London, 1996; p 9.
23. Arai, T.; Sasai, H.; Yamagushi, K.; Shibasaki, M. *J. Am. Chem. Soc.* **1998**, *120*, 441.
24. Ketter, A.; Glahsl, G.; Herrmann, R. *J. Chem. Res., (S)* **1990**, 278; *J. Chem. Res., (M)* **1990**, 2118.

Conformationally controlled (entropy effects), stereoselective vibrational quenching of singlet oxygen in the oxidative cleavage of oxazolidinone-functionalized enecarbamates through solvent and temperature variations

J. Sivaguru,^a Marissa R. Solomon,^a Hideaki Saito,^{a,c,d} Thomas Poon,^e
Steffen Jockusch,^a Waldemar Adam,^{f,g} Yoshihisa Inoue^{c,d} and Nicholas J. Turro^{a,b,*}

^aThe Department of Chemistry, Columbia University, New York, NY 10027, USA

^bThe Department of Chemical Engineering, Columbia University, New York, NY 10027, USA

^cThe Department of Applied Chemistry, Osaka University, 2-1 Yamada-oka, Suita 565-0871, Japan

^dThe Entropy Control Project, ICORP, JST, 4-6-3 Kamishinden, Toyonaka 560-0085, Japan

^eJoint Science Department, W. M. Keck Science Center, 925 North Mills Avenue, Claremont McKenna,
Pitzer, and Scripps Colleges, Claremont, CA 91711, USA

^fInstitute für Organische Chemie, Universität Würzburg, D-97074 Würzburg, Germany

^gThe Department of Chemistry, University of Puerto Rico, Facundo Bueso 110, Rio Piedras, PR 00931, USA

Received 8 November 2005; revised 3 January 2006; accepted 13 January 2006

Available online 5 June 2006

We dedicate this work to our appreciated friend and distinguished colleague, Professor Sigfried Huenig
(University of Würzburg), on the occasion of his 85th birthday

Abstract—On photooxygenation (methylene blue as sensitizer) of *E/Z* enecarbamates, equipped with the oxazolidinone chiral auxiliary, the oxidative cleavage of the alkenyl functionality releases the enantiomerically enriched methyldeoxybenzoin (MDB) product. The *extent* (% ee) as well as the *sense* (*R* vs *S*) of the stereoselectivity in the MDB formation depends on the choice of the alkene configuration; the efficacy of stereocontrol may be tuned by appropriate solvent and temperature conditions. Highlighted is the finding that the formation of the preferred MDB enantiomer (*R* or *S*) depends for the *E* isomer on the chosen solvent and temperature, but not for the corresponding *Z* isomer. The activation parameters for the various solvents disclose that differential entropy effects ($\Delta\Delta S^\ddagger$) dominate the conformationally more flexible *E* diastereomers. As mechanistic rationale for this unprecedented conformationally imposed stereochemical behavior, we propose the competitive action of stereoselective vibrational quenching of the attacking singlet oxygen by the enecarbamate versus sterically controlled stereoselective oxidative cleavage of its double bond.

© 2006 Elsevier Ltd. All rights reserved.

1. Introduction

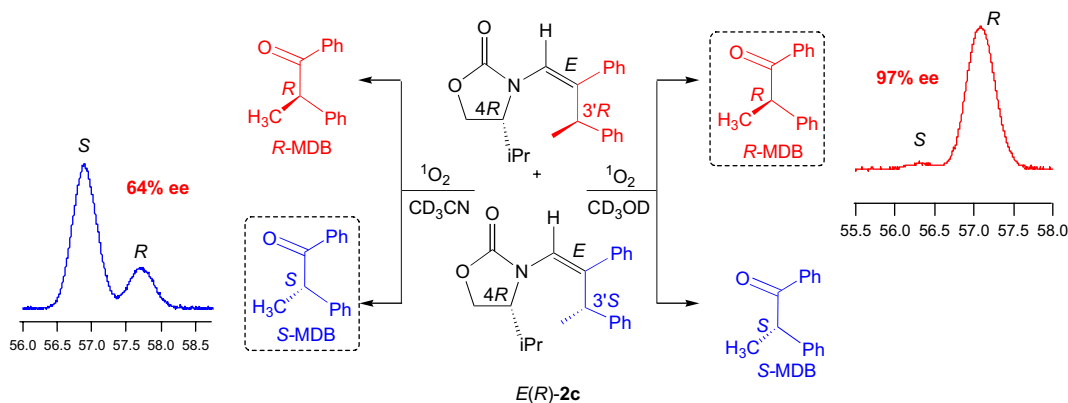
The success in achieving a high enantioselectivity in photochemical reactions^{1–3} depends on how effectively the spatial requirements of the process are manipulated within the short lifetimes of the excited states.⁴ To imprint stereocontrol in the photoproduct, organized assemblies^{5–10} have been employed with varying degrees of success; however, obtaining a high enantioselectivity in solution still constitutes a

formidable challenge.^{1–3} In this regard, a novel concept, which we have explored in the stereoselective photooxidative cleavage of chiral enecarbamates, involves selective deactivation (quenching) of one of the diastereomers in a pair of chiral excited states.^{11,12} Indeed, a high degree of stereocontrol may be imprinted in the photoproduct, but depending on the oxidant and the reaction conditions, the sense of the stereoselectivity may be reversed (Scheme 1).^{11–13}

Previously we have shown^{14–16} that such a photooxidative cleavage of enecarbamates actually entails a photooxygenation reaction,^{17–20} in which the diastereomerically pure [*1'S,2'S*] dioxetane intervenes, as exemplified for the chiral *Z*-configured enecarbamates in Figure 1. The salient reactivity feature in the exposed snapshot is the preferential

Keywords: Chiral auxiliary; Conformational effects; *E/Z* isomers; Mechanism; Photooxygenation; Substituent effects; Stereoselectivity; Vibrational quenching.

* Corresponding author. Tel.: +1 212 854 2175; fax: +1 212 932 1289; e-mail: njt3@columbia.edu



Scheme 1. Stereoselective photooxidative cleavage of oxazolidinone-functionalized *E*-encarbamates.

quenching of the electronically excited $^1\text{O}_2$ as it attacks from below, such that in addition to the steric preference for the approach of $^1\text{O}_2$ from above, the synergistic interplay of quenching and steric hindrance dictates the observed high diastereoselectivity. Moreover, the stereoselection in the dioxetane formation is independent of the configuration at the C-3' position of the alkyl side chain and the size of the alkyl substituent at the C-4 position of the oxazolidinone chiral auxiliary. Both, the methyl as well as the isopropyl derivatives $1'Z,4R(\text{Me}),3'S$ -**2b** and $1'Z,4R(\text{iPr}),3'R$ -**2c** afford the corresponding $[1'S,2'S]$ dioxetanes in diastereomeric ratios (dr) of about 95:5. For comparison, the encarbamate **Z-2a** without a substituent at the C-4 position of the oxazolidinone, i.e., the parent ring, displays no diastereoselectivity whatsoever in the dioxetane formation of the [2+2] cycloaddition with $^1\text{O}_2$.^{14–16}

In the present work, for comparison with the *Z* diastereomer, we have explored the photooxidative cleavage of the *E-2* encarbamates (see the structure matrix of Chart 1). These are equipped with the oxazolidinone chiral auxiliary for asymmetric induction, to yield MDB and **3** as photoproducts (Scheme 2).^{11,12} Analogous to the previously studied *Z* isomer,^{14–16,21} ca. 50:50 diastereomeric mixtures of the *R/S* isomers at the C-3' position in the alkene side chain were used, to assess how effective the stereocontrol would be in

the kinetic resolution. These derivatives constitute versatile and informative substrates for the study of conformational, electronic, stereoelectronic, and steric effects on the stereoselectivity in the photooxidation of the alkene functionality.^{11,12,14–16,21} Methylene blue was used to generate the singlet oxygen for the photooxidative cleavage of the alkenyl functionality in these chiral encarbamates to produce the optically active MDB product.

The extent of and the sense in the enantioselectivity were assessed for the *E* geometry of the alkene as function of (a) the alkyl substituent at the C-4 position of the oxazolidinone chiral auxiliary (see Chart 1), (b) the configuration of the alkyl substituent at the C-4 position of the oxazolidinone chiral auxiliary, (c) the solvent, and (e) the reaction temperature. Herewith we report the results of this extensive investigation, which evidently show that the difference in the spatial arrangement offered by the *E* versus *Z* diastereomers of the encarbamates is crucial. Furthermore, for achieving high stereoselectivity in the formation of the MDB product during the photooxygenation of the *E* encarbamates, we conjecture that the singlet oxygen is preferentially deactivated (quenched) in one of the epimeric transition structures for the *E*-encarbamate/ $^1\text{O}_2$ encounter complexes. Such selective quenching of diastereomeric excited states constitutes a promising *stereochemical tool*

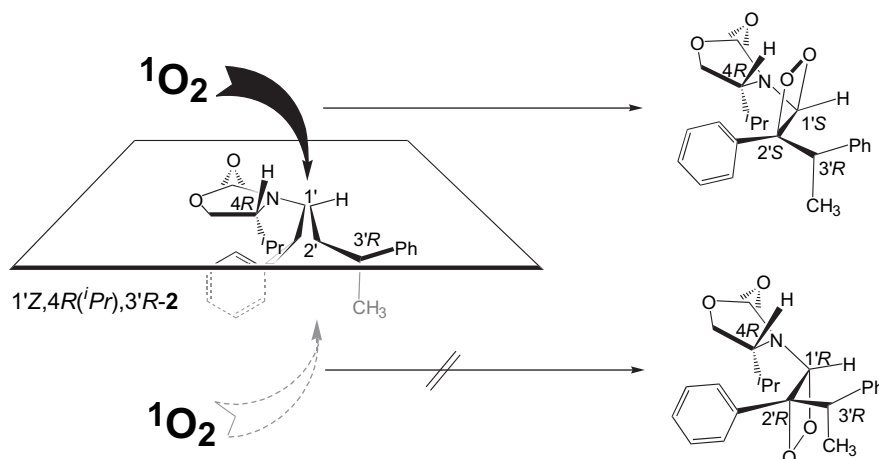


Figure 1. Preferred π -facial attack of $^1\text{O}_2$ from above controlled by the steric shielding of the 4-isopropoxyloxazolidinone substituent in the *Z* encarbamates.

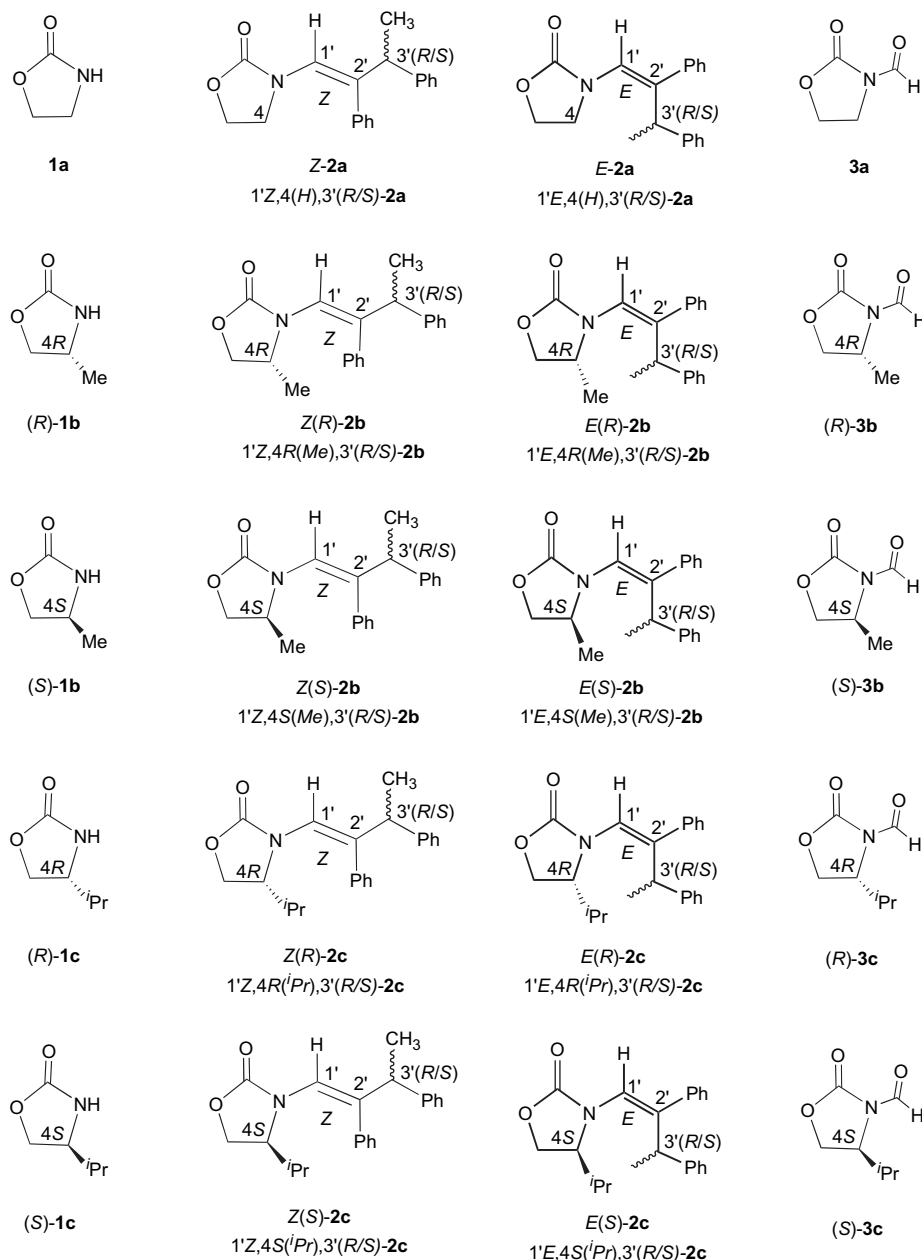


Chart 1. Structure matrix.

to effect the enantioselective photooxidative cleavage of chiral alkenes.

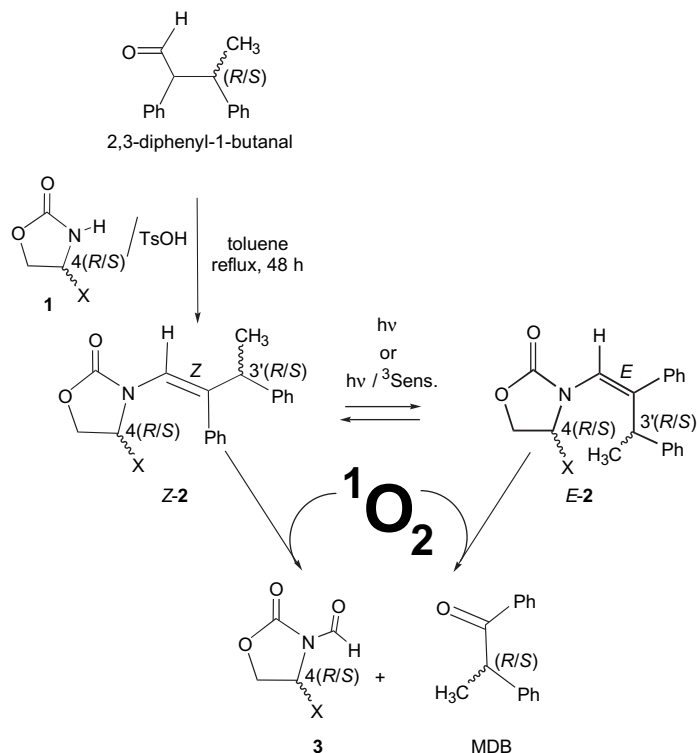
2. Experimental

2.1. Materials

All regular solvents were purchased from Aldrich and the deuterated solvents from Cambridge Isotope Labs and used as received. CDCl_3 was stored over sodium bicarbonate prior to use. Flash chromatography was carried out on silica gel, while 2-mm thick silica gel plates (EMD 60F) were employed for preparative TLC. Commercially available compounds were purified by standard procedures. The *Z*-2 enecarbamates were synthesized by a previously published procedure.^{11,12,14–16}

2.2. Methods

2.2.1. General procedure for the synthesis of the *E* enecarbamates *E*-2. A sample of 0.150 mmol of *Z*-2 (see Chart 1, Scheme 2) was dissolved in 20 mL of CH_2Cl_2 and placed into a quartz test tube, fitted with a rubber septum, gas delivery needle, and vent needle. The solution was purged for 20 min with dry N_2 gas and then irradiated at 254 nm in a Rayonet photochemical reactor for 20–30 min under a positive N_2 pressure. GC analysis of the photolysate showed that the photostationary state (*Z/E*=52:48) was reached after 20 min. The solvent was removed at ca. 25 °C and 15 Torr on a rotatory evaporator. The residue was loaded onto a preparative TLC plate and eluted with a 2:1 mixture of hexane and methyl *tert*-butyl ether (MTBE). The faster running fraction was extracted with a 1:1 mixture of CH_2Cl_2 and EtOAc



Scheme 2. Synthesis and photooxygenation of 4-oxazolidinone-functionalized *Z* and *E* enecarbamates.

to recover the starting material (*Z*-2). The slower running fraction was extracted with a 1:1 mixture of CH_2Cl_2 and EtOAc , to give 0.07 mmol of the corresponding *E*-2.

2.2.1.1. *E*(*R*)-2b. *E*(*R*)-2b was obtained in 95% yield according to the above general procedure. The two diastereomers 1'*E*,4*R*(Me),3'*R*-2b and 1'*E*,4*R*(Me),3'*S*-2b were separated on a preparative TLC plate by eluting with 2:1 hexane/methyl-*tert*-butyl ether mixture.

2.2.1.2. 1'*E*,4*R*(Me),3'*R*-2b. ^1H NMR (300 MHz, CDCl_3) δ^{ppm} =1.45 (d, J =6.10, 3H), 1.55 (d, J =7.14, 3H), 4.00 (m, 1H), 4.11 (m, 1H), 4.49 (m, 2H), 5.90 (s, 1H), 7.06 (m, 2H), 7.32 (m, 8H); ^{13}C NMR (75 MHz, CDCl_3) δ^{ppm} =16.9, 18.0, 39.4, 54.4, 120.7, 126.7, 127.4, 127.9, 128.3, 128.6, 129.4, 138.8, 143.6, 148.6, 157.1, 158.9; MS (FAB): $\text{M}+\text{H}^+$ Calcd 308.1572, Exptl 308.1644.

2.2.1.3. 1'*E*,4*R*(Me),3'*S*-2b. ^1H NMR (300 MHz, CDCl_3) δ^{ppm} =1.42 (d, J =5.93, 3H), 1.51 (d, J =7.23, 3H), 3.89 (m, 1H), 4.01 (m, 1H), 4.49 (m, 2H), 5.93 (s, 1H), 7.08 (m, 2H), 7.28 (m, 8H); ^{13}C NMR (75 MHz, CDCl_3) δ^{ppm} =17.4, 18.3, 54.6, 69.6, 121.2, 126.7, 127.5, 127.9, 128.2, 128.7, 129.5, 139.0, 143.6, 148.6, 159.0, 162.7; MS (FAB): $\text{M}+\text{H}^+$ Calcd 308.1572, Exptl 308.1656.

2.2.1.4. *E*(*R*)-2c. *E*(*R*)-2c was obtained in 95% yield according to the above general procedure. The two diastereomers 1'*E*,4*R*(*i*Pr),3'*R*-2c and 1'*E*,4*R*(*i*Pr),3'*S*-2c were separated on preparative TLC plate by eluting with 2:1 hexane/methyl-*tert*-butyl ether mixture.

2.2.1.5. 1'*E*,4*R*(*i*Pr),3'*R*-2c. ^1H NMR (300 MHz, CDCl_3) δ^{ppm} =0.76 (d, J =7.03, 3H), 0.86 (d, J =6.85, 3H), 1.33 (d,

J =7.20, 3H), 2.00–2.12 (m, 1H), 3.65 (ddd, J =8.10, 4.23, 3.66, 1H), 4.04 (dd, J =8.95, 4.33, 1H), 4.10 (t, J =8.68, 1H), 4.32 (q, J =7.20, 1H), 5.89 (s, 1H), 6.96–7.01 (m, 2H), 7.10–7.22 (m, 8H); ^{13}C NMR (75 MHz, CDCl_3) δ^{ppm} =14.6, 17.8, 18.4, 28.2, 39.2, 62.7, 63.1, 121.0, 126.3, 127.5, 127.6 (2C), 127.7 (2C), 128.2 (2C), 129.0 (2C), 138.9, 143.1, 146.1, 157.1; MS (FAB): $\text{M}+\text{H}^+$ Calcd 336.1958, Exptl 336.1972.

2.2.1.6. 1'*E*,4*R*(*i*Pr),3'*S*-2c. ^1H NMR (300 MHz, CDCl_3) δ^{ppm} =0.87 (d, J =6.92, 6H), 1.39 (d, J =7.20, 3H), 2.01–2.15 (m, 1H), 3.75 (ddd, J =8.70, 4.78, 3.92, 1H), 4.08 (dd, J =8.95, 4.88, 1H), 4.19 (t, J =8.80, 1H), 4.28 (q, J =7.20, 1H), 5.88 (s, 1H), 6.84–6.87 (m, 2H), 7.07–7.27 (m, 8H); ^{13}C NMR (75 MHz, CDCl_3) δ^{ppm} =15.6, 17.3, 18.6, 29.5, 39.5, 63.2, 63.9, 121.9, 126.7, 127.9, 128.0 (4C), 128.7 (2C), 129.4 (2C), 138.4, 142.2, 144.9, 157.1; MS (FAB): $\text{M}+\text{H}^+$ Calcd 336.1958, Exptl 336.1961.

2.2.1.7. *E*(*S*)-2c. *E*(*S*)-2c was obtained in 95% yield according to the above general procedure. The two diastereomers 1'*E*,4*S*(*i*Pr),3'*R*-2c and 1'*E*,4*S*(*i*Pr),3'*S*-2c were on preparative TLC plate by eluting with 2:1 hexane/methyl-*tert*-butyl ether mixture.

2.2.1.8. 1'*E*,4*S*(*i*Pr),3'*S*-2c. ^1H NMR (300 MHz, CDCl_3) δ^{ppm} =0.85 (d, 3H), 0.92 (d, 3H), 1.42 (d, 3H), 2.11–2.18 (m, 1H), 3.71–3.76 (ddd, 1H), 4.12 (dd, 1H), 4.19 (t, 1H), 4.41 (q, 1H), 5.97 (s, 1H), 7.06–7.11 (m, 2H), 7.20–7.34 (m, 8H); ^{13}C NMR (75 MHz, CDCl_3) δ^{ppm} =15.1, 18.5, 19.0, 28.2, 39.9, 62.9, 63.2, 121.4, 126.7, 127.9, 128.1 (4C), 128.7 (2C), 129.5 (2C), 138.9, 143.3, 146.6, 157.1; MS (FAB): $\text{M}+\text{H}^+$ Calcd 336.1958, Exptl 336.1952.

2.2.1.9. 1'E,4S(iPr),3'R-2c. $^1\text{H NMR}$ (300 MHz, CDCl_3) δ^{ppm} =0.96 (d, 6H), 1.42 (d, 3H), 2.12–2.22 (m, 1H), 3.81–3.87 (ddd, 1H), 4.16 (dd, 1H), 4.28 (t, 1H), 4.37 (q, 1H), 5.96 (s, 1H), 6.93–6.97 (m, 2H), 7.16–7.35 (m, 8H); $^{13}\text{C NMR}$ (75 MHz, CDCl_3) δ^{ppm} =15.6, 17.3, 18.6, 29.5, 39.5, 63.2, 63.9, 121.9, 126.7, 127.9, 128.0 (4C), 128.7 (2C), 129.4 (2C), 138.4, 142.2, 144.9, 157.1; MS (FAB): $\text{M}+\text{H}^+$ Calcd 336.1958, Exptl 336.1950.

2.3. Instrumentation

GC analyses were carried out on a Varian 3900 gas chromatograph, equipped with an auto-sampler. A Varian Factor-4 VG-1ms column ($l=25$ m, $\text{id}=0.25$ mm, and $\text{df}=0.25$ μm) was employed for the separation on the achiral stationary phase, with a program of 50 °C for 4 min, raised to 225 °C at 10 °C min^{-1} , and kept at 225 °C for 10 min. A Varian CP-Chirasil-DEX CB column ($l=25$ m, $\text{id}=0.25$ mm, and $\text{df}=0.25$ μm) was used for the separation on the chiral stationary phase, with a program of 135 °C for 70 min, raised to 200 °C at 15 °C min^{-1} , and kept at 200 °C for 30 min. The $^1\text{H NMR}$ and $^{13}\text{C NMR}$ spectra were recorded on BRUKER spectrometers (Model DPX300 or DRX300).

2.3.1. Photooxygenation of Z and E enecarbamates (see Chart 1). The appropriate Z or E enecarbamate **2** (see Scheme 2) and methylene blue sensitizer in 0.7 mL of the desired deuterated solvent (the enecarbamate concentration was 3.0×10^{-3} M and that of methylene blue was 3.7×10^{-4} M) were placed into the NMR tube, sealed with a rubber septum, and fitted with a gas delivery needle and a vent needle. Dry O_2 gas was purged through the sample for 20 min, while irradiating with a 500-W halogen lamp, equipped with a cutoff filter (<500 nm). After irradiation, the samples were submitted to $^1\text{H NMR}$ spectroscopy to determine the conversion (kept below 50%). The mass balance (based on unreacted enecarbamate and formed MDB product) and the conversion (based on unreacted enecarbamate) were determined by GC analysis on an achiral stationary phase, with 4,4'-di-*tert*-butylbiphenyl as calibration standard. The enantioselectivity (% ee) of the MDB product was determined by GC analysis on a chiral stationary phase.

3. Results

To assess the diastereoselectivity in the oxidative cleavage of the chiral enecarbamate substrate *E-2* as a function of temperature and solvent, the photooxygenation under a variety of conditions was examined. Evans' chiral auxiliary^{22,23} was chosen as the essential stereochemically directing entity and was introduced into the enecarbamate substrate *Z-2* by condensing the 4-alkyl-substituted oxazolidinones with the 2,3-diphenyl-1-butanal (see Scheme 2). The 1-phenylethyl substituent at the C-3' position of the double bond was selected to minimize the *ene* reaction;^{11,12,14–16} the required coplanar alignment of the only allylic hydrogen atom is encumbered. The *E-2* diastereomer was prepared by direct or sensitized photochemical isomerization of *Z-2*, followed by chromatographic separation (Scheme 2).²⁴ Analogous to the previously studied Z diastereomer,^{13–15} the photooxygenation of the *E-2* enecarbamate gave the expected chiral methyldeoxybenzoin (MDB) and the oxazolidinone

aldehyde **3** (see Scheme 2) quantitatively on complete conversion of the substrate. To recall, the thermally labile dioxetane intermediate was previously detected at –35 °C and was shown to decompose readily at room temperature (ca. 20 °C) into MDB and aldehyde **3**.^{13–15}

To assess the diastereoselectivity in the oxidative cleavage of the chiral enecarbamate substrate *E-2* as a function of temperature and solvent, the photooxygenation under a variety of conditions was examined. The new results for the *E-2* diastereomers are collected in Table 1, together (for comparison purposes) with the relevant data of the already published *Z-2* diastereomers.^{13–15} As for the previously studied *Z-2* diastereomers,^{13–15} we employed a ca. 50:50 diastereomeric mixture of the *R* and *S* isomers at the C-3' position also in the photooxygenations of the *E-2* enecarbamates. The conversion was kept below 50% to avoid overoxidation, which would therewith distort the ee values.

The negligible effect of the alkyl substituent at the oxazolidinone C-4 position in the photooxidative cleavage of the chiral enecarbamates **2** is exemplified for the *E* diastereomer with the methyl [*E(R)-2b*] and the isopropyl [*E(R)-2c*] groups (Table 1). In CDCl_3 at 18 °C the *E(R)-2b* (entry 2) gave the *R*-MDB enantiomer with an ee value of 67% at 19% conversion ($s=5.9$) and the *E(R)-2c* (entry 2) an ee value of 63% at 17% conversion ($s=5.0$). The respective s factors (see Eq. 1) convincingly express the relatively low response to the steric factors of the oxazolidinone chiral auxiliary. For this reason, hereafter we shall concentrate on the isopropyl derivative *E-2c*.

As already demonstrated previously for the Z series of diastereomers,^{13–15} the sense of the enantioselectivity in the MDB product is opposite, while the extent of diastereomeric control in the photooxidative cleavage of the *E* enecarbamates is the same (within the experimental error) for the *R* and *S* antipodes at the C-4 position (Table 1). This is clearly evident in the % ee data for the *E(R)-2c* and *E(S)-2c* isomers, as exemplified by their photooxygenation in CD_2Cl_2 at 20 °C. As expected, the reversal in the enantioselectivity sense was also seen for *E(R)-2c* (entries 5–7) and affords the *S*-MDB (34% ee at 25% convn), whereas *E(S)-2c* (entries 17–19) leads to the *R*-MDB (28% ee at 29% convn) enantiomer as final oxidation products.

The effect of the solvent type and polarity was examined by comparing the polar aprotic solvent CD_3CN , the polar protic solvent CD_3OD , and the halogenated solvents CD_2Cl_2 and CDCl_3 , which are of relatively low polarity. For the photooxidative cleavage of the *E-2c* substrate, the solvent dependence of the diastereoselectivity follows the order CD_3CN (30%) \sim CD_2Cl_2 (34%) $<$ CDCl_3 (63%) $<$ CD_3OD (85%) at the common temperature of about 18–20 °C (Table 1, entries 9, 5, 2 and 13, respectively); the ee values are given in parentheses. Evidently, the best diastereoselectivity is obtained for the hydrogen-bonding solvent methanol (entry 13), whereas the lowest control is displayed by the aprotic acetonitrile (entry 9) at the same temperature. The relatively high ee value in chloroform-*d* (entries 1–4) is quite striking. Mechanistically most revealing is the finding that the *R*-MDB enantiomer is the favored product in CDCl_3 and CD_3OD (entries 2 and 13, respectively), but the *S*-MDB isomer

Table 1. Determination of the stereoselectivity factor (*s*) for the formation of (*R/S*)-MDB product in the photooxygenation^a of *E(R)*-**2b**, *E(R)*-**2c**, and *E(S)*-**2c** as a function of solvent and temperature

Entry	Temp (°C)	Solvent	<i>E(R)</i> - 2b			<i>E(R)</i> - 2c		
			MDB ^b (% ee)	Conv ^c (%)	<i>s</i> ^d	MDB ^b (% ee)	Conv ^c (%)	<i>s</i> ^d
1.	50	CDCl ₃	—	—	—	8 (<i>S</i>)	5	1.2
2.	18		67 (<i>R</i>)	19	5.9	63 (<i>R</i>)	17	5.0
3.	−15		85 (<i>R</i>)	14	14.0	78 (<i>R</i>)	37	13.0
4.	−40		86 (<i>R</i>)	52	45.0	88 (<i>R</i>)	43	31.0
5.	20	CD ₂ Cl ₂	7 (<i>S</i>)	10	0.9	34 (<i>S</i>)	25	2.3
6.	−20		62 (<i>R</i>)	23	5.1	27 (<i>R</i>)	65	2.7
7.	−60		95 (<i>R</i>)	31	59.0	82 (<i>R</i>)	54	40.0
8.	50		—	—	—	64 (<i>S</i>)	23	5.5
9.	18	CD ₃ CN	28 (<i>S</i>)	18	0.5	30 (<i>S</i>)	34	2.1
10.	−15		0	55	1.0	0	28	1.0
11.	−40		45 (<i>R</i>)	33	3.3	58 (<i>R</i>)	37	5.2
12.	50		—	—	—	70 (<i>R</i>)	30	7.6
13.	18	CD ₃ OD	75 (<i>R</i>)	17	8.1	85 (<i>R</i>)	34	19.0
14.	−15		80 (<i>R</i>)	13	10.0	90 (<i>R</i>)	17	23.0
15.	−40		86 (<i>R</i>)	13	15.0	94 (<i>R</i>)	12	37.0
16.	−70		—	—	—	97 (<i>R</i>)	8	72.0
17.	20	CD ₂ Cl ₂	—	—	—	28 (<i>R</i>)	29	2.0
18.	−20		—	—	—	36 (<i>S</i>)	59	3.4
19.	−60		—	—	—	88 (<i>S</i>)	56	45.0

^a The *E* enecarbamate concentration is 3.0×10^{-3} M and 3.7×10^{-4} M for the methylene blue sensitizer.

^b The enantiomeric excess (% ee) of the MDB product, determined by GC analysis on a chiral stationary phase.

^c Conversion (convn) of enecarbamates determined by GC analysis on an achiral stationary phase with 4,4'-di-*tert*-butylbiphenyl as calibration standard, and by ¹H NMR spectroscopy; averages of three runs, within 5% error of the stated values.

^d Calculated from Eq. 1.

dominates in CD₂Cl₂ and CD₃CN (entries 5 and 9, respectively). Thus, the selectivity cannot be attributed to the solvent polarity alone in the photooxidative cleavage of the *E*-**2** enecarbamates.

Still more intriguing for mechanistic considerations is the temperature dependence of the ee values for the *E*-**2c** substrate (Table 1). Only in methanol the extent of the diastereoselectivity is relatively constant (note the high ee value of 97% at −70 °C, i.e., nearly perfect stereocontrol!) and the

same enantiomer, namely *R*-MDB, is formed over the entire temperature range from −70 to +50 °C (entries 12–16). In the other solvents, depending on the temperature, a change in the sense from the usual *R*-MDB to the *S*-MDB isomer is observed. For example, very good stereocontrol (ee value of 88%) in favor of *R*-MDB is found in chloroform-*d* at −40 °C (entry 4), but the *S*-MDB isomer is preferred with very poor diastereoselectivity (ee value of only 8%) at +50 °C (entry 1). This inflection in the enantioselectivity sense (*R* to *S* isomer) occurs in CDCl₃ above +18 °C (entries

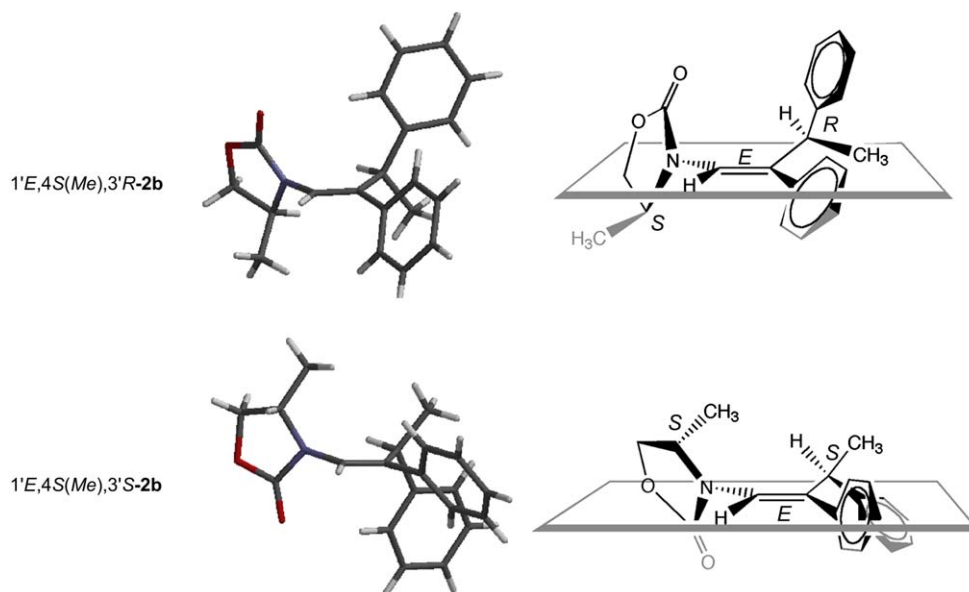


Figure 2. X-ray crystal structure (Ref. 25) of 1'*E*,4*S*(Me),3'*R*-**2b** and 1'*E*,4*S*(Me),3'*S*-**2b**.

1 and 2), while in CD_2Cl_2 it takes place between $+20\text{ }^\circ\text{C}$ and $-20\text{ }^\circ\text{C}$ (entries 5 and 6). In the case of CD_3CN , the temperature at which the change of sense takes place is $-15\text{ }^\circ\text{C}$ (entry 10), as indicated by the 0% ee value in the MDB product (see Table 1). These profound selectivity trends require careful mechanistic scrutiny, to understand the details of the photocleavage pathway.

To enable a detailed mechanistic rationalization of the favored attack by $^1\text{O}_2$ on the double bond of the enecarbamate, the structural details of the chiral enecarbamate must be known reliably. Fortunately, we succeeded in crystallizing the methyl derivative $E(S)\text{-2b}$ from ether/hexane and obtained its solid-state structure by X-ray crystallography (Fig. 2).²⁵

As displayed in Figure 2, both diastereomers $1'E,4S(\text{Me}),3'R\text{-2b}$ and $1'E,4S(\text{Me}),3'S\text{-2b}$ are contained in the same unit cell. Inspection of the crystal structure reveals that the oxazolidinone carbonyl is almost perpendicular to the plane of the double bond, such that the nitrogen lone pair is contained within that plane for conjugation with the carbonyl group. The phenyl substituent on the double bond is also twisted out of conjugation, to minimize the steric interactions with the phenethyl side chain. Presumably, polarity factors of the oxazolidinone functionality and steric interactions with the alkyl side chain are minimized in the observed conformation.

4. Discussion

The salient features of photooxygenation of the $E\text{-2}$ and the $Z\text{-2}$ diastereomers of the enecarbamates are three-fold:

- While the photooxidative cleavage of the $E\text{-2}$ isomer affords the MDB product in high (up to 97%) enantioselectivity (Table 1), the ee value for the $Z\text{-2}$ isomer is quite low (only 30% at best) under comparable reaction conditions;^{11,12,14–16}
- The enantiomeric excess in the MDB product depends substantially on the solvent and the temperature of the photooxygenation for the $E\text{-2}$ isomer (Table 1), but that is not the case for the corresponding $Z\text{-2}$ enecarbamate;^{11,12,14–16}
- Not only does the extent of stereoselection (% ee value) of the $E\text{-2}$ diastereomer vary extensively as a function of solvent and temperature (Table 1), but also the favored configuration (R vs S enantiomers of MDB) changes, i.e., there is an inversion point in the sense of the stereoselectivity.

This divergent behavior in the stereocontrol displayed by the two geometrical isomers E and Z needs to be mechanistically rationalized in terms of the trajectory of the $^1\text{O}_2$ attack onto the double bond during the photooxidative cleavage of the enecarbamate substrate. Since we have employed for the photooxygenation a ca. 50:50 diastereomeric mixture of enecarbamates $E\text{-2}$ (R/S epimers at the $C\text{-3'}$ stereogenic site of the alkyl side chain), the stereoselection in the present study entails a case of *kinetic resolution*. Thus, the enantiomeric excess in the MDB product, which is formed in the double-bond cleavage, reflects the differentiation in the reaction rates of the enecarbamate photooxidation. For such

kinetic resolution, the so-called stereoselectivity factor (s) applies (Eq. 1),^{26–29} which is a quantitative measure (corrected for the extent of conversion) of the relative reaction rates for the two stereoisomers in question. In the present photooxygenation of the enecarbamates $\mathbf{2}$, the s factor for the two epimers from the substrate conversion and the MDB enantiomeric excess. A large value will translate into high enantiomeric excess in the MDB product even at 50% conversion (see Fig. 3). This is the case, for example, in the photooxidation of the $E(R)\text{-2c}$ substrate in CD_3OD at $-70\text{ }^\circ\text{C}$ with the s factor of $\mathbf{72}$ (see Table 1, entry 16).

$$s = \frac{k_R}{k_S} = \frac{\ln[1 - C(1 + ee_{\text{MDB}})]}{\ln[1 - C(1 - ee_{\text{MDB}})]} \quad (1)$$

where C is the conversion and ee_{MDB} is the ee value of the MDB product.

As a practical utilization of such a high s factor for the *kinetic resolution* with $^1\text{O}_2$, the photooxygenation of $E(R)\text{-2c}$ was run in CD_3OD at $-70\text{ }^\circ\text{C}$ up to nearly 50% conversion. The $R\text{-MDB}$ product was separated from the reaction mixture by chromatography and an ee value of 97% was obtained. The unreacted $1'E,4R(^i\text{Pr}),3'S\text{-2c}$ enecarbamate was then quantitatively photooxidized at room temperature to afford the $S\text{-MDB}$ product with an ee value of 97%. This remarkable case of $^1\text{O}_2$ stereoselection was previously coined as *photochemical Pasteur-type kinetic resolution*.^{11,13,26–29}

To understand the temperature dependence of the enantiomeric excess in the MDB product for the photooxygenation of $E(R)\text{-2c}$ in the various solvents, the differential activation parameters ($\Delta\Delta S^\ddagger$ and $\Delta\Delta H^\ddagger$) were computed with the help of Eyring relation (Eq. 2):^{2,30,31}

$$\ln(k_R/k_S) = \Delta\Delta S^\ddagger_{R-S}/R - \Delta\Delta H^\ddagger_{R-S}/RT \quad (2)$$

The $\Delta\Delta S^\ddagger$ and $\Delta\Delta H^\ddagger$ data for the $E(R)\text{-2b}$ and $E(R)\text{-2c}$ diastereomers are collected in Table 2, together with the previously investigated $Z(R)\text{-2c}$ in CD_2Cl_2 for comparison.¹⁰

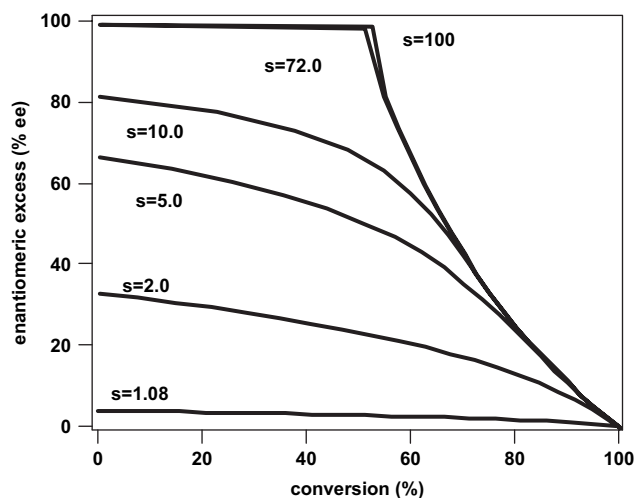


Figure 3. The dependence of the enantiomeric excess of the MDB product on the conversion of chiral oxazolidinone-functionalized enecarbamates as a function of the stereoselectivity factor (s).^{26–29}

Table 2. Solvent dependence of the differential activation parameters^a for the photooxygenation of *E(R)*-2b, *E(R)*-2c, *E(S)*-2c, and *Z(R)*-2c in different solvents

Entry	Solvent	<i>E(R)</i> -2b		<i>E(R)</i> -2c	
		$\Delta\Delta H^\ddagger$ (kcal mol ⁻¹)	$\Delta\Delta S^\ddagger$ (cal mol ⁻¹ K ⁻¹)	$\Delta\Delta H^\ddagger$ (kcal mol ⁻¹)	$\Delta\Delta S^\ddagger$ (cal mol ⁻¹ K ⁻¹)
1	CDCl ₃	-4.9	-14	-4.5	-14
2	CD ₂ Cl ₂	-6.6	-23	-4.0	-15
3	CD ₃ CN	-4.4	-17	-4.5	-17
4	CD ₃ OD	-1.5	-1.0	-2.5	-4.9
<i>E(S)</i> -2c					
5	CD ₂ Cl ₂			5.3	19.0
<i>Z(R)</i> -2c					
6	CD ₂ Cl ₂			-0.2	0.4

^a $\Delta\Delta H^\ddagger$ and $\Delta\Delta S^\ddagger$ were computed from Eq. 2.

The data for the *E*-2 isomer in the aprotic solvents CDCl₃, CD₂Cl₂, and CD₃CN display (Table 2, entries 1–3) a pronounced temperature dependence of the MDB enantiomeric excess, namely, a relatively high contribution by the differential activation entropy term ($|\Delta\Delta S^\ddagger| \geq 14$ cal mol⁻¹ mol⁻¹), as well as an appreciable contribution by the differential activation enthalpy term ($|\Delta\Delta H^\ddagger| \sim 4$ kcal mol⁻¹). As may be seen from the differential Eyring relation (Eq. 2), the change in the % ee values (or $\Delta\Delta G^\ddagger$) depends both on the entropic and enthalpic terms. Since the $\Delta\Delta H^\ddagger_{R-S}/RT$ term is proportional to the reciprocal temperature (Eq. 2), the $\ln(k_R/k_S)$ value is determined mostly by the enthalpic contribution at low temperatures; however, as the temperature increases, the relative contribution from the $\Delta\Delta S^\ddagger_{R-S}/R$ term increases and begins to override the $\Delta\Delta H^\ddagger_{R-S}/RT$ term at some temperature. Eventually, the sign of the $\ln(k_R/k_S)$ value inverts and the enantioselectivity sense switches, provided that the $\Delta\Delta H^\ddagger_{R-S}$ and $\Delta\Delta S^\ddagger_{R-S}$ terms possess the same sign, as is the case here for the photooxygenation of the *E*-2 isomer (Table 2, entries 1–3). Such entropy effects are indicative of conformational factors,^{2,30,31} which in the present case are dictated, presumably, by the stereogenic center at the C-3' position of the phenethyl side chain.

In contrast, the corresponding *Z*-2c isomer is insensitive to temperature, as convincingly exposed by the near-zero $\Delta\Delta S^\ddagger$ and $\Delta\Delta H^\ddagger$ terms in CD₂Cl₂ with opposite sign (Table 2, entry 6);^{2,30,31} consequently, irrespective of what temperature is chosen, the *R*-enantiomeric MDB product is enhanced (as $\Delta\Delta S^\ddagger$ and $\Delta\Delta H^\ddagger$ compensate each other upon temperature variations due to the opposite sign), but in modest preference. Similarly, in the protic CD₃OD solvent, also for the *E*-2 isomer a small temperature dependence is observed (Table 1, entries 12–16), again corroborated by the small $\Delta\Delta S^\ddagger$ and $\Delta\Delta H^\ddagger$ values (Table 2, entry 4). As a consequence of the low entropy and enthalpy contributions, in the protic methanol (notice the same sign for $\Delta\Delta S^\ddagger$ and $\Delta\Delta H^\ddagger$; upon decreasing the temperature the contribution from $\Delta\Delta H^\ddagger$ will increase slightly), the response of the *E*-2 isomer to temperature is nominal; certainly the sense of the enantioselectivity is not changed.

An effective visual display of these experimental trends in the temperature dependence of k_R/k_S as a function of the solvent nature is given in Eyring plots for *E*-2c (Fig. 4). The

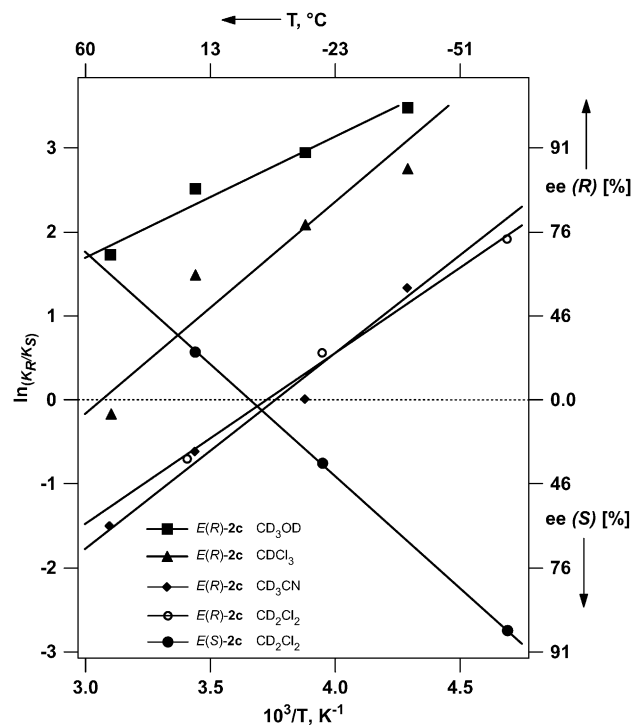


Figure 4. Eyring plots for the stereoselective photooxygenation of *E(R)*-2c and *E(S)*-2c enantiomers in various solvents.

nearly parallel lines (similar slopes) bring out the fact that the extent of enthalpic contribution ($\Delta\Delta H^\ddagger$) is about the same as that in the diverse solvents, but the crossing of the 0% ee line reflects the change in the sense of specification of the favored configuration for the MDB enantiomer. Another point that is focused well in Figure 4, is the mirror imaging of the two lines for the *E(R)*-2c [—○—] and *E(S)*-2c [—●—] diastereomers upon photooxygenation in CD₂Cl₂, which conveys the stereocontrol by the stereogenic center at the C-4 position of the oxazolidinone chiral auxiliary. The similar magnitudes but opposite signs of the $\Delta\Delta S^\ddagger$ and $\Delta\Delta H^\ddagger$ terms for the oppositely configured *E(R)*-2c and *E(S)*-2c diastereomers in CH₂Cl₂ (Table 2; entries 2 and 5, respectively) are dictated by mirroring of the two lines in Figure 4. The intersection of the two lines signifies the temperature (*inversion* temperature, -3 °C for CD₂Cl₂) at which the entropic contribution equals the enthalpic contribution, which will be reflected in the 0% ee value in the MDB product.

These conspicuously complex temperature and solvent effects on the stereoselectivity of the *E* and *Z* enantiomers photooxygenation shall now be mechanistically scrutinized. As already anticipated, conformational factors may be responsible for the difference in the sensitivity response between the *E* and *Z* oxazolidinone-functionalized enantiomers toward solvent and temperature variations. To assess such conformational factors, detailed X-ray crystal structures of the *E* and *Z* diastereomers should be helpful; however, such structures are not necessarily definitive, since our photooxygenations are conducted in the solution phase and not in the solid state, for which the actual conformations may differ appreciably. The pertinent crystal structures are given in Figure 5, which disclose some significant conformational differences.

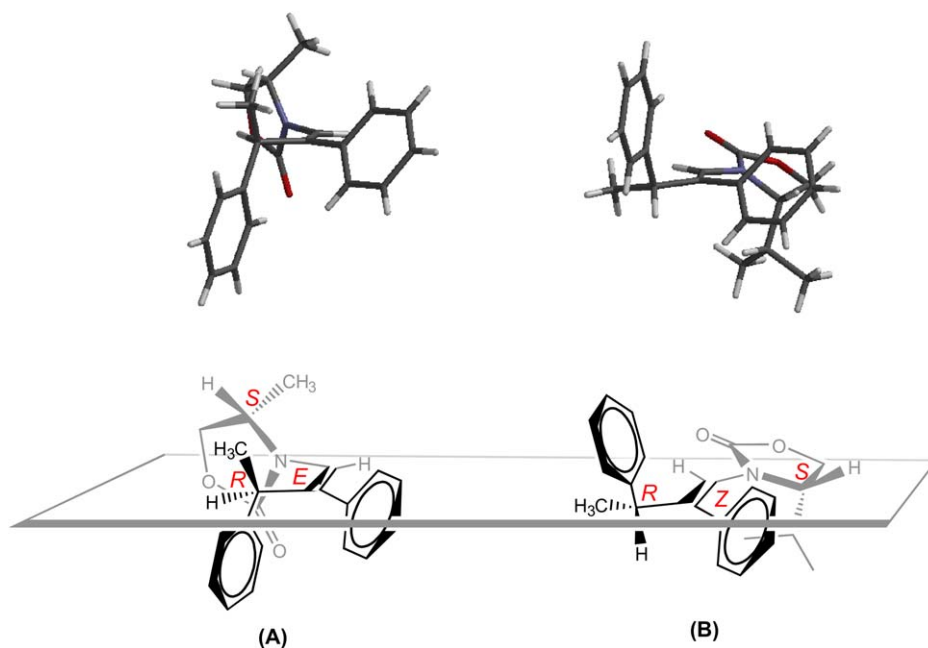


Figure 5. Comparison of the favored conformers for the *E*-4*S*(Me),3'*S*-**2b** (A) and *Z*-4*S*(*i*Pr),3'*S*-**2c** (B) enecarbamates, as revealed by the corresponding solid-state structures, of the *E*-4*S*(Me),3'*S*-**2b** (A) and *Z*-4*S*(*i*Pr),3'*S*-**2c** (B) enecarbamates (for clarity, only the 4*R*,3'*S* epimers are shown), which disclose some pertinent conformational differences. It should, however, be emphasized that in (A) we are using the *methyl* derivative, whereas in (B) the *isopropyl* one; unfortunately, the crystal structures are not available for the same alkyl group at the C-4 position of the oxazolidinone chiral auxiliary; nevertheless, for the present discussion it is not the substituent in the oxazolidinone chiral auxiliary that counts, but the *E* and *Z* geometries of the double bond.

As illustrated in Figure 5, the oxazolidinone carbonyl of the *E* isomer (C-3'*S* epimer) is oriented above the plane of the double bond (for the other C-3'*R* epimer, the oxazolidinone carbonyl is oriented below),²⁵ compared to the coplanar alignment of the *Z* isomer (see Fig. 5).^{13–15} Moreover, molecular models and quantum-chemical computations suggest that the *Z* diastereomer^{13–15} is conformationally more rigid than the *E* one. The greater flexibility of the *E* conformer appears to be due to less steric encumbrance between the imposing phenyl and oxazolidinone groups. Therefore, we speculate that the more mobile *E* conformer is more susceptible to solvent and temperature variations, as confirmed by the larger $\Delta\Delta S^\ddagger$ contribution (Table 2). Correspondingly, the greater rigidity of the *Z* conformer makes it less sensitive to solvent and temperature variations, as reflected by the lower $\Delta\Delta S^\ddagger$ values (Table 2). Further work would be required, to confirm the higher flexibility of the *E* conformer, e.g., NOESY and NOE NMR spectroscopy as well as theoretical studies would be helpful.

The enthalpy–entropy plot for both the *E* and *Z* enecarbamates is shown in Figure 6. The differential activation parameters fall on a single straight line passing through the origin, which indicates that the same diastereo-differentiating mechanism operates, irrespective of (a) the configuration of the double bond [*E* or *Z*], (b) the alkyl substituent at the C-4 position [Me or *i*Pr], (c) the configuration of the C-4 substituent [*R* or *S* isomer], and (d) the solvent that is employed.

A pertinent aspect to be rationalized is the higher stereoselectivity of the *E* compared to the *Z* enecarbamate. It is truly remarkable that the smallest possible oxidant, namely *singlet oxygen*, is subject to such high stereocontrol. To understand the higher stereocontrol for the *E* isomer, we shall explore now the details of the trajectory for the incoming ¹O₂

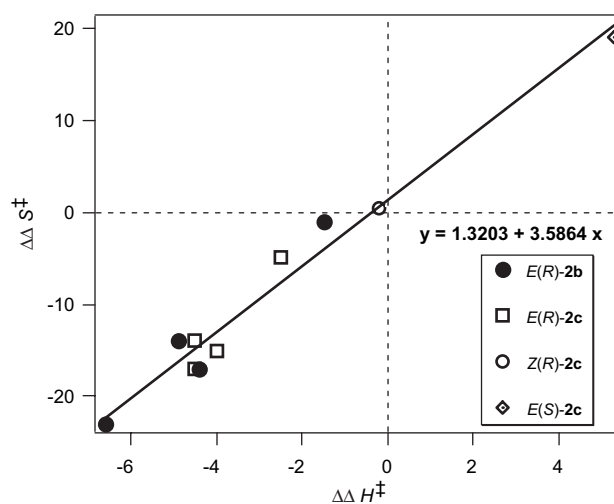


Figure 6. Plot of $\Delta\Delta S^\ddagger$ versus $\Delta\Delta H^\ddagger$ for the photooxygenation of *E*(*R*)-**2b**, *E*(*R*)-**2c**, *E*(*S*)-**2c**, and *Z*(*R*)-**2b**.

onto the double bond of the chiral enecarbamate, to reveal the critical oxidant/substrate interactions in the attack. As exemplified in Figure 2, the configuration at the C-3' position, i.e., 3'*R* versus 3'*S*, plays an important role in aligning the oxazolidinone carbonyl with respect to the face of the double bond. In 1'*E*,4*S*(Me),3'*R*-**2b**, the oxazolidinone carbonyl is oriented toward the top face of the double bond, whereas in the 1'*E*,4*S*(Me),3'*S*-**2b** epimer it is steered toward the bottom face. Although it is well known that polar groups may facilitate the facial selectivity of singlet oxygen,³² in the present case, this alone does not explain the high selectivity for the *E* isomer. The reason is that the relative spatial arrangement of the carbonyl and the phenethyl groups is the same in both the structures and, thus, equal

amounts of the *R*- and *S*-MDB enantiomers would be expected. Evidently, besides conformational and steric factors, additional interactions must be involved.

We propose that the high stereocontrol in the *R*-MDB versus *S*-MDB formation for the photooxidative cleavage of the *E* isomer is the consequence of selective π -facial quenching of the electronically excited singlet oxygen by the enecarbamate substrate. In this context, it is well known that the lifetime of singlet oxygen in deuterated solvents is much higher than non-deuterated ones,^{17–20} since C–H bond vibrations deactivate $^1\text{O}_2$ to its triplet ground state.³³ In view of the higher flexibility of *E* enecarbamates, conformations may be populated, in which one π face of the double bond exposes a larger number of C–H bonds for selective quenching³³ of the incoming excited $^1\text{O}_2$. In the present case of *kinetic resolution*, to generate selectively the *R*-MDB enantiomer in excess from the $3'R/3'S$ diastereomeric pair, the $3'S$ epimer must be preferentially quenched and thereby accumulates. We have previously shown low selectivity in the MDB product for photooxidation of both *E* and *Z* enecarbamates with ozone—a reactive ground state species.³⁴ A more careful inspection of the solid-state structures for the $3'R/3'S$ diastereomeric pair in Figure 2 reveals that in the $3'R$ epimer, the methyl groups of the oxazolidinone ring and the phenethyl side chain are located on opposite π faces of the double bond, whereas in the $3'S$ epimer these methyl groups are on the same side (in the shown structure, above the plane of the double bond). If such conformationally imposed structural differences apply also in the solution phase, the attacking $^1\text{O}_2$ is more efficiently deactivated by the $3'S$ epimer and the *R*-MDB enantiomer is favored, as observed in aprotic solvents at subambient temperature (Table 1). The more efficient stereocontrol (higher % ee values in favor of the *R*-MDB enantiomer) as the temperature is decreased (Table 1), may arise from populating in solution, the favored conformations of the $3'R/3'S$ diastereomeric pair. Consequently, at the lower temperature limit, the *R*-MDB enantiomer is favored due to more effective $^1\text{O}_2$ quenching, whereas at the higher temperature limit the proportion of *S*-MDB product increases because the mechanism of selective π -facial quenching is depreciated as a result of efficient conformational equilibration. In the latter situation, presumably steric effects override physical deactivation of the electronically excited $^1\text{O}_2$. Evidently, the complex stereoselectivity behavior presently observed in the photooxidative cleavage of the chiral enecarbamates **2** (Table 1, Fig. 4) is a delicate balance between the steric interactions and quenching in the $^1\text{O}_2$ /substrate encounter, imposed by temperature-dependent and solvent-dependent conformational preferences.

5. Conclusion

It should be evident that the extensive stereochemical properties embodied in the chiral oxazolidinone-substituted enecarbamates (i.e., the chirality center at the C-4 position of the oxazolidinone ring, the chirality center at the C-3' position of the phenethyl side chain, and the *E/Z* configurations of the alkene functionality) make these substrates informative molecular probes to explore the mechanistic intricacies of kinetic resolution in the photooxidative cleavage of the alkene double bond to the enantiomerically enriched MDB.

The stereoselection of the kinetically preferred MDB enantiomer depends not only on the alkene geometry (*Z/E*), the size of the C-4 alkyl substituent (H, Me, ^tPr) in the oxazolidinone ring, and the configuration (*R/S*) at the C-3' stereogenic center of the phenethyl side chain, but also on the nature of the solvent and the reaction temperature. The conformationally more flexible *E* diastereomer responds sensitively to such reaction conditions (ee values of up to 97%), whereas the conformationally more rigid *Z* diastereomer behaves impervious to such manipulation (ee values of up to 30%). We argue that the stereochemical consequences of such conformational effects (entropy control) are stereoselective quenching of $^1\text{O}_2$ by vibrational deactivation (a novel concept), in competition with stereoselective oxidative double-bond cleavage subject to steric interactions on the attacking $^1\text{O}_2$.

Acknowledgements

The authors at Columbia thank the NSF (CHE 01-10655 and CHE-04-15516) for generous support of this research. W.A. is grateful for the financial support from the Deutsche Forschungsgemeinschaft, Alexander-von-Humboldt Stiftung, and the Fonds der Chemischen Industrie. T.P. acknowledges the support of the W.M. Keck Foundation. H.S. and Y.I. gratefully acknowledge a JSPS research for fellowship for young scientists (08384) for young scientists to H.S. The authors thank Dr. Sara G. Bosio for initiating the work on the photooxygenation of *Z* enecarbamates.

References and notes

1. Inoue, Y.; Ramamurthy, V. *Chiral Photochemistry*; Marcel Dekker: New York, NY, 2004; pp 685.
2. Inoue, Y. *Chem. Rev.* **1992**, *92*, 741–770.
3. Rau, H. *Chem. Rev.* **1983**, *83*, 535–547.
4. Turro, N. J. *Proc. Natl. Acad. Sci. U.S.A.* **2002**, *99*, 4805–4809.
5. Turro, N. J.; Cheng, C. C.; Abrams, L.; Corbin, D. R. *J. Am. Chem. Soc.* **1987**, *109*, 2449–2456.
6. Ramamurthy, V. *Photochemistry in Organized and Confined Media*; Wiley-VCH: New York, NY, 1991.
7. Garcia-Garibay, M. A. *Acc. Chem. Res.* **2003**, *36*, 491–498.
8. Sivaguru, J.; Natarajan, A.; Kaanumalle, L. S.; Shailaja, J.; Uppili, S.; Joy, A.; Ramamurthy, V. *Acc. Chem. Res.* **2003**, *36*, 509–521.
9. Sivaguru, J.; Shailaja, J.; Uppili, S.; Ponchot, K.; Joy, A.; Arunkumar, N.; Ramamurthy, V. Achieving Enantio and Diastereoselectivities in Photoreactions Through the Use of a Confined Space. In *Organic Solid-State Reactions*; Toda, F., Ed.; Kluwer Academic: Dordrecht, The Netherlands, 2002; pp 159–188.
10. Poon, T.; Turro Nicholas, J.; Chapman, J.; Lakshminarasimhan, P.; Lei, X.; Adam, W.; Bosio Sara, G. *Org. Lett.* **2003**, *5*, 2025–2028.
11. Poon, T.; Sivaguru, J.; Franz, R.; Jockusch, S.; Martinez, C.; Washington, I.; Adam, W.; Inoue, Y.; Turro, N. J. *J. Am. Chem. Soc.* **2004**, *126*, 10498–10499.
12. Sivaguru, J.; Poon, T.; Franz, R.; Jockusch, S.; Adam, W.; Turro, N. J. *J. Am. Chem. Soc.* **2004**, *126*, 10816–10817.
13. *Chem. Eng. News* **2004**, *82*, 7.
14. Adam, W.; Bosio, S. G.; Turro, N. J. *J. Am. Chem. Soc.* **2002**, *124*, 14004–14005.

15. Adam, W.; Bosio, S. G.; Turro, N. J. *J. Am. Chem. Soc.* **2002**, *124*, 8814–8815.
16. Adam, W.; Bosio, S. G.; Turro, N. J.; Wolff, B. T. *J. Org. Chem.* **2004**, *69*, 1704–1715.
17. Wasserman, H. H.; Murray, R. W. *Singlet Oxygen*; Academic: New York, NY, 1979.
18. Gollnick, K.; Kuhn, H. J. *Singlet Oxygen*; Wasserman, H. H., Murray, R. W., Eds.; Academic: New York, NY, 1979.
19. Foote, C. S. *Acc. Chem. Res.* **1968**, *1*, 104–110.
20. Frimer, A. A. *Singlet Oxygen*; CRC: Boca Raton, 1985; Vol. 1–4.
21. Poon, T.; Turro, N. J.; Chapman, J.; Lakshminarasimhan, P.; Lei, X.; Jockusch, S.; Franz, R.; Washington, I.; Adam, W.; Bosio, S. G. *Org. Lett.* **2003**, *5*, 4951–4953.
22. Evans, D. A.; Bartoli, J.; Shih, T. L. *J. Am. Chem. Soc.* **1981**, *103*, 2127–2129.
23. Ager, D. J.; Prakash, I.; Schaad, D. R. *Chem. Rev.* **1996**, *96*, 835–876.
24. Saito, H.; Sivaguru, J.; Jockusch, S.; Inoue, Y.; Adam, W.; Turro, N. J. *Chem. Commun.* **2005**, 3424–3426.
25. Detailed X-ray structure analysis of the *E* enecarbamates will be published elsewhere.
26. Kagan, H. B.; Fiaud, J. C. *Top. Stereochem.* **1988**, *18*, 249–330.
27. Keith, J. M.; Larrow, J. F.; Jacobsen, E. N. *Adv. Synth. Catal.* **2001**, *343*, 5–26.
28. Martin, V. S.; Woodward, S. S.; Katsuki, T.; Yamada, Y.; Ikeda, M.; Sharpless, K. B. *J. Am. Chem. Soc.* **1981**, *103*, 6237–6240.
29. Chen, C. S.; Fujimoto, Y.; Girdaukas, G.; Sih, C. J. *J. Am. Chem. Soc.* **1982**, *104*, 7294–7299.
30. Buschmann, H.; Scharf, H.-D.; Hoffmann, N.; Esser, P. *Angew. Chem., Int. Ed. Engl.* **1991**, *30*, 477–515.
31. Otera, J.; Sakamoto, K.; Tsukamoto, T.; Orita, A. *Tetrahedron Lett.* **1998**, *39*, 3201–3204.
32. Prein, M.; Adam, W. *Angew. Chem., Int. Ed. Engl.* **1996**, *35*, 471–494.
33. Turro, N. J. *Tetrahedron* **1985**, *41*, 2089–2098.
34. Sivaguru, J.; Saito, H.; Poon, T.; Omonuwa, T.; Franz, R.; Jockusch, S.; Hooper, C.; Inoue, Y.; Adam, W.; Turro, N. J. *Org. Lett.* **2005**, *7*, 2089–2092.